Genetic and molecular mechanisms mediating sperm cell formation in *Arabidopsis thaliana*

Thesis submitted for the degree of Doctor of Philosophy

Nadia Taimur

Department of Biology

September 2012

I dedicate this thesis to my parents for their unconditional love and endless support

Abstract

A study of molecular and genetic mechanisms mediating the formation of twin sperm cells in *Arabidopsis thaliana*

In flowering plants, the male gametophyte produces a pair of functional sperm cells that are transported to the embryo sac for double fertilisation. Asymmetric division of the microspore establishes the germline and division of the germ cell results in two sperm cells, however, the molecular mechanisms governing the germ cell specification and division are yet to be uncovered. DUO1 has been identified as a germline-specific MYB binding transcription factor that coordinates germ cell division with gamete specification. One of the major objectives of this thesis is the characterization of an EMS-induced germ cell division mutant termed as *duo pollen 5 (duo5)* in *Arabidopsis*. Mutant *duo5* germ cells were shown to elongate and enter mitosis but fail to complete the division cycle. Genetic analysis showed that *duo5* is an incompletely penetrant gametophytic mutation that has reduced transmission thorough the male. Map based cloning defined *duo5* to a genetic interval of ~250 kb region on the lower arm of chromosome IV. The thesis also explores the expression and regulation of two novel DUO1-activated zinc finger genes, *DAZ3* and *DAZ3L*. The reduction in the activity of both promoters in *duo1* germ cells suggested that DUO1 is required for their activation in the male germline. Analysis suggests that DUO1 possibly employ both direct and indirect mechanisms to activate DAZ3 and DAZ3L. Furthermore, analysis of protein fusion constructs demonstrated that DAZ3 and DAZ3L expression is predominantly localized in the sperm cell cytoplasm and this expression pattern persists in the developing pollen tubes. The analysis of DAZ3 expression in germ cell division mutants revealed that late activation of DAZ3 promoter is independent of germ cell division. The work demonstrated, will further add to the knowledge of male gametophyte development and will provide new opportunities to understand molecular and genetic mechanisms involved in the production of two plant sperm cells.

Acknowledgements

It is a pleasure to thank those who made this thesis possible. First and foremost, I would like to thank Allah; our Lord, the All-Knowing, the Almighty, the most Merciful and the most Compassionate. Prayers and peace be upon His prophet Mohammed, the last messenger for all humankind.

I would like to express my deepest gratitude to my supervisor Prof David Twell. I appreciate Prof David Twell for his excellent supervision, endless support and consistent encouragement throughout the PhD project. My heartfelt appreciation also goes to my PhD advisor Prof Pat Heslop-Harrison for his immensely positive and valuable suggestions as well as encouragements during yearly progress assessments.

I take the chance to thank and express my gratitude to all my friends for their encouragement, advice and understanding. I am very thankful to all my colleagues in the lab specially Hoda for being my closest and caring friend I can ever have and for her endless support, Michael for his help and for his positive suggestions regarding DAZ3 project. I am also grateful to Ugur, Mihai and Nick for their kind help and friendship that made my experience in the lab a memorable one. My special thanks goes out to the past Twell lab members, Said, Gael Le Trionnaire and Sofia for their constant encouragement, friendship and kind words in troubled times. I would also like to thank Trudie Allen and Anna Sidorova for their help and assistance.

Without the support of all members of my family, I wouldn't have found the courage to overcome all the difficulties during this work. I am very grateful to my dear family, my father and my mother for their daily phone calls, my sisters and my brothers for their love and continuing support. Thanks a lot for being my lovely family and for always there for me.

I would also like to acknowledge the Higher Education Commission of Pakistan (HEC) and University of Science and Technology Kohat (KUST), Pakistan for the financial support provided to me during my PhD studies. Finally, I would like to thank everybody who was involved in this work as well as expressing my apology to those I did not mention in this acknowledgment.

Nadia

Table of contents

List of Figures

List of Tables

Abbreviations

A	adenine
APC/C	Anaphase promoting complex/cyclosome
ATP	adenosine triphosphate
BAP	6-benzylaminopurine
bp	base pair
BSA	bovine serum albumin
C	cytosine
^{o}C	degrees centigrade
CDKA;1	Cyclin-dependent kinase A;1
cDNA	complementary DNA
chi (X^2)	Chi-square statistic
cm	centimetre
CCS52	cell cycle switch 52 gene
CDK	Cyclin-dependent kinase
Cdc	cell division control
Cdh1	Cdc20 homologue 1
D-box	destruction box
dCAPS	derived cleaved amplified polymorphic sequences
CDS	coding sequence
DIC	Differential interference contrast
CKI	CDK inhibitory subunit
CSM	Cdc20-specific motif
CYC	Cyclin
DAA1	DUO1 activate ATPase
DAP	days after pollination
DAPI	4',6-diamidino-2 phenylindole dihydrochloride
DAT	DUO1-activated target
DEL	DP-E2F Like
DNA	deoxyribonucleic acid
dNTP	deoxynucleotide triphosphate
DUO1	Duo Pollen-1
DUO2	Duo Pollen-2
DUO3	Duo Pollen-3
DUO4	Duo Pollen-4
E1	Ubiquitin-activating enzyme
E2	Ubiquitin-conjugaing enzyme
E2F	Adenovirus E2 promotor binding factor
E3	Ubiquitin-ligase
EDTA	ethylenediaminetetraacetic acid
EMS	ethyl methanesulfonate
F1,F2,F3	first, second, third generation after a cross

FBL17	F-box-Like 17
FDA	fluorescein diacetate
fm	fentamole
g	gram
g	gravity
G	guanine
GCS1 / HAP2	Generative cell-specific-1 / hapless-2
gDNA	genomic DNA
GEX2	Gamete expressed-2
GFP	green fluorescent protein
GRSF	germline-restrictive silencing factor
GUS	beta-glucuronidase
H2B	histone H2B
kb	kilobase pair
Kda	kilodalton
KRP	Kip-related protein
l	litre
LB media	Luria Bertani media
M	molar
MBS	MYB binding site
MES	2-(N-Morpholino)ethanesulfonic acid
mg	milligram
MGH3	male gamete-specific histone-3
MGU	Male germ unit
ml	millilitre
mM	millimolar
mRFP	monomeric red fluorescent protein 1
mRNA	messenger RNA
MS	Murashige and Skoog
MT	microtubules
ng	nanogram
OD	optical density
p	plasmid
PPB	Pre-prophase band
PCR	polymerase chain reaction
PCR11	PLANT CADMIUM RESISTANCE
pg	picogram
prom	promoter
PSSM	position-specific scoring matrix
qRT-PCR	quantitative RT-PCR
RBR	Retinoblastoma-related
RenLUC	Renilla luciferase protein
Rluc	Renilla luciferase activity

RNA	ribonucleic acid
RNAi	RNA interference
ROI	region of interest
rpm	revolutions per minute
RSAT	regulatory sequence analysis tools
RT	room temperature
SCF	Skp, Cullin, F-box containing E3 ligase complex
RT-PCR	reverse transcriptase-PCR
SEM	standard error of the mean
SNP	single nucleotide polymorphisms
SSLP	Single Sequence Length Polymorphism
T	thymine
T1	first generation of transformed Arabidopsis plants
TAE	tris-acetate EDTA
TAIR	The Arabidopsis Information Resource
T-DNA	transfer DNA
TEM	Transmission electron microscopy
Tm	melting temperature
TIO	Two-in-one
TIP5;1	Tonoplast intrinsic protein-5;1
Tris	tris(hydroxymethyl)aminomethane
Triton X-100	(t-Octylphenoxypolyethoxyethanol)
U	enzyme units
mg	microgram
ml	microlitre
mM	micromolar
UTR	untranslated region
V	volts
VCK	Vegetative cell kinase
v/v	volume per volume
WD-40	Tryptophan–aspartate dipeptide repeat motif
w/v	weight per volume
WT	wild type

Chapter 1 Introduction

1.1 The life cycle of flowering plants

Flowering plants represent one of the most successful and largest groups of plants which dominate the vegetation of most of the terrestrial ecosystems. The life cycle of flowering plants alternate between a reduced haploid gametophytic generation and a dominant diploid sporophytic generation. The haploid gametophyte is morphologically distinct from the diploid sporophyte and consists of three celled male gametophyte (pollen) and seven- celled female gametophyte (embryo sac) (Maheshwari, 1950) both harbouring a unique germline transcriptome profile. Sporophyte represents the main plant body and consists of roots, shoots, leaves and flowers. The gametophytic phase of the life cycle starts with the formation of haploid microspores and megaspores, which are produced as a result of meiotic divisions in specialized floral tissues. The haploid products of meiosis undergo a further round of mitosis to form the haploid gametophyte that is responsible for the production of male and female gametes. The coordinated fusion of two pairs of male and female gametes give rise to two distinct fertilisation products, the embryo and the endosperm, a phenomenon termed as double fertilisation (Berger, 2008). The flowering plants owe their evolutionary success to certain unique features including presence of genetically active haploid (gametophyte) and diploid (sporophyte) phases of life cycle, absence of a germline, and a double fertilisation event during sexual reproduction to produce an embryo and a nutritive tissue called endosperm (Walbot and Evans, 2003).

1.1.1 Sexual reproduction in flowering plants

Meiosis occurs in the life cycle of all sexually reproducing eukaryotes and is a unique and essential part of the life cycle. Sexual reproduction in flowering plants involves transition from the sporophytic stage to the gametophytic stage via meiosis (Bhatt *et al.*, 2001). Plants undergo several developmental transitions during their life cycle. The floral transition is one of the major transitions from the adult vegetative state to the reproductive state. Flowers, the reproductive organs of angiosperm, are more varied than the equivalent structures of any other group of organisms (Barrett, 2002). Unlike animals, where germline is established early in embryogenesis and remain as separate

stem cell populations (Hayashi and Surani, 2009; Strome and Lehmann, 2007), flowering plants have an undifferentiated stem cell population in the shoot apical meristems. The shoot apical meristem switches from producing vegetative structures to reproductive structures in response to environmental signals such as available nutrients, day length, light intensity, light quality, and ambient temperature as well as endogenous signals transmitted by plant hormones (Bäurle and Dean, 2006; Parcy, 2005).

The development of the male (anther) and female (ovule) reproductive structures from somatic tissue are dependent on the process of meiosis and initiate the basic process of development in plants. Although the male and female gamete production in higher plants is similar, the fate of the male and female meiotic products is distinct. During male gamete production, all four meiotic products called microspores develop to produce fully viable pollen grains (McCormick, 2004; Scott *et al.*, 2004). In contrast, during female gamete production, only one of the four meiotic products called megaspores, give rise to the 7-celled female gametophyte and the remaining megaspores undergo programmed cell death. The development of female gametophyte (the embryo sac or megagametophyte) takes place within the ovule, which is located inside the carpel of the flower. In the developing ovule, a single cell from the internal tissue, called nucellus, differentiated into the female meiocyte or megaspore mother cell. The megaspore mother cell undergoes meiosis to generate four spores, three of which undergo programmed cell death. The remaining proximal megaspore at the chalazal end completes three rounds of mitosis to generate eight nuclei. Subsequent cellularization results in the formation of seven cells: three antipodal cells, two synergids, one egg cell and one central cell (Alandete-Saez *et al.*, 2008; Drews and Goldberg, 1989; Drews and Yadegari, 2002). The male germline is established when the haploid microspore divides asymmetrically to produce a small germ cell engulfed within a large vegetative cell. The germ cell undergoes a final round of mitosis to produce twin sperm cells. The two sperm cells are transported by the pollen tube to the haploid female reproductive cells of the embryo sac where they participate in double fertilisation. Inside the female reproductive tissue, one sperm cell fuses with the haploid egg cell to form the diploid zygote, whereas the second sperm cell fuses with the diploid central cell to form triploid endosperm that nourishes the embryo through seed development (Weterings and Russell, 2004) (Figure 1.1).

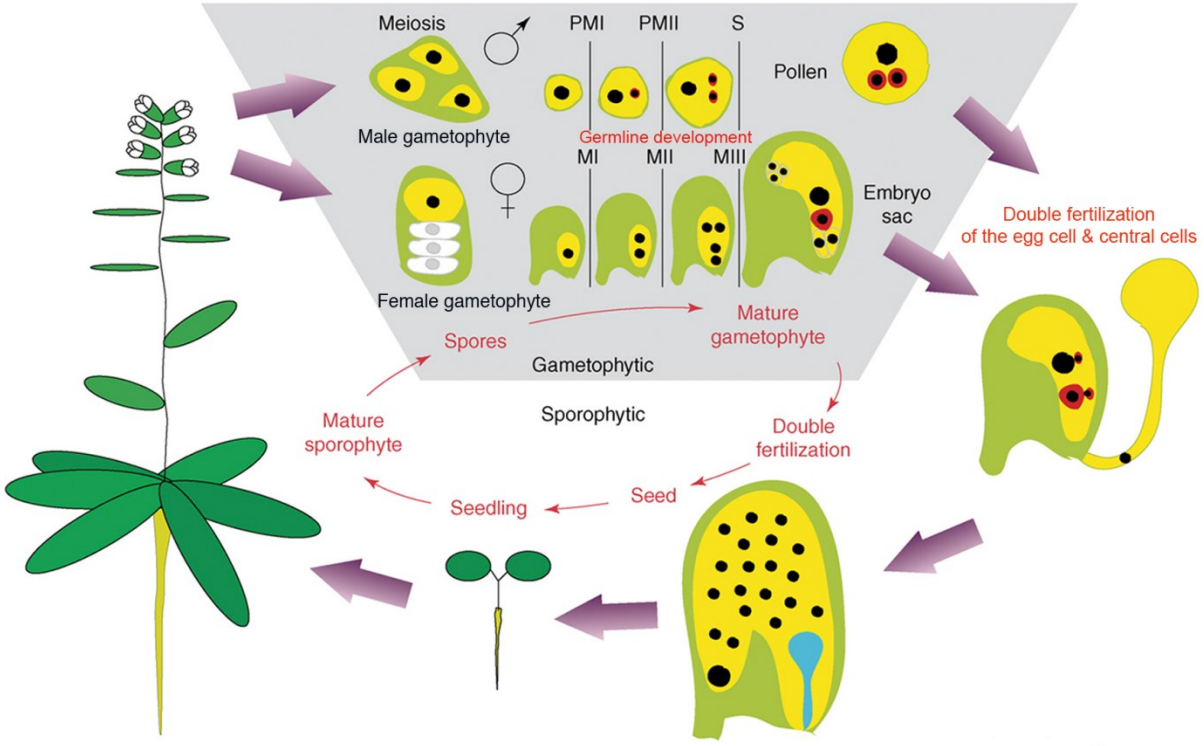

Figure 1.1: The life cycle of *Arabidopsis thaliana* alternates between sporophyte and gametophyte phases. The diploid sporophyte undergoes meiosis to produce haploid gametophytes. Microspores undergo two mitotic divisions to produce twin sperm cells (marked red). Haploid megaspores produce seven-celled female gametophytes as a result of three mitotic divisions. The female gametophyte consists of the egg cell (red), three antipodal cells at the chalazal end (proximal) end, two synergid cells at the micropylar (distal) end and the central cell (black). The two sperm cells are transported to the embryo sac through the pollen tube, which results in double fertilization. During double fertilization, one sperm cell fertilizes the egg to form the embryo, while the second sperm cell fuses with the central cell to form the triploid endosperm. The endosperm nourishes the developing embryo to generate a mature seed, which is dispersed and eventually germinate and give rise to a new generation. The process of double fertilization thus represents the end of the gametophytic stage and the beginning of the sporophytic stage. Adapted from (Berger *et al.*, 2006).

1.1.2 Cellular analysis of pollen development

In flowering plants the shoot apical meristem converts to a reproductively determined inflorescence meristem upon receiving appropriate environmental cues (Amasino, 2010). The floral meristem produces floral organs in concentric rings or whorls from centre to edge: pitils, stamens, petals and sepals (Irish, 2010; Smyth *et al.*, 1990). In flowering plants the formation of gametes occurs within specialized reproductive structures called stamen and carpel. The floral meristem of *Arabidopsis* is composed of three histologically distinct cell layers with separate lineages. The outermost L1 layer establishes the epidermis and stomium which is essential for dehiscence and pollen release. The male reproductive organs, stamens, are derived from periclinal divisions of L2 layer of the floral meristem (Jenik and Irish, 2000). The innermost L3 layer contributes to the formation of a connective, vascular bundle and inner part of tapetum (Goldberg *et al.*, 1993; Scott *et al.*, 2004). Stamens consist of an anther, the site of pollen development, and a stalk-like filament, which transmits water and nutrients to the anther and positions it to aid pollen dispersal. The anther contains both non-reproductive and reproductive tissues that are responsible for the production and release of mature pollen grains. In the case of male gametophyte, the pollen development takes place in anther in two distinct phases i.e. microsporogenesis and microgametogenesis (Scott *et al.*, 2004).

1.1.2.1 Microsporogenesis

In microsporogenesis, the middle L2 layer within anther primordia produces the archesporial cells which divide mitotically to produce primary parietal cells (PPC) and primary sporogenous cells (PSC). Further mitotic divisions in primary parietal cells give rise to several concentric layers that differentiate into the endothecium, middle layer and innermost tapetum. The tapetum surrounds the sporogenous cells and serves to nourish the developing microspores during the process of pollen mother cell meiosis and microspore maturation. On the other hand the primary sporogenous cells give rise to microsporocytes or male mieocytes or pollen mother cells (PMC). These pollen mother cells become enclosed in an impermeable β-1,3-glucan wall (callose), isolating meiocyte from sporophyte cells. The diploid pollen mother cells undergo two meiotic divisions to produce a tetrad of haploid microspores. The unicellular microspores are

released from the tetrad by the activity of callase enzymes containing endoglucanase and exoglucanase, from the inner nutritive layer of the stamen, the tapetum (Scott *et al.*, 2004). The disruption in the activity of tapetal enzymes results in so called *quartet (qrt)* mutant phenotypes in which the four products of microsporogenesis remain fused and pollen grains are released as tetrads. Three genes required for tetrad dissolution have been described in *Arabidopsis* and include *qrt1, qrt2,* and *qrt3*. The molecular identity and function of *QRT2* gene has not yet been resolved, but *QRT1* gene encodes a pectin methylesterase whereas *QRT3* encodes a tapetum-specific polygalacturonase involved in the degradation of the pollen mother cell wall (Francis *et al.*, 2006; Preuss *et al.*, 1994; Rhee *et al.*, 2003).

1.1.2.2 Microgametogenesis

In newly released microspores the nucleus is positioned in the centre and many small vacuoles are distributed throughout the cytoplasm. During microgametogenesis the microspores enlarge and small vacuoles coalesce to produce a single large vacuole that is associated with migration of the nucleus of the microspore to a peripheral position against the cell wall (Owen and Makaroff, 1995; Yamamoto *et al.*, 2003). The polarized microspores then undergo two rounds of mitotic divisions. PMI represents a key event that results in a distinct asymmetric division of the microspore into two unequal cells i.e. a large vegetative cell and smaller germ cell. The larger vegetative cell makes the pollen grain itself, has dispersed nuclear chromatin and accumulates a very dense cytoplasm containing lipids, proteins and carbohydrates (McCormick, 2004). The small germ cell contains highly condensed chromatin and contains few organelles and stored metabolites. The asymmetric division of the microspore at PMI is known to be essential for the correct germ cell fate specifications and that vegetative cell fate is a default developmental pathway (Eady *et al.*, 1995; Twell *et al.*, 1998). The two cells have a distinct cytoplasm and unique gene expression profile that give them their distinct structures and cell fates.

Prior to the division, the germ cell migrates to the centre of the pollen and undergoes further morphogenesis to acquire an elongated or spindle-like shape, thought to be maintained by a cortical cage of bundled microtubules (Cai and Cresti, 2006; Palevitz and Cresti, 1989). The vegetative cell is arrested at G1 phase of the cell cycle but the smaller germ cell undergoes a further mitotic division, called Pollen Mitosis II to

produce twin sperm cells. A physical association is formed between the two sperm cells and the nucleus, called the male germ unit (MGU), which is common to both bicellular species and tricellular species (Dumas *et al.*, 1998; Lalanne and Twell, 2002). During maturation of *Arabidopsis* pollen, the vegetative cell accumulates carbohydrate and lipid reserves as well as transcripts and proteins that are required for rapid pollen tube growth (Pacini, 1996). Also the accumulation of sugars (disaccharides), amino acids (proline) and glycine betane serve as osmoprotectants for cellular membranes and proteins during pollen dehydration (Schwacke *et al.*, 1999). The larger vegetative cell nurtures the germ cell and later forms a pollen tube that grows through the style and delivers the two sperm cells to fertilise the haploid egg cell and diploid central cell.

1.1.2.3 The timing of germ cell division in flowering plants

The timing of germ cell division to from two sperm cells is regulated differently among plant species. There are two different patterns in relation to the timing of PMII, identified in seed plants. Approximately 70% of angiosperm plant families (Brewbaker, 1967) and all extant non-flowering seed plants (Friedman, 1999; Rudall and Bateman, 2007), pollen mitosis II take place after pollen germination and therefore bi-cellular pollen is released from anthers. Whereas in a number of unrelated angiosperm families, pollen mitosis II takes place within the pollen grain prior to anthesis and is considered to be more advanced state in angiosperm evolution (Brewbaker, 1967). *Nicotiana tabacum* produce bicellular pollen at anthesis while many important model and food crop plants such as *Arabidopsis thaliana, Oryza sativa, Triticum vulgare* and *Zea mays* produce advanced but often short-lived tricellular pollen grains (Singh and Bhalla, 2007; Twell *et al.*, 2006). Further studies suggest that among higher plants there is variability in the timing of the cell cycle associated with sperm cell development and fertilisation. Different patterns of sperm cell cycle can be found in angiosperm species that shed bicellular and tricellular pollen (Friedman, 1999).

1.1.3 Significance of Pollen Mitosis I and asymmetric cytokinesis

In plant cells, the asymmetric cytokinesis followed by PMI is critical for correct germ cell fate and ensures that the cell fate determinants are correctly segregated and confined by a new cell wall. The cytoskeleton is also likely to play a central role in determining both nuclear migration and the division plane. The control of microspore nuclear

migration, organization of asymmetric mitotic spindle and phragmoplast microtubule arrays and division orientation are key processes in establishing the male germline.

1.1.3.1 Significance of asymmetric nuclear division

The first mitotic division is a strikingly asymmetric division that produces two daughter cells of different sizes and developmental fates (Twell *et al.*, 1998). In tobacco, the treatment of microspores using microtubule inhibitors or centrifugation caused a symmetrical PMI, producing two equal-sized daughters expressing the vegetative cell fate marker LAT52-GUS. These results suggested that asymmetric division at PMI is required for correct germ cell differentiation. Also the vegetative cell fate is the default fate during pollen development and that the activation of vegetative cell-specific genes can be uncoupled from nuclear division and cytokinesis (Eady *et al.*, 1995; Tanaka and Ito, 1980, 1981). Two general models have been formulated to elucidate the distinct cell fates of the two daughter cells after PMI. Both the models propose that the vegetative-cell genes are controlled by a microspore-expressed gametophytic factor that accumulate and reach a certain threshold at PMI and provide mechanisms for vegetative cell-specific gene repression in germ cell. In the passive-repressive model, the gametophytic factor is excluded from the germ cell pole as a result of division asymmetry, thereby preventing activation of genes specific to vegetative cell. Moreover, lack of sufficient gametophytic factor would maintain high histone H1 concentration in the germ cell, promoting condensed chromatin state and repression of vegetative cell specific genes. According to the second active-repression model, the gametophytic factor is distributed in both vegetative cell and germ cell. However, an additional germ cell-repressor is concentrated at the germ cell pole that blocks the action of the gametophytic factor, resulting in inactivation of vegetative cell-specific genes in the germ cell (Eady *et al.*, 1995; Twell *et al.*, 1998).

Another mechanism of male germline gene repression in non-germ cells has been identified that involve the repressor protein called GRSF (Germline Specific Silencing Factor). GRSF is a nuclear protein which is ubiquitous in non-germ cells and is absent from the male germ cells. GRSF recognizes the silencer elements in the promoters of the genes specific to the germline and represses their activation in non-germ cells (somatic cells, vegetative cell). Immunolocalization experiments using antibodies to GRSF showed that the GRSF protein is present in uninucleate microspores and in the

vegetative cell after PMI but absent from the germ cell. The absence of GRSF from the germ cell may result in transcriptional derepression mechanism promoting expression of germ cell specific genes and thus account for the differential gene expression and distinct cell fates at PMI (Haerizadeh *et al.*, 2006).

1.1.3.2 Significance of asymmetric cytokinesis

The characteristic asymmetric cytokinesis at PMI mostly relies on the asymmetry generated by the pre-mitotic cytokinesis apparatus. Moreover, the asymmetric cytokinesis at PMI differs from that in somatic cells in several aspects. First, preprophase band (PPB) of microtubules is absent from gametophytic cytokinesis and is not involved in marking the future division plane, second, a unique hemispherical cell plate is formed to enclose the eccentric germ cell nucleus and third the nuclei resulting from pollen mitosis are immediately differentiated (Mascarenhas, 1975; Tanaka, 1997; Terasaka and Niitsu, 1995; Van Lammeren *et al.*, 1985). The absence of PPB in microspore mitosis was earlier reported for *Brassica* (Hause *et al.*, 1993), *Gasteria* (Van Lammeren *et al.*, 1985), and for *Tradescantia* (Terasaka and Niitsu, 1990).

In dividing microspores of orchids, an MT array named generative pole MT system (GPMS) was observed between the plasma membrane and the prophase microspore nucleus prior to the assembly of the spindle (Brown and Lemmon, 1991). However, this MT array was not observed in dividing microspores expressing a green fluorescent protein (GFP)-tubulin marker in *A. thaliana* and tobacco (Oh *et al.*, 2010a; Oh *et al.*, 2010b). At late anaphase and telophase during pollen mitosis I, microtubules are reorganized into the bipolar phragmoplast array between two reforming nuclei. Remarkably, the phragmoplast expands centrifugally in a curved fashion and consequently, a curved cell plate is formed separating the germ and the vegetative cell (Brown and Lemmon, 1994; Liu *et al.*, 2011; Terasaka and Niitsu, 1995).

Gametophytic mutants that influence division polarity and cytokinesis include *tio* (Oh *et al.*, 2005), *gem1* (Park *et al.*, 1998; Twell *et al.*, 2002), *gem2* (Park *et al.*, 2004), *kinesin-12A/12B* (Lee *et al.*, 2007) and *hit-1/tes-1* (Oh *et al.*, 2008) and have been shown to disrupt pollen patterning and formation of germline. The *sidecar pollen* (*scp*) was identified as a gametophytic mutant that affects microspore division (Chen and McCormick, 1996). Recent analysis of the *sidecar pollen* mutant in *Arabidopsis* showed

that *SCP* is important for the correct timing and control of division orientation of microspore but not for nuclear migration (Oh *et al.*, 2010c).

1.1.4 Germ cell migration, morphogenesis and division

The products of the asymmetrical mitosis are well differentiated in the early bi-nucleate pollen, which contains the peripheral germ cell within larger vegetative cell. During subsequent growth and development the germ cell undergoes changes in position and morphology before committing to the second phase of mitotic division.

1.1.4.1 Germ cell migration

Immediately after asymmetric division, the germ cell is located against the pollen wall. The formation of hemispherical callose wall constitutes the initial partition between the nascent germ cell and the vegetative cell. This callose wall is subsequently degraded allowing the germ cell to detach from the intine wall layer and migrate inwards. Inside the cytoplasm of the vegetative cell this newly internalized germ cell is surrounded by two closely associated plasma membranes, resulting in a unique cell-within-cell structure (Park and Twell, 2001). After detachment from the pollen wall, the thin-walled germ cell rounds up to become spherical and remains peripheral in the early bi-cellular stage of pollen development (Boavida *et al.*, 2005). In the *Arabidopsis* gametophytic mutant *limpet pollen (lip*), the germ cell fails to migrate into the pollen grain after PMI such that the germ cell or the sperm cells remain at the periphery (Howden *et al.*, 1998).

The cytoskeleton is also implicated in germ cell migration, immediately after PMI. During the early pollen stage of tobacco, actin filaments remain associated with the germ cell wall and the vegetative nucleus and function during migration of both germ cell and vegetative nucleus towards the centre of the pollen, away from the pole (Zonia *et al.*, 1999).

Recent studies suggest the most prominent role of microtubules at early and mid-bicellular stage of pollen development. At early bicellular stage, the microspore and pollen culture of *Brassica napus,* developed *in vitro,* displayed parallel arrangement of cortical and endoplasmic microtubules to the long axis of germ cell. Moreover, during germ cell migration, multiple thick and longitudinal bundles of endoplasmic microtubules of the germ cell reorganize and start to surround the germ cell. Later when

the germ cell took more central position within vegetative cell, thick bundles of longitudinally arranged microtubules radiating from the cytoplasm near the germ cell plasma membrane assembled at the narrow end of germ cell, close to the vegetative cell nucleus forming a comet-like microtubule tail. These studies demonstrated that the endoplasmic microtubules are involved in germ cell detachment from the pollen wall, its migration towards vegetative nucleus as well as germ cell shape changes. Moreover, the studies also suggests that the cortical microtubules of germ cell which form a basket-like structure around germ cell, could play protective role during germ cell migration (Dubas *et al.*, 2012).

1.1.4.2 Germ cell morphogenesis

A critical aspect of germ cell differentiation after detachment from the pollen wall is the change in the shape of the cell from a spherical to a spindle shape, accompanied by a corresponding change in the shape of the nucleus. Detailed studies have demonstrated that basket-like arrays of cross-bridged microtubules (Palevitz and Tiezzi, 1992) play a significant role in maintenance of cell shape, morphogenesis and participation in germ cell division. The morphogenesis of the nascent germ cell to form an elongated, lenticular or spindle shape is associated with the reorganization of the microtubule arrays located in the cortical germ cell cytoplasm. Previous studies have established that immature isolate germ cells have spheroidal shape, with meshwork of microtubules (Zhou and Yang, 1991). These microtubules elongate and take up position in the longitudinal parallel bundles, causing the germ cell shape change from spheroidal to spindle-like. A slightly spiraled cage or basket of microtubule bundles surrounds the nucleus residing in the thin cytoplasmic layer (Del casino *et al.*, 1992). The essential requirement of microtubules bundles in maintaining germ cell shape is suggested by the fact that microtubule-perturbing drugs prevent the elongation of the germ cell (Sanger and Jackson, 1971).

Recent studies have highlighted the importance of endoplasmic and sub-cortical microtubules in provoking changes in the germ cell shape (Dubas *et al.*, 2012). In maize, an α-tubulin-YFP line expressing the fusion protein under the control of the endogenous promoter was reported to be exclusively germline specific. The analysis of germline specific tubulin marker line at late bicellular stage showed basket-like microtubule structure around the germ cell nucleus that continued into tail-like

extensions at both poles of the germ cell. The length of these tail-like microtubule extensions further increased during pollen maturation both between sperm cells and opposite poles (Kliwer and Dresselhaus, 2010). These tail-like extensions or cytoplasmic projections are polarised towards vegetative nucleus and become associated with a pre-formed groove on the surface of the vegetative nucleus (McCue *et al.*, 2011). In tobacco, a GFP fluorescent α-tubulin6 reporter protein has highlighted the cytoplasmic extensions emanating from germ cell towards vegetative nucleus, demonstrating the presence of microtubules within the cytoplasmic projections in living cells (Oh *et al.*, 2010a; Oh *et al.*, 2010b). This shift in germ cell morphogenesis may help to streamline the germ cell and facilitate its passage through the narrow confines of rapidly growing pollen tubes.

1.1.4.3 Germ cell division

In plant species that shed tricellular pollen, germ cell division takes place in the developing pollen tube. In contrast, plant species that tricellular pollen, germ cell division takes place within the pollen grain prior to anthesis. The second mitotic division within the pollen grain involves typical mitosis with the formation of a cell plate. However, germ cell division within the developing pollen tube is unusual because the spatial constraints in the germ cell confine the cell plate to a highly oblique or longitudinal orientation (Terasaka and Niitsu, 1989).

The most investigated aspects of GC division include the establishment of the mitotic spindle and metaphase plate and the mode of cytokinesis. In the pollen tubes of monocot *Endymion non-scriptus,* changes in the distribution of microtubules within the germ cell were studied. It was illustrated that, at prophase stage, the cytoplasmic microtubules decline in favour of mitotic spindle fibres (Burgess, 1970). In tobacco, pre-mitotic germ cells have a highly elongated structure and condensed nuclear chromatin. The chromatin undergoes further condensation as the cell enters prophase. Microtubules are also programmed to disappear from the cytoplasm of the germ cells of tobacco as well as *Ornithogalum virens* at the time the mitotic spindle is arranged (Charzynska and Cresti, 1993; Yu and Russell, 1993). The oblique arrangement of the mitotic spindle results in atypical alignment of chromosomes to the mitotic spindle (Palevitz, 1990; Palevitz and Cresti, 1989; Taylor *et al.*, 1989; Terasaka and Niitsu, 1989; Yu and Russell, 1993). The origin and distribution of the kinetochore fibres that connect the condensed

chromosomes to the pole of mitotic spindle at metaphase stage has been a contentious issue. In species like *Rhododendron* and *Tradescantia,* chromosomes are arranged perpendicular to the obliquely oriented metaphase spindle (Liu and Palevitz, 1991; Palevitz, 1990; Palevitz and Cresti, 1989; Taylor *et al.*, 1989), while in *Hyacinthus* the kinetochores are conventionally distributed along the equatorial plane (Del casino *et al.*, 1992). In tobacco, kinetochore fibres are irregularly distributed along the length and depth of the germ cell (Yu and Russell, 1993). The metaphase spindle of *Ornithogalum virens* mostly consists of kinetochore fibres, located in one plane perpendicular to the pole of spindle axis (Banaś *et al.*, 1996).

In *Ornithogalum virens,* the anaphase is characterized by a shortening of kinetochore fibres and considerable elongation of the mitotic spindle, a characteristic of germ cell mitosis in both bicellular and tricellular species (Banaś *et al.*, 1996; Charzynska and Lewandowska, 1990; Yu and Russell, 1993). According to Liu and Palevitz (1992), the axial system of microtubules and kinetochore fibres reorganise into two thick bundles (superbundles). As a result, chromatids of each pair segregate to different superbundles bound to opposite ends. However, in tobacco germ cell division, the movement of chromosomes results from the convergence of the dispersed poles into pointed poles upon which all kinetochore fibres focus as well as shortening of kinetochore bundles and separation of anaphase poles (Yu and Russell, 1993).

At late anaphase the sister chromatids reach the opposite poles and in the region between the two separated nuclei the phragmoplast microtubules give rise to phragmoplast, which in turn produces a cytokinetic cell plate (Charzynska *et al.*, 1989; Yu and Russell, 1993). This mode of germ cell division is documented in bicellular and tricellular pollen of several plant species including *Hordeum vulgare* (Charzyńska *et al.*, 1988), *Brassica napus* (Charzynska *et al.*, 1989), *Nicotiana tabacum* (Palevitz, 1993; Yu and Russell, 1993), *Lilium* (Xu *et al.*, 1990), *Ornithogalum* (Banaś *et al.*, 1996), and *Rhododendron* (Taylor *et al.*, 1989). In these species, cytokinesis is accompanied by phragmoplast formation, which then guides the assembly of a cell plate that partitions the cytoplasm. However cytokinesis in *Tradescantia* and *Hyacinthus* is not characterized by the formation of either distinct phragmoplast or cell plate. In the absence of phragmoplast in *Tradescantia*, cytokinesis is accomplished by furrowing process (Del casino *et al.*, 1992; Palevitz and Cresti, 1989). One of the most prominent

features of germ cell cytokinesis is the absence of F-actin from the spindle or from phragmoplast throughout division indicating that actin filaments are not required in the cell plate formation at pollen PMII (Palevitz and Tiezzi, 1992).

1.2 Genetic and transcriptomic approaches to dissect gametophyte gene functions

In recent years, major advances in genetic and genomic technologies have made it possible to study processes of cell fate specification and cellular function during pollen development. The combination of forward and reverse genetics approaches provides powerful tools to dissect pollen developmental pathways in both male and female gametophytes that remain inaccessible for direct inspection (Page and Grossniklaus, 2002). Also recent advancements in high-throughput technologies such as microarrays has enabled analyses of the haploid gene expression on a much larger scale and helped to reveal the transcriptional profile of male gametophyte in greater detail (Redman *et al.*, 2004; Rehrauer *et al.*, 2010).

1.2.1 Screens for male gametophyte mutants

The quest to decipher gene functions at different pollen developmental stages remains one of the major strands in *Arabidopsis* research. Genetic analysis of gametophytic mutants remains a challenge because not all gametophytic mutations can be scored directly for easily observable mutant phenotype, compared with sterile mutants. Because male specific gametophytic mutations can be transmitted from one generation to another as heterozygotes therefore, plants homozygous for mutations could not be recovered. Also the phenotype of the heterozygous mutant plants often appear wild type and therefore require further analysis for identification of the mutant (Procissi *et al.*, 2001). According to previous studies, various screens for mutations affecting gametophytic viability and function have resulted in isolation of a small percentage of fully defective male gametophytic mutants (Bonhomme *et al.*, 1998; Feldmann *et al.*, 1997; Howden *et al.*, 1998). Nevertheless, numerous forward (from-phenotype-to-gene) and reverse (from-gene-to-phenotype) genetic approaches have proved useful in isolating gametophytic mutants and genes influencing male gametophyte development and function. Two forward genetic approaches have been adopted to identify mutants

affecting pollen development. These include morphological screening of pollen from mutagenized plants using histochemical staining for DNA (Chen and McCormick, 1996; Park *et al.*, 1998) or callose (Johnson and McCormick, 2001). The second approach exploits marker segregation ratio distortion to identify mutants with reduced transmission through male or female gametes (Bonhomme *et al.*, 1998; Grini *et al.*, 1999; Howden *et al.*, 1998; Johnson *et al.*, 2004; Lalanne *et al.*, 2004; Procissi *et al.*, 2001).

1.2.1.1 Segregation distortion screens

Insertional mutagenesis screens mostly employ DNA elements that are able to insert at random within the genome, such as transposons or T-DNA that harbour dominant antibiotic or herbicide resistance markers. The segregation distortion screen is based on the fact that if an insertion inactivates an essential male or female gametophytic gene, then the ratio of resistant to sensitive individuals in a self-progeny progeny would deviate significantly below the expected 3:1 segregation ratio. In case the hemizygous T-DNA/transposon line segregates at a ratio of 1:1 for resistant to sensitive progeny, it would indicate that the insertion failed to transmit through either male or female gametophyte. Therefore, segregation ratio distortion screens can be used as a reliable indicator of a gametophytic defect in genes involved in post-pollination events (Howden *et al.*, 1998).

The genetic screens for segregation ratio distortion have led to the identification of a number of gametophytic mutant phenotypes caused by T-DNA insertions (Bonhomme *et al.*, 1998; Feldmann *et al.*, 1997; Grini *et al.*, 1999; Howden *et al.*, 1998; Johnson *et al.*, 2004) or transposons (Lalanne *et al.*, 2004).

A unique collection of more than 14,000 *Arabidopsis* transformants was generated with the seed co-cultivation method (Feldmann, 1991). An initial screening of 142 of these transformed lines on medium containing the selective agent, kanamycin resulted in the identification of 17 lines that failed to segregate the kan^R trait in the Mendelian manner for dominant allele (Feldmann *et al.*, 1997).

Approximately 1000 independent *Arabidopsis* transformants harbouring at least one T-DNA insert were screened for the segregation of Hygromycin resistant seedlings in a progeny of selfed T3 plants. This screening strategy led to the identification of eight

independent putative T-DNA tagged gametophytic mutants that reproducibly exhibited distorted segregation ratio approaching 1:1. These included the cellular morphogenesis mutant, *limpet (lip)* pollen mutant that fails to complete germ cell migration, one male specific progamic phase mutant and four lines showing significant effects on male and female transmission (Howden *et al.*, 1998).

Similarly, another T-DNA insertional mutagenesis screen mainly focused on identification of highly penetrant T-DNA transmission defect lines (*Ttd*) showing 1:1 segregation for kanamycin resistance. Genetic analysis of 38 of these T-DNA transmission defect *(Ttd)* lines confirmed eight as male-specific mutants, with 0-1% T-DNA transmission through the pollen (Bonhomme *et al.*, 1998).

An alternative approach was based on the segregation distortion of nearby visible markers to screen for EMS-induced gametophytic mutants. A multiply-marked chromosome I (mm1), carrying five visible recessive markers, was used to identify gametophytic mutants only in close proximity to the markers. Seven gametophytic mutations were isolated that exhibited a marked reduction in transmission through the male (*mad1, mad2, mad3* and *mad4)* or through both male and female gametes *(bod1, bod2, bod3*), displaying pleiotropic phenotypes (Grini *et al.*, 1999).

In another screening procedure, gametophytic mutants were identified by distorted ratio segregation utilizing an herbicide resistance marker (Basta) and the T-DNA element containing a LAT52:GUS pollen-specific reporter genes, providing a cell-autonomous tag for pollen grains that carry an insertion. The screen performed in a *quartet* genetic background yielded a total of 32 haploid-disrupting heterozygous mutations called *hapless* (*hap*) that defined genes required for pollen grain development, pollen tube growth within the stigma/style and pollen tube growth and guidance in the ovary (Johnson *et al.*, 2004).

In a different approach, a transposon insertion mutagenesis screen was adopted and Ds transposon insertion lines were created. The screen was based on the segregation ratio distortion of a population of Ds transposon insertion lines containing single enhancer trap (DsE) or gene-trap (DsG) elements marked with kanamycin resistance (Moore *et al.*, 1997; Sundaresan *et al.*, 1995). This strategy was employed to identify transposon-tagged genes that have gametophytic roles (Moore *et al.*, 1997; Page and Grossniklaus,

2002) and, in particular, to identify genes that are required for post-pollination pollen development in *Arabidopsis*. From a population of 3359 Ds transposon insertion lines, 20 independent lines showed stably reduced segregation ratios arising from reduced genetic gametophytic transmission. These included 10 "*ungud*" mutants, affecting both male and female gametogenesis and 9 "*seth*" mutants affecting pollen function during progamic development and one male-specific mutant termed *halfman* affecting microsporogenesis (Lalanne *et al.*, 2004).

1.2.1.2 Pollen morphological screens

Chemical or radiation mutagenesis offers many advantages for isolating a collection of mutants that are defective for a particular process of interest. Mutations can be introduced in *Arabidopsis* genome as single nucleotide changes using chemical mutagens, such as ethyl methanesulfonate (EMS), or as small deletions using physical mutagens such as X-rays or UV irradiation. EMS predominantly generates G/C to A/T point mutations which could lead to a total loss of gene function by creating a premature stop codon or alter functionally critical amino acids. Both physical (Chen and McCormick, 1996) and chemical mutagenesis screens (Johnson and McCormick, 2001; Lalanne and Twell, 2002; Park *et al.*, 1998) have been employed to identify lesions in genes involved in male gametophyte development.

Morphological screening of pollen from mutant lines mutagenized with fast neutrons and EMS have yielded a wide range of novel phenotypes affecting different stages of pollen development. A morphological screen based on mutagenesis of *Arabidopsis* No-0 seeds with fast neutrons identified *sidecar pollen (scp)* mutant that affects microspore division asymmetry and cell fate. Pollen from M1 plants was stained with DAPI and scored for aberrant pollen phenotype. Heterozygous *sidecar pollen (scp)* mutant plants were identified based on abnormal pollen morphology in approximately half of the pollen population (Chen and McCormick, 1996). Similarly, an EMS-based pollen morphological screen led to the isolation of pollen mutants in which pollen grains stained for callose before anther dehiscence. The male gametophytic mutant *raring-to-go* was identified as an unusual mutant in that some of the pollen in *raring-to-go (rtg)* plants prematurely hydrate, germinate, and form pollen tubes within the anther. Several other *rtg*-like mutants, as well as novel mutants were also isolated, including *gift-wrapped pollen (gwp)*, *polka dot pollen (pdp)*, and *emotionally fragile pollen (efp)* that

exhibited unexpected patterns of callose staining and precocious pollen germination (Johnson and McCormick, 2001).

In another EMS-derived mutant screen, pollen was screened for mutants with deviations from the wild type tricellular pollen morphology. Mature pollen from approximately 10,000 mutagenized M2 plants (Nossen (No-0) background) was stained with DAPI and analysed for aberrant pollen cell division phenotypes using fluorescence microscopy. The genetic screen yielded 15-20 independently induced mutants that affected the stereotypical pollen cell division and pollen intracellular architecture (Park *et al.*, 1998). Mutations identified from the screen could be grouped into three categories i.e. 1) mutants affecting microspore division symmetry and cytokinesis, 2) mutants affecting male germ unit organization and 3) mutants affecting germ cell division. The *Gemini pollen (gem)* mutant produced twin pollen, affecting division asymmetry at PMI. MOR1/GEM1 is a member of the MAP215 family of microtubule-associated proteins and is involved in microtubule assembly and is associated with interphase, spindle and phragmoplast microtubule arrays (Park *et al.*, 1998; Park and Twell, 2001; Twell *et al.*, 2002). The *two-in-one pollen (tio)* mutant, previously termed *solo pollen* mutant, failed to undergo normal cytokinesis at PMI. TIO is the plant homologue of the Ser/Thr protein kinase FUSED and localises to the midline of the phragmoplast where it has an essential role in cell plate expansion (Oh *et al.*, 2005).

The morphological screen also identified a distinct class of pollen mutants that showed defects in the integrity and/or the positioning of the male germ unit (MGU), termed as *germ unit malformed (gum)* and *male germ unit displaced (mud)*. In *gum* mutants, the vegetative nucleus is positioned adjacent to the pollen grain wall, separate from the two sperm cells, whereas in the *mud* mutants the intact MGU is displaced to the pollen grain wall. Genetic analysis revealed that both mutations show reduced pollen transmission and thus act in a gametophytic manner. Further cytological analysis revealed that correct MGU assembly is required for efficient transmission of the male gametes through the pollen (Lalanne and Twell, 2002).

The most remarkable class of mutants identified in the EMS mutagenesis screen produced bicellular pollen at anthesis and hence termed *duo pollen (duo)*. The *duo pollen (duo)* mutant class consists of six individual mutants termed *duo1, duo2, duo3, duo4, duo5* and *duo6* arising in different M_1 parental groups (Durbarry and Twell

Unpublished). Analysis of DAPI-stained pollen using epifluorescence microscopy showed that *duo* mutants shed bicellular pollen grains, containing a vegetative nucleus and an undivided germ cell. The *duo* mutants identified in the screen were isolated as heterozygous mutants and were mapped to different chromosomal locations. These mutants displayed very similar but distinct aberrant germ cell phenotypes and hence were classified into two main groups based on the shape of the undivided germ cell nucleus, after staining with DAPI that specifically stains the nuclear DNA. The first group comprised of *duo1, duo2* and *duo3* that borne round germ nuclei at anthesis. The second class included *duo4, duo5* and *duo6*, whereby mature pollen produce frequently elongated germ nuclei. Asymmetric microspore division is completed in these mutants; however, the resulting germ cell fails to enter or complete division at pollen mitosis II (Durbarry *et al.,* 2005; Durbarry and Twell Unpublished). Heterozygous *duo1* and *duo2* mutants produce approximately 50% bicellular pollen containing a single germ cell showing complete penetrance of the mutations. Phenotypic analysis suggest that *duo2* mutant germ cells enter mitosis but arrest at prometaphase, whereas, mutant germ cells in *duo1* complete S-phase but fail to enter mitosis (Durbarry *et al.*, 2005). This thesis describes phenotypic and genetic analysis of *duo5* mutant pollen as well mapping strategies to identify the position of the *duo5* locus, mapping progress and limitations.

1.2.2 Male gametophyte gene expression studies and transcriptomics

Completion of the Arabidopsis genome sequence (*Arabidopsis* Genome Initiative 2000) and associated public databases i.e. A*rabidopsis* Information Resource (TAIR) and the TIGR *Arabidopsis thaliana* database, availability of various transcriptomic datasets for pollen transcriptome (Honys and Twell, 2004; Pina *et al.*, 2005), recently available data for sperm cell transcriptome (Borges *et al.*, 2008), and availability of pollen specific research tools and protocols (Johnson-Brousseau and McCormick, 2004) are important landmarks that will help in deciphering the role of various important genes involved in pollen development.

1.2.2.1 Pollen transcriptomic studies

The first conclusive evidence of gene expression during pollen development was based on isozyme (Pedersen *et al.*, 1987) and RNA hybridization studies (Mascarenhas, 1990), that suggested an extensive pollen gene expression programme. New high-throughput

technologies such as microarrays (Hennig *et al.*, 2003; Honys and Twell, 2003), serial analysis of gene expression (SAGE) technology (Lee and Lee, 2003) and expressed sequence tags (EST) (Engel *et al.*, 2003), have facilitated the comprehensive analysis of male gametophyte gene expression on a global scale. Amongst these techniques, microarray is one of the most effective and commonly used methods to identify a range of transcripts in the target tissue. In the pioneering studies, two different platforms were used to investigate mature pollen transcriptome, including serial analysis of gene expression (SAGE) technology (Lee and Lee, 2003) and GeneChip microarray (Becker *et al.*, 2003; Honys and Twell, 2003). The GeneChip approach, exploiting 8K Affymetrix AG microarrays, provided analysis for mature pollen from *Arabidopsis* ecotype Landsberg *erecta* (L*er*), based on approximately one-third of the *Arabidopsis* genome (Honys and Twell, 2003). Expression data obtained from the 8K GeneChip array suggested significant 61% overlap of the pollen transcriptome with that of sporophyte. Moreover, with further improvement in gene chip technologies, an improved Affymetrix 23K *Arabidopsis* ATH1 array, harbouring 22,591 genes, allowed the analysis of more than 80% of the *Arabidopsis* genome (Redman *et al.*, 2004). In one of the studies, the new ATH1 array was used to generate transcriptomic data covering four stages of male gametophyte development (uninucleate microspore, bicellular pollen, tricellular pollen and mature pollen) for ecotype Landsberg *erecta* (L*er*) (Honys and Twell, 2004). In two additional studies, (Pina *et al.*, 2005; Zimmermann *et al.*, 2004) ATH1 data sets for mature pollen from ecotype Columbia was reported. The combined analysis of these datasets and the final normalised data identified 5000 to 7000 genes expressed in the mature male gametophyte. Extending the analysis to four pollen developmental stages, the total number of genes expressed during pollen development and function was estimated to be over 14,000. Surprisingly, only 5% represented genes showed strictly pollen-specific expression pattern (Borg *et al.*, 2009; Honys and Twell, 2004) Another key finding was the gradual decrease in the number of expressed genes from early (nearly 12000 active genes in microspore and bicellular pollen) to late phase (just over 7000 genes expressed in tricellular pollen and mature pollen). The genes expressed at the late phase of pollen development are mostly involved in cell wall metabolism, cytoskeleton and cell signalling, highlighting functional specialization of pollen in preparation for maturation and rapid pollen tube growth (Borg *et al.*, 2009; Honys and Twell, 2004).

In another landmark experiment, microarray datasets were generated from isolated sperm cells. Pollen from *Arabidopsi*s ecotype Columbia (Col-0), expressing eGFP marker driven by a germline specific *GEX2* promoter, was mechanically disrupted and subjected to fluorescence-activated cell sorting (FACS). Pollen grains were disrupted in order to free sperm cells and then purify GFP-marked sperm cells based on their GFP signal, size and presence of DNA. Microarray data sets were also generated for seedlings and pollen as a repeat analysis. A total of 5,829 (27% of the total 22,392 genes on the ATH1 array) genes transcripts were detected specifically in sperm cells compared to 33% and 64% genes in pollen and seedlings respectively. The vast majority of the genes (3,813) expressed in the sperms cells were also detected in pollen vegetative cell (Borges *et al.*, 2008).

Transcriptomic datasets are also available for progamic phases of pollen development, encompassing post-pollination events. The genome-wide expression profiling of pollen tubes grown *in vitro* identified a set of genes that are expressed in the pollen tube but not in pollen (Wang *et al.*, 2008). Whereas, expression profiles of *in vitro* and semi *in vivo* grown pollen tubes, growing through the pistil, exhibit more diverse gene expression profile compared with pollen tubes grown *in vitro* (Qin *et al.*, 2009).

Moreover, male gametophyte-specific genes are often characterised by very high expression levels, highlighting their importance in the specialized gametophytic programmes. The availability of transcriptomic datasets has made it possible to carefully select reverse genetics targets based on co-expression and overcome the genetic redundancy encountered in genetic screens (Honys *et al.*, 2006; Honys and Twell, 2004).

1.2.2.2 Gene expression studies in the male germline of flowering plants

Pioneering studies of gene expression in the male germline have been mainly focused on species with larger and more accessible germline, including male germline of tobacco, maize, lily and *Plumbago* (Russell, 1991; Tanaka, 1988; Uchiumi *et al.*, 2006; Zhang *et al.*, 1998). The availability of comparatively larger germline cells in both bicellular and tricellular model plant species tobacco, lily, maize, and *Plumbago* have permitted the development of techniques for isolation and purification of male germline. To isolate the male germline cells, pollen grains or *in vitro* grown pollen tubes are first

subjected to mechanical or enzymatic disruption, followed by separation of germline cells from the vegetative cell debris by density gradient centrifugation (Tanaka, 1988; Xu *et al.*, 2002), micromanipulation (Chen *et al.*, 2006; Zhang *et al.*, 1998) or fluorescence-activated cell sorting (FACS) (Engel *et al.*, 2003). Moreover, cDNA libraries and EST (expressed sequence tag) sequencing projects, derived from purified germline cells, provided first insight in to the unique male germline transcriptome. Comparative analysis of the male germline transcriptome datasets generated from tobacco, maize, lily and *Plumbago* indicated overlap of germline expressed genes in these taxa and expression of similar classes of genes in their germline. Further investigation targeted at male germline transcript identity, led to the identification of germline-specific transcripts which include *Lily Generative Cell1 (LGC1)* (Xu *et al.*, 1999b), *gcH2A* and *gcH3* encoding histone isoforms (Xu *et al.*, 1999a), a polyubiquitin gene *LG52* (Singh *et al.*, 2002) and Generative Cell Specific1 (GCS1) from lily germ cells (Mori *et al.*, 2006). Several male germline specific genes homologous to those expressed in the germline of other species have been characterised in *Arabidopsis*. A homologue of the lily gene *GCS1* (*HAP2*), and three genes homologous to maize sperm cell expressed genes (*GEX1*, *GEX2*, and *GEX3*), are examples of genes identified in *Arabidopsis*. *GCS1/HAP2* that encodes a gamete surface protein required for pollen tube guidance and gamete fusion represents a conserved male germline transcriptional signature in flowering plants (Alandete-Saez *et al.*, 2008; Engel *et al.*, 2005; Mori *et al.*, 2006; Von Besser *et al.*, 2006).

1.2.3 Expression of transcription factor families during pollen development

Generally, the abundance and variability of transcription factors is higher in plants than in the other kingdoms. Approximately 5% of *Arabidopsis* genome code for at least 1533 genes encoding putative transcription factors (Riechmann *et al.*, 2000). In *Arabidopsis* germline, the early and late gene expression programmes require coordinated regulation at transcriptional level. Out of 1350 predicted transcription factors in the *Arabidopsis* genome, anchored on the Affymetrix ATH1 Genome Array, 612 gave reliable expression signal in the developing male gametophyte (542 early, 405 late) (Twell *et al.*, 2006). According to Honys and Twell (2004) the most overexpressed transcription factor families in the male gametophyte with more than 25 members include CCAAT

family, C2H2 zinc finger, WRKY, bZIP, TCP and GRAS gene families. On the contrary, AUX/IAA, HSF, bHLH, NAC, AP2-EREBP, HB, R2R3-MYB, MADS and C2C2 zinc finger gene families were all under-represented. During early (microspore and bicellular) and late phase (tricellular and mature pollen) of pollen development, two major transcription factor gene sets could be distinguished. One major group of predominantly early expressed genes belonged to NAC, WRKY, TCP, ARF, Aux/IAA, HMG-box and Alfin-like transcription factors families. While the second smaller group, comprised of C2H2 or TUBBY transcriptional families, showed predominately late expression profiles (Honys and Twell, 2004). According to Borges *et al.,* (2008), members of MYB-type transcription factors family showed higher expression in the sperm cells. Another sperm cell-specific transcription factor (At4g35700) identified only in the sperm cell transcriptome belonged to C2H2 zinc finger family and showed the highest expression of all the transcription factors. This thesis mainly focuses on the characterization and expression analysis of the sperm cell-specific zinc finger proteins At4g35700 called DAZ3 and its homologue at4g35610 called DAZ3L.

1.2.3.1 The role of MYB Transcription Family in plants

MYB proteins are a large superfamily of transcription factors. The v-MYB gene of avian myeloblast virus was the first MYB gene identified (Klempnauer *et al.*, 1982). Analysis of the complete *Arabidopsis* genome sequence has resulted in identification of about 198 genes in the MYB superfamily, most of them encoding proteins with only two tryptophan-rich repeats. Such plant MYB proteins are called R2R3-MYB proteins. Plant MYB genes encode proteins with DNA-binding domains called MYB domains. These domains are composed of one, two or three conserved motifs of approximately 52 amino acid residues. These repeated motifs or MYB domains bind to major groove of target DNA by its helix-turn-helix structure, interacting with bases and phosphates. There are regularly spaced tryptophan residues, which form a tryptophan cluster in the helix-turn-helix structure, a characteristic of a MYB repeat (Saikumar *et al.*, 1990). According to the number of the MYB repeats, MYB transcription factors can be divided into four subfamilies, namely 1R, 2R (R2R3), 3R (R1R2R3) and 4R (R1R2R3R4) MYBs which contain one, two, three or four MYB repeats, respectively, with R2R3 MYBs being the largest subfamily (Dubos *et al.*, 2010; Stracke *et al.*, 2001). A phylogenetic comparison of members of rice and *Arabidopsis* MYB family suggest a

rapid expansion in *Arabidopsis* MYB superfamily after it diverged from monocots. The *Arabidopsis* genome contains a total of 198 MYB genes, out of which 126 are R2R3-type, 5 are MYB3R, 64 are MYB-related and 3 are atypical MYB genes (Yanhui *et al.*, 2006). The first plant MYB gene was identified from *Zea mays* and was called *ZmMYBC1* (*C1*), which is required for anthocyanin synthesis in the aleurone of maize kernels (Paz-Ares *et al.*, 1987). Members of MYB family are involved in a variety of biological functions including phenylpropanoid metabolism (Grotewold *et al.*, 1994), biotic and abiotic stress (Segarra *et al.*, 2009), cell shape such as AM MIXTA (Noda *et al.*, 1994), cellular differentiation (Kang *et al.*, 2009; Oppenheimer *et al.*, 1991), hormone responses i.e. AtMYB2 (Urao *et al.*, 1993), GAMYB and CpMYB (Gubler *et al.*, 1995), formation of B-type cyclin (Ito *et al.*, 2001) or during plant defence reactions i.e. NtMYB1 (Liu *et al.*, 2008b; Yang and Klessig, 1996). Several R2R3-MYB proteins have been implicated with roles in plant development. AtMYB33 and AtMYB65 appear to act redundantly to facilitate both anther and pollen development (Millar and Gubler, 2005). Recent studies have shown that the MYB genes are post-transcriptionally regulated by microRNAs; for instance, AtMYB33, AtMYB35, AtMYB65 and AtMYB101 genes involved in anther or pollen development are targeted by miR159 family, thus restricting their expression solely to the developing anthers (Allen *et al.*, 2007). Gibberellins (GAs) also play important roles in anther development. A MYB transcription factor termed as GAMYB is involved in GA-regulated gene expression in anthers (Aya *et al.*, 2009; Kaneko *et al.*, 2004; Tsuji *et al.*, 2006). One of the mutants, *gamyb-4* shows abnormal enlarged tapetum and could not undergo normal meiosis and is involved in early anther development in rice (Liu *et al.*, 2010). Similarly, important plant hormone, jasmonic acid and its chemical derivatives (collectively known as jasmonates) are key regulators of stamen development and pollen maturation. Three MYB transcription factors MYB108, MYB21 and MYB24 are involved in jasmonate response in stamens. Analysis of plants with insertions in these genes show reduced male fertility associated with delayed anther dehiscence, reduced pollen viability, and decreased fecundity (Mandaokar and Browse, 2009; Mandaokar *et al.*, 2006). Moreover, MYB proteins are also involved in female fertility. AtMYB98 controls the differentiation of the synergid cells during female gametophyte development and mutant *myb98* synergid cells have defects in filiform apparatus and pollen tube guidance (Punwani *et al.*, 2008). Among male gametophytic mutations in male germline,

AtMYB125/DUO1 represents the first germline specific R2R3 MYB transcription and is shown to be a key regulator of germ cell division and differentiation (Brownfield *et al.*, 2009a; Durbarry *et al.*, 2005; Rotman *et al.*, 2005).

1.2.3.2 The role of C2H2 Zinc Finger Transcription Family in plants

The C2H2 zinc finger transcription family consisting of 176 members forms one of the largest transcription families in *Arabidopsis*. According to *in silico* analysis 0.7% of all genes in *Arabidopsis* encode C2H2-type zinc finger proteins (Englbrecht *et al.*, 2004). These proteins are involved in wide range of functions and can bind to DNA, RNA and proteins. All the C2H2 zinc finger proteins contain a DNA binding motif of 30 amino acids including two conserved cysteins and two histidines tetrahedrally bound to one zinc ion to form a compact finger structure containing β-hairpin and an α-helix. Structural studies of crystalline zinc finger DNA complexes have revealed that the α-helix makes contact with the major groove of DNA (Choo and Klug, 1997). The first zinc finger protein in plants, ZPT2-1 was reported in *Petunia*, and was characterized as DNA binding protein involved in anthocyanin production in petals (Takatsuji *et al.*, 1992). Later studies led to the identification of other zinc finger proteins that are active during flower development. One such example is SUPERMAN (SUP), which maintains the boundary between third and fourth whorls of flower (Sakai *et al.*, 1995). Similarly SUP-like protein i.e. RABBIT EARS (RBE) was identified and shown to play role in petal development and maintaining boundaries of homeotic gene expression between whorls (Krizek *et al.*, 2006). Some zinc finger proteins have been identified that act redundantly e.g. NUB acts redundantly with JAG to promote the growth of the pollen-bearing microsporangia of the anthers and the carpel walls of the gynaecium (Dinneny *et al.*, 2006).

The numbers of zinc finger domains vary in different zinc finger proteins. The C2H2 zinc finger proteins in plants can be distinguished from other eukaryotes in two structural features. First, in multiple fingered plant C2H2-type proteins, the zinc finger domains are separated by long spacers that vary in length and sequence from protein to protein, whilst in animals and yeast, zinc finger domains are clustered and separated by a short spacer of six to eight amino acids (Klug and Schwabe, 1995; Sakamoto *et al.*, 2004). Second, most of the C2H2 plant zinc finger proteins have an invariant DNA-binding, QALGGH motif in the zinc protein helices, while animals and yeast lack this

motif (Takatsuji, 1999). Further *in vitro* analysis of these motifs have revealed that each amino acid of this conserved sequence is essential for DNA-binding activity of C2H2-type zinc finger proteins (Kubo *et al.*, 1998). Thus, the substitution of the second G (Glycine) residue of the SUPERMAN protein to D (Aspartic Acid) resulted in loss of function of SUPERMAN (Sakai *et al.*, 1995). Moreover, most members of this group share putative nuclear localisation sequences as well as repression domains. The repression activity is acquired via their ethylene-responsive element-binding factor (ERF)-associated amphiphilic repression (EAR) domain (Englbrecht *et al.*, 2004). According to recent analysis of EAR containing transcription factors, C2H2 family is the largest family of repression motif containing proteins. The EAR motif sites are mainly located in the C- terminal region but are also located in the N-terminal and middle region of protein sequence (Kagale *et al.*, 2010). In a study, Hiratsu *et al.,* (2002) demonstrated that SUPERMAN is an active repressor and its repression activity via a single EAR motif in the carboxy-terminal region is essential for normal flower development. Similarly, another protein called KNUCKLES, which contains a single zinc finger and an EAR repression motif, encodes SUP-like protein and has been suggested to function as a transcriptional repressor of cellular proliferation (Payne *et al.*, 2004). In plants it has been shown that zinc finger proteins are involved in diverse activities i.e. regulating floral and vegetative organ formation, gametogenesis in anthers and stress responses (Takatsuji, 1999).

1.3 Plant cell cycle regulation

In eukaryotes, a number of cellular processes such as cell division, cell growth and differentiation are regulated by activities of the cell cycle. Single eukaryotic cell divides into two cells by going through a well regulated mitotic cell cycle. It is a unidirectional succession of events divided into four sequentially ordered phases, termed as G1 (Gap1), S (Synthesis phase), G2 (Gap2) and M (Mitotic phase). Synthesis and Mitotic phases are the two major active phases of the cell cycle and are separated by gap phases. During the S phase the cell's genome is duplicated via DNA replication, followed by mechanical redistribution of the duplicated chromosomes into daughter cells during M phase, followed by cell division (cytokinesis). The M-phase represents the only microscopically visible stage and consists of four consecutive phases, pro-, meta-, ana- and telophases preceding the cytokinesis, whereas the rest of the cell cycle is referred to

as interphase. Progression through the cell cycle is regulated at two major checkpoints, the G1/S transition and the G2/M transition. These checkpoints ensure chromosome integrity and the completion of each stage of the cell cycle before the initiation of the following stage. Abnormal progression of S-phase results in cell cycle arrest at G1/S checkpoint whereas irregularity in mitotic progression causes induction of M-phase checkpoint (Cools and De Veylder, 2009). In plants, the mechanical structures allowing separation of the chromosomes during mitosis start with the reorganization of the cytoskeleton early in G2 phase. The first mitotic event comprises of prophase where the chromatin condensation begins, accompanied by the breakdown of the nuclear envelope and appearance of spindle microtubules radiating from poles. At metaphase, chromosomes align at the metaphase plate attached to kinetochore microtubules. In the following anaphase, extension of spindle microtubules and depolymerisation of kinetochore microtubules result in the separation of sister chromatids and their subsequent movements towards the opposite pole. The separated nuclei decondense in telophases and are further surrounded by a newly formed nuclear envelope. The karyokinesis is followed by the division of the cytoplasm which marks the end of mitosis. The plane of the newly forming cell wall is in plants is defined by the preprophase band visible in early prophase. The interphase arrays of cortical microtubules that are transversely arranged with respect to the main axis of growth rearrange into a narrow cortical ring of the preprophase band. The band is specific to plants and marks the future division plane. The band dissociates as the mitotic spindle is built, which segregates the chromosomes during anaphase. The microtubules then rearrange again to form the phragmoplast which initiates the synthesis of the new cell wall between two newly formed daughter cells (Kost *et al.*, 1999). In certain specialized cell types such as trichomes and cells within leguminous nodules, cells undergo endoreduplication, a process characterised by repeated cycle of DNA replication (Foucher and Kondorosi, 2000; Joubès and Chevalier, 2000).

1.3.1 Overview of plant cell cycle machinery

In higher plants, activity of many regulatory proteins including CDKs (cyclin-dependent kinases), cyclins, CAKs (CDK-activating kinases), CKI (CDK inhibitors) such as KRPs (Kip-Related Proteins), the retinoblastoma protein (RBR), E2F/DP transcription factors, APC/C (Anaphase Promoting Complex/Cyclosome), WEE kinases, etc. control the

progression through cell cycle phases (Stals and Inze, 2001).

The central regulators of the cell cycle progression belong to a specific class of highly conserved serine-threonine protein kinases, termed as cyclin-dependent kinases (CDKs) due to their activation by association with regulatory subunits, cyclins. Plant CDKs carries a highly conserved heptapeptide motif consisting of proline, serine, threonine, alanine, isoleucine, arginine and glutamic acid (PSTAIRE). The canonical sequence PSTAIRE resides within the cyclin binding domain of the CDK protein. Plant CDKs can be classified into 7 different groups, from A to G, based on the characteristic amino acid cyclin binding motif. CDKA carries the PSTAIRE hallmark; CDKB is characterized by PPT(A/T)LRE and CDKD by N(I/F)TALRE, indicating two subgroups within these CDK types; CDKC shows a PITAIRE motif; CDKE a SPTAIRE and the last motif known is PLTSLRE found in CDKG (Mironov *et al.*, 1999; Vandepoele *et al.*, 2002). Only two CDKs i.e. CDKA and CDKB have been shown to directly regulate cell cycle progression (Menges *et al.*, 2005; Vandepoele *et al.*, 2002). Among the CDKs, plants possess only one gene that encodes A-type CDK and therefore, is the only plant CDK active at G1/S phase. B-type CDKs are are unique to plants and their activity is linked with the G2/M transition phase (Dewitte and Murray, 2003; Joubès *et al.*, 2000). Furthermore, CDKD and plant specific CDKF function as CDK-activating kinases, while, CDKC and CDKE are presumed to regulate transcription, as deduced from the function of their mammalian homologs (Umeda *et al.*, 2005). All eukaryotic CDKs contain a catalytic cleft, with ATP- and substrate-binding sites placed between the N-terminal and C-terminal lobes. However, access to these binding sites remains restricted by a loop of the CDK known as T-loop. A CDK-activating kinase (CAK) carries out the phosphorylation of a conserved threonine 160 residue within the T-loop. This positive phosphorylation brings about conformational change, exposing the active binding sites for cyclin binding (Dewitte and Murray, 2003; Joubès *et al.*, 2000; Vandepoele *et al.*, 2002). CDK activities are negatively regulated via inhibitory phosphorylation of amino-terminal residues around threonine-14 and tyrosine-15, carried out by a tyrosine protein kinase also known as WEE1, thereby inhibiting ATP fixation and substrate binding of CDK. In order to activate the CDK-CYC complex the phosphogroups at position 14 and 15 have to be removed by the CDC25 phosphatase. The activity of WEE1 is high during S and G2 phases when it is able to inhibit CDK function, whereas during G2/M transition WEE1 is phosphorylated by major M phase

kinase known as Polo-like kinase 1 (PLK1), which triggers its proteasomal degradation allowing mitotic entry (Watanabe *et al.*, 2004). WEE1 is the only protein kinase to be a putative negative regulator of A- and B-type CDKs. (Sorrell *et al.*, 2002; Sun *et al.*, 1999). Further mechanisms of modulating CDK activity exist through the actions of two classes of CDK inhibitors or CKIs i.e. Kip-Related Proteins (KRPs) and SIAMESE (SIM)/SISMESE-RELATED (SMR) proteins. KRPs share a 31 amino acid residue with a member of the mammalian Kip/Cip family of CDK inhibitors, hence termed as Kip-Related Proteins (Komaki and Sugimoto, 2012; Van Leene *et al.*, 2010). The *Arabidopsis* genome encodes seven KRPs, KRP1–KRP7, and at least 13 SIM/SMRs (Churchman *et al.*, 2006; De Veylder *et al.*, 2001; Lui *et al.*, 2000; Torres Acosta *et al.*, 2011). KRPs are small proteins with a C-terminal domain (CTD) that is required for CDK- or cyclin-binding and their inhibitory function (De Clercq and Inzé, 2006; De Veylder *et al.*, 2001). Previous studies have revealed that all KRPs can interact with D-type cyclins i.e. CYCD1;1, CYCD2;1, and CYCD3;1 (Wang *et al.*, 1997; Zhou *et al.*, 2003). Recent proteomic analyses in *Arabidopsis* have validated these studies, and uncovered that all seven KRPs co-purify solely with CYCDs and CDKA, strongly suggesting that KRPs inhibit the activity of the CYCD–CDKA complex (Van Leene *et al.*, 2011). Moreover, analysis of double and multiple mutants from five single Arabidopsis KRP T-DNA mutants (KRPs1, 2, 5, 6, 7), revealed that KRPs function redundantly in a dosage dependent manner (Cheng *et al.*, 2013). A second class of CDK inhibitors, consisting of SIM/SMR proteins was first identified in *Arabidopsis* and show localised sequence similarity to KRPs within the C-terminal cyclin binding domain. These proteins are only found in plants, including rice, maize, tomato, and poplar. The founding member, SIM is required to repress the mitotic cell cycle in endoreduplicating trichomes by direct binding with CYCD-CDKA complex (Churchman *et al.*, 2006). Another member of the SIM/SMR family, called LOSS OF GIANT CELLS FROM ORGANS (LGO) or SMR1 promotes endoreduplication in the sepal epidermal cells. The loss of function mutant *smr1/lgo* causes additional cell divisions instead of endoreduplication, whereas, overexpression of SMR1/LGO produces additional giant cells (Roeder *et al.*, 2010).

The activation of CDKs requires binding to another group of regulatory proteins known as cyclins. The name cyclins (CYCs) stems from the transient and cyclical appearance of these proteins during the cell cycle (Evans *et al.*, 1983). In plants five different types

of cyclins exist (A, B, C, D, H types) based on sequence organization. Approximately 50 genes in *Arabidopsis* code for cyclin-related proteins out of which 32 cyclins have putative roles in cell cycle regulation consisting of 10 A-type, 11 B-type, 10 D-type, and 1 H-type cyclins (Menges *et al.*, 2005). Generally, A-type cyclins control S to M phase transition and are destroyed around G2/M transition. B-type cyclins are involved in G to M transition and M phase progression and are destroyed as cells enter anaphase (Inze and De Veylder, 2006). D-type cyclins control progression through G1 and into S phase, in response to external signals for example phytohormones and nutrient availability. However, the expression of CYCD genes is not specific to the G1/S phase, and some are expressed at the G2/M phase (Menges *et al.*, 2005). In Arabidopsis, A type cyclins are divided into 3 subfamilies i.e. the CYCA1, CYCA2, and CYCA3 subfamilies, which include two, four, and four genes, respectively (Wang *et al.*, 2004). CYCBs also comprise of three subfamilies CYCB1, CYCB2 and CYCB3. Both CYCB1 and CYCB2 subfamilies contain five members while CYCB3 subfamily is represented by single member. The G1 cyclins, CYCDs consist of seven subfamilies, CYCD1 toCYCD7. The CYCD3 subfamily has three members, the CYCD4 subfamily has two and all the other groups have a single member. The *Arabidopsis* CYCA1 and CYCA2 show a peak of expression at the G2/M phase, whereas CYCA3 is expressed during the G1/S transition phase and S phase in synchronized *A. thaliana* suspension cells. A number of CYCA proteins can bind to CDKA and CDKB proteins. CYCA2;3 was shown to form a complex with CDKB1;1 and promote the mitotic cell cycle (Boudolf *et al.*, 2009). In another study it was revealed that revealed that the CYCA3;1–CDKA;1 complex phosphorylates histone H1 and retinoblastoma related (RBR) protein *in vitro* (Takahashi *et al.*, 2010). Mutation of CYCA2;3 result in increased ploidy levels in *Arabidopsis* (Imai *et al.*, 2006). On the contrary, overexpression of CYCA result in ectopic cell division, delayed differentiation and increase expression of S phase specific genes (Takahashi *et al.*, 2010). All members of CYCB family peaks at G2/M transition phase and have the ability to interact with CDKA, CDKB1, and CDKB2 (Boruc *et al.*, 2010; Menges *et al.*, 2005; Van Leene *et al.*, 2010). Previous studies have demonstrated their role in positive regulation of cell division by ectopically expressing CYCB1;1 under the control of the CDKA;1 promoter. The increased expression of CYCB1;1 promote root growth without altering organ morphology (Doerner *et al.,* 1996). Furthermore, overexpression of CYCB2;2 in rice enhances root growth by increasing cell number,

indicating that CYCB2;2 can stimulate cell division (Lee *et al.*, 2003). Promoter deletion analysis of CYCB1;1 from *Catharanthus* and *Nicotiana* has led to the identification of M-phase specific activator (MSA) elements. The promoters of genes expressed during G2 and M phase contain these elements and are recognized by three MYB repeat (MYB3R) transcription factors which were first identified in tobacco as NtMYBA1, NtMYBA2 and NtMYBB (Ito *et al.*, 2001). Of these, NtMYBA1 and NtMYBA2 function as transcriptional activator of G2–M-specific genes, including CYCAs and CYCBs, while NtMYBB acts as their transcriptional repressor. In *Arabidopsis,* out of five MYB3R genes, two members MYB3R1 and MYB3R4 are the closest homologs of NtMYBA1 and NtMYBA2. In the *myb3r1 myb3r4* double mutants expression of many G2 to M-specific genes carrying the MSA elements is dramatically down-regulated. This suggests the existence of an alternative mechanism, potentially mediated by other MYB proteins, controlling the transcription of G2–M phase genes (Haga *et al.*, 2011). Most of the CYCD genes are expressed during G1 and S phase, but some, such as CYCD3;1, are transcribed during the G2 and M phase. The majority of the CYCD proteins can interact with CDKA;1. The overexpression of some CYCD genes accelerates the entry of the cell into the S phase suggesting that CDKA–CYCD complexes regulate the G1/S transition (Dewitte *et al.*, 2003).

Cyclin proteins have a sequence of 100 amino acids known as the cyclin box which is required for CDK binding and activation (De Veylder *et al.*, 1997). Plant A and B type cyclins contain a destruction box in the N terminal region, which is required for ubiquitin/26S proteasome-mediated degradation (Weingartner *et al.*, 2004). D-type cyclins expression is also regulated by proteolysis in response to nutrient conditions (Planchais *et al.*, 2004). Mitotic cyclins (CYCAs and CYCBs) degradation is mainly mediated by anaphase promoting complex/cyclosome (APC/C), which is mostly active from mid-M phase (anaphase) to the end of G1 phase during the cell cycle, whereas, G1 cyclins i.e. D type cyclins are usually marked for degradation by Skp-Cullin1-F-Box (SCF) complex during G1-S transition. Both APC/C and SCF are most important E3 ubiquitin ligase complexes involved in cell cycle regulation (Vodermaier, 2004). The activity of APC depends on the interaction of two APC activators: CELL DIVISION CYCLE 20 (CDC20) and CDC20 HOMOLOG 1 (CDH1), called FIZZY (FZY) and FIZZY-RELATED (FZR) in *Drosophila,* respectively. In plants, the CDH1 activators are known as the *CELL CYCLE SWITCH 52* (*CCS52*) genes (Cebolla *et al.*, 1999), and

are classified into A- and B-type subgroups, namely CCS52A and CCS52B. The deregulation of these proteins inhibits entry into mitosis and also induces endoreduplication (Tarayre *et al.*, 2004; Vinardell *et al.*, 2003). The *Arabidopsis* APC/C consists of at least 11 core subunits and among them its catalytic core proteins, APC2 and APC11, have structural similarities to the components of the SCF complex (Capron *et al.*, 2003; Van Leene *et al.*, 2010). In *Arabidopsis* genome, all 11 APC/C subunits except of *APC3* are encoded by single genes. Two isoforms exist for APC3, namely *APC3a/CDC27a* and *APC3b/HOBBIT* (*HBT*) (Capron *et al.*, 2003; Lima *et al.*, 2010). Analysis have shown that APC subunits mutants including *apc2, apc3b*, *apc6* and *apc8*, accumulate mitotic cyclins in the embryo sacs, suggesting mitotic CYCs are substrates of the plant APC/C (Capron *et al.*, 2003; Kwee and Sundaresan, 2003; Zheng *et al.*, 2011). Similarly, single mutants in *apc2* and *apc10* or *apc3a apc3b* double mutants display female gametophytic lethality whereas mutation in APC8 causes defects in male gametogenesis (Capron *et al.*, 2003; Eloy *et al.*, 2011). Also, mutation of either APC8 or APC13 results in decreased biogenesis of miR159, which targets a male germline specific regulator, DUO1, an important transcriptional activator of CYCB1;1. The loss of function mutations of *apc8* and *apc13* results in increased transcription of CYCB1;1, hence contributing to the male gametophytic defect (Brownfield *et al.*, 2009a; Palatnik *et al.*, 2007; Zheng *et al.*, 2011). The SCF complex is a major class of E3 ligases in plants and consists of four components: RING-finger protein Roc1/Rbx1/Hrt1, cullin1/Cdc53, and Skp 1(adaptor protein) and the F-box proteins. The F-box proteins share a 40 amino acid conserved domain, which is called F-Box at the N-terminus (Xu *et al.*, 2009). In the C terminal, the F-Box protein contains a protein domain that binds substrate/target proteins, in a phosphorylation dependent manner and represents a critical step in SCF dependent proteolysis. The SCF complex is considered to be active throughout the cell cycle but targeting only phosphorylated proteins (Bachmair *et al.*, 2001). In plants, the F box protein termed as FBL17, that is part of an E3 SCF-type ubiquitin ligase an E3 SCF-type ubiquitin ligase complex in pollen, is expressed during the male gametogenesis after first asymmetric division and targets the KRP6 and KRP7 thus enabling activation of CDKA/CYCD complex, allowing progression of the germ cells through S phase (Kim *et al.*, 2008).

Another key regulator of the cell cycle is the most highly conserved tumor suppressor Retinoblastoma protein (RB) which functions as a negative regulator of the G1/S

transition. RB protein interacts with E2F (adenovirus E2 promoter-binding factor (E2F) that forms a dimer with the Dimerization Protein DP to become functional) and CDK/CYC complexes. RETINOBLASTEMA-RELATED (RBR) is a plant homolog of the animal tumor suppressor Retinoblastoma protein (RB) and *Arabidopsis* genome encodes a single RBR protein (Vandepoele *et al.,* 2002). The non-phosphorylated RBR binds to the heterodimeric transcription factor E2F/DP and masks the transcriptional activation domain rendering it in active. During G1 phase, CDKA/CYCD complex phosphorylates RBR and thus release E2F/DP to allow transcription of their target genes promoting S phase entry (Attwooll *et al.*, 2004; Boniotti and Gutierrez, 2001). Abolishing activity of RBR gene causes excessive cell proliferation and defects in cell differentiation during megagametogenesis and in roots and shoots (Borghi *et al.,* 2010; Chen *et al.,* 2009; Ebel *et al.,* 2004). Moreover, inactivation of RBR protein activity produces hyperplasia in young leaves and increases ploidy in older leaves (Desvoyes *et al.,* 2006).Similarly loss of RBR affects the vegetative lineage and prevents arrest of cell division typical of vegetative cell fate during male gametophyte development (Chen *et al.,* 2009) (Figure 1.2).

1.3.2 Cell cycle progression and cytokinesis

The cell cycle is a series of events that result in cell division and proliferation. During division a cell progresses through four consecutive phases (G1, S, G2, M) consisting of two major transitions: G1 to S phase when cells get ready for DNA duplication and G2 to M phase when they divide in to two cells.

1.3.2.1 G1 to S phase transition

During G1 and S phase cells are committed to acquire all the machinery necessary to correctly replicate their genome. CDKA/CYCD complexes are the primary mediators of G1/S transition. Prior to entry into S phase, the inhibition of CDKA kinase activity by KRPs is removed via SCF mediated degradation of KRP proteins. Likewise, inhibitory phosphorylation of CDKA by WEE1 kinase is relaxed by the phosphatase activity of CDC25. In the beginning of G1, the levels of CYCD increase in cells in response to hormones and growth factors, and allow formation of CDKA/CYCD complex, which becomes active after phosphorylation by CDK-activating kinases. This active complex phosphorylates the RBR protein associated with E2F/DP heterodimeric complex,

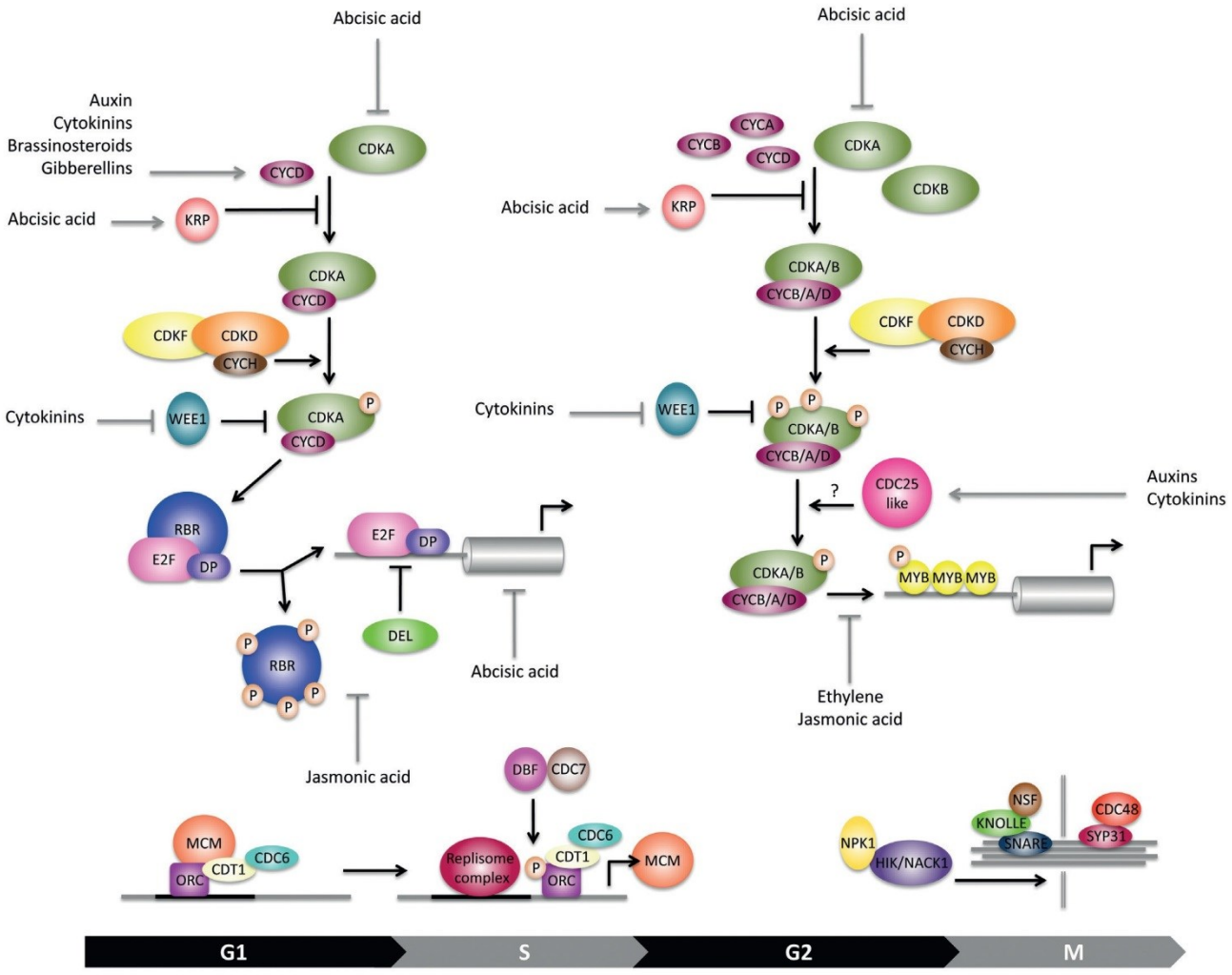

Figure 1.2: Plant cell cycle overview: Schematic representation of the cell cycle components and events that characterize G1/S-phase and G2/M-phase transitions. The stages of cell cycle are highlighted whereby cells in gap phase 1 (G1) undergo DNA replication (S), progress to gap phase 2 (G2) and then enter the mitotic phase (M) to complete the division cycle. CDK-cyclin complexes mainly regulate the progression of cell cycle to the S -and M- phases and represent the main component of the pathway. The activity of CDK is regulated by positive factors such as CDK activating kinases (CAK) as well as CDK inhibitors. The negative and positive phosphorylation by WEE1 and CDC25 respectively, also mediate the activity of CDK in the control of cell cycle progression. The hormonal control of the cell cycle is also pinpointed in this scheme. Adapted from (Pereira *et al.*, 2012).

allowing release of E2F/DP complex from inhibitory interaction with RBR. The released E2F/DP heterodimer binds to E2F-binding sites in target promoters. This triggers G1 to S phase transition by initiation of the transcription of genes involved in DNA replication, DNA repair and chromatin regulation (Takahashi *et al.*, 2008; Vandepoele *et al.*, 2005). The *Arabidopsis* genome contains three E2F proteins (E2Fa, E2Fb and E2Fc) and two DP proteins (DPa and DPb). E2Fa and E2Fb function as transcriptional activators whereas E2Fc plays largely a repressor role during cell proliferation (De Veylder *et al.*, 2007).

According to recent studies a new G1/S module has been proposed and comprise the transcriptional regulators E2F and RBR, the F-box protein FBL17, CDK inhibitors of the KRP class, and CDKA;1 (Zhao *et al.*, 2012). This module describes four steps of negative regulation mediating G1/S progression i.e. RBR repressing FBL17 (Zhao *et al.*, 2012), FBL17 mediating degradation of KRPs (Gusti *et al.*, 2009; Kim *et al.*, 2008; Zhao *et al.*, 2012), KRPs inhibiting CDKA;1 (Nakai *et al.*, 2006; Wang *et al.*, 2006), and inhibitory phosphorylation of RBR by CDKA;1. The negative feedback of RBR protein is brought about in four steps centred around FBL17 that mediates the degradation of CDK inhibitors but is itself directly repressed by RBR. The sequence of events proposed by Zhao *et al.* (2012) are as follows: RBR represses E2F that activates FBL17, which, in turn, releases the repression of CDKA;1 that can then phosphorylate RBR, presumably leading to its complete inactivation. Furthermore, the transition from G1 to S phase is dependent on the dosage sensitivity of CDKA;1 towards CDK inhibitors i.e. KRPs.

1.3.2.2 G2 to M phase transition

A cascade of events similar to G1/S transition occurs during the G2/M transition and mainly involves CDKA and CDKB associating with CYCA, CYCD and particularly CYCB to form CDK/CYC complexes. These complexes are negatively regulated either through specific bindings of KRP proteins to CDK and cyclins preventing their association to form complex or activity of the assembled CDK/CYC complex is inhibited by its direct phosphorylation through WEE1 in response to replication stress or DNA damage. The inactive CDK/CYC complex is then activated by the phosphatase activity of CDC25. In the beginning of the G2 phase, CYCB expression increases and therefore, active CDK/CYCB complexes are formed (Inze and De Veylder, 2006).

These complexes are able to phosphorylate a variety of G2 specific transcription factors such as CYCA, CYCB, CDC20, cytokinesis-specific syntaxin KNOLLE and kinesin-like protein NACK1. Mainly MYB transcription factors are involved in G2/M transition, which recognise the M-phase specific activator (MSA) elements in the promoters of the M phase specific genes. In tobacco, NtMYBA1 and NtMYBA2 bind to MSA elements in CYCB promoter and activate its expression. The factors initiating the transcription of NtMYBA genes are not known but it has already been demonstrated that activity of tobacco MYB transcription factors depend on phosphorylation by CDK/CYC complexes (Araki *et al.*, 2004; Ito *et al.*, 2001; Menges *et al.*, 2005).

At the completion of mitosis, cyclins are degraded through ubiquitination by APC (anaphase promoting complex) targeting them to the 26S proteasome. Cytokinesis in plants is initiated by microtubules assemblage to form phragmoplast at the centre of the cell division plane. A number of cytokinesis-specific genes are active at this stage e.g. a complex of proteins comprising SNARE (a complex of membrane anchoring proteins), SYP31 (a syntaxin) and CDC48 that interact with KNOLLE and regulate the process of vesicle fusion at the cell plate (Heese *et al.*, 2001).

1.3.3 Significance of male gametophyte cell cycle

Pollen represents a model system to explore cell cycle controls, differentiation as well as establishment and maintenance of cell fate. During pollen development two mitotic divisions represent key events required for the formation of functional sperm cells, essential for double fertilisation. The components of cell cycle machinery have been shown to actively participate in mediating mitotic divisions in the male germline. Identification of genes defective in cell cycle functions have proved useful in understanding the male gametophyte cell cycle control. A major cell cycle component, CDKA;1 has been shown to play critical role during germ cell division. The analysis of T-DNA mutant in CDKA;1 exhibit slow S phase and hence delayed germ cell entry in mitosis, The cdka;1 mutant pollen develops a vegetative cell similar to the wild type but only one germ cell (Aw *et al*., 2010). Similarly, disruption of F box Like 17 (FBL17), also show single germ cell phenotype as displayed by *cdka;1* (Gusti *et al.*, 2009; Kim *et al.*, 2008). Loss of RBR is gametophyte-lethal because mitotically derived cells from the megaspore fail to differentiate into a functional female gametophyte as well as in male

gametophyte results in vegetative cell proliferation (Borghi *et al.*, 2010; Chen *et al.*, 2009). Another important male gametophyte cell cycle regulator is a germ cell specific R2R3 MYB gene in *Arabidopsis* called DUO1 which controls male gamete formation in plants. According to Berger and Twell, (2011), cell cycle progression during pollen development can be elucidated based on the events of the two consecutive mitotic divisions. Following the microspore division, the CDK inhibitors KRP6 and KRP7 are present in both the vegetative cell and the germ cell. At this stage FBL17 is transiently expressed only in germ cells and therefore, result in degradation of KRP6 and KRP7, leading to removal of CDKA/CYCD inhibition (Kim *et al.*, 2008). Likewise, two RING-finger E3 ligases, RING-H2 group F1a (RHF1a) and RHF2a have been shown to be involved in KRP6 turnover during gametogenesis (Liu *et al.*, 2008a). The activated CDKA/CYCD further phosphorylates RBR which in turn relieves RBR mediated E2F/DP repression, allowing the progression of the germ cell through S phase. The vegetative cell exits cell cycle at G1 phase due to the absence of FBL17 and continued inhibition of CDKA by KRPs, as well as repression of S phase promoting E2F/DP complex via non-phosphorylated RBR (Chen *et al.*, 2009). At G2/M transition, DUO1 and DUO3 activate an overlapping set of G2/M regulators, including DUO1-dependent activation of CYCB1;1 that results in the progression into mitosis (Brownfield *et al.*, 2009a). DUO3 also a controls progression of the germ cell mitosis via CYCB1;1 independent pathway (Brownfield *et al.*, 2009b) (Figure 1.3).

In higher plants the successful fusion of male and female gametes occurs when both gametes have reached a synchronous cell cycle phase prior to fertilisation and during karyogamy. In *Arabidopsis*, the newly formed sperm cells within pollen grains in anthers, rapidly enter S phase of the cell cycle and at the time of pollination contain approximately 1.5C DNA. The synthesis phase continues in the pollen tube and the sperm nuclei attain DNA content of 1.75C by the time it has reached ovary. The sperm cells achieve DNA content of 2C whilst in the embryo sac just prior to double fertilisation (Friedman, 1999).

1.4 Genetic analysis of pollen development

The highly reduced male gametophyte has great significance as a subject of research

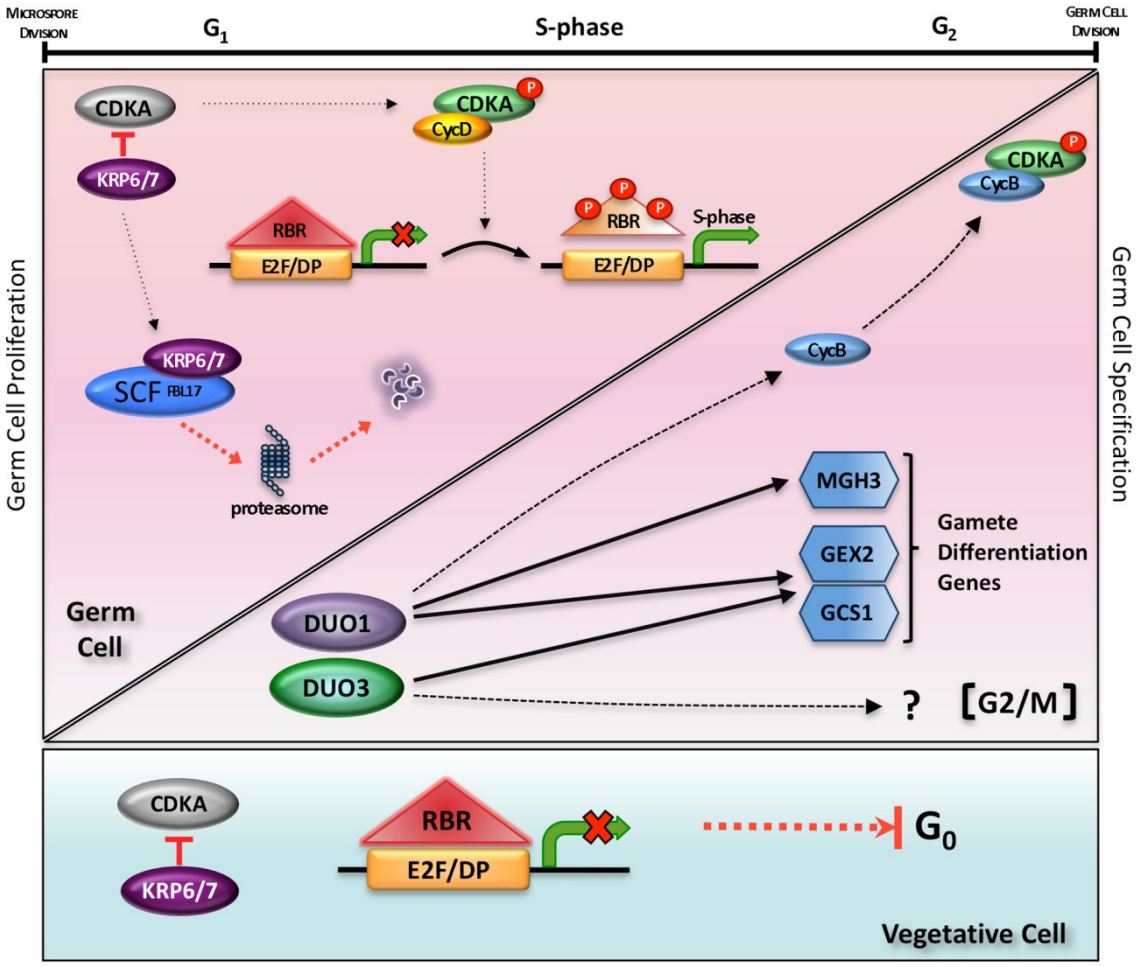

Figure 1.3: Schematic illustration of the events during germ cell proliferation and specification. Prior to entry into S phase, CDKA kinase activity is inhibited by KRPs present in both germ and vegetative cells. At this stage FBL17 is transiently expressed only in germ cells and therefore, results in degradation of KRP6 and KRP7, leading to the removal of CDKA/CYCD inhibition. The activated CDKA/CYCD further phosphorylates RBR, which in turn relieves RBR mediated E2F/DP repression, allowing the progression of the germ cell through S phase. Whilst the vegetative cell exits cell cycle at G1 due to absence of FBL17 and continued inhibition of CDKA by KRPs, as well as repression of S phase promoting E2F/DP complex via non-phosphorylated RBR. At G2/M transition, DUO1 and DUO3 activate an overlapping set of G2/M regulators, including DUO1-dependent activation of CYCB1;1 that results in progression into mitosis. The coordinated association of DUO1 and DUO3 is therefore essential for the production of fully differentiated sperm cells. Adapted from (Borg *et al.*, 2009).

because of its simple cell lineage and occurrence of highly coordinated developmental events. Mutation affecting male gametophyte can be easily scored in the segregating population of pollen grains and hence represent an ideal system to test genetic led hypothesises. Several genetic studies employing mutagenic screens and transcriptome analysis have provided substantial understanding of pollen gene functions at different stages of development (Figure 1.4). An overview of genes affecting male gametogenesis has been presented in this section.

1.4.1 Genes affecting microspore division

Asymmetric division of the haploid microspore is a prerequisite to set aside the germline and establish two dimorphic cells i.e. large vegetative cell and a smaller germ cell, with different cell fates (Eady *et al.*, 1995). The first genetic screens were developed exploiting chemical and physical mutagens (Chen and McCormick, 1996; Park *et al.*, 1998) to identify gametophytic genes that affect microspore division and cell fate.

The first male gametophytic mutant reported in *Arabidopsis* represents novel mutant named *sidecar pollen* (*scp*) that affects the microspore division symmetry. In *sidecar pollen,* microspores undergo symmetrical division followed by asymmetric division of one daughter cell to produce second vegetative cell and two sperm cells, thus producing a striking four celled pollen grain. Pollen harbouring *scp* mutation delay the timing of mitosis and alter the orientation of mitotic segregation. Positional cloning of the mutation has revealed that the gene responsible for the *scp* phenotype encode a plant specific *LATERAL ORGAN BOUNDRIES DOMAIN/ASYMMETRIC LEAVES2-like* (*LBD27/ASL29*) protein that belongs to the LBD/ASL protein family. *SCP* represents currently the only putative transcription factor that is essential for expression of genes with functions in microspore division (Oh *et al.*, 2010c).

Another microspore division mutant, *gemini pollen1 (gem1)* affects the nuclear migration and microspore division asymmetry resulting in equal, unequal, and partial microspore division phenotypes. *GEM1,* also known as *MOR1* (Whittington *et al.*, 2001) is homologous to conserved MAP215 family of microtubule-associated proteins that stimulate growth of interphase spindle and phragmoplast microtubule arrays.

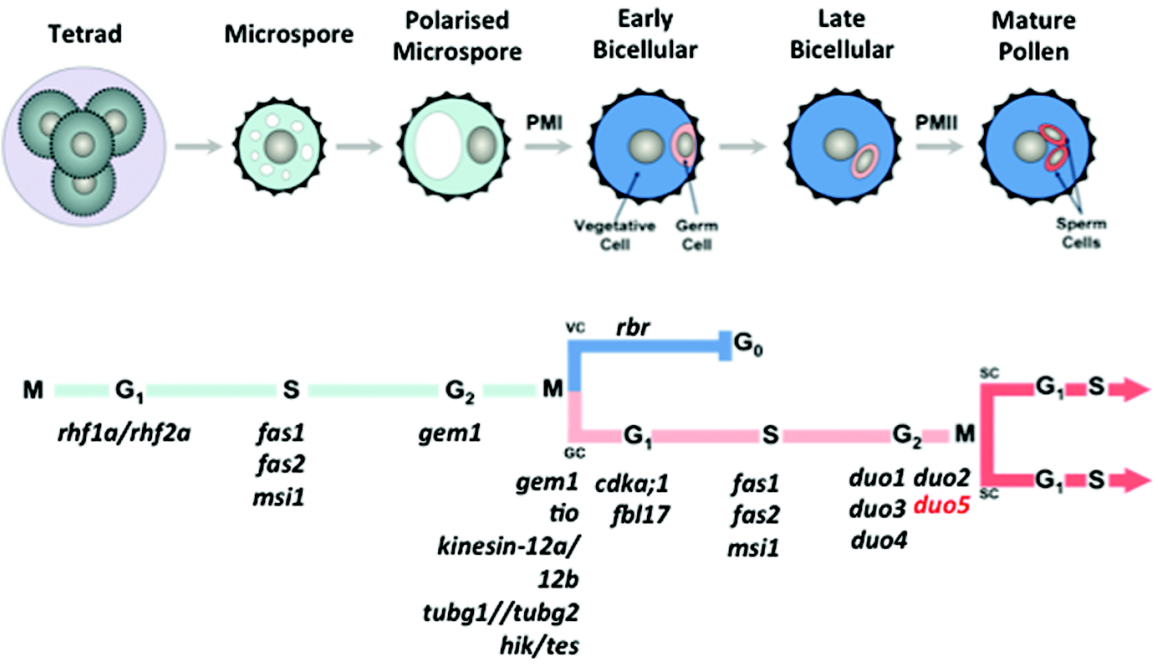

Figure 1.4: The development of male gametophyte in *Arabidopsis.* Schematic diagram representing morphological changes during male gametophyte development (top panel) along a timeline of cell cycle phases. Listed below the time line are known mutants affecting specific stages of male germline formation in *Arabidopsis*. During microsporogenesis, diploid pollen mother cells undergo meiotic division to produce a tetrad of haploid microspores. The released microspores undergo a highly asymmetric mitotic division called Pollen Mitosis I (PMI) to produce a large vegetative cell and small germ cell. Whilst the vegetative cell exits cell cycle, the germ cell elongates and undergoes a further mitotic division called Pollen Mitosis II (PMII) to form two sperm cells. The sperm cells continue through the cell cycle and reach G2 phase when delivered to the embryo sac. VC, vegetative cell; GC, germ cell; SCC, sperm cell (adapted from Borg *et al.,* 2009).

Similarly, *GEM2* genes affect cell polarity and cytokinesis not only in microspores, but also in roots and embryo sacs, however, the gene remains to be identified (Park *et al.*, 2004; Twell *et al.*, 2002). The gametophytic role of TMBP200, a tobacco orthologue of MOR1/GEM1 was investigated by analysing microspore-targeted TMBP200 knockdown lines. The RNAi lines examined, exhibited division defects in microspore polarity, division asymmetry and cytokinesis (Oh *et al.*, 2010b). Similarly, analysis of mutations in two functionally redundant gamma tubulin genes, TUBG1 and TUBG2 has highlighted their role in spindle organization to establish correct microspore division asymmetry (Pastuglia *et al.*, 2006).

Unlike mutants described above with defects in division asymmetry at PMI, *two-in-one* (*tio*) represents a novel mutant that affects the asymmetric cytokinesis. TIO encodes a plant homologue of the Ser/Thr protein kinase FUSED, and localises to the phragmoplast midline, where it plays vital role in centrifugal cell plate expansion. The *two-in-one* (*tio*) mutant exhibits a cytokinesis defect with the formation of incomplete cell plates that fail to expand. The *tio* microspore completes the nuclear division but fails to complete cytokinesis resulting in a binucleate pollen grain with a vegetative cell fate (Oh *et al.*, 2005). Two members of KINESIN-12 family proteins i.e. PAKRP1/ KINESIN-12A and PAKRP1L/ KINESIN-12B also localise to the middle region of the phragmoplast. The two proteins act redundantly to organize phragmoplast microtubules during cytokinesis in the microspore that is essential for cell plate formation (Lee *et al.*, 2007). In tobacco, kinesin related proteins, NACK1 and NACK2 play critical role in somatic cell cytokinesis by activating the NACK–PQR MAP kinase pathway. Their *Arabidopsis* orthologue, *HINKEL* (*HIK*) and *TETRASPORE* (*TES*) are a functionally redundant gene pair required for cell plate expansion during male gametophytic cytokinesis and double mutant *hik-1/tes-1*microspores produces binucleate pollen grains with cell plate expansion and cytokinesis defects similar to *tio* microspores (Oh *et al.*, 2008).

These studies suggest that failure of microspore cells to divide asymmetrically has severe repercussions on formation and correct differentiation of germ cell lineages. Furthermore, correct segregation of cell fate determinants followed by confinement in a new cell wall is critical for specifying the differing fates of the vegetative and germ cells at PMI (Berger and Twell, 2011).

1.4.2 Genes affecting germ cell division

Pollen development takes place in two distinct and sequential phases i.e. microsporogenesis and microgametogenesis. The end products of microsporogenesis consist of four haploid microspores released in the anther locule by dissolution of callose wall. Further expansion of microspore results in formation of large vacuole and migration of the nucleus to a peripheral position against the cell wall. The polarised microspore then undergoes a highly asymmetric division, called Pollen Mitosis I (PMI), to produce a bicellular pollen grain with a small germ cell engulfed within the cytoplasm of a large vegetative cell. The vegetative cell exits the cell cycle after PMI whereas the germ cell undergoes another round of mitosis at PMII and produces two sperm cells that participate in double fertilisation. An increasing number of mutants have been described in *Arabidopsis* that block PMII and produce bicellular pollen at anthesis consisting of single germ cell (Borg *et al.*, 2009).

A number of cell cycle genes are known to affect germ cell division. Progression of the cell cycle requires different regulatory proteins, which include cyclin-dependent kinases (CDKs), cyclins, cyclin-dependent kinase inhibitors (CKIs), and retinoblastoma-related proteins (Stals and Inze, 2001). *CDKA;1* or A-type cyclin dependent kinase is an important cell cycle regulator that plays essential role in germ cell division. Analysis of T-DNA insertion mutants in *CDKA;1* revealed germ cell division failure and delay of DNA synthesis phase (Iwakawa *et al.*, 2006; Nowack *et al.*, 2006). The second mitosis in germ cell is missing or severely delayed, leading to mature pollen with a single germ cell instead of two sperm cells. However, majority of the undivided *cdka;1* germ cells undergo PMII during pollen tube growth and successfully fertilises the egg cell, whereas karyogamy does not take place in the central cell (Aw *et al.*, 2010).

FBL17 is one of the components of the SCF ubiquitin-ligase complexes that consist of Skp1 and CUL1 that form the SKP1-CUL1-F-box (SCF) E3-ubiquitin protein ligase complex and is plays critical role in the ubiquitination of substrates for 26S proteasome mediated proteolysis (Kipreos and Pagano, 2000). Analysis of T-DNA insertion mutants suggest that disruption of the *F-Box Like 17 (FBL17)* gene results in the formation of a single germ cell, which produces same phenotype as is observed in *cdka;1*

mutants (Kim *et al.*, 2008). Interestingly the mutant germ cell is able to fertilise the egg cell producing an embryo that aborts early in development due to lack of endosperm production. *FBL17* is transiently expressed in the germ cell after PMI and targets the CDK inhibitors KRP6 and KRP7 for proteasome-dependent degradation thus removing the inhibition of CDKA activities allowing the germ cell to progress through S-phase. It has been shown that FBL17 is not expressed in the vegetative cell and the presence of KRP6 and KRP7 are proposed to inhibit CDKA;1 activity preventing the vegetative cell nucleus from progressing through the cell cycle (Kim *et al.*, 2008). Recent studies suggest that the interplay between E2F and RBR regulates *FBL17* expression and that activity of both CDKA;1 and FBL17 control S-phase entry during both the first and second mitotic division during male gametogenesis (Zhao *et al.*, 2012).

In contrast to *cdka;1* mutant pollen, a mutation in plant retinoblastoma-related protein RBR results in hyperproliferation of both vegetative and germ cells leading to pollen with four sperm cells. The hyperproliferation phenotype due to lack of RBR is dependent on CDKA;1 activity since introduction of *cdka;1* mutant allele rescues the hypomorphic *rbr* pollen. In addition, loss of RBR activity prevents cell fate establishment in a fraction of RBR-defective vegetative cells that behave like microspores and further divide asymmetrically to produce an additional cell with vegetative fate, germ cell fate, or mixed fate identity. Thus, RBR is a critical cell cycle regulator, primarily controlling cell cycle progression and cell fate. The RBR repression of E2F/DP pathway as well as KRP dependent CDKA;1 inhibition are two fundamental mechanisms that ensure the exit of vegetative cell at G1 phase as well as G1/S progression of germ cell through the cell cycle (Chen *et al.*, 2009). Recently it has been shown that asymmetric divisions in the shoot and root cells of *Arabidopsis* depend on the function of CDKA;1 that operates through a transcriptional regulation system mediated by RBR (Weimer *et al.*, 2012).

Chromatin integrity is another important factor that contributes to germ cell division. Analysis of Chromatin Assembly Factor-1 pathway mutants that include *fas1, fas2,* and *msi1* has revealed that correct chromatin assembly is important for male gametophyte cell division. Loss of CAF1 function delays the cell cycle pace in the germ cell, preventing the G2-M transition. CAF-1 pathway mutants display different points of arrest, with some failing to divide at PMI and PMII whereas some divide

successfully producing two sperm cells. However, CAF1 deficiency does not have any impact on the vegetative cell differentiation and function. Mutant bicellular CAF-1 deficient pollen grains correctly activate germ cell fate markers and can fertilise either the egg or central cell (Chen *et al.*, 2008).

Similarly the *duo pollen* (*duo*) mutants represent another distinct and novel class of gametophytic mutants that complete normal asymmetric division but fail to enter or complete generative cell division and thus show distinct phenotypes (Durbarry *et al.*, 2005). Six *duo* mutants have been identified that specifically fail to undergo germ cell division and remain arrested in a bicellular condition at anthesis. These mutations act gametophytically and are male-specific. These *duo* mutants represent different loci and can be classified into two main groups based on the shape of the undivided germ cell nucleus. The first group comprises *duo1, duo2* and *duo3* that bear round germ nuclei at anthesis. The second class includes *duo4,* and *duo5*, which have frequently elongated germ cell nuclei (Durbarry and Twell, 2005 unpublished). Heterozygous *duo1, duo2* and *duo3* mutation results in approximately 50% bicellular pollen grains at anthesis containing a densely packed germ cell nucleus and a diffuse vegetative cell nucleus. In the case of *duo2,* mutant germ cells enter mitosis and arrest at prometaphase, while *duo1* and *duo3* mutant germ cells complete S phase but fail to enter mitosis (Durbarry *et al.*, 2005). The expression of DUO1 is restricted to the male germline, whereas DUO3 is involved in essential developmental roles in cell cycle progression and cell specification in both gametophytic and sporophytic tissues (Brownfield *et al.*, 2009b). DUO1 is an important transcriptional regulator and is involved in activation of genes required for germ cell cycle progression and sperm cell specification. In a recent study, DUO1 regulatory network has been uncovered through which it coordinates mitotic cell cycle progression and sperm cell specification programmes. The output of the study revealed 63 putative target genes, out of which 14 have been validated as DUO1 targets and hence designated as DUO1-activated target (DAT) genes (Borg *et al.*, 2011).

A set of redundant C_2H_2–type zinc finger proteins DAZ1 (At2g17180) and DAZ2 (At4g35280) represent a group of male germline specific transcription factors that are direct targets of DUO1. The role of these two proteins was determined by analysing knockout T-DNA insertion lines in both genes. No pollen phenotype could be determined for *daz1* and *daz2* alleles when analysed separately. However, combination

of double *daz1/daz2* heterozygous mutants (*daz1-1*/+; *daz2-1*/+) produced pollen with bicellular pollen phenotype similar to *duo1* mutant. Double heterozygous *daz1/daz2* mutants produced 25% of aberrant pollen anthesis whereas homozygous heterozygous (hom-het) mutant combinations (*daz1-1/daz1-1*; *daz2-1*/+ and *daz1-1*/+ ; *daz2-1/daz2-1*) produced approximately 50% bicellular pollen suggesting that both proteins act redundantly to control germ cell division (Borg *et al.*, 2014).

1.4.3 DUO1, a master regulator of germ cell division and specification

Morphological screening of pollen from EMS-derived mutant individuals in Nossen (No-0) background resulted in identification of DUO1, a unique germ cell specific R2R3 MYB transcription factor in *Arabidopsis*, which controls male gamete formation in plants. As discussed earlier in section 1.4.2, mutant *duo1* germ cells fail to enter PMII but this failure does not prevent entry of germ cell into S phase (Rotman *et al.*, 2005). DUO1 encode two tryptophan-rich repeats (R2R3), with DNA binding domains called MYB domains which bind to the major groove of target DNA by helix-turn-helix structure, interacting with bases and phosphates (Saikumar *et al.*, 1990).

Further analysis using reverse transcriptase PCR revealed that DUO1 transcripts peak at the bicellular pollen stage during male gametogenesis prior to germ cell mitosis, validating its status as key germline-specific regulator vital for G2/M transition. In addition, failure of *duo1* germ cell to enter mitosis is caused by the lack of core cell cycle component, CYCB1;1 specifically required at G2/M transition, suggesting that CYCB1;1 expression is DUO1-dependent. Moreover, functional characterization of *duo1* mutants demonstrate that mutant germ cells are unable to carry out fertilisation suggesting that *duo1* not only cause cell cycle defect but also lack key features of gamete differentiation (Brownfield *et al.*, 2009a).

It has been demonstrated that DUO1 regulates germline specific genes including *MGH3* (*MALE-GAMETE-SPECIFIC HISTONE H3*) encoding germline specific histone H3.3 variant (Okada *et al.*, 2005), *GEX2* (*GAMETE EXPRESSED 2),* encoding a putative membrane associated protein (Engel *et al.*, 2005), and *GCS1 (GENERATIVE CELL SPECIFIC 1)* encoding sperm cell surface protein required for fertilisation (Mori *et al.*, 2006). Analysis of GFP expression driven by these target promoters in *duo1* mutants has shown no expression or weak GFP signal in mutant germ cells. The lack of

expression of *GCS1* in *duo1* germ cells results in infertility of mutant *duo1* pollen demonstrating that absence of DUO1 also suppresses expression of GCS1 suggesting that activation of GCS1 is DUO1-dependent. These studies suggest that DUO1 plays dual role in male germline development and is required for germ cell division and germ cell specification to form functional twin sperm cells (Brownfield *et al.*, 2009a).

In addition, DUO1 was ectopically expressed in seedlings using a resistant DUO1 cDNA (mDUO1) with an altered nucleotide sequence at microRNA159 binding site. An estradiol inducible promoter was used to drive the expression of mDUO1 in sporophytic tissue. The induction of mDUO1 also results in expression of its target genes MGH3, GEX2 and GCS1, however, its expression is not sufficient to induce CYCB1;1 transcripts (Brownfield *et al.*, 2009a) This ability of *DUO1* to activate its targets in ectopic tissues has been exploited by carrying out a time-course microarray experiment using an estradiol-inducible m*DUO1* construct (Zuo *et al.*, 2000). This strategy was adopted to identify additional regulatory targets of *DUO1*. The output of this study revealed 63 putative targets that showed a high fold increase of expression after induction of *DUO1*. Out of these, 14 target genes have been shown to be regulated by DUO1 through binding to canonical MYB sites in target promoters (Borg *et al.*, 2011). These putative *DUO1*-targets represent various gene families including germline enrich genes required for germline development and specification. The experiment has been further explained in Chapter 4 (Section 4.1).

DUO3 is another positive germline regulator and like DUO1, is required for germ cell division and sperm cell specification. DUO3 shares regulatory targets in common with DUO1 and is also involved in activation of *GCS1* and *GEX2*. It has been shown that in absence of DUO3, the normal expression of germline markers *GCS1* and *GEX2* is suppressed. However, the germline expression of DUO1 dependent *MGH3* gene is independent of DUO3 activation. Similarly, the expression of CYCB1;1 persists in *duo3* germ cells but not in *duo1* germ cells suggesting that unlike DUO1, DUO3 promotes entry into mitosis independent of CYCB1;1. Thus, a set of molecular markers, suppressed in both *duo1* and *duo3* germ cells suggest a distinct overlapping control of germline differentiation genes by DUO1 and DUO3. However, mechanisms these two germline regulators employ to activate common target genes during germline development still remain elusive (Figure 1.3) (Brownfield *et al.*, 2009a).

Furthermore, *in silico* analysis of *DUO1* gene has revealed that its sequence share high identity with nucleotides corresponding to the MYB domain of 11 different *DUO1* like proteins and has been found to be evolutionarily conserved among at least seven plant families in two major evolutionary clades, monocots and eudicots (Haught and Twell, 2007 unpublished). *DUO1* homologues are also present in bicellular (*Nicotiana tabacum*) and tricellular pollen species (maize, rice and *Arabidopsis*) but also in non-flowering plants like *Selaginella moellendorfii* and *Physcomitrella patens* (Brownfield *et al.*, 2009a). Furthermore, it provides an excellent opportunity to investigate the evolution of tricellular pollen in flowering plants and more interestingly if the role of *DUO1* is conserved as a regulator of germ cell division then it may have played an important role in heterochronic changes involved in the evolution of tricellular pollen in flowering plants (Rotman *et al.,* 2005).

1.5 Aims and objectives

The identification and characterization of germ cell division mutants has led to the discovery of many important germline regulators including DUO1. The short life cycle of male gametophyte and its dependence on the sporophyte for its existence, makes the genetic analysis challenging. Forward and reverse genetic approaches have been used as powerful tools for the identification and characterization of the division mutants. The major aim of this PhD project was to understand the biological processes involved in the male gametophyte development. The identification of *duo* pollen mutants in a morphological screen in Twell lab provided the opportunity to gain further knowledge of the male gametophyte development and its role in plant reproduction. One of the *duo* mutants called *duo5* belongs to elongated class of pollen mutants and produces a highly elongated germ cell nucleus. The characterization of *duo5* mutant was carried out to determine its phenotype, analyse its genetics and identify the *duo5* locus by fine mapping. Furthermore, the role of novel germline genes was investigated to gain an insight into germ cell division and sperm cell specification.

1) The first major objective of the thesis was to characterize *duo5* mutant. The third chapter of the thesis describes phenotypic as well as genetic characterization of *duo5 pollen* mutant. The specific aims of the experiments were as follows:

Analysis of DAPI stained *duo5* pollen using epifluorescence microscopy to determine

the nuclear morphology of mutant pollen. Also pollen viability was assessed using vital stain, fluorescein diacetate (FDA). The cell fate of both germ and vegetative cell was determined by introducing vegetative and germ cell fate markers to monitor cell fate specifications. Furthermore, ultrastructure of the *duo5* mutant was analysed by transmission electron microscopy to establish the bicellularity of *duo5* mutant pollen. To determine the patterns of germ cell ontogeny in wild type and *duo5* mutant pollen by examining DAPI stained pollen from various bud stages using epifluorescence microscopy. Moreover, nuclear DNA content of the mutant *duo5* germ cells was measured to determine the precise point of development arrest.

Another specific aim of the experiments was to characterise the *duo5* mutant genetically. This involved performing tetrad analysis, using *quartet1* (*qrt*) mutants and the number of aberrant pollen in the *quartet* and analysing genetic transmission through the male and the female gametes to determine the gametophytic nature of the mutation. In addition, the *duo5* locus was further narrowed down using molecular markers i.e. dCAPS and SSLP.

2) The second major objective was to explore the role of two novel zinc finger proteins in male germline development. The identification of *DUO1*-activated zinc finger proteins in the *DUO1* overexpression microarray experiment represent novel genes, and their analysis will provide valuable information about the role of zinc finger proteins in the male germline development. One of these genes, DAZ3 and its homologue DAZ3L were chosen for further analysis.

The two zinc finger proteins were validated as DUO1 targets and their expression pattern was analysed during pollen development. The promoter and protein fusion constructs were studied to examine male germline specificity and specific expression in nucleus/cytoplasm in wild type pollen. Also these constructs were analysed in the *duo1* background to determine *duo1*-dependence of these genes. Also the expression was analysed in pollen developmental stages and sporophytic tissues to validate germ cell specific expression and confirm the findings of the transcriptomic data. To determine the role of *DAZ3* in sperm cell function its expression was analysed in other germ cell mutants like *fbl17* and *cdka;1* to help determine its role in sperm cell differentiation.

Chapter 2 Materials and methods

2.1 Plant materials and chemicals used for experiments

Plant materials were grown at the university of Leicester botanic gardens and brought into the laboratory every week. Plants are mostly received from the garden at the rosette stage, prior to bolting. Seeds for *quartet* analysis, *qrt1/qrt1* (L*er* accession) were provided by D. Preuss. The germ cell fate marker line GEX2-GFP was supplied by Sheila McCormick. Other germ cell fate markers used include ProMGH3:H2B-GFP, ProLAT52:H2B-GFP, ProKinase:H2B-GFP and ProDAZ3:H2B-GFP were generated in the Twell laboratory (Borg *et al.*, 2011; Brownfield *et al.*, 2009a).

All Chemicals and materials used in different experiments were purchased from Melford Laboratories,Sigma-Aldrich, Thermo Fisher Scientific, PerkinElmer, BioGene, Calbiochem, Promega, Duchefa Biochemie, DHAI PROCIDA and Lehle seeds. Purification kits were purchased from Qiagen, Sigma-Aldrich and Bioneer. Enzymes and other reagents were obtained from Invitrogen, Finnzymes, New England Biolabs, Novagen, Sigma-Aldrich and Bioline. Companies from which equipment and instruments were purchased are indicated in the materials and methods.

2.2 Preparation of plant materials and storage

2.2.1 Preparation of soil for seed sowing and growth conditions

Arabidopsis thaliana plants ecotype Columbia (Col-0), Nossen (No-0) and Landsberg *erecta* (L*er*) were grown either in soil in 3:1:1 compost (Levington(R): vermiculite: sand or plated on MS0 growth media with or without an appropriate selection. Plants were grown in standard greenhouse conditions with 16 hours light regime and a temperature of 22^{o}C. *Nicotiana tabacum* cv.SR-1 was grown in Levington M2 compost (Scotts, UK), under greenhouse conditions of 25ºC, variable humidity, and 16 hr of day light.

2.2.2 Seeds surface sterilization and plating on media

Seeds were surface sterilised with 70% (v/v) ethanol (containing 0.5% Triton X-100) for 5 minutes followed by incubation in 100% (v/v) ethanol for 1 minute. The seeds were

dried on the sterile filter paper for 15-20 minutes. For plating primary transformants, 100-150 mg of T1 seeds were plated on MS0 media with appropriate selection. In the case of selection on soil, similar amount of seeds were sown on soil with appropriate selection. From the second generation of transformants, seeds were plated on MS0 media utilizing appropriate antibiotic selection. For selection of kanamycin or a hygromycin resistance, seeds were selected on MS0 medium with 35-50 µg/ml kanamycin or 20 µg/ml hygromycin, respectively. Non-transformed seeds were plated on MS0 media without selection. A ventilated lid was placed on the seeds sown in soil and kept on for two weeks to maintain humidity. All the seeds were stratified at 4^{o}C for three days, and then incubated in the growth room set at 22^{o}C with variable humidity and continuous light.

2.2.3 Preparation of media for plant tissue culture

Arabidopsis seeds were plated on Murashige and Skoog salt media (Duchefa Biochemie). 4.3g of MS salt was dissolved in 950 ml of deionised water with no added sucrose (MS0) or with 1-3% (w/v) sucrose. The pH of the media was adjusted to 7.0 with 5N NaOH and autoclaved for 20 minutes at 120◦C and 15psi on liquid cycle. To make MS agar for plating, 0.6% (w/v) of Phyto Agar (Duchefa Biochemie) was added prior to autoclaving.

2.2.4 Antibiotics for selection of transformed plants

Antibiotic	Working concentration
Cefotaxime (Melford Lab, UK)	200 mg/ml
Gentamycin (Melford Lab, UK)	100 mg/ml
Kanamycin (Melford Lab, UK	50 mg/ml
Hygromycin (CALBIOCHEM)	20 mg/ml
Glufosinate ammonium (BASTA)	30 mg/ml
DL-Phosphinothricin (Melford Lab,UK)	10 mg/ml

To make working stocks at desired concentration as listed above, antibiotics were dissolved in deionised water and stored at -20^{o}C.

2.2.5 Emasculation and crossings of *Arabidopsis* plants

The female parent plant was selected on the basis of 5-6 fully developed inflorescences with large buds whereas plants that have started to form siliques were chosen as pollen donors or male parent. Mature siliques as well as opened flowers and buds that already had a white tip were removed from the female parent inflorescence with fine forceps. Very small buds were also removed from the inflorescence leaving 3-5 buds of the right size. A flower bud was opened by inserting the tip of one pair of forceps between petals and sepals. The immature anthers were removed with the other pair of forceps. The forceps were cleaned with a piece of tissue and the procedure was repeated for the remaining buds. A double knot was tied around the stem of inflorescence with a piece of thread to mark the emasculated inflorescence. After 2-3 days the stigma on top of the carpel had developed rough and sticky surface (the cross works best when the papillae cells are nicely erect). The stigma was pollinated with mature pollen from the male parent. The pollinated inflorescence was marked with a coloured thread and the cross documented. The siliques matured after 20-25 days. The siliques were harvested by cutting them into a paper bag or in eppendorf tubes. The siliques were left at room temperature for a couple of days to dry. Occasionally male sterile *ms1-1* plants were used as female. This plant was pollinated without emasculation.

2.2.6 Plant tissue storage

All isolated plant tissues (including seedlings, rosette leaves, cauline leaves and flowers with mature pollen grains) for DNA and RNA extraction were weighed, flash frozen in liquid nitrogen and stored at –80^{o}C.

2.3 Bacterial culture and storage

2.3.1 Bacterial strains

(Escherichia . coli)	*(Agrobacterium. tumefaciens)*
α-select (Bioline)	
DH5α	GV3101
DB3.1	

2.3.2 Bacterial growth conditions

Escherichia coli (E. coli) and *Agrobacterium tumefaciens (A. tumefaciens)* cultures were grown at 37^{o}C and 28^{o}C respectively either on plates in an incubator (LEEC Ltd, UK) or in liquid medium on an orbital shaker (SANYO Gallenkamp, UK) at 200 rpm. Cultures were grown over night, for two days or until desired optical density was reached.

2.3.3 Bacterial growth media

E. coli and *A. tumefaciens* were grown in Luria Bertani Broth medium (LB Broth) consisting of 1% (w/v) tryptone, 1% (w/v) NaCl and 0.5% (w/v) yeast extract. For bacterial growth on plates, 1.5% (w/v) bacto-agar was added to the media before autoclaving. The media pH was adjusted to 7.0 with 5N NaOH and autoclaved for 20 minutes at 120^{o}C and 15 psi on liquid cycle. In some instances, ready mix LB media was used (Melford) so no pH adjustment was necessary.

2.3.4 Antibiotics for bacterial selection

	Working concentration (mg/ml)	
Antibiotic	***E.coli***	***A.tumefaciens***
Rifampicin (Melford Lab, UK)	n.a	50 mg/ml
Gentamycin (Melford Lab, UK)	n.a	50 mg/ml
Spectinomycin (MelfordLab, UK)	100mg/ml	100 mg/ml
Kanamycin (Melford Lab, UK)	50 mg/ml	50 mg/ml
Ampicillin (Melford Lab,UK)	30 mg/ml	30 mg/ml
Chloromphenicol (Sigma)	30 mg/ml	20 mg/ml

2.3.5 Long term storage of bacterial strains

A single bacterial colony was used to inoculate 5 ml LB medium containing appropriate antibiotics and was left to grow overnight. 700 µl aliquot of the overnight bacterial culture was transferred to a cryogenic storage tube and mixed with 300 µl sterile 50% (v/v) glycerol. The cells were flash frozen in liquid nitrogen and stored at -80^{o}C. The strains were recovered by streaking a small portion of the frozen culture on agar medium containing appropriate selection and grown as required.

2.3.6 Bacterial transformations

2.3.6.1 Preparation of competent *E. coli* cells

Competent *E. coli* cells were prepared as described previously (Hanahan, 1983). A single *E. coli* colony was grown in 25 ml of SOB media (2% Bactotryptone, 0.5% Yeast extract, 10 mM NaCl, 2.5 mM KCl, 10 mM MgCl2, and 10 mM MgSO4) at 37^{o}C, 200 rpm. A 1 ml aliquot of the overnight culture was inoculated into 100 ml of pre-warmed LB along with tetracycline and allowed to grow at 30^{o}C. 1 M $MgCl_2$ was added to a final concentration of 20 mM (2 ml of 1 M $MgCl_2$) and the cells were grown until OD_{600} reaches 0.45-0.55. The bacterial cells were transferred to a sterilised 50 ml tube and incubated on ice for 30 minutes and centrifuged at 4^{o}C, 5000 *g* for 5 minutes. The bacterial pellet was resuspended in 50 ml of prechilled $Ca^{2+}Mn^{2+}$ solution (Sodium acetate 40 mM, $CaCl_2$ 100 mM, $MnCl_2$ 70 mM, pH adjusted to 5.5 with 1 M HCl and filter sterilised) and incubated on ice for 45 minutes. The bacterial cells were centrifuged at 5,000 rpm for 5 minutes, the supernatant was discarded and pellet was gently resuspended in 5 ml of $Ca^{2+}Mn^{2+}$ solution containing 15% (v/v) glycerol. A 200 µl aliquot of the cells was dispensed into 1.5 ml tubes, frozen in liquid nitrogen and then stored at -80^{o}C.

2.3.6.2 Transformation of competent *E. coli* cells

For transformation of *E. coli*, 200 µl aliquot of competent cells was removed from -80^{o}C freezer and thawed on ice for 10 minutes. 50 µl of the competent cells was aliquot into four eppendorf tubes. 1 µl (~125 ng) of plasmid or half of the ligation / recombination reaction was added into a 50 µl aliquot, was gently mixed by flicking the tube and incubated on ice for 30 minutes. The mixture was heat shocked in a water bath at 42^{o}C for 45 seconds, then transferred back on ice for a further 2 minutes. 950 µl of LB media was added and the culture was incubated at 37^{o}C for 1 hr with gentle shaking (200 rpm). The resulting cells (100 µl) were spread on LB agar plates containing antibiotic selection, allowed to dry and the plates then incubated overnight at 37oC. The resulting transformants were later identified by colony PCR.

2.3.6.3 Preparation of competent *A. tumefaciens* cells

An *Agrobacterium* strain (GV3101) containing an appropriate helper T_i plasmid

(pMP90) was grown in 5 ml of LB medium along with selective antibiotic (50 µg/ml Rifampicin, 50 µg/ml Gentamycin) overnight at 28^{o}C on a shaker (200 rpm). A 2 ml aliquot of the overnight culture was added to 50 ml of LB medium in a 250 ml flask. The culture was grown at 28^{o}C with vigorous shaking (250 rpm) until the OD_{600} reaches 0.5-1.0. The cell suspension was chilled on ice and centrifuged at 3000 *g* for 10 minutes at 4^{o}C. The supernatant was discarded and the cells were resuspended in 1 ml of 20 mM ice-cold $CaCl_2$ solution. A 100 µl aliquot of the cells was quickly dispensed into pre-chilled microfuge tubes, flash frozen in liquid nitrogen and stored at -80^{o}C.

2.3.6.4 Transformation of competent *A. tumefaciens* cells

For transformation of *Agrobacterium*, 0.5 – 1 µg of plasmid DNA was added into the frozen aliquot and incubated at 37^{o}C for 5 min to heat-shock the cells. 1 ml of LB medium was added to the mixture, and then incubated at 28^{o}C with gentle shaking (200 rpm) shaker for 2-4 hours. The culture was then centrifuged for 30 seconds at 5000 rpm and the supernatant was discarded. Transformed cells were resuspended with the remaining solution and then spread on LB agar plate containing appropriate antibiotics. The plates were incubated at 28^{o}C for 2 days. The colonies were obtained after 2-3 days and identified by colony PCR.

2.4 Nucleic acid isolation procedure

2.4.1 Genomic DNA isolation

2.4.1.1 Small scale isolation of genomic DNA using CTAB extraction method

About 1-2 cauline or rosette leaves were collected in a 1.5 ml eppendorf tube containing 200-300 glass beads (Sigma-Aldrich) of size 425-600 micron and were frozen in liquid nitrogen. The leaf tissue was ground for 10-12 seconds in a Silamet amalgam mixer (Ivoclar Vivadent, UK) at room temperature. 250 µl of DNA extraction buffer (1.4 M NaCl, 3% (w/v) CTAB, 20 mM EDTA, 100 mM Tris-Hcl pH8) was added, vortexed briefly and incubated for 15 minutes at room temperature. An equal volume of chloroform: IAA (24:1) (250 µl) was added, mixed thoroughly and centrifuged for 10 minutes at 13000 rpm. The upper aqueous phase (200 µl) was transferred to a fresh eppendorf tube, containing 0.7 volumes (140 µl) of isopropanol. The mixture was

incubated for 5 minutes at room temperature and then centrifuged for 7 minutes at 13000 rpm. The supernatant was discarded and the pellet was washed with 1 ml of 70% (v/v) ethanol and centrifuged for 5 minutes at 13000 rpm. Ethanol was poured off and the pellet was vacuum dried for 5 minutes or left at room temperature for 30 minutes to dry. The dried pellet was resuspended in 100 µl of deionized water (DW) and incubated at 55^{o}C for 5 minutes. The DNA solution was then stored at -20^{o}C.

2.4.1.2 Large scale isolation of genomic DNA using High-throughput extraction method

Isolation of *Arabidopsis* genomic DNA was carried out following a protocol based on Edwards buffer (Edwards *et al.*, 1991) adapted for high-throughput extraction. This technique involves the crude extraction of DNA from leaf material ground with glass beads. Typically this method is used to extract a large number of tissue samples in a 96 microtiter plate format, using a shaker TissueLyser Siegen, Germany). Leaf tissue sections of about 0.5 cm^2 were collected into individual 1.2 ml collection microtubes in a 96-tube box resting on ice, with each microtube containing 0.5 cm of 1.5-2.5 mm glass beads (BDH, UK). Once all samples were collected, the tissue was flash frozen by placing the tube box in liquid nitrogen. Next, samples were ground by shaking at 30 Hz for 30 seconds using TissueLyser Siegen, Germany). This step was repeated after rotating the rack of tubes so that the tubes nearest to the TissueLyser were now outermost. After disruption of the leaf tissue, 400 µl of extraction buffer (200 mM Tris of 1 M pH 8 (or 7.5), 250 mM NaCl of 5 M, 25 mM EDTA of 0.5 M, 0.5% SDS of 10 %) was added to each microtube using the 300 µl multi-channel pipette with 300 µl tips.The mixture was centrifuged with microplate adaptors at 3,000 × *g* for 30 min at 4ºC. Next, 200 µl of supernatant from each sample was transferred into new 1.2 ml collection microtubes in another 96-tube box, and 200 µl of isopropanol was added to each microtube, mixed by inverting 3-4 times. DNA was pelleted by centrifuging with microplate adaptors at 3,000 × *g* for 20 min at room temperature and the supernatant was discarded. To wash the pellet, 200 µl of 70% (v/v) ethanol was added and then poured off, leaving the samples to dry in the sterile hood. DNA pellet was resuspended in 60 µl of sterile dH_20, and was then used immediately or stored at –20ºC.

2.4.2 Total RNA isolation

Isolation of total RNA was performed Spectrum™ Plant Total RNA Kit (Sigma-Aldrich) according to the manufacturer's instructions. Tissue samples were collected from seedlings, rosette leaves, flowers containing mature pollen and mature pollen pellets, frozen in liquid nitrogen and stored at -80ºC. Approximately 50-100 mg of frozen tissues were ground to fine powder in liquid nitrogen. 500 µl of Lysis solution containing 2-β-mercaptoethanol (adding10 µl of 2-β-mercaptoethanol to 1 ml Lysis buffer) was pipetted into the tissue powder, vortexed and ground again to completely resuspend it in the solution. After all the tissue was ground, the samples were transferred to microfuge tubes and then incubated 56ºC for 3-5 minutes. The samples were centrifuged at maximum speed (14000 rpm) for 3 minutes in a benchtop centrifuge set at 4ºC. The lysate was transferred into a filtration column (blue) and collection tube and centrifuged at maximum speed for 1 minute. While pipetting care was taken to avoid the pellet. The spin column was discarded and 500 µl of the Binding solution was added to the clear lysate and mixed immediately and thoroughly by pipetting 5-6 times. 700 µl of the mixture was then transferred to binding column (red) in a collection tube and centrifuged at maximum speed for 1 minute. The flow-through was discarded and the column returned to the collection tube. The column was washed first with 500 µl Wash Solution 1, centrifuged at maximum speed for 1 minute and flow-through discarded. The same procedure was repeated using 500 µl of Wash Solution 2. The flow-through was discarded and column returned back to the collection tube and centrifuged at maximum speed for 1-2 minutes to dry. The Binding column was transferred to a clean 2 ml collection tube and 50 µl of the Elution solution was added directly in the centre of the binding matrix inside the column. The tube was left to sit for 1-2 minutes and then centrifuged again at maximum speed for 1 minute. The column was discarded and the purified RNA samples were quantified by spectrophotometer and verified by gel electrophoresis before being stored at -20ºC.

2.4.3 Measuring RNA purity

The purity of the RNA was analysed using a spectrophotometer by measuring the absorbance at 260 and 280nm, and then calculating the ratio between the absorbance values (Abs260 : Abs280). For pure RNA, a ratio of 1.9-2.1 is expected if the RNA is

suspended in buffer at pH 7 (10 Mm Tris.Cl, pH 7.5). If the RNA is dissolved in water, a lower ratio value was expected as water is not buffered and the pH interferes with absorbance (i.e. low pH result in low absorbance due to change in ionic concentration).

2.4.4 Quantification of nucleic acids

Following RNA or DNA isolation, 1 µl of the total RNA or genomic DNA was separated on a 1.5% (w/v) agarose gel to assess the quality of the isolation. To measure the concentration of the nucleic acids, the absorbance at 260nm (Abs260) was measured using Philips, PU-870 spectrophotometer. 1 Abs260 unit equates to 40 µg/ml of RNA or 50 µg/ml of double stranded DNA.

Concentration (ng/µl) of RNA = 40 x Abs260 x dilution factor

Concentration (ng/µl) of DNA = 50 x Abs260 x dilution factor

Total amount (ng) = Concentration (ng/µl) x total volume of extraction (µl)

The above criterion is based on the extinction coefficient (a measure of how well RNA absorbs electromagnetic radiation) calculated for RNA or DNA suspended in pure water. Nucleic acid samples were diluted 1/50 or 2/100 in pure water and loaded into a quartz cuvette. In the case of RNA samples special considerations were taken to use RNAse-free water and an RNAse-free quartz cuvette. A fixed wavelength (260nm) was selected and a blank was set using RNAs-free water. The quartz cuvette containing the RNA sample was loaded and placed in the appropriate cell. The quartz cuvette was cleaned prior to the addition of each sample. The Abs260 reading was recorded for each sample and the total concentration of RNA was determined with the above criteria using Microsoft excel software. The concentration of the RNA was verified by running fixed amounts of RNA on a 1.5% (w/v) agarose gel.

2.4.5 Isolation of plasmid DNA from bacterial cultures

Transformed Plasmid DNA was isolated from *E. coli* and *A. tumefaciens* using GenElute Plasmid Miniprep Kit (Sigma-Aldrich, UK) according to manufacturer's instructions. Single colonies of transformed bacteria were inoculated in 5 ml LB media containing appropriate antibiotics. A 1.5 ml of the overnight culture was transferred into an eppendorf tube and centrifuged for 1 minute at 13000 rpm. The supernatant was

discarded and the pelleted cells were resuspended in 200 µl of Resuspension solution by brief vortexing or pipetting up and down to thoroughly resuspend the cells until homogenous. Then 200 µl of Lysis solution was added to lyse the cells and the tube was gently inverted (6-8 times) to achieve a homogenous, clear and viscous mixture. Immediately, 350 µl of Neutralization/Binding solution was added and the suspension was mixed gently to precipitate cell debris and the associated bacterial chromosomal DNA. Lysed bacterial cells were centrifuged for 10 minutes at 13000 rpm to precipitate cell debris, proteins, lipids and chromosomal DNA. A binding column was prepared by adding 500 µl of Column preparation solution to GenElute Miniprep Binding column assembled in a provided microcentrifuge tube and centrifuged at 13000 rpm for 30 seconds to 1 minute. The flow through was discarded. The clear upper phase was transferred into the prepared spin column and centrifuged for 1 minute at 13000 rpm. The flow-through was discarded and 500 µl of Optional Wash solution was added to the spin column and centrifuged for 1 minute at 13000 rpm. The column was washed with 750 µl of diluted Wash Solution containing 70% (v/v) ethanol and centrifuge for 1 minute at 13000 rpm. The supernatant was discarded and the column was centrifuged for an additional minute at 13000 rpm. The column was then transferred into a clean collection tube and 50 µl of 10 mM Tris-Cl pH 7.5 or water was added an elutant to the middle of the column. The column was left for 1 minute before being centrifuged at 13000 rpm for 1 minute to elute the plasmid DNA.

2.5 DNA synthesis by polymerase chain reaction (PCR)

2.5.1 Primer design

Different oligonucleotide primer pairs were designed to amplify genomic DNA, cDNA, cloned products and vector sequences (Appendix Table A1). Primers were designed either manually or using softwares i.e. *Primer3* (Rozen and Skaletsky, 2000) and MacVector.

For genomic and cDNA sequence amplification, primers were designed with length ranged between 20 – 25bp and melting temperature (Tm) between 60 – 65ºC. When possible, a Guanidine and Cytosine nucleotides (GC) clamp was also included at the 3'-OH end for stable primer binding. The PCR products amplified for cDNA and genomic DNA sequences ranged in sizes between 250 – 1200bp. For gateway recombination, the

primers designed included 12bp att sites for use in MultiSite Gateway® recombination reactions. Additional 1 or 2 nucleotides were also added to keep the sequence in frame. The PCR product sizes varied between 600 – 1200bp with an optimum melting temperature of 60ºC. Any problems arising with annealing temperatures, such as low yield or incorrect fragment size, were tackled by using a temperature gradient to select the optimal temperature for that specific reaction (Figure 2.1).

All primers were ordered from Sigma-Aldrich and resuspended in an appropriate volume of Tris buffer or water (10 mM Tris-Cl, pH 8.0) to achieve a stock concentration of 100 µM. A 5 µM working solution of primers was prepared for use in PCR reactions. All primers were stored at -20ºC.

2.5.2 PCR DNA amplifications

PCR reagents including Taq-polymerase, 10xNH4 buffer and MgCl2 were obtained from Bioline. dNTPs were obtained from either Bioline or Invitrogen, UK. For amplification of cloning products, proof reading enzymes, Phusion (Finnzymes) DNA polymerases were used instead. The DNA template was diluted1:100 for plasmid DNA and genomic DNA samples and 1:10 for cDNA samples. The parameters used to amplify PCR products varied according to the product size and melting temperature T_m or primers used. The annealing temperature was set 5-10ºC below the primer melting temperature and an optimum annealing temperature was determined using gradient PCR. Double stranded DNA was denatured either at 96ºC with BioTaq or 98ºC with Phusion. Primer extension time was set at 72ºC for 30 seconds per 1kb of product with BioTaq and 15 seconds per 1 kb of product with Phusion. A minimum number of cycles were used for amplifying promoters and coding sequences used for cloning. PCR reactions were carried out using one of the three different thermocyclers: TProfessional Basic Gradient (Biometra), Primus96 Plus (MWG-Biotech) and Mastercycler Gradient (eppendorf). The PCR product was analysed by agarose gel electrophoresis. To perform a general purpose PCR reaction using BioTaq DNA polymerase following parameters were applied: Denaturing: 96ºC for 20 seconds, Annealing: 55-65ºC for 30 seconds and Extension: 72ºC for 30 seconds per1kb, and finally 72ºC for 5 minutes.

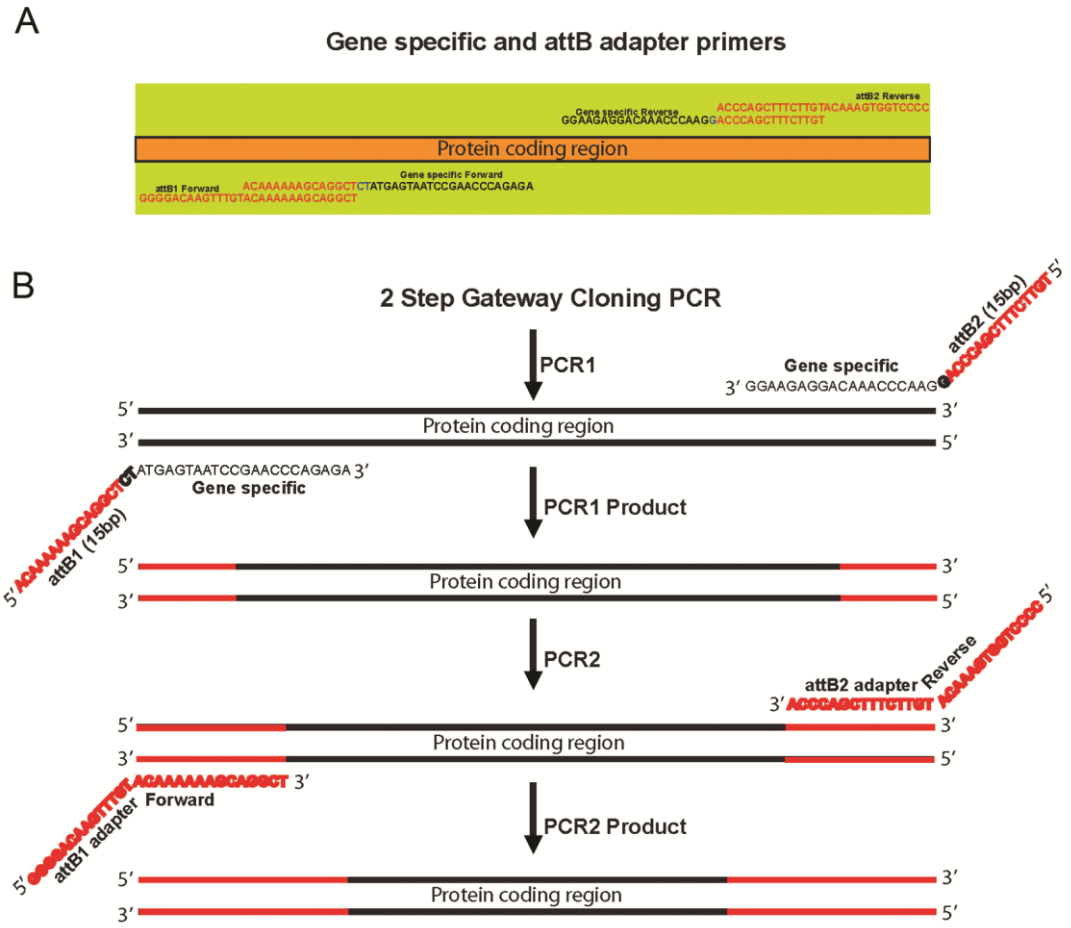

Figure 2.1: Two step Gateway cloning PCR experiment. (A) Schematic diagram depicting sequences of gene specific forward and reverse primers containing 15 base pair overlap with attB primers (indicated in dark red). These primers are used to amplify coding sequence in PCR1 in a typical two-step Gateway cloning PCR experiment. Adapter primers, attB1 forward and attB2 reverse, indicated in bold red are used in the second PCR that results in the target coding region flanked by the attB recombination sequences. **(B)** An illustration depicting the two-step PCR amplification strategy. The first PCR makes use of 5' and 3' gene specific primers that incorporates a portion of attB (dark red sequences) sites in the PCR product 1. The second PCR proceeds with forward and reverse attB primers that generate the complete attB1 and attB2 sites, producing attB-PCR substrate that is suitable for recombination. The PCR product is further subcloned into pDONR221 in a MultiSite Gateway BP reaction that facilitates production of an entry clone.

A 20μl BioTaq PCR reaction for general purpose was set up as follows:

Reagents	Volume	Final concentration
Water	12.4 µl	
10x NH4 buffer	2.0 µl	1x
50 mM MgCl2	1.0 µl	2.5 mM
10 mM dNTPs	0.5 µl	0.25 mM
5 µM F primer	0.5 µl	0.125 µM
5 µM R primer	0.5 µl	0.125 µM
DNA template	1.0 µl	
Taq polymerase 5U/µl	0.1 µl	1 U
	20 µl	

A 20μl BioTaq PCR reaction for mapping was set up as follows:

Reagents	Volume	Final concentration
Water	13 µl	
10x NH4 buffer	2.0 µl	1x
50 mM MgCl2	0.8 µl	2 mM
2m M dNTPs	2.0 µl	0.2 mM
20 µM F primer	0.5 µl	0.5 µM
20 µM R primer	0.5 µl	0.5 µM
DNA template	1 µl	
Taq polymerase 5U/µl	0.2 µl	1 U
	20 µl	

2.5.3 High fidelity PCR for cloning

For Gateway® recombination cloning, PCR products were amplified using Phusion® High-Fidelity Polymerase (Finnzymes). Phusion DNA polymerase generates PCR products with high efficiency and accuracy of amplification. The sequences of gene specific primers contain a 15 base pair overlap with attB primers to avoid designing long and expensive primers. A first reaction (PCR1) is carried out to generate the required product and a second reaction (PCR2) is carried out with relevant attB adapter primers using the product amplified in PCR1 in order to extend the attB sites prior to

Gateway® recombination (Figure 2.1). The first PCR incorporates a portion of attB recombination sequences in the PCR product 1, whereas, second PCR proceeds with forward and reverse attB primers that generate the complete attB1 and attB2 sites, producing attB-PCR substrate that is suitable for recombination.

PCR1: A 25μl Phusion PCR reaction for PCR1

Reagents	Volume	Final concentration
Water	14.2 µl	
5x HF buffer	5.0 µl	
5 mM MgCl2	1.0 µl	0.2 mM
10 mM dNTPs	0.5 µl	0.2 mM
5 µM F primer	1.5 µl	0.3 µM
5 µM R primer	1.5 µl	0.3 µM
DNA template	1.0 µl	
Phusion 2U/µl	0.3 µl	0.6 U
	25 µl	

PCR2: A 50μl Phusion PCR reaction for PCR2

Reagents	Volume	Final concentration
Water	15.4 µl	
5x HF buffer	10.0 µl	
5 mM MgCl2	2.0 µl	0.2 mM
10 mM dNTPs	1.0 µl	0.2 mM
5 µM F primer	8.0 µl	0.8 µM
5 µM R primer	8.0 µl	0.8 µM
PCR product	5.0 µl	
Phusion 2U/µl	0.6 µl	0.6 U
	50 µl	

The buffers that were used to make master mixes were supplied with the Phusion enzyme. dNTPs were supplied by either Bioline or Invitrogen. The DNA template was diluted 1:100 for plasmid DNA and genomic DNA samples in PCR 1 reactions. The cycling conditions used for Phusion PCR1 were as follows: 98ºC for 2 minutes, 10 cycles of 98ºC for 20 seconds, 55-65ºC for 30 seconds and 72ºC for 15 seconds per

1kb, and finally 72ºC for 5 minutes. The cycling conditions for Phusion PCR2 were as follows: 98ºC for 2 minutes, 10 cycles at 98ºC for 20 seconds, 45ºC for 30 seconds and 72ºC for 15 seconds per 1kb, 20 cycles of 98ºC for 20 second, 55ºC for 30 seconds and 72ºC for 15 seconds per 1kb and finally 72ºC for 5 minutes.

2.6 Reverse Transcription PCR (RT-PCR)

Total RNA isolated from plant tissues i.e. leaves, flowers and mature pollen. The samples were first DNase treated with Amplification Grade DNase I (Sigma-Aldrich) according to manufacturer's instructions. Depending on the volume of total RNA, the 10x Reaction Buffer was diluted to 1x and the same volume of DNaseI added to the sample followed by incubation at room temperature for 15 minutes. The same volume of STOP solution was then added and the sample incubated at 70◦C for 10 minutes to denature the DNaseI. Samples were kept on ice in preparation for first-stand cDNA synthesis.

First strand cDNA was synthesised with a standard amount of total RNA primed with oligo dT primers using M-MLV reverse transcriptase (Promega). 750ng-1µg of DNAse-treated total RNA was used in the first strand cDNA synthesis reactions. Where appropriate, an RT negative control reaction containing no reverse transcriptase was included during cDNA synthesis. To determine transcript abundance of genes of interest, a 1:10 dilution of first strand cDNA was used as a template in general BioTaq PCR reactions using gene-specific primers.

Approximately 750 ng-1µg of total RNA was placed in 0.2 ml microfuge tubes on ice along with 0.5 µg of oligo dT per µg of RNA in a volume of ≤15 µl. This mixture was mixed, spun briefly and heated in a thermocycler to 70ºC for 5 minutes then cooled immediately on ice to prevent secondary structure reforming. The following was then added to each tube:

M-MLV 5x Reaction Buffer	5.0 µl
10 mM dNTPs	1.25 µl
M-MLV RT	200 U
Nuclease-free water	up to 25.0 µl

The tubes were then mixed and incubated at 42ºC for 1 hour in a thermocycler. The

cDNA was stored at -20ºC or used directly for PCR analysis. PCR reaction mixture was prepared in a 0.2 ml microfuge tube that was kept on ice, mixed and spun briefly. The expression of the target template was detected by analysing the RT-PCR product using agarose gel electrophoresis.

2.7 DNA modification and agarose gel electrophoresis

2.7.1 Digestion of DNA with restriction endonucleases

Restriction digest of PCR products and plasmid DNA was performed with varying enzymes according to requirements. Digests were carried out in an appropriate buffer and incubated at 37◦C (or any other appropriate temperature) for 1 hour and 30 minutes. When more than one restriction enzyme was used, an appropriate buffer was selected that gave optimal activity for both enzymes. In cases where the buffer is not appropriate for both enzymes, iterative single digests were performed. The digest reaction was set up as follow:

Restriction digest reaction	Volume
DNA	1 µg
Buffer	2.0 µl
10xBSA (1mg/ml)	2.0 µl
Restriction enzyme (10U/µl)	0.5 µl
Water	Up to 20 µl

All the enzymes and reagents used were purchased from New England Biolabs (NEB), UK.

2.7.2 Separation of DNA by agarose gel electrophoresis

Identification and purification of different DNA fragments of different sizes from PCR products, restriction digest and purified plasmids were performed by agarose gel electrophoresis. A similar technique was also used for the visualization of extracted total RNA. Agarose gel was made up with 1x Tris-acetate buffer (TAE) (40MmTris base, 20 mM glacial acetic acid, 1 mM EDTA) supplemented with 0.5 µg/ml ethidium bromide. According to the size of the DNA fragments, the concentration of agarose gels varied between 1 % (w/v) to 4 % (w/v). Based on a method from (Sambrook and Russell

David, 1989) samples were mixed with 1x Orange G DNA loading buffer or gel loading dye (10x Gel loading buffer: Orange G 0.5 % (w/v), glycerol 50 % (v/v)) then were loaded into gel wells. The loaded gel was placed in the electrophoresis tank and a voltage of 10V/cm was applied to separate the fragments for approximately 30 minutes. The DNA / RNA fragments were visualized under UVP transilluminator (BioDoc – ItTM System, U.S.A) and the size and quantity of the DNA fragments were determined by comparing with a standard DNA ladder (New England Biolabs)

50 X TAE stock:

242 g Tris-base
57.1 ml Glacial acetic acid
100 ml of 0.5 M EDTA (pH 8.0)
Made up to 1L volume of water

To make a working solution of 1x TAE, 20 % (v/v) of the 50x TAE stock was used to make 10x TAE. 10 % (v/v) of 10x TAE was then used to make a final working solution of 1x TAE.

2.8 Purification of DNA

2.8.1 DNA Purification from agarose gel

DNA fragments required for sequencing or cloning were purified from agarose gels using a GenElute Gel Extraction kits (Sigma-Aldrich, UK) according to manufacturer instructions. The DNA fragment was excised from the agarose gel with a clean scalpel or razor blade. The gel slice was weighed and three gel volumes (100 mg = 100 µl) of Gel Solubilization Solution were added. The sample was then incubated at 50-60ºC for 10 minutes with occasional vortexing to dissolve the gel. A binding column was prepared by adding 500 µl of Column Preparation Solution to a GenElute Binding Column G placed in a 2 ml collection tube and then centrifuged for 1 minute. Once the agarose had dissolved completely, one gel volume of isopropanol was added to the mixture. The gel solution mixture was then pipetted into GenElute Binding Column G and centrifuged for 1 minute at 13000 rpm. The flow-through was discarded and a 700 µl aliquot of Wash Solution was added to the column to remove all traces of agarose. The column was centrifuged for 1 minute at 13000 rpm and the flow-through discarded.

The column was centrifuged for an additional 1 minute at 13,000 g to remove any traces of the remaining ethanol. The binding column was placed into a clean 1.5 ml microfuge tube, 30 µl of Elution Solution or 10 mM Tris-Cl pH 7.5 or water was added to the centre of the column and allowed to stand for 1 minute. The DNA was eluted by centrifugation at 13000 rpm for 1 minute. Eluted DNA was used directly for cloning reactions or stored at -20ºC.

2.8.2 PCR DNA Purification

In the cases where the primer set used to amplify DNA fragment for cloning or sequencing showed high specificity (i.e. no non-specific products were amplified) and the fragment size ranged between 100bp-1kb, a GenElute PCR Clean-up Kit (Sigma-Aldrich, UK) was used instead of GenElute Gel Extraction Kit due to its higher recovery of purified DNA. Following a PCR reaction, five volumes of Binding Solution was added to the sample, mixed thoroughly and pipetted onto GenElute plasmid mini spin column. The column was centrifuged for 1 minute at 13000 rpm and the flow-through discarded. 500 µl of diluted Wash Solution was added and the column centrifuged for 1 minute. The flow-through was discarded and the column was centrifuged for an additional 1 minute. The column was placed into a clean 1.5 ml microfuge tube, 30 µl of Elution Solution or 10 mM Tris-Cl pH 7.5 or water was added to the centre of the column and allowed to stand for 1 minute. The DNA was eluted by centrifugation at 13000 rpm for 1 minute. Eluted DNA was used directly for cloning reactions or stored at -20ºC.

2.9 Cloning by Gateway® recombination

The Gateway® technology is based on the bacteriophage lambda site-specific recombination system that facilitates the integration into *E. coli* chromosome. The principle of this recombination system based on the recombination courses between site specific attachment(*att*) sites *att*B on the *E. coli* chromosome and *att*P on the lambda chromosome to give rise to *att*L and *att*R (Landy, 1989). For high throughput DNA cloning, a gateway recombination technology (Invitrogen, UK) was used instead of a traditional conventional cloning. DNA fragments were first amplified by PCR using primer pairs that incorporate the recombination sites (attB1 and attB2) at the 5' and 3' -

OH end of the DNA fragment. Depending on the specificity of the primers, the PCR product was then purified either by GenElute Gel Extraction kits (Sigma-Aldrich, UK or GenElute PCR Clean-up Kit (Sigma-Aldrich, UK). The concentration of purified product together with the vector was determined by agarose gel electrophoresis using a standard DNA ladder. The PCR product was cloned into the expression vector in two subsequent steps.

2.9.1 Multisite Gateway® Cloning

Multisite Gateway® recombination cloning (Invitrogen, UK) was used to clone the genes. DNA fragments were first amplified by PCR using primer pairs with flanking *att* recombination sites (attB1, attB2, attB3 and attB4) at the 5' and 3' ends to amplify the DNA fragment. Then, the PCR product was purified by gel extraction. The fragment of interest was inserted into stable vectors for expression and functional analysis, using two cloning steps:

Step 1: BP reaction

In the first Gateway® recombination reaction, 125 ng of purified gel product was recombined into 75 ng of donor vector to generate entry clones. Following overnight incubation at room temperature, the reaction was terminated by the addition of 0.5 µl of proteinase K (2 µg/µl) and incubation at 37ºC for 10 minutes.

BP-reaction	
PCR product	~125 ng
PDONR vector	~75 ng
BP Clonase II	1 µl
TE buffer	up to 5 µl

The reaction was terminated with 0.5 µl of proteinase K enzyme by incubating at 37ºC for 5 minutes to denature the clonase enzymes. 2.5 µl of the total reaction was used for transformation of commercial E. coli cells (α-select) (Bioline). The transformed cells were grown in 950 µl LB medium for one hour, then plated onto agar plates with appropriate selection, and incubated at 37ºC for approximately 16 hours. The colonies were screened by colony PCR using pDONRF/R M13 primer set to identify the

presence of the correct plasmid. Positives colonies were used to setup 5 ml overnight culture and the plasmid was isolated from the bacteria and verified by restriction digest and sequencing before being used for the second step cloning.

Step 2: LR recombination reaction

Verified entry clones were used to recombine the insert into the destination vector in a LR reaction. For single site LR reaction, the recombination of 125 ng of the entry clone and 75 ng of the desired destination vector were used in a second ligation reaction catalysed by the enzyme LR Clonase II enzyme (Invitrogen). For Multisite LR reaction, the recombination 5fmol of each entry clone and 10fmol of the desired destination vector were catalysed with the LR Clonase II Plus enzyme (Invitrogen).

LR-reaction	
Destination vector	~75 ng
Entry clone	~125 ng
LR Clonase II	1 µl
TE buffer	up to 5 µl

Two-site LR-reaction	
Destination vector	10 fmol
pDONRP4-P1R entry clone	5 fmol
pDONR221 entry clone	5 fmol
LR Clonase II Plus	1 µl
TE buffer	up to 5 µl

Three-site LR-reaction	
Destination vector	10 fmol
pDONRP4-P1R entry clone	5 fmol
pDONR221 entry clone	5 fmol
pDONR221 entry clone	5 fmol
LR Clonase II Plus	1 µl
TE buffer	up to 5 µl

The reaction was incubated overnight at room temperature and then terminated by adding 0.5 µl of proteinase K enzyme and incubating at 37ºC for 10 minutes. 2.5 µl of the total reaction was used to transform *E. coli* cells (α-select) and the colonies were screened by PCR. Positively screened colonies were inoculated in 5 ml of LB overnight culture was setup and recombinant plasmid was isolated and used for restriction analysis and sequencing when appropriate. Verified expression vectors were then mobilized into *A. tumefaciens* (GV3101) for transformation of *Arabidopsis* plants.

The formula to calculate the ng of plasmid DNA needed to achieve the desired f mols is as follows:

ng needed = desired f mol x size of vector (bp) x (660 x 10-6)

2.9.2 Sequencing of DNA

Purified PCR product and isolated recombinant plasmid were sent to John Innes Centre lab (The Genome Analysis Centre, Norwich, UK) for sequence confirmation. 50 ng of PCR product or 150 ng of plasmid DNA in a total of 20 µl was sent for sequencing, According to the submission requirements. Sequencing primers at a 1.5 pmol/µl concentration were sent along with plasmid DNA. In the case of entry clones, M13 primers were used to sequence recombined inserts. Depending on the length of sequencing required (maximum of 500bp per reaction), more than one set of primers were sent to provide full coverage of sequenced regions in the event more than 500 bp was analysed. Sequencing result in ABI format were downloaded from the JIC website (http://jicgenomelab.co.uk/account.html) and analysed with the MacVector sequence analysis program (MacVector, U.S.A). Sequence pattern was confirmed by analysing alongside chromatogram files and the predicted sequences using the Align to Reference feature in MacVector.

2.10 Generation of transgenic plants

2.10.1 Transformation of *Arabidopsis thaliana*

Arabidopsis plants were transformed by the floral dip method as described before (Clough and Bent, 1998) with some modifications. Healthy plants were grown under a 24 hour light regime with primary bolts clipped when the plants were approximately 2-

5cm tall. Plants were left to grow auxilliary buds for ~1 week then fully developed inflorescences were clipped and the plants supplemented with Miracle-Gro All Purpose Concentrated Plant Food (Scotts). After 1 week, the plants had numerous inflorescences and unopened floral buds. Plants were prepared for transformation by clipping off siliques and fully open flowers.

A single colony from the desired *Agrobacterium* strain was used to a 5 ml culture of LB containing appropriate antibiotic selection. Cells were allowed to grow to saturation overnight at 28ºC with vigorous shaking (220 rpm). A 400 µl aliquot of the culture was subcultured into a 1 litre conical flask containing 400 ml of fresh LB media with antibiotic selection and cultured to saturation overnight at 28ºC with vigorous shaking (220 rpm). Cells were then centrifuged at 3500 rpm for 20 minutes and resuspended in 1 litre of infiltration medium (2.17 g/l half strength MS salts, 3.16 g/l full strength Gamborg B5 vitamins, 0.5 g/l MES, 50 g/l sucrose, 10 µg/l 6-benzylaminopurine). Just before dipping, 300 µl of Silwet L-77 (Vac-In-Stuff, Lehle Seeds) was added per litre of resuspended culture. The above-ground part of the plants was dipped in the *Agrobacterium* solution for ~30 seconds with gentle agitation. Dipped plants were then kept under a nylon autoclave bag for 16 to 24 hours in order to maintain high humidity. Plants were then watered and grown normally with loose branches tied around a stake with twist-ties once the plants started to mature and set seed. Once the siliques were mature, watering was stopped and the plants were kept in a drying room for ~2 weeks. The dry seed was harvested and selected on plates and/or soil containing appropriate selection to identify primary transformants.

2.10.2 Transient transformation of *Nicotiana tabacum* leaf

Argrobacterium-mediated transient transformation of *Nicotiana tabacum* leaf in *Nicotiana tabacum* cv. SR-1 leaf epidermal cells, following an adapted protocol of the agroinfiltration method (Sparkes *et al.*, 2006), using Sigma reagents. Single colonies of transformed *Agrobacterium tumefaciens* GV3101 (pMP90) were inoculated in 5 ml of LB media containing appropriate antibiotics and incubated overnight at 28ºC with constant shaking of 200 rpm. Cells were harvested from a 1.5 ml aliquot of the overnight culture by centrifugation at 1,000g and the pellet resuspended in 1 ml of infiltration media (280 mM D-glucose, 50 mM MES, 2 mM Na3PO4.12H2O, 0.1 mM

acetosyringone). The cells were washed by resuspending in another 1 ml of infiltration media to remove traces of antibiotic and the OD600 measured using a Pye Unicam PU 8650 spectrophotomer (Philips). The *Agrobacterium* solutions were then combined according to the experiment at an OD600 of 0.1 for reporter and effector vectors and an OD600 of 0.02 for the Renilla luciferase control vector. 4-6 week old *Nicotiana tabacum* plants were grown in greenhouse conditions but placed under a white fluorescent lamp for 1 hour before infiltration to ensure fully open stomata. Generally the 3rd and 4th large leaves from the apical mersitem were chosen for infiltration. Each infiltration was carried out four times, on both sides of the midrib region on two separate leaves. The *Agrobacterium* solutions were taken up in 1 ml syringes and the underside of the leaf prepared by gently rubbing a 0.5 cm^2 region to remove the cuticle. The syringe tip was then placed against the rubbed regions and the *Agrobacterium* solutions gently infiltrated whilst directly supporting the front of the leaf with a finger. Infiltrated areas were marked and labelled with a permanent black marker pen. Gloves were sprayed with 70% (v/v) ethanol in between infiltrations to prevent cross contamination. Plants were placed in a growth chamber under normal growth conditions and left for 2 days. Infiltrated regions were excised and used in dual luciferase assays.

2.10.3 Dual Luciferase assays

Luciferase reporter activity resulting from transient expression assays was quantified following an adapted protocol of the dual luciferase reporter assay (Sherf *et al.*, 1996). *Agrobacterium*-infiltrated *Nicotiana tabacum* leaf regions were excised using a size 7 cork borer. The excised leaves were ground in clean pestle and mortars in 500 µl of 1x Passive Lysis Buffer (Promega) until extracts appeared homogenous (~30 seconds). The leaf extracts were centrifuged at 4ºC at 14,000 g to pellet cell debris. The extracts were kept on ice while assaying for dual luciferase activity. Fresh luciferase assay buffers were prepared and enzyme substrates added only prior to priming the injectors of a Clinilumat LB9502 luminometer (Berthold). A total of 20 ml of firefly luciferase assay buffer and 20 ml of Renilla luciferase assay buffer is enough to prime each injector and assay around 40-45 leaf extracts. Luciferase reaction buffers were prepared with slight modification of published non-commercial recipes (Dyer *et al.*, 2000). The firefly luciferase assay buffer (25 mM glycylglycine, 15 mM KPO4 pH 8.0, 4 mM EGTA, 2 mM ATP, 1 m M DTT, 15 mM MgSO4, 0.1 mM CoA, 75 µM luciferin with

final pH adjusted to 8.0) and Renilla luciferase assay buffer (1.1 M NaCl, 2.2 mM Na2EDTA, 0.22 M KPO4 pH 5.1, 0.44mg/ml BSA, 1.43 µM coelenterazine with final pH adjusted to 5.0) were prepared. The injectors of the luminometer were primed with the assay buffers and two separate 25 µl aliquots separately assayed for luciferase activity with 200 µl of each assay buffer. Luciferase activity consisted of photon counts detected over 10 seconds with an integration time of 1 second. Uninfiltrated tobacco leaf extract was also assayed to assess leaf background and subtracted from the luciferase activity of the infiltrated regions. A normalised dual luciferase activity (FLuc/RLuc) was calculated for each infiltration by dividing firefly luminescence activity (FLuc) with Renilla luminescence activity (RLuc).

2.11 Cytological Analysis

2.11.1 Visualization of pollen nuclei with DAPI

Pollen nuclear morphology was visualized by staining with 4',6-diamidino-2 phenylindole (DAPI) as described in previous studies (Park *et al.*, 1998). 4-5 fully open flowers were collected in an eppendorf tube containing 300 µl of 10 µg/ml DAPI in GUS buffer (0.1 M sodium phosphate pH 7.0, 1 mM EDTA, 0.1% (v/v) Triton X-100). DAPI stock solution was made by dissolving DAPI powder in distilled water (0.4 mg/ml DAPI; high grade, Sigma). Pollen grains were released into the DAPI solution by brief vortexing and centrifuged for 5 seconds in a picofuge (Stratagene, UK). 3 µl of the pollen pellet was transferred to a microscope slide, gently pressed down with a cover slip, sealed with nail varnish to prevent sample from drying, and viewed under fluorescence microscope (Nikon ECLIPSE 80i, Japan) or confocal scanning laser microscope (Nikon ECLIPSE TE2000-E, Japan).

DAPI staining solution	
GUS buffer	10 ml
DAPI (10 µg/ml)	8 µl

For screening pollen from a large scale population, mature pollen from 1 – 2 single open flowers was collected into a 96–well microtiter plate containing 100 µl of DAPI solution. Pollen grains were released from the flowers by gently tapping the microtiter

plate and pollen nuclei were visualised under an inverted fluorescence microscope (Zeiss Axiophot 100). For analysis of spores at earlier developmental stages, buds were separated and sequentially arranged based on their position on the floral axis with +1 representing a first fully open flower and approximately -12 stage representing early released microspores (Lalanne and Twell, 2002). Flowers buds were dissected on microscope slide into 5 µl of DAPI solution or 0.3 M mannitol using a dissecting microscope (Zeiss STEM1 SV8). Anthers were firmly pressed with fine forceps and dissecting needle to release the spores, coverslip was mounted and the samples and gently squashed onto tissue paper to flatten the samples. The cover slip was sealed with nail varnish and visualised under fluorescence microscope. The pollen was analysed for reporter constructs using Nikon ECLIPSE 80i, Japan or confocal scanning laser microscope, Nikon ECLIPSE TE2000-E, Japan.

2.11.2 Fluorescein diacetate (FDA) staining for pollen viability

Pollen grain viability was determined cytologically by visualising cellular esterase activity with 0.1mg/ml fluorescein diacetate (FDA) in 0.3M mannitol (Eady *et al.*, 1995). 1-2 open flowers were agitated into 96-well microtiter plate containing 100 µl of freshly made FDA stain. After 5 minutes of incubation at room temperature, the pollen was examined with FITC filter set on Zeiss Axiovert 100 at low power (x10/x20 objectives) to prevent photobleaching.

FDA stain	
0.3 M Mannitol	990 µl
10 mg/ml FDA (in acetone)	10 µl

2.11.3 *In vitro* pollen germination assays

For pollen *in vitro* germination assay, mature pollen at the stage of anther dehiscence was transferred to slides or in the wells of a 24 well plates with the germination medium (1 mM CaCl2, 0.01% (w/v) Boric Acid, 18% Agarose (w/v), 1 mM Ca(NO3)2, 1 mM MgSO4 and 10 % (w/v) Sucrose in distilled water, pH adjusted to 7). Germination occurred in a moist chamber at 25ºC in constant light overnight. Samples were stained with a mixture of DAPI and GUS buffer for 1 hour and viewed under a fluorescence

microscope using an UV-filter. A newly developed *in vitro* pollen germination protocol (Rodriguez-Enriquez *et al.*, 2013) was used. According to the protocol, pollen was placed in contact with a cellulose membrane overlying an agarose-based medium containing 18% (w/v) sucrose, 0.01% (w/v) boric acid, 1 mM CaCl2, 1 mM Ca(NO3)2, 1 Mm KCl, 300 mg/l casein enzymatic hydrolysate (N-Z-Amine A, Sigma C0626), 100 mg/l myo-inositol, 100 mg/l ferric ammonium citrate, 0.25 mM spermidine and pH adjusted to 8.0 with KOH. The slides were placed in a vertical position in a humid sealed box and incubated in the dark at 24°C for 10 to 12 hours. The cellophane membrane with germinated pollen was carefully removed with forceps from the agarose pad and placed on drop of the liquid germination media of same composition as the solid germination media without agarose on a new slide. A cover slip was placed on the cellophane membrane and then sealed with nail varnish. The slide was visualized under a fluorescence microscope using partial bright field optics and appropriate filter set.

2.11.4 Microscopy and image processing

All images were captured using different cameras and objectives depending on the microscope used and type of image to be captured. When using the Nikon ECLIPSE TE2000-E (Nikon, Japan) inverted fluorescence microscope, a mercury lamp was used as an excitation source together with a Plan Fluor 40x/1.3 NA oil immersion objective or a Plan Fluor 60x/1.25 NA oil immersion objective. DIC images were captured with a Micropublisher 3.3 RTV colour CCD camera (QImaging, Canada) and fluorescence images were captured with an ORCA-ER cooled CCD camera (C4742-95-12ERG, Hamamatsu Photonics, Japan). Images were previewed, captured and saved using Openlab 5.0.2 software (Improvision, UK) in TIFF format. When using the Nikon ECLIPSE 80i (Nikon, Japan), an LED-based excitation source (CoolLED, presicExcite) was used together with a Plan Fluor 40x/1.3 NA oil immersion objective or a Plan Apo VC 60x/1.4 oil immersion objective. Fluorescence images were captured with a DS-QiMc cooled CCD camera (Nikon, Japan). Images were previewed, captured and saved using NIS-Elements Basic Research v3.0 software (Nikon, Japan) in JPEG2000 format. For confocal laser scanning microscopy (CLSM), the Nikon ECLIPSE TE2000-E (Nikon, Japan) microscope was employed using the C1 confocal module (Nikon, Japan). A Melles Griot Argon Ion (excitation 488 nm) and Melles Griot Helium- Neon (excitation 543 nm) were used as laser excitation sources. CLSM was operated using the

EZ-C1 control unit and associated imaging software. Images of dissected siliques were captured using a 3-CCD colour video camera (JVC, KY-F55B) mounted on a dissecting microscope (Zeiss STEMI SV8). The video camera was linked to a Neotech IGPCI capture card and images previewed, captured and saved using Image Grabber PCI 1.1 software on running on Mac OS 9. All subsequent image processing was undertaken using Adobe Photoshop CS version 8.0.

2.11.5 Fluorescence and relative DNA content

Relative DNA content of mutant germ cell nuclei was measured based on the resulting fluorescence of DAPI stained nuclei. Similarly, the mean signal intensity of fluorescent fusion nuclear proteins was based on the fluorescence of sperm cell nuclei. Images were captured on a Nikon ECLIPSE 80i (Nikon, Japan) fluorescence microscope using a DS-QiMc cooled CCD camera (Nikon, Japan) camera and Plan Fluor 60x/1.25 NA oil immersion objective. The exposure time was determined empirically in order to avoid image saturation and kept constant during image capture of all mutants or transgenic lines analysed (300ms exposure in the case of the final experiment). NIS-Elements BR v3.0 software (Nikon, Japan) was used to process the captured images in order to determine the total pixel intensity (TPI) of manually defined regions of interest (ROI) encompassing germ cell and/or sperm cell nuclei. The ROI was defined using the auto-detect feature within the measurements panel. This ROI was then duplicated and used to measure the TPI of the cytoplasmic background within the same pollen grain. The true fluorescence of the germ cell and/or sperm cell nucleus was obtained by subtracting the cytoplasmic background TPI from the nuclear TPI. Each batch of images corresponding to a germ cell division mutant or a certain transgenic line was processed and the mean TPI calculated.

For measuring DNA content of mutant germ cells, mature pollen from fully opened flowers from wild type and mutant plants was collected in eppendorf tubes and fixed in 3:1 95% (v/v) ethanol: acetic acid for about 24 hours at 4°C. Samples were vortexed again for few seconds, flowers were taken out of the tube and pollen pelleted in centrifuge for 40 seconds at full speed (16000g). The fixative solution was removed from the tube using P-100 pipette; afterwards 400 µl of 75% ethanol was added and centrifuged again for 40 seconds. The ethanol was removed and 200 µl of GUS buffer

(0.1 M sodium phosphate, pH 7.0, 1 mM EDTA, 0.1% (v/v) Triton X-100) was added to wash pellet of fixative and ethanol. GUS buffer was removed after centrifuging again for 40 seconds. DAPI solution (0.1 M sodium phosphate, pH 7.0, 1 mM EDTA, 0.1% (v/v) Triton X-100, 0.4 mg/ml DAPI) was added to the sample and after 5 minutes the pollen was pelleted by spinning. A coverslip was mounted, gently squashed to flatten the samples and sealed with nail varnish. The samples were then visualised under an epifluorescence microscope, NIKON ECLIPSE 80i. DAPI Images were captured and relative fluorescence values were recorded using fixed area. A single nucleus was selected and readings were recorded. The net values for nuclei were obtained by recording initial reading of the nucleus and subtracting a corresponding background reading from the cortical cytoplasm. In order to standardise the relative fluorescence per C value, the DNA content of *duo2* was also measured at anthesis since it arrests in mitosis and possesses 2C DNA content (Durbarry *et al.*, 2005). The TPI for *duo2* was determined as 2.0C and relative DNA content was calculated for the mutants analysed.

2.12 Statistical analysis

Statistical analysis was performed using Microsoft Excel and statistical software package GraphPad Prism 5.0. To determine whether the average fluorescence value of sperm nuclei and the germ nuclei and the average fluorescence value from the mutant germ nuclei were statistically significant from each other, one-tailed *t-test* (Microsoft Excel software) was used assuming unequal variance was applied. The parametric student's t-test or non-paramteric Mann-Whitney U test was used to compare two data sets. Multiple comparisons were performed by means of the parametric analysis of variance (ANOVA) test or the non-parametric Kruskal-Wallis test. To determine which data sets differ in the multiple comparisons, post hoc analysis was carried out with a Tukey-Kramer test following ANOVA analysis or Dunn's multiple comparison test following the Kruskal-Wallis test. All tests were two-sided and a p-value less than $\alpha = 0.05$ was considered to be statistically significant.

The statistical assessment of genetic data was carried out with the Chi-square ($\chi 2$) test using Excel in order to determine whether the ratio of observed phenotype was significantly different from the expected ratio of phenotypes. Statistically significant outcomes were determined using significance (α) level of 0.05.

Chapter 3 Characterization of *duo5* pollen mutant

3.1 Introduction

The use of forward genetic screens has resulted in isolation of mutants affecting various aspects of pollen development in *Arabidopsis*. A number of genetics screens have been employed for male gametophyte specific mutants identification using two separate approaches, i.e. segregation distortion screens (Bonhomme *et al.*, 1998; Feldmann *et al.*, 1997; Grini *et al.*, 1999; Howden *et al.*, 1998) and the direct phenotypic screens to identify gametophytic mutations resulting in abnormal pollen grain development (Chen and McCormick, 1996; Johnson and McCormick, 2001; Lalanne and Twell, 2002; Park *et al.*, 1998). In particular, a mutagenesis screen involving DAPI-based analysis of pollen from an EMS-derived *Arabidopsis* population led to the identification of a unique class of mutants, termed as *duo* pollen mutants (described in section 1.2.1.1) (Durbarry *et al.*, 2005). This class comprises of six male gametophyte-specific heterozygous mutants. Analysis of DAPI stained mature pollen from these individual mutant lines revealed their distinct bicellular phenotype with defects in germ cell division. Each of these mutants exhibits a different germ cell phenotype and can be categorised in two groups based on the shape of the DAPI-stained germ cell nuclei. One group comprises of *duo* mutants (*duo1, duo2, duo3*) with round germ cell nucleus, whereas another group consists of mutants (*duo4, duo5, duo6*) displaying elongated germ cell morphology. Further analysis revealed that all these mutants represent different genes as they all mapped to different chromosomal locations (Durbarry *et al.,* 2005; Durbarry and Twell Unpublished). One of the *duo* mutants called *duo5* belongs to a class of pollen mutants that produces a highly elongated germ cell nucleus. The mature pollen from heterozygous mutant produces 40% to 46% aberrant pollen, which shows characteristic single germ cell phenotype. This mutant represents a unique lesion and has been assigned a distinct chromosomal position, on the lower arm of the chromosome four.

This chapter describes the cytological and genetic characterization of the *duo5* mutant. The first part of the chapter explains the pollen cytology of heterozygous and homozygous *duo5* mutant pollen using fluorescence as well transmission electron microscopy (TEM) to establish the bicellularity of the mutant germ cells. Furthermore, the pollen viability and cell fate of the mutant germ cells was determined using vital

stains and various cell fate markers respectively. The second part of the chapter illustrates the point in development where *duo5* deviates from the normal pollen developmental pathway and shows morphological differences between wild type and mutant germ cell development. The third part of the chapter investigates the gametophytic nature of the *duo5* mutant by analysing various backcrossed lines for segregation in selfed progeny as well as examining the transmission efficiency of the *duo*5 mutant through male and female gametes. In addition, tetrad analysis was performed to further get an insight into the gametophytic nature of the *duo5* mutant. Furthermore, the previously identified map position of *duo5* was further narrowed down to 250kb by applying previous and new molecular markers both north and south of the putative mutant *duo5* locus.

3.2 Phenotypic analysis of *duo5*

3.2.1 Pollen cytology and phenotypic classes in mature *duo5* pollen

Mature pollen from the *duo5* mutant was examined by light and fluorescence microscopy to determine pollen morphology and phenotype. The initial observation of the *duo5* mutant by fluorescence microscopy showed bicellular pollen consisting of a diffusedly stained vegetative nucleus and highly stained, germ cell nucleus lying close to the vegetative nucleus. Pollen grains from wild type and *duo5* were similar in size and appearance as observed under light and fluorescence microscopy (Figure 3.1).

Pollen from a number of independent plants (n=4) was stained with DAPI to observe the nuclear morphology and frequency of aberrant pollen in *duo5* plants. Analysis of pollen from wild type Nossen plants (n=4) showed no aberrant pollen phenotypes and the number of DAPI stained pollen (n=795) observed showed tricellular pollen morphology (Appendix Table A2). In the case of *duo5* mutant, DAPI staining of pollen (n=1181) from heterozygous plants showed that 40% to 46% of the pollen population contain single germ cell nucleus at mature pollen stage (Appendix Table A3). The germ cell nucleus showed different phenotypic classes that included elongated (Figure 3.1B-C), round (Figure 3.1D-E) and irregular or abnormal nuclei (Figure 3.1F). The elongated germ nuclei are present frequently as compared to round and irregular germ cell nuclei (Figure 3.1C). Approximately 62% of the mutant germ nuclei (in a mutant pollen population) show germ nucleus elongation and do not enter mitosis. The presence

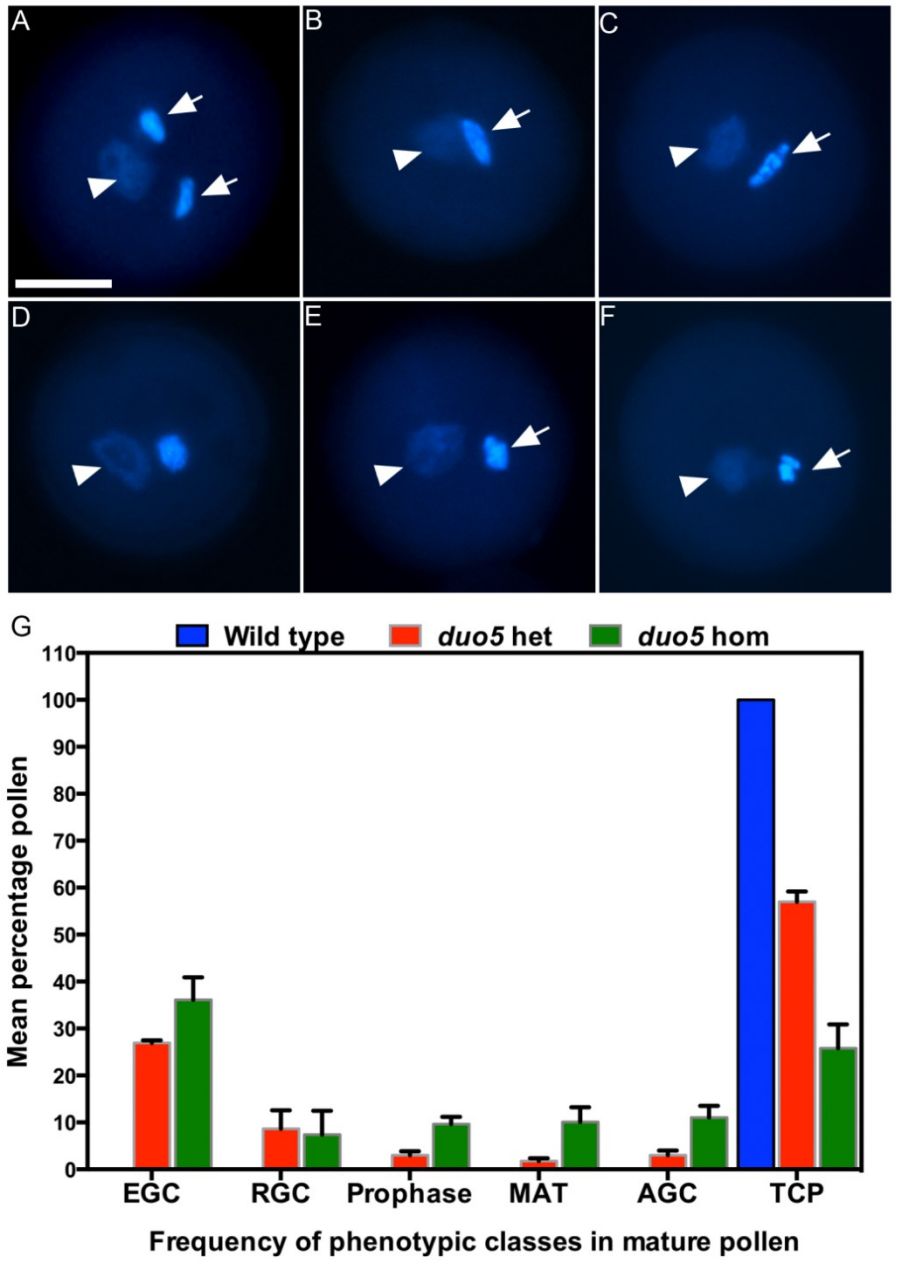

Figure 3.1: Nuclear morphology of wild type and *duo5* pollen and frequency of pollen phenotypic classes. Mature pollen from wild type and mutant plants was stained with DAPI and screened using fluorescence microscopy. Counts were made from different heterozygous and homozygous *duo5* individual lines. Data is derived from >600 pollen counted from backcrossed individual lines (n=4). **(A-F)** DAPI stained pollen from different phenotypic classes, showing **(A)** wild type pollen with two sperm cells, **(B-C)** highly stained, single elongated mutant germ cell nuclei, **(D-E)** round mutant germ cell nuclei and **(F)** mutant germ cell showing condensed chromosomes. The arrows indicate sperm cell and mutant germ cell nuclei, whereas arrowheads indicate vegetative nuclei. A diffusedly stained vegetative nucleus (arrowhead) is present in close association with the sperm cells in the wild type and germ cells in the mutant pollen. (**G)** A bar graph representing frequency of pollen phenotypic classes in heterozygous and homozygous *duo5* pollen at anthesis. Scale bar = 10µm. EGC, elongated germ cell; RGC, round germ cell; MAT, prophase-metaphase-anaphase; AGC, abnormal germ cell; TCP, tricellular pollen. Error bars represent the standard error of the mean.

of condensed chromosomes that appear as dots and threads suggests that approximately 11% of the germ cell nuclei displaying mitotic figures and 7% in abnormal phenotypic classes (representing abnormal prophases) enter mitosis. Approximately 62.5% of the mutant germ cells exhibiting mitotic figures are arrested at prophase, with few of the nuclei able to progress further and make sperm cells (Appendix Table A3, Figure 3.1G). This data suggests that *duo5* mutation is not fully penetrant and may show partial transmission through the male parent. The DAPI screening of segregating progeny in a selfed *duo5* heterozygous population showed an increase in the proportion of *duo5* plants as compared to wild type plants indicating presence of putative homozygotes. The ratio of wild type to mutant plants in heterozygous *duo5* back crossed lines significantly deviate from 1:1 ratio suggesting that a proportion of *duo5* germ cells are able to divide and transmit through male parent and produce putative homozygotes. The presence of homozygotes has not been observed in completely penetrant *duo* mutants including *duo1*, *duo2*, *duo3* and *duo4*.

Interestingly, putative *duo*5 homozygotes were identified from the selfed mutant progeny and pollen counts from different inflorescences in each homozygote was done to score the mutant phenotype percentage. The result obtained showed double the percentage of aberrant pollen in homozygote as compared to mutant pollen percentage in heterozygote. The mutant pollen percentage for putative *duo5* homozygotes ranged from 75% to 82% with the similar aberrant pollen phenotype as observed in heterozygous *duo5* mutant pollen (Appendix Table A4). In DAPI stained *duo5* homozygous mature pollen (n=614), different mutant germ cell phenotypic classes were scored that include highly stained elongated germ nuclei, elongated germ nuclei at different stages of mitosis, round germ nuclei, compact germ nuclei showing abnormal mitosis and a proportion of pollen with two sperm cells (Appendix Table A4). Plant phenotype was normal indicating specific effects on male gametophyte development.

Detailed analysis of mutant pollen phenotype in both *duo5* heterozygous and homozygous lines suggests that mutant germ cells not only show division defects but also abnormal elongation of a proportion of mutant germ nuclei. In homozygous *duo5* lines (n=4), approximately 15% of the mutant germ cells show condensed chromosomes, appearing abnormally round, representing abnormal prophase stage. Similarly, 48% of total pollen population show abnormally elongated germ nuclei in

preprophase stage of development. Despite abnormal morphogenesis approximately 26% of the *duo5* germ cells displaying mitotic figures and 15% abnormal prophasic germ nuclei enter mitosis. Of the mutant germ cells exhibiting mitotic stages, 49% stay in prophase and the rest enter other mitotic stages. This suggests that the division is not completely blocked and that some of the mutant germ cells divide and form two sperm cells. The mean percentage of tricellular pollen at anthesis in both heterozygous and homozygous *duo5* pollen population is 57% and 25.9% respectively (Figure 3.1G), which shows that a proportion of mutant germ cells divide to form two sperm cells.

The mean percentage aberrant pollen frequency calculated for *duo5* heterozygous and homozygous mutants was 43% and 74% respectively, lower than the expected frequency of 50% for a fully penetrant male gametophytic lethal mutation (Appendix Table A3, Table A4). In heterozygous *duo5* pollen population the remaining 7% of the aberrant pollen that carry *duo5* show an apparently wild type pollen phenotype. This partially reduced penetrance was confirmed in *duo5* homozygotes which produced 74% phenotypically aberrant pollen. According to the transmission efficiency of *duo5* heterozygote through the male, approximately 22% of the pollen carrying *duo5* successfully transmit the mutation whereas, 78% pollen fail to successfully fertilise an ovule (discussed in section 3.3.1). Based on this, approximately 78% of aberrant pollen should show a visible phenotype in homozygotes which is similar to the frequency observed (74%) in *duo5* homozygotes.

It can be further concluded that *duo5* is an incompletely penetrant gametophytic mutation and a proportion of mature mutant germ cells are able to divide and produce viable pollen. Furthermore, the two sperm cells are able to transmit the mutation through male parent resulting in an increase in the mutant progeny as well as generating homozygotes.

3.2.2 Ultrastructural analysis of *duo5* mature undehisced pollen using TEM

The observation that *duo5* mutant germ nuclei appear arrested at germ cell division raises the issue of bicellularity of mutant germ cells. To address this question, ultrastructural analysis by transmission electron microscopy was carried out on homozygous *duo5* mutant pollen and was compared to wild type pollen.

Before division the germ cells in the wild type pollen occupy a cortical position in the cytoplasm of the vegetative cell. When the newly formed germ cell is detaching, the germ cell callosic wall is degraded and the subsequent internalized germ cells are surrounded by two closely associated plasma membranes (Park and Twell, 2001). Assuming that first mitotic division and the associated morphological changes in *duo5* mutant pollen follow the wild type pollen developmental pattern, it can be hypothesized that *duo5* mutant pollen grains are bicellular. To test this hypothesis, ultra-thin sections from mature undehisced stage (-1 bud stage) were observed for *duo5* mutant and compared with wild type.

Examination of the sections (n=35) from mature undehisced pollen stage in homozygous duo5 do not show differences in cytoplasmic constituents compared with wild type pollen (n=22). For example the number and distribution of lipid bodies (circular electron dense bodies) appear similar in both wild type and mutant *duo5* pollen (Figure 3.2). In homozygous *duo5* mature pollen, approximately 80% of pollen population exhibited mutant phenotype and the rest of the population showed a wild type phenotype. It was easy to identify mutant germ cells in sections due to the higher percentage of elongated germ cells. The sections that contained a single germ cell were selected for *duo5* germ cell ultrastructure analysis. The sections in mutant *duo5* passed through the nucleus of the germ cell, revealing the longer dimensions and cytoplasmic constitution of the mutant germ cells (Figure 3.2E-F). Similarly, the two sperm cells contained inside the pollen grain, exhibited elongated profiles with characteristic irregular membrane protrusions (Figure 3.2A-B). The elongated mutant germ cells could easily be distinguished from the wild type sperm cells based on the abnormal elongation of the mutant germ cells. In addition, round mutant germ cells were also observed in homozygous *duo5* pollen sections that showed distinct round germ cell morphology (Figure 3.2C-D). These observations correlated well with the previous epifluorescence microscopic analysis of DAPI stained wild type and homozygous *duo5* mature pollen. In addition, pollen grains from homozygous lines exhibiting different germ cell phenotypic classes appeared indistinguishable from wild type pollen grains in pollen size and morphology (discussed in the section 3.2.1).

At mature undehisced stage, wild type pollen contains two sperm cells with intact double plasma membranes. Sections from wild type pollen containing two sperm cells

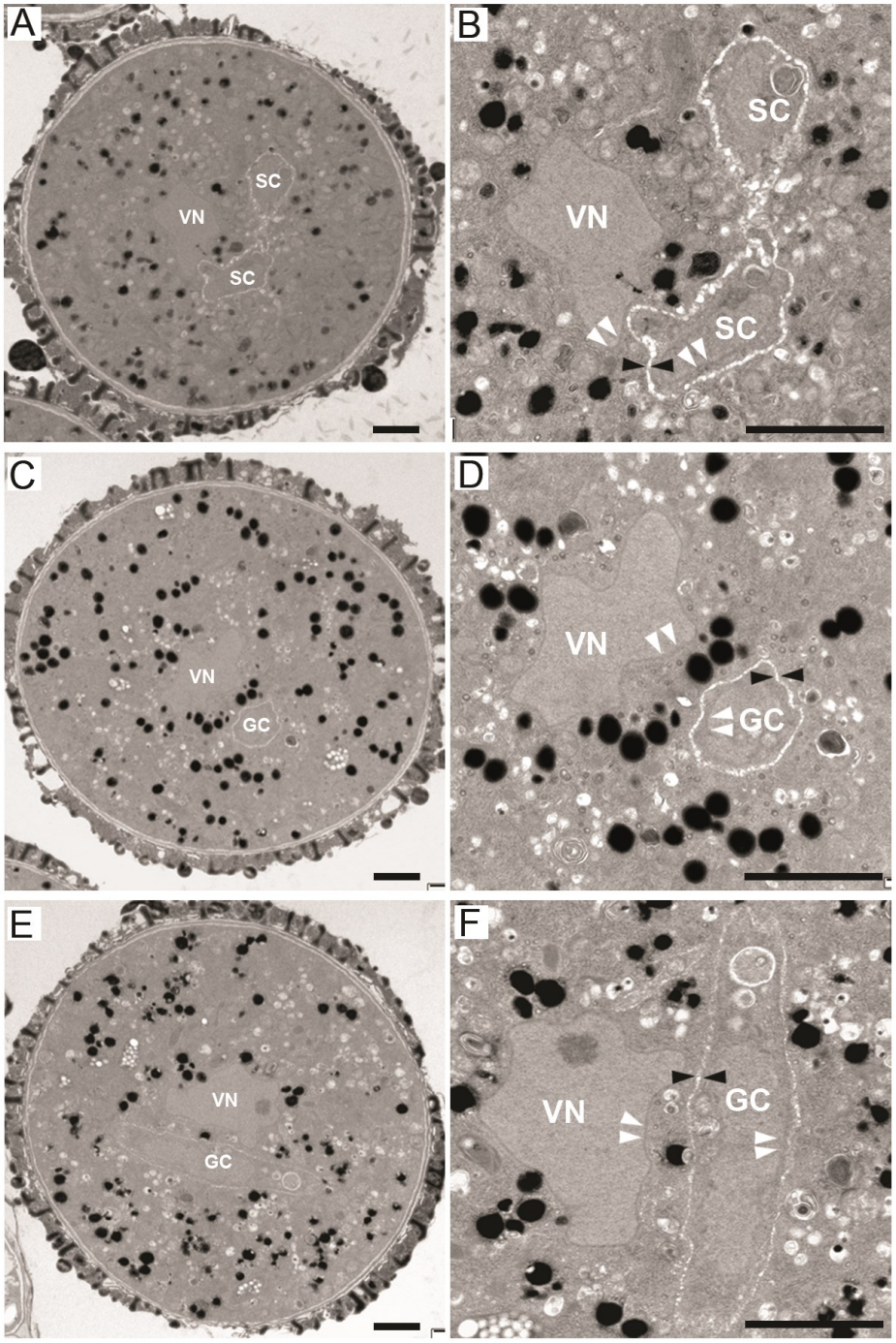

Figure 3.2: Transmission electron micrographs of wild type and *duo5* pollen sections at mature undehisced stage. (A-B) Ultra-thin section of wild type mature pollen depicting vegetative nucleus and two sperm cells surrounded by intact plasma membranes. **(B)** Image showing the vegetative nucleus and the sperm cell in close association. Sperm cells are surrounded by intact cell membranes (black arrowheads). **(C-F)** Mature *duo5* pollen grain with single round **(C-D)** and elongated germ cell **(E-F)** alongside vegetative nucleus (VN) surrounded by vegetative cytoplasm identical to wild type. The elongated and round *duo5* germ cells are also enclosed by intact plasma membranes as indicated by black arrowheads and show association with the vegetative nucleus. White arrowheads indicate the nuclear envelope and black arrowheads indicate double membranes enclosing the germ cells. VN = vegetative cell nucleus, GN = mutant germ cell nucleus, SC = sperm cells. Scale bars represent 5µm.

in paired configuration were chosen for comparison. It can be inferred (Figure 3.2C-D, E-F) from the observation that *duo5* mutant germ cells have intact plasma membranes and thus are bicellular. The germ nuclei are extended along the length of germ cell and thus show elongated morphology. The vegetative cytoplasm also showed similarity in both wild type and mutant germ cells.

3.2.3 Pollen viability of mature *duo5* pollen

Pollen viability is one of the most important aspects of male sterility. Viable pollen is competent to germinate a pollen tube and deliver two male gametes to the embryo sac. Pollen viability is assessed by 1) cytochemical staining of the grain, 2) by evaluating pollen *in vitro* and *in vivo* germination tests and 3) analysing final seed set in plants fertilised with particular pollen sample. Of these, pollen staining tests are widely used to assess pollen viability by using dyes such as Alexander staining, fluorescein diacetate (FDA) staining, and I2/KI (iodine-potassium iodide) staining. The Alexander's staining method assesses pollen viability by yielding a magenta-red colour in normal pollen grains and blue green in aborted pollen grains (Alexander, 1969). FDA stains living cells green whereas, dead cells are non-fluorescent (Jones and Senft, 1985). In the iodine-potassium iodide staining method, iodine reacts with starch in normal pollen grains, resulting in black staining (Zhu *et al.*, 2004).

FDA is a cell-permeant esterase substrate that can serve as viability probe to measure two features of the pollen grain i.e. the presence of hydrolytic enzymes capable of cleaving the diacetate portion of fluorescein diacetate and secondly the presence of an intact membrane required for intracellular retention of the fluorescent product. FDA is permeable to cell membranes in its native state, and after entry into a living cell the acetate moieties are cleaved by cytoplasmic esterases, producing fluorescein that is photoactive under UV light. The fluorescein accumulates in the pollen grains if the membranes are intact and diffuses out of the cells lacking membrane integrity. Hence, viable cells show bright green fluorescence, whereas dead cells are non-fluorescent (Jones and Senft, 1985).

In order to address the question whether *duo5* pollen is viable, mature pollen grains from heterozygous *duo5* and wild type plants were stained with the vital stain, FDA to assay the integrity of the vegetative cell plasma membrane. Vital staining for plasma

membrane integrity showed that in wild type approximately 86% (n = 412) of the pollen grains were viable and in *duo5* approximately 79% (n = 576) of mature pollen grains were viable. Percentage viability of wild type and mutant pollen was analysed using the Chi-squared test. The statistical analysis showed that the percentage pollen viability of mutant pollen is not significantly different from the wild type pollen (Table 1). The result thus suggests that pollen viability is not affected in heterozygous *duo5* pollen population.

Table 1: Pollen viability analysis in wild type and *duo5* plants

Mutant pollen membrane integrity and cell viability is analysed by fluorescence microscopy using the vital stain, fluorescein diacetate (FDA). Viable pollen shows bright green fluorescence whereas non-viable pollen is non-fluorescent under UV fluorescence. FCR (+) = Fluorochromasia positive, FCR (-) = Fluorochromasia negative, VPO = Viable pollen observed, NVPO = Nonviable pollen observed, TP = Total pollen, %NVPO = %nonviable pollen observed, %VPO = %Viable pollen observed, %VPE = %viable pollen expected.

							% based on Wild type viable pollen		
Genotype	**Lines (n)**	**VPO**	**NVPO**	**TP**	**% NVPO**	**% VPO**	**% VPE**	**X^2 value**	**Significance (α=0.05) X2=3.84**
Wild type	2	412	67	479	13.99	86.01	–	–	–
duo5 het	2	576	156	732	21.31	78.69	86.01	0.6229	ns

This finding also correlated well with the phenotypic observations of DAPI stained pollen from wild type and mutant plants. No abnormalities were observed in the mutant and wild type pollen, suggesting that *duo5* pollen viability is not affected.

Mutant pollen derived only from heterozygous *duo5* plants was stained with because at the time the staining assay was performed homozygous *duo5* plants had not been identified in a selfed heterozygous mutant population. However, with the availability of *duo5* homozygotes, viability of heterozygous and homozygous *duo5* pollen from freshly dehisced anthers was further assayed by *in vitro* germination method following a newly developed protocol by Rodriguez-Enriquez *et al.* (2013) (described in section 2.11.3). An agarose–based pollen germination media was prepared and made into a circular or rectangular pad on a microscope slide, with a cellulose membrane overlaid on the agarose pad. Pollen was placed in contact with the cellulose membrane by holding an inverted flower with tweezers and gently brushing it across the surface to spread the pollen uniformly. The slides were placed vertically in a humid sealed box and incubated in the dark at 24°C for 10 to 12 hours. The cellophane membrane with germinated

pollen was carefully removed with forceps from the agarose pad and placed on a new slide with a drop of the liquid germination media of same composition as the solid germination media without agarose. The germinated pollen was observed with fluorescent microscopy using bright field optics. A pollen grain was considered germinated when pollen tube length was at least equal to or greater than the grain diameter. Pollen from Col-0 and No-0 wild type was also germinated along with pollen from mutant heterozygous and homozygous plants. Germination percentage (%) was determined by dividing the number of germinated pollen grains by the total number of pollen viewed.

Table 2: *In vitro* pollen germination in wild type and *duo5* plants

Mature pollen from wild type and *duo5* mutant plants was placed on cellulose membrane overlaying an agarose-based pollen germination media. The germination potential of *duo5* mutant pollen was assessed and compared with wild type pollen. The number of germinated and non-germinated pollen was calculated and Chi-squared analysis performed. The analysis suggests that mean percentage germination of pollen from *duo5* heterozygous plants is not significantly different from wild type (p = 0.05). GPO = Germinated pollen observed, NGPO = Non-germinated pollen observed, TP = Total pollen, %NGPO = %non-germinated pollen observed, %GPO = %Germinated pollen observed, %GPE = %Germinated pollen expected.

						X^2 based on WT (No-0) germinated pollen			
Genotype	**Lines (n)**	**GPO**	**NGPO**	**TP**	**% NGPO**	**% GPO**	**% GPE**	**X^2 value**	**Significance (α=0.05) X2=3.84**
WT (Col-0)	2	193	55	248	22.2	77.8	–	–	–
WT (No-0)	3	309	165	474	34.8	65.2	–	–	–
duo5 het	4	495	247	742	33.29	66.71	65.2	0.1	ns
duo5 hom	4	291	548	839	65.32	34.68	65.2	41.096	*

Mean percentage pollen germination was calculated for wild type (Col-0, No-0) and mutant pollen population (heterozygous and homozygous *duo5*) and compared (Table 2). At 10 to 12 hours of germination, about 78% and 65% of pollen from Col-0 (n=2) and No-0 (n=3) wild type plants respectively (Figure A1(A-B), germinated and formed pollen tubes. The mean percentage germination rate of pollen from *duo5* heterozygous lines (n=4) was 66.7%, similar to wild type (No-0) (Figure A1(C). However, average germination rate of pollen from homozygous *duo5* lines (n=4) reduced to approximately 35% (Figure A1(D). The Chi-squared analysis revealed that the mean percentage germinated pollen in heterozygous *duo5* mutants is not significantly different from wild type germinated pollen (Figure A1(E). However, germination rate of homozygous *duo5*

pollen reduced significantly ($X^2 = 41.096$, $p < 0.05$) from mean percentage germination rate of heterozygous *duo5* and wild type pollen grains. This represented approximately 50% lower germination rate compared with wild type suggesting that pollen viability of majority of the homozygous *duo5* pollen population is significantly affected. According to the transmission efficiency through male parent, approximately 22% of the pollen carrying the mutation successfully fertilises the ovules. However, pollen germination assay suggest that a higher proportion representing 35% of homozygous *duo5* pollen population is able to germinate and form pollen tubes.

Analysis of seed fertility (seed set) represents one of the most accurate tests of pollen viability. Once established that pollen tube germination of heterozygous *duo5* pollen is similar to wild type and that a proportion of *duo5* pollen in homozygous mutant's plants is viable, the next step was to determine whether selfed heterozygous mutant plants have full seed sets or reduced seed sets. Selfed plants heterozygous for fully penetrant male gametophytic mutations are expected to produce 50% undeveloped seeds. This estimate is based on the assumption that mutant and wild type pollen tubes are guided equally to the embryo sac but mutant pollen tubes fail to initiate fertilisation, resulting in reduced seed sets. Further analysis was carried out by dissecting 10 days old mature siliques from wild type, *duo5* heterozygous and homozygous selfed plants under the dissecting microscope to identify aborted seeds and ovules. Siliques (n=7) from a wild type plant in a selfed segregating population contained approximately 99% (n=415) normal green seeds that turned brown at maturity (Figure A2(A-B) and only 1% (n=5) aborted seeds. Similarly, siliques (n=6) from a selfed heterozygous mutant plant produced approximately 87% (n=290) normal seeds (Figure A2(C-D) as well as 13.4% reduced seed set (6.6% early aborted seeds, n=22); 6.9% aborted ovules, n=23) (Figure A2(G-H). This represented an increased rate of successful fertilisation than expected 50%. However, selfed siliques (n=6) from a selfed homozygous *duo5* plant exhibited 93.4% reduced seed set (52.6% early aborted seeds, n=175; 41% aborted ovules, n=137) (Figure A2(E-F, G-H). Unlike wild type siliques that contain full and green seeds, siliques from *duo5* homozygous and heterozygous plants contain undeveloped ovules and early aborted seeds. The aborted/undeveloped ovules appear as white stubs that do not turn brown on desiccation whereas, early aborted seeds appear as small brown shriveled structures that typically turn brown as silique matures. Also white to pale green translucent structures represents mutant seeds that abort at silique maturity

(Figure A2(E-F). A Chi-squared analysis revealed that the percentage seed failure in heterozygous *duo5* siliques is significantly lower than the expected 50% seed abortion for fully penetrant male gamete defective mutations ($X^2 = 26.8$, $p < 0.05$). One possibility for the enhance seed fertility in heterozygous *duo5* plants could be that approximately 36.5% the mutant pollen tubes are able to deliver sperm cells to the ovules and successfully initiate fertilisation resulting in seed development whereas, the remaining 13.5% are able to reach ovules but fail to initiate fertilisation (Figure A2(G). Another explanation could be that due to pollen tube guidance defects, the majority of the *duo5* pollen tubes (~36.5%) are not able to compete with the wild type pollen tubes and thus wild type pollen tubes would preferentially increase the percentage seed set. A Kruskal-Wallis ANOVA revealed that that the percentage seed abortions observed was different amongst the genotypes analysed ($p < 0.0001$). Furthermore, Dunn's *post ad hoc* test revealed that percentage seed abortion in siliques form *duo5* homozygous plant is significantly different ($p < 0.001$) form the percentage seed abortion in siliques form a wild type plant (Figure A2(H). Taken together, these data suggest that the significant reduction in seed set observed in selfed *duo5* homozygous plants could be due to failure of fertilisation by the mutant pollen tube that results in approximately 52% early aborted seeds. The remaining 41% ovule abortion results from lack of fertilisation, which could indicate that *duo5* germ cells are not competent to fertilise or according to the pollen germination assay, majority of the mutant pollen is not viable and therefore is not able to germinate pollen tubes to reach the ovules in pistils. Similarly, it can be assumed that enhanced seed set in *duo5* heterozygous siliques may result from the wild type pollen tube that compensates for *duo5* pollen tube failure.

The phenomenon of enhanced fertility in heterozygous *duo5* siliques can further be investigated by crossing *duo5* pollen onto *ms1-1* or wild type pistils and analysing the siliques 3 days after pollination (DAP) by clearing and examining the number of ovules that had received one or two pollen tubes. Similar analysis could be performed to determine the fertilisation defects in the developing embryo and/or endosperm, fertilised by the mutant *duo5* pollen. Moreover, silique length measurements could be performed in wild type as well heterozygous and homozygous *duo5* plants to determine if full or reduced seed set correspond to the silique length in wild type and mutant plants respectively. Additionally, these analyses will provide further insights into the role of *duo5* in male fertility defects.

3.2.4 Cell fate analysis of *duo5* pollen

The asymmetric division of the haploid microspore results in the formation of a vegetative cell and a germ cell that have a distinct cytoplasm and unique gene expression profile that give them their distinct structures and cell fates (Twell *et al.*, 1998). To determine if arrest of the germ cell division in the *duo5* mutant is associated with cell fate changes, plants expressing different cell fate markers were crossed into *duo5* plants.

Vegetative cell fate was determined by introducing the vegetative cell fate markers, ProLAT52:H2B-GFP and ProKinase:H2B-GFP into heterozygous *duo5* plants (Brownfield *et al.*, 2009a; Twell, 1992). A single insertion marker line in a heterozygous mutant background is predicted to show 50% reporter gene expression if there is no effect on cell fate. In the case of completely penetrant gametophytic mutation, 50% of the mutant and 50% of wild type pollen from F1 plants will show marker line expression. To determine the vegetative cell fate, DAPI stained pollen from *duo5* F1 plants was scored for GFP expression using epifluorescence microscopy. Only the vegetative nucleus showed GFP signal, indicating that vegetative cell fate is not affected in the absence of germ cell division (Figure 3.3). The expression of the reporter gene in vegetative nucleus was determined by counting the number of pollen grains with and without GFP signals in both mutant and wild type pollen populations (Figure 3.3A-B, C-D). The mean percentage mutant pollen population expressing ProLAT52:H2B-GFP constituted 50% of the total mutant population. Similarly, mutant pollen from *duo5* mutant plants harbouring ProKinase:H2B-GFP (Khatab and Twell unpublished) also exhibited approximately 50% of the GFP expression. The mean percentage calculated for wild type pollen exhibiting GFP signal in a wild type pollen population was also 50% for the two vegetative cell markers analysed in *duo5* mutant background. The equal proportion of wild type and mutant GFP positive pollen observed in heterozygous *duo5* plants indicate that vegetative cell fate is maintained in the absence of germ cell division (Figure 3.4A).

To examine whether the *duo5* mutation affects germ cell fate, germline-specific markers were introduced into heterozygous *duo5* mutant plants. The *Arabidopsis* male germline-specific histone H3 marker, ProMGH3: H2B-GFP, *Arabidopsis* gamete expressed-2

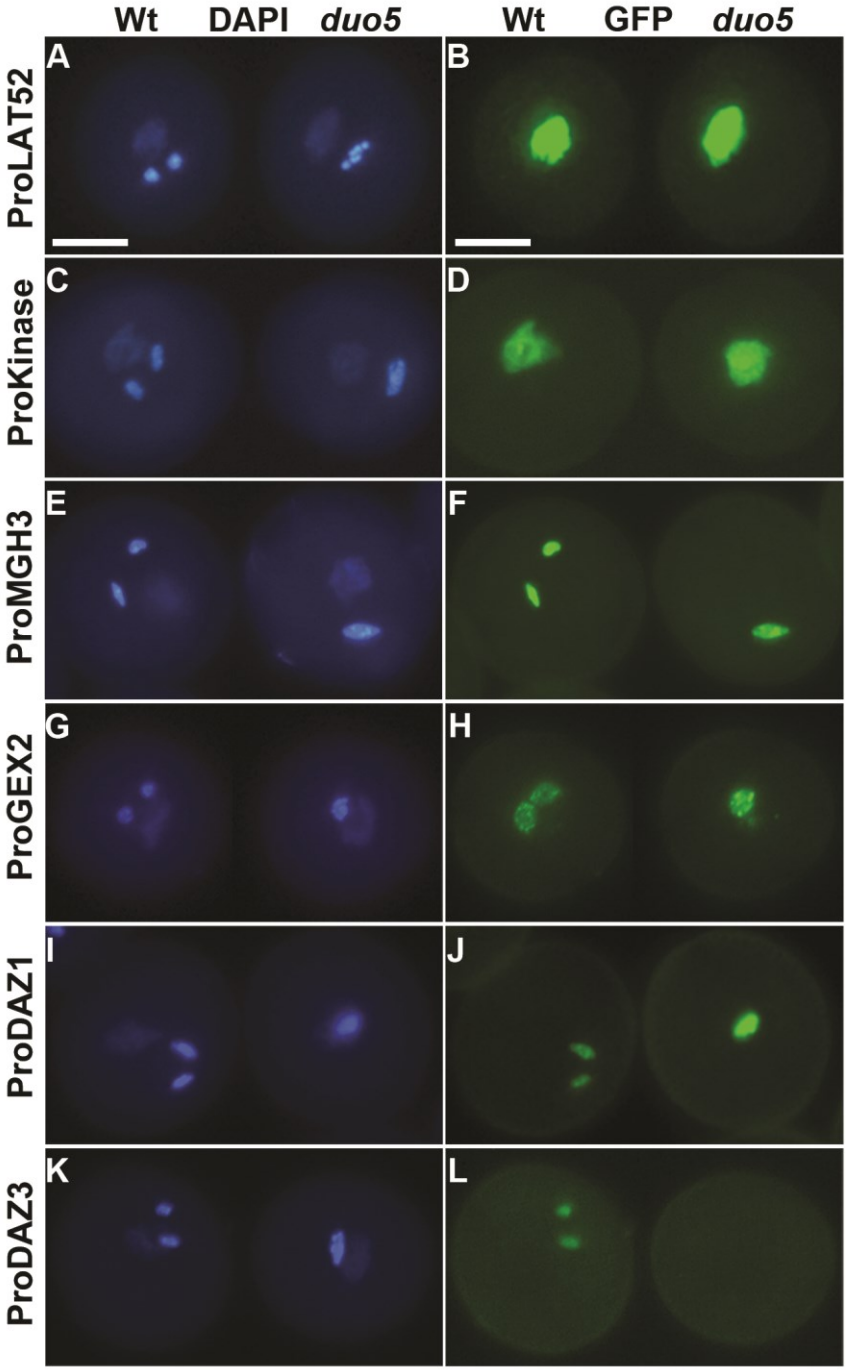

Figure 3.3: Expression analysis of cell fate markers in wild type and *duo5* pollen. (A-L) Examples of pollen grains from different heterozygous *duo5* mutant plants, expressing individual cell fate markers as viewed by fluorescence microscopy. Each image has a wild type pollen to the left and a mutant pollen to the right. DAPI stained images are shown in the left panel whereas the right panel represents corresponding GFP images expressing germ cell fate markers. (**A-D)** Normal expression of vegetative cell fate markers, ProLat52:H2B-GFP and ProKinase:H2B-GFP, is observed in vegetative nucleus of both mutant and wild type pollen. Similarly germ cell fate markers **(E-F**) ProMGH3:H2B-GFP, **(G-H)** ProGEX2-GFP**, (I-J**) and ProDAZ1:H2B-GFP are expressed normally in the mutant germ cells. **(K-L).** In the case of ProDAZ3:H2B-GFP, no expression is observed in the mutant germ cells indicating that *duo5* germ cells lack germ cell differentiation factors. Scale bars =10μm.

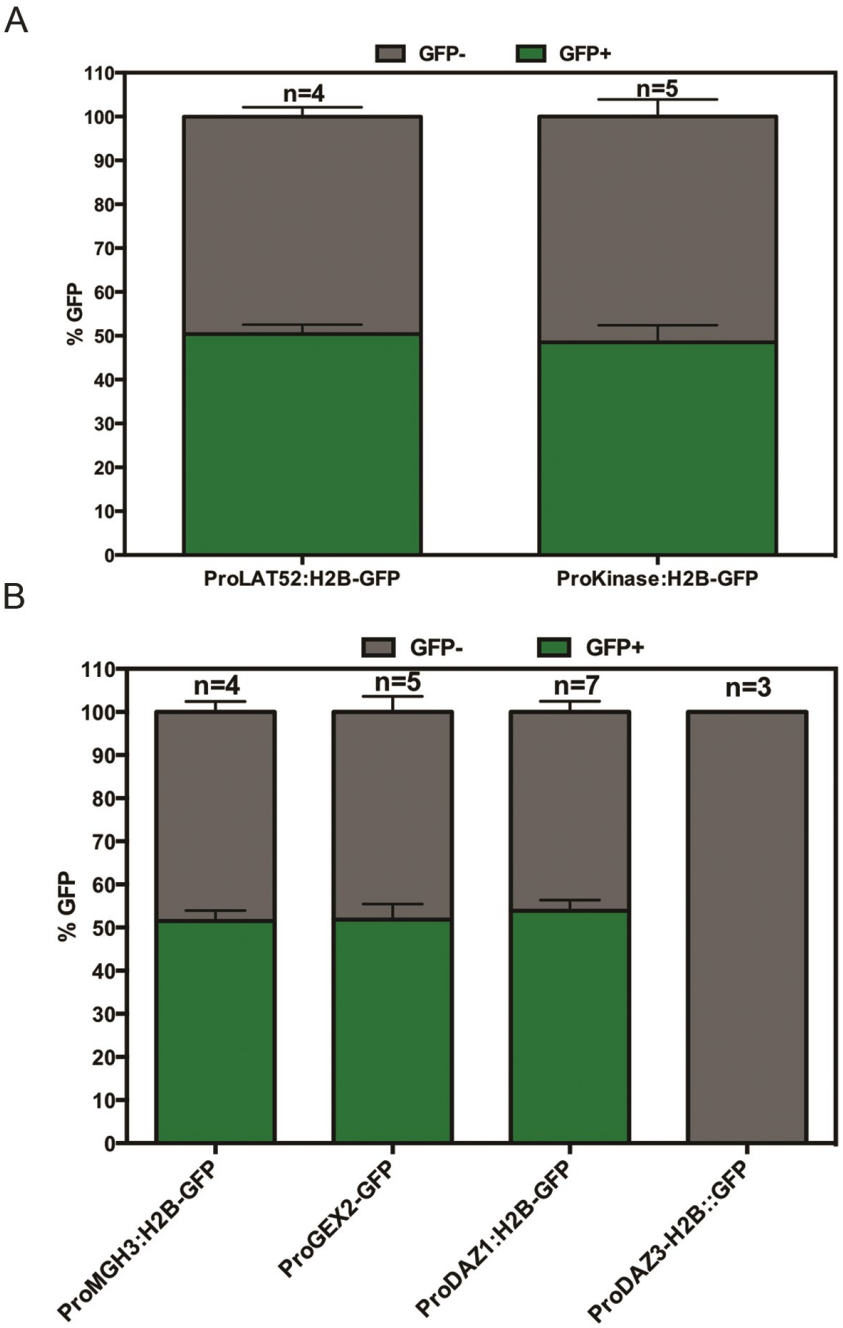

Figure 3.4: Qualitative fluorescence analysis of cell fate markers in wild type and *duo5* pollen. The mean percentage pollen showing GFP expression in *duo5* single germ cells in heterozygous *duo5* plants harboring various cell fate markers was determined by counting DAPI stained pollen for GFP expression. Counts were carried out on F1 lines with *duo5* phenotype. **(A)** The mutant population of *duo5* germ cells in individual heterozygous lines (n>3) was analyzed for vegetative cell fate markers. Approximately equal proportion of GFP+ and GFP- mutant pollen was observed indicating normal vegetative cell fate. (**B)** Bar chart representing germ cell fate analysis utilizing germ cell fate markers ProMGH3-H2B:GFP, ProGEX2-GFP and ProDAZ1-H2B:GFP in individual *duo5* heterozygous lines. The mean percentage frequency of GFP+ and GFP- mutant pollen shows that the germ cell fate is normal in undivided *duo5* germ cells. No GFP expression was observed in the single germ nuclei for ProDAZ3-H2B:GFP marker, suggesting absence of germ cell maturation factors in undivided *duo5* germ cells. Error bars represent the standard error of the mean for n number of individuals analyzed.

marker, ProGEX2-GFP and *DUO1*-activated zinc finger protein1, ProDAZ1:H2B-marker lines (Borg *et al.*, 2011; Brownfield *et al.*, 2009a; Engel *et al.*, 2005; Okada *et al.*, 2005) were crossed into *duo5* mutant plants. The expression of the three germ cell markers was observed specifically in mutant *duo5* germ cells (Figure 3.3). Independent counts were carried out and the mean percentage of GFP positive wild type and mutant pollen was determined for different germ cell fate markers analysed in in heterozygous *duo5* F1 plants. The mean percentage of wild type and *duo5* pollen scored in heterozygous *duo5* plants harbouring ProMGH3:H2B-GFP marker line was 49% and 51% respectively (Figure 3.3E-F). For ProGEX2-GFP marker, the mean percentage of both wild type and *duo5* pollen expressing GFP was 52% and 51% respectively (Figure 3.3G-H). In heterozygous *duo5* plants harbouring ProDAZ1:H2B-GFP, 49% t of the wild type pollen showed GFP signal whereas 50% of the mutant pollen expressed GFP in germ cells (Figure 3.3I-J). The equal proportion of mutant and wild type pollen expressing germ cell fate markers, suggests that germ cell fate is maintained in *duo5* mutant germ cells (Figure 3.4B). Similarly, a new sperm cell-specific marker, ProDAZ3:H2B-GFP (Borg *et al.,* 2011) was introduced in *duo5* plants to monitor expression in mutant germ cells. The expression of the marker is detected in sperm cells late after germ cell division and represents an important germ/sperm cell differentiation marker. Pollen was stained with DAPI and expression of the GFP reporter was determined by scoring pollen grains with GFP signal in both wild type and *duo5* pollen populations. No GFP expression could be detected in *duo5* germ cells (Figure 3.3K-L). In the case of wild type pollen, 50% of the wild type pollen population carrying the transgene exhibited GFP signal. The absence of GFP signal from mutant germ cells suggests that functional maturation of these germ cells could be impaired in the absence of DAZ3, resulting in incomplete differentiation of *duo5* germ cells (discussed in the section 5.4). The absence of DAZ3 expression in the undivided mutant germ cells can possibly delay the maturation of these germ cells resulting in post fertilisation defects including ovule and seed abortion.

3.2.5 *duo5* deviates from wild type pollen development at germ cell division

Examining pollen from successive bud stages in the mutant and the wild type plants provide valuable information about pollen development. In order to determine the step

in the pollen developmental pathway where *duo5* deviates from the normal pollen development, pollen grains from both the wild type and the mutant *duo5* plants were examined from different bud stages. Buds stages were established based on their arrangement on the floral axis, with +1 representing the first fully open flower containing mature tricellular pollen. The first and second unopened buds were designated as -1 and -2 stages harbouring immature tricellular pollen (Lalanne and Twell, 2002). Anthers from these bud stages were dissected; pollen was released in DAPI solution and examined by the epifluorescence microscopy. Counts were made at several stages of pollen development. No abnormalities were observed during microspore development in both wild type and mutant plants. The pattern of asymmetric microspore division in both the wild type and the mutant plants followed the same developmental path including polarization of the microspore nucleus and its subsequent division.

The germ cell formed after pollen mitosis I showed round morphology at -8 bud stage both in wild type and *duo5* mutant lines. Approximately 100% of the pollen population showed round germ cell morphology in both wild type and mutant plants. At -7 bud stage the mean percentage pollen with round germ cells was 95% and 80% in wild type and *duo5* heterozygous lines respectively. The pollen population in homozygous *duo5* lines exhibiting round germ cells remained 100%. At -6 bud stage approximately 85% and 70% of the germ cell showed round germ cell morphology in wild type and heterozygous *duo5* plants respectively. In the case of *duo5* homozygous lines, 100% of the germ cells maintained round germ cell morphology. The pollen population was highly synchronous and consisted mostly of bicellular pollen. At -5 and -4 bud stages a proportion of germ cells entered mitosis. The pollen population no longer remained synchronous and germ cells at different stages of mitosis were observed along with bicellular and tricellular pollen. The percentage of tricellular pollen at these bud stages was used as a measure of tricellular pollen development.

In the wild type plants, the percentage of tricellular pollen observed at -5 and -4 bud stages was 8.7% and 49% respectively corresponding with the appearance of mitotic figures. The proportion of tricellular pollen at the later bud stages was 100% marking the completion of the germ cell division (Appendix Table A5, Table A6, Figure 3.5A). In heterozygous *duo5* plants higher percentage of tricellular pollen at -5 stages was

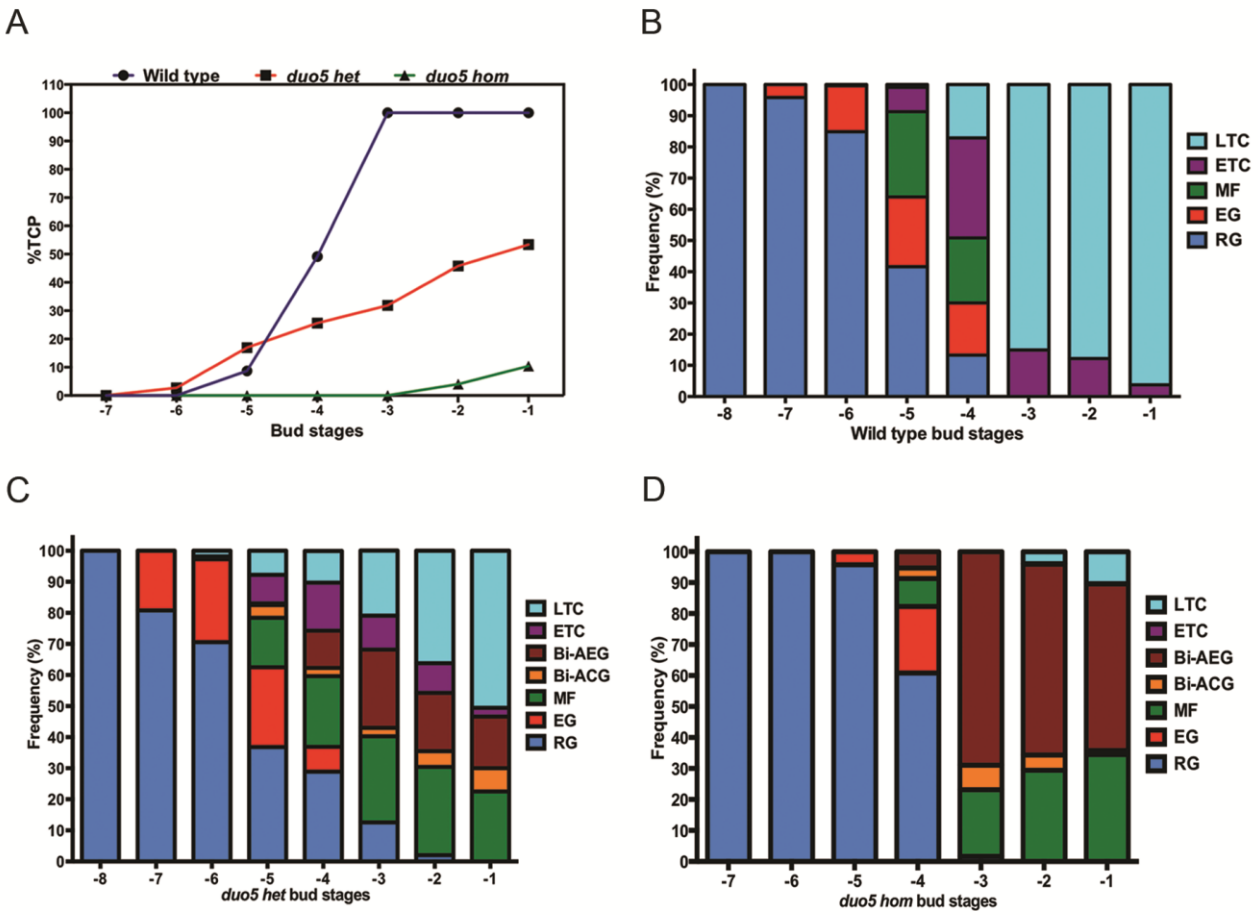

Figure 3.5: Graphs showing the frequency of different classes of pollen grains observed at different bud stages. (A) Graph showing the mean percentage tricellular pollen at different developmental stages in the wild type and in *duo5* mutant individuals. Blue, red and green lines represent frequency of tricellular pollen in wild type, heterozygous *duo5* and homozygous *duo5* mutants respectively at different bud stages during development. **(B-D)** represent compositions of pollen population in individual buds before, during and after germ cell division. Pollen from individual wild type and mutant lines (n>3) was dissected in DAPI from 2-3 mature long anthers from buds at different developmental stages and counts were made using DAPI fluorescence filter. Different classes of pollen grain were scored i.e. round germ cell nuclei (RG), elongated germ cell nuclei (EG), mitotic figures (MF), bicellular abnormally elongated germ cell nuclei (Bi-AEG), bicellular abnormally condensed germ cell nuclei (Bi-ACG), early tricellular pollen (ETC) and late tricellular pollen (LTC).

observed as compared to the wild type. About 17% of the population at -5 bud stage consisted of tricellular pollen. The percentage of tricellular pollen at -4 and -3 bud stage was not very high, consisting of 26% and 32% tricellular pollen respectively. At (-1) bud stage a maximum of 53% of tricellular pollen was observed in heterozygous *duo5* plants (Appendix Table A5, Table A7, Figure 3.5A). Similarly in homozygous *duo5* plants tricellular pollen were not observed until -2 bud stage. The percentage of tricellular pollen observed at -2 and 1- bud stage was 4% and 10.4% respectively (Appendix Table A5, Table A8, Figure 3.5A).

These results show that pollen development in the wild type and the *duo5* mutant plants remain similar until germ cell formation. The deviation from normal pollen development occurs at germ cell division, which usually takes place at -5 bud stage. The *duo5* mutation thus causes division defect at the germ cell stage of pollen development. The bud stages are not perfectly coincident between plants which can explain variation in the percentage tricellular pollen at -5 and -4 bud stages.

3.2.6 M phase of cell cycle is delayed in *duo5* mutant germ cells

The analysis of germ cells progression into M phase of the cell cycle is best studied when consecutive bud stages are analysed for the composition and nuclear morphology of different pollen populations. To understand the defects associated with germ cell division in *duo5*, the cell cycle stage of the male germline was analysed in wild type and *duo5* mutant. The pollen grains from different bud stages before, during and after germ cell division, spanning -6 to -1 bud stages, were analysed in both the wild type and the mutant *duo5* plants.

Eight successive bud stages were analysed for pollen composition. The observations were first made for the wild type bud stages. DAPI stained pollen dissected from anthers was analysed by fluorescence microscopy. At -8 bud stage, the pollen population consisted of germ cells that were detaching from the pollen wall, along with germ cells that were internalized. In the next bud stages i.e. -7 and -6 germ cells nuclei appeared round and cortical in position, marking late interphase. The later bud stages, -5 and -4, had variable pollen composition consisting of mitotic stages, bicellular and tricellular pollen. Both elongated and round germ cell nuclei were observed. The round germ nuclei underwent morphogenesis to acquire an elongated shape that marked entry into

mitosis. The large majority of mitotic figures were observed at -5 and -4 bud stages. As second mitotic division is not synchronous in anthers, the proportion of pollen in different mitotic stages in these buds varied in different inflorescences. In the subsequent bud stages (-1 and -2) a uniform pollen population consisting of two sperm nuclei was observed (Table A6, Figure 3.5B).

In the case of heterozygous *duo5* plants, the composition of pollen populations in -8, -7 and -6 bud stages was similar to that in the wild type pollen. The germ nuclei in *duo5* pollen elongated normally like the wild type pollen. The same proportion of germ cells in mitosis, in *duo5* and wild type pollen were observed at -5 and -4 bud stages. However, in the wild type pollen population no mitotic figures could be seen at -3 bud stage and onwards. Whereas in the *duo5* pollen population mitotic stages prevail until pollen dehiscence, which suggests that *duo5* germ cells enter mitosis but fail to complete division (Table A7, Figure 3.5C).

The pollen population in different bud stages in homozygous *duo5* plants showed a different trend. More than 95% of the germ cell nuclei in -7, -6 and -5 bud stages retain a round morphology. At -4 bud stage, 21% of germ cells elongate, while more than 60% of the germ cell population is still round. A small fraction of these elongated germ cells enter prophase. A dramatic change in events occurs at -3 bud stage when nearly 68% of the germ nuclei have elongated morphology and the rest progress to different mitotic stages, alongside germ nuclei (~ 8%) with abnormal mitotic arrest phenotypes. A small proportion of germ nuclei (1.69%) with a round phenotype were also observed (Appendix Table A8). The same pattern is observed in -2 and -1 bud stages, along with the formation of tricellular pollen at very low frequency i.e. 4% and 10.4% respectively. A large proportion of germ nuclei at prophase arrest could be seen in -2 and -1 bud stages (Figure 3.5D). This suggests that *duo5* germ cells are unable to divide due to a delay in mitotic progression which leads to division defect.

3.2.7 Patterns of germ cell ontogeny in wild type and *duo5* mutant pollen

According to the developmental analysis, *duo5* mutant germ cells elongate and enter mitosis but are not able to complete the division cycle. To analyse mitotic defects in *duo5*, the sequence of events during M phase of germ cell division was determined in

wild type and then compared to the *duo5* pollen mutant.

In wild type plants, germ nuclei before division elongate and then progress through different mitotic stages to form twin sperm cells. The mitotic figures were observed only in -5 and -4 bud stages. During these stages, the germ nuclei first enter prophase, which is marked by the appearance of five thread-like chromosomes and as a result of further condensation they appear as five compact chromosomes. These five chromosomes align on a plane in the metaphase stage. During anaphase two sets of chromosomes separate and move towards the spindle poles. At telophase stage the sperm cell nuclei are round. Sperm nuclei undergo partial de-condensation and begin to elongate (Figure 3.6B-G). Pollen at different stages of mitosis in -4 and -5 bud stages were scored and the mitotic index calculated (Appendix Table A9, Figure 3.6J). The mean percentage frequency of mitotic figures observed for -5 and -4 bud stages in wild type was 24% (Appendix Table A10) (n=1002 pollen).

The germ cells at early bicellular stage in heterozygous *duo5* plants showed the same morphology as the wild type. The germ cell nuclei elongated and appeared less condensed prior to mitosis. Later in the development, the increase in condensation could be observed due to an increase in DAPI fluorescence. The majority of the germ cells at different stages of mitosis could be seen at -5 and -4 bud stages. Abnormal mitotic figures were also observed in which chromosomes failed to align correctly and formed highly compact structures (Figure 3.7). At later stages (-3 to -1) mutant germ nuclei showed different condensation patterns. Nearly half of the elongated mutant germ nuclei, with visible five dots as chromosomes, were scored as prophase nuclei and the rest appeared less condensed indicating that they have not entered mitosis. The overall mean percentage mitotic index in heterozygous *duo5* mutant (Appendix Table A10) was 23.43% (n=5715).

Similarly, homozygous *duo5* mutant germ cells showed the same patterns of mitotic progression at different bud stages. The majority of the elongated mutant germ cells showed less chromatin condensation and appeared in interphase, while a proportion of germ cells were clearly in prophase (Figure 3.7). The mitotic figures observed at different stages (-4 to -1 bud stages) were counted and the mean percentage frequency calculated for different homozygous *duo5* lines was 23.6 % (n=3018) (Appendix Table A10).

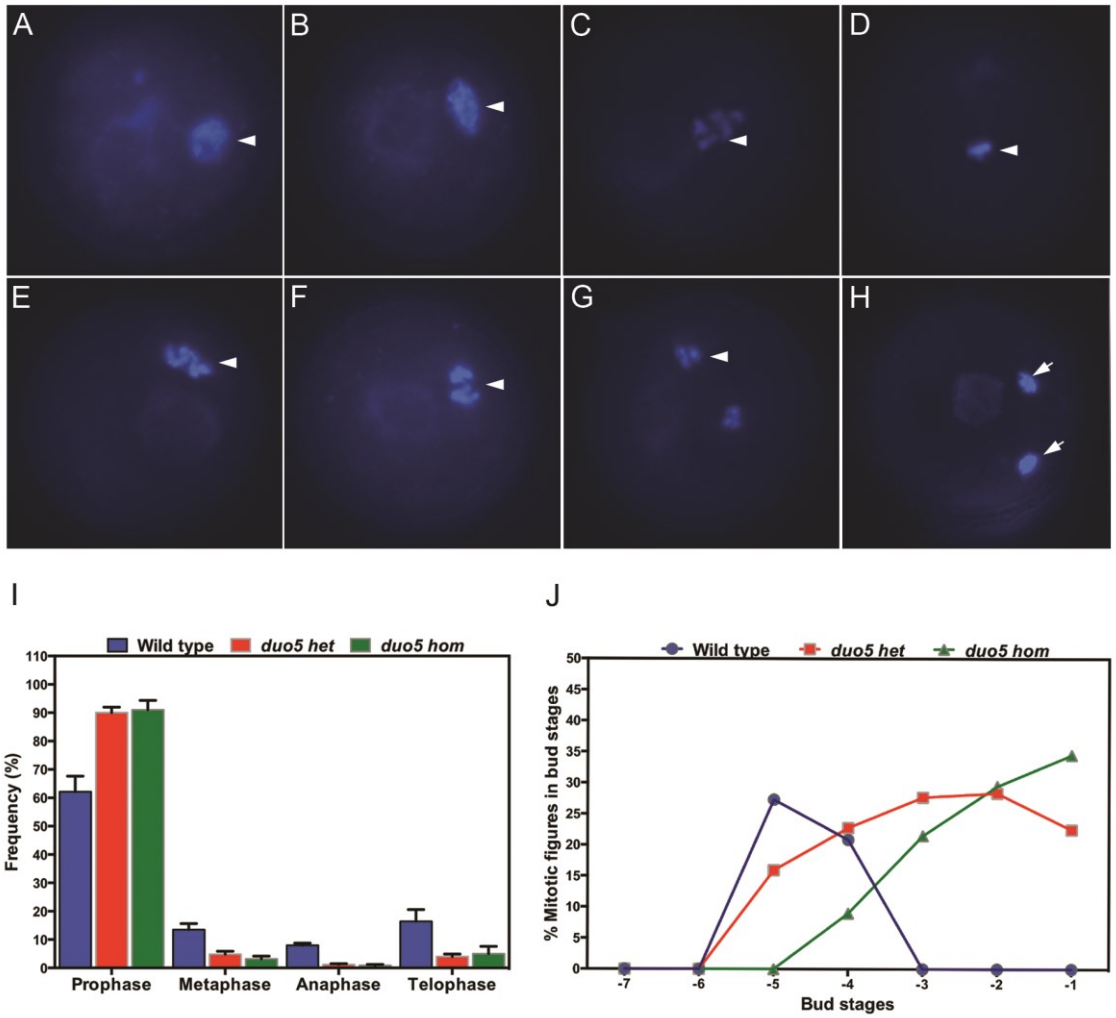

Figure 3.6: Images depicting mitotic progression and morphology of the wild type germ nuclei, during development. Pollen from wild type bud stages was dissected out in DAPI and observations were carried out under DAPI fluorescence. **(A-B)** Image depicting round and elongated germ cells before entering mitosis. **(C)** Germ cell with prophase stage showing five condensed chromosomes. **(D)** Metaphase showing germ nucleus viewed as perpendicular to spindle axis. **(E-F)** Pollen grains depicting early and late anaphase stages during mitosis, **(G)** followed by telophase stage with two groups of chromosomes separated. Two newly formed sperm cells **(H)** at the completion of the germ cell division. Scale bar represents 10µm. **(I)** The mitotic figures were counted and grouped according to the mitotic stage. Frequencies were calculated from pooled data from -5, and -4 bud stages in wild type and -5 to -1 bud stages in *duo5* mutant. Higher frequency of prophase nuclei were observed in *duo5* mutant pollen as compared to wild type while the mean percentage of metaphase and anaphase mitotic figures was greatly reduced in *duo5* mutant germ cells. Error bars represent the standard error of the mean. Arrowheads indicate germ cells at different developmental stages, while arrows indicate newly formed sperm cells. **(J)** Graph illustrating mean percentage of mitotic figures at different bud stages during development of wild type and *duo5* mutant lines. The mean percentage mitotic figures calculated for homozygous *duo5* lines appear at -5 bud stage and increase significantly during development compared to the wild type buds. In the case of heterozygous *duo5* plants, mitotic figures appear at -6 bud stages as observed in wild type buds. However, the mean percentage of mitotic figures remains high in the succeeding bud stages in *duo5* heterozygous lines, indicating delayed mitotic germ cell arrest.

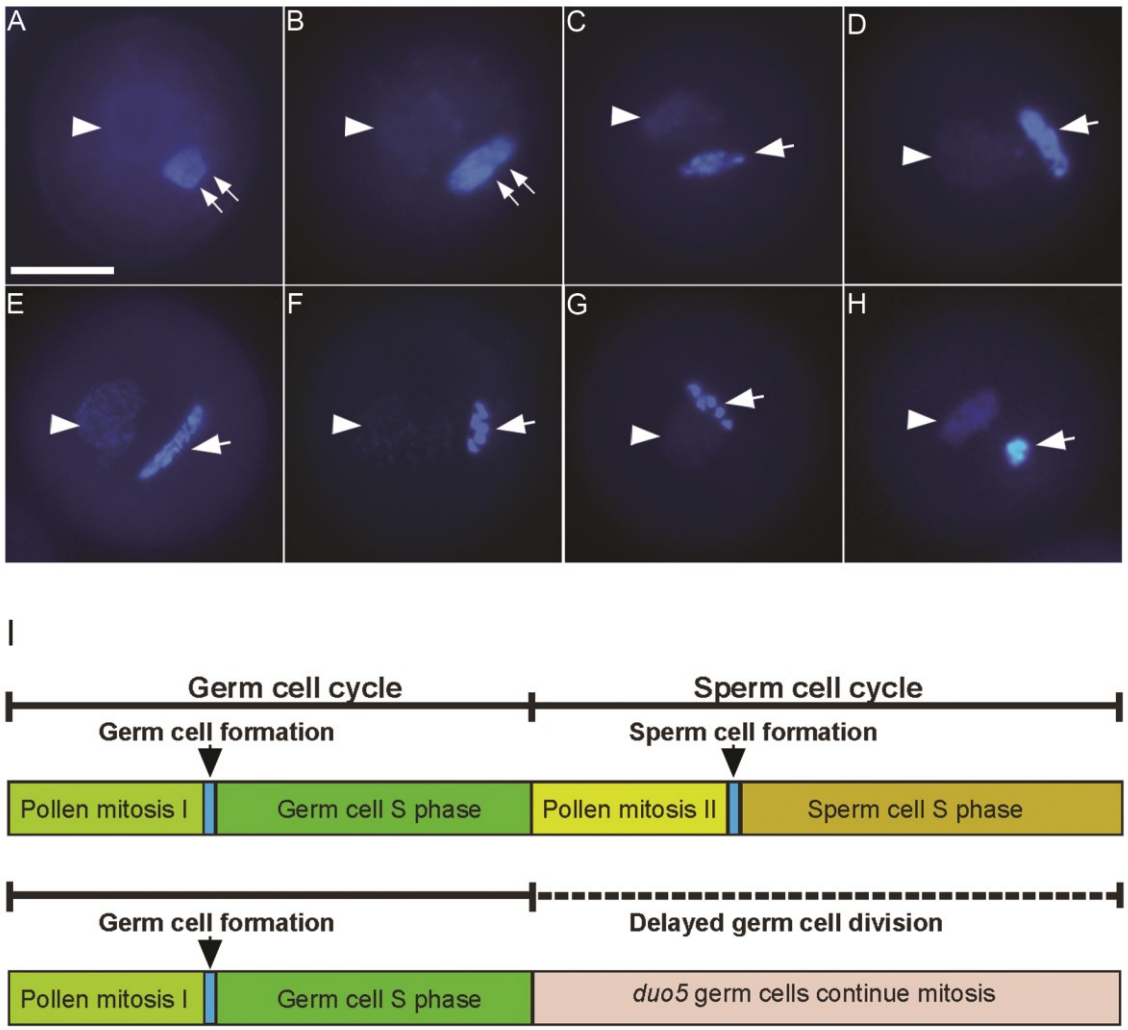

Figure 3.7: Progression of germ cell division and observation of nuclear morphology of DAPI stained *duo5* mutant pollen. Pollen from heterozygous and homozygous *duo5* lines was dissected out of the buds in DAPI and analyzed for aberrant phenotypic classes. Images **(A)** and **(B)** represent normal morphology of round and elongated germ cells before mitosis. **(C-E)** represent different phenotypes of elongated mutant germ cells showing **(C)** elongated germ nucleus with partially condensed chromatin displaying elongation similar to wild type germ nucleus and **(D-E)** abnormally elongated germ nuclei. **(F-G)** represent pollen grains depicting mutant germ nuclei at prophase stage with five dots portraying five chromosomes while **(H)** shows abnormal mitosis with condensed chromosomes congressed together with abnormally compact germ cell chromatin. Arrowheads indicate the vegetative nuclei, while arrows indicate undivided *duo5* germ cells observed under DAPI fluorescence filter. Scale bar represents 10µm. **(I)** Schematic diagram of cell cycle progression in the wild type and *duo5* mutants illustrating the stage at which *duo5* deviates from normal pollen developmental pathway. The germ cells in wild type plants complete DNA replication and enter pollen mitosis II to form two sperm cells, while *duo5* germ cells completes S phase and enter mitosis but further progression is delayed and germ cells fail to exit mitosis as a result of prophase arrest.

According to the mean mitotic index, mutant germ cells follow the wild type mitotic pattern but stay longer at prophase. An increased frequency of germ cells at prophase is scored both in heterozygous and homozygous *duo5* mutants as compared to wild type. In the wild type pollen 62% of the germ cells in mitosis are at prophase stage whereas 90% and 91% of the mitotic germ cells in heterozygous and homozygous *duo5* mutant pollen respectively remain at prophase stage (Appendix Table A9, Figure 3.6I-J). This increase could arise if mutant *duo5* pollen stays longer or arrests during early steps of the mitotic cell cycle. The reduced number of germ cells at later mitotic stages as compared to wild type supports the idea of prophase arrest in mutant *duo5* pollen (Figure 3.7I). In summary these results are consistent with distinct mitotic defects in cell cycle progression in *duo5* mutant compared with wild type plants. In wild type plants, the germ cells complete DNA replication and contain 2C DNA content. These germ cells then enter mitosis and form two sperms cells, which re-enter S phase before anthesis. However, *duo5* germ cells complete S phase and enter mitosis, but predominantly fail at prophase stage. The prophase arrest impairs the ability of the mutant germ cells to complete mitotic division before anthesis (Figure 3.7I).

3.2.8 Mutant *duo5* germ cells show higher DNA content

Observations of DAPI stained mature *duo5* mutant pollen show intense staining of mutant germ nuclei, which suggests that mutant germ nuclei also undergo DNA replication but are unable to divide. To confirm this observation, the nuclear DNA content of dehisced mutant germ nuclei was measured and compared to the nuclear DNA content of other germ cell division mutants including *fbl17* (Kim *et al.*, 2008), *duo1-1*, and *duo2* (Durbarry *et al.*, 2005).

According to previous studies (Coleman and Goff, 1985) DAPI-stained pollen grains fluoresce in proportion to DNA content. To measure the DNA content mature pollen from both homozygous and heterozygous *duo5* mutants was fixed in a fixative solution to reduce the variability of DAPI staining. For analysis 3-4 open flowers were placed in microfuge tube containing fixative solution (3:1 ethanol:acetic acid), vortexed to release the pollen and allowed to fix for 24 hours at 4°C. The flowers were then removed and the tube centrifuged at 16,000g for 30 seconds to pellet the pollen. The fixative solution was removed, replaced with 75% (v/v) ethanol and the pellet gently resuspended before

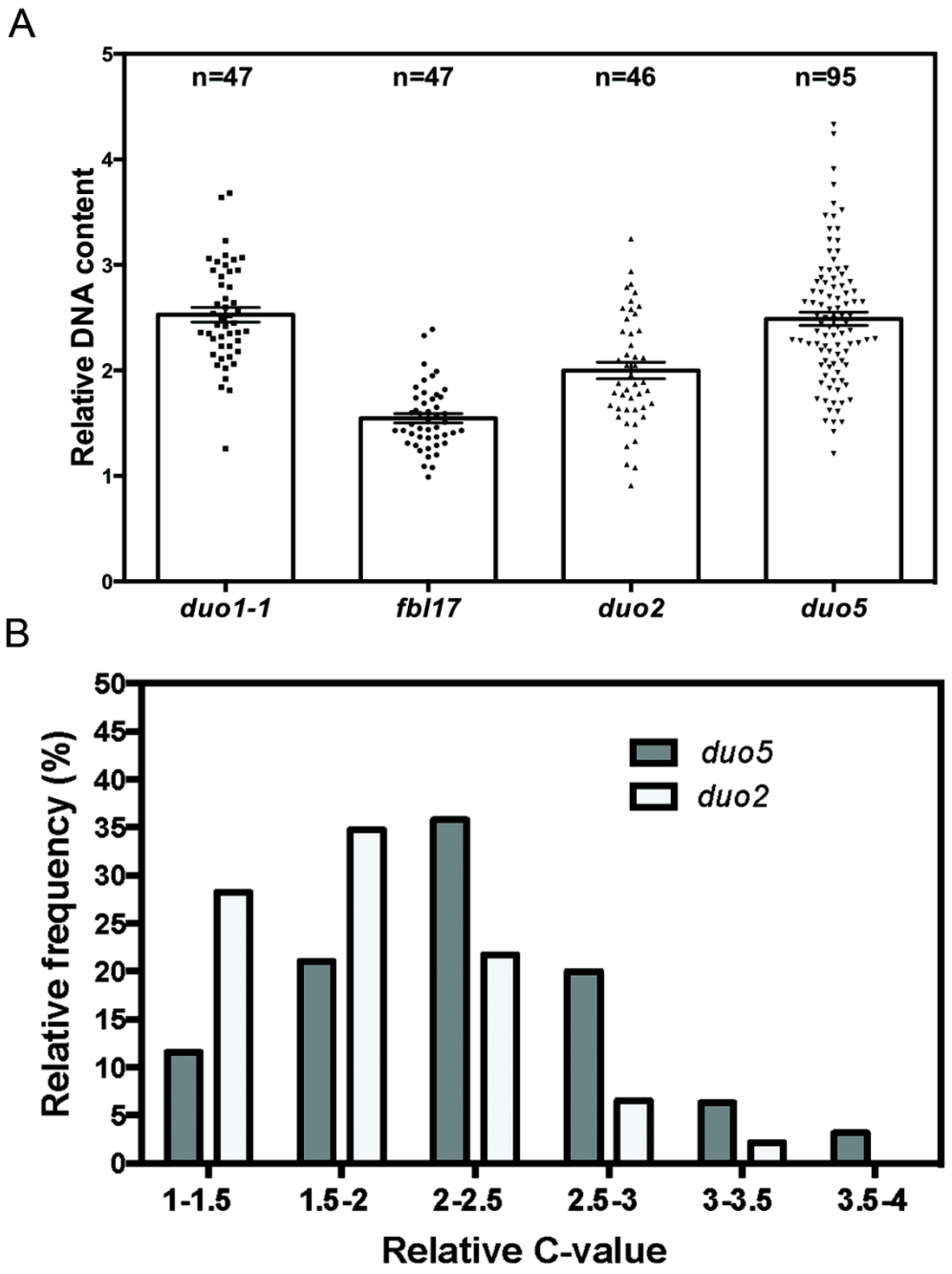

Figure 3.8: Relative DNA content measurement of the mutant *duo5* germ cells. (A) Scatter diagram showing average nuclear DNA content of *duo5* germ cell nuclei compared with that of *fbl17*, *duo2* and *duo1-1* germ nuclei. Mature pollen from each mutant was fixed overnight and then stained with DAPI and mounted on slides. Images were captured randomly using standardized conditions to calculate total pixel intensity of manually defined regions of interest encompassing germ cell nuclei. The mean total intensity calculated for n number of germ cells was corrected for the background and then normalized to 2C DNA content, the mean fluorescence of *duo2* germ cells (Durbarry *et al.,* 2005). The mean C-values are indicated along each bar for the mutants analyzed and the error bars indicate the 90% confidence interval for the calculated mean. **(B)** Distribution of the DNA content of *duo5* and *duo2* germ cells to determine the range of DNA content in the mutant germ cells. The variation in *duo5* germ cells suggests that the amount of DNA content vary in different classes of *duo5* germ cells.

storing at 4°C. Once ready to analyse, the fixed pollen samples were centrifuged at 16,000g for 30 seconds to pellet the pollen. The ethanol was removed and the pellet resuspended in GUS buffer (0.1 M sodium phosphate, pH 7.0, 1 mM EDTA, 0.1% (v/v) Triton X-100) to wash pellet of fixative and ethanol. The pollen was again pelleted by centrifugation at 13000 rpm for 30 seconds and resuspended with DAPI in GUS buffer (0.1 M sodium phosphate, pH 7.0, 1 mM EDTA, 0.1% (v/v) Triton X-100, 0.4 mg/ml DAPI) and analysed by fluorescence microscopy. Images were captured at standard exposure settings and DAPI fluorescence was measured in mutant germ nuclei as described in the section 2.11.5.

The DNA content of *duo5*, *fbl17*, *duo1* and *duo2* germ cells was determined following the procedure described above. The *fbl17* mutant is in Col-0 background, whereas *duo5*, *duo1* and *duo2* are EMS mutants in Nossen background. It was previously demonstrated that mutant germ cells in *duo2* complete S phase, enter mitosis and arrest at prometaphase and hence show 2C DNA content at anthesis, whereas more than 2C DNA content was measured in mature mutant *duo1* germ cells that complete S phase but skip mitosis and continue DNA replication, increasing their DNA content to 2.46C (Durbarry *et al.*, 2005). Similarly, the *fbl17* germ cells undergo incomplete DNA replication and therefore the average DNA content measured in the germ cells was 1.52C and 1.38C , previously reported in two different studies (Gusti *et al.*, 2009; Kim *et al.*, 2008). As *duo2* germ cell nuclei produce a mean fluorescent intensity of 2C, it was used as a reference to calculate DNA content of *duo5* mutant germ cells. The DNA content of *duo1-1* and *fbl17* was also measured at the same time and used as control.

The relative C values for the mutants were calculated from DAPI fluorescence values normalized to the mean fluorescence of *duo2* (2C) germ nuclei. The average fluorescence values calculated for *duo5* mutant germ cells corresponded to 2.49C (Figure 3.8A), similar to mean DNA content in *duo1* mutant (Durbarry *et al.*, 2005). The average DNA contents of *duo1, duo2* and *fbl17* were calculated as 2.53C, 2C and 1.55C respectively. The DNA content values in these mutants represented good control and the average C value of *duo5* mutant was compared with these values to determine the stage of germ cell cycle arrest in *duo5* germ cells. Multiple comparisons test was performed by means of the ANOVA test. The analysis revealed that the average DNA content values were significantly different among the germ cell division mutants ($p <$

0.001). To determine which of the C values are significantly different, a Tukey-Kramer multiple comparison *post ad hoc* test was employed (Benjamini and Braun, 2002), and the analysis revealed that average C values of most of the mutants differ significantly from each other. However, no significant difference was found between the average DNA contents of *duo1-1* and *duo5* germ nuclei. Interestingly, the DNA content measured in individual mutant *duo5* germ cells varied suggesting that a proportion of mutant germ cells nuclei re-enter S-phase similar to *duo1* and *duo3* thereby increasing average DNA content to 2.49C (Brownfield *et al.*, 2009a).

The range of DNA contents in mutant *duo5* germ cells was compared with that of *duo2* germ cell nuclei (Figure 3.8B). The range of relative DNA contents based on DAPI fluorescence was greater among *duo5* germ cell nuclei as compared to *duo2* germ cell nuclei. The greater variation in *duo5* germ cells thus reflects the variation in the amount of DNA in different *duo5* germ cells. Approximately 21% of the *duo5* germ cells show relative C-value close to 2C, whereas a subpopulation consisting of 55% of the germ cells has DNA content more than 2C. This suggests that a group of undivided *duo5* germ cells acquire 2C DNA content and remain at G2/M phase whereas a subpopulation of *duo5* germ nuclei with more than 2C DNA content at anthesis skip mitosis and enter another round of DNA synthesis.

3.3 Genetic analysis

3.3.1 Genetic transmission analysis

The transmission efficiency (TE) of the mutant allele through the male or female gamete describes the fraction of mutant alleles that are successfully transmitted to the progeny compared with the wild type allele (Howden *et al.*, 1998). If the mutant allele is transmitted with 100% efficiency, test cross progeny should segregate 1:1 for wild type to mutant plants, assuming that there are equal numbers of both alleles segregating at meiosis. In *duo5*, transmission of the mutant allele through female gametes was found to be normal where 80% of the megagametophytes carrying *duo5* successfully transmitted the mutation, whereas, only 22% transmission through male parent was observed demonstrating gametophytic nature of the *duo5* mutation (Table 3). A Chi-squared test shows that TE values for male transmission differ significantly from expected 1:0 ratio. Similar Chi-squared analysis revealed that TE values for female transmission do not

A

Parent	Genotype	*+/duo5*	+/+	TP	% *duo5*	TE (%)
Female	*+/duo5 X +/+*	93	116	209	44.5%	80
Male	*+/+ X +/duo5*	56	253	309	18%	22

B

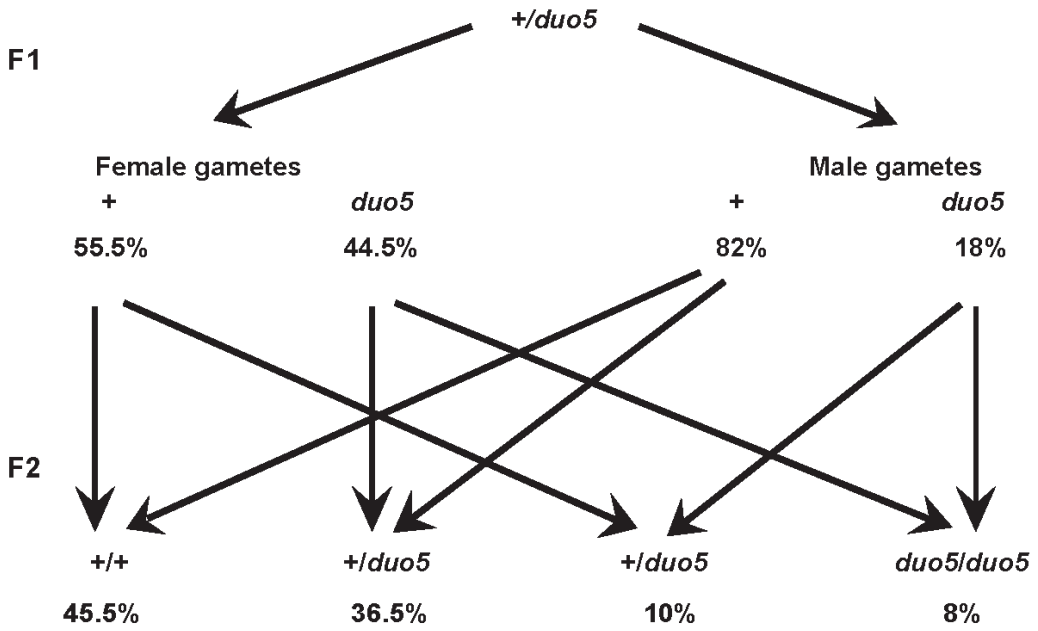

C

+/duo5 selfed progeny	*+/duo5* and *duo5/duo5*	+/+
Predicted	54.5%	45.5%
Observed	(105) 62%	(64) 38%

Figure 3.9: Genetic transmission analysis and illustration of predicted and observed progeny in selfed *duo5* heterozygotes based on observed frequency of *duo5* plants in test cross progeny. (A) Progeny from reciprocal test crosses as well as selfed heterozygous mutant plants was examined by analysing DAPI stained pollen from the progeny with epifluorescence microscopy and the percentage of mutant and wild type plants calculated. The transmission efficiency (TE) represents the percentage of mutant alleles successfully transmitted through the male or female gametes. **(B)** An illustration depicting the predicted frequency of *duo5* and wild type alleles in male and female gamete population in *duo5* heterozygous lines based on the observed frequency of mutant and wild type plants in transmission crosses. The observed frequency of *duo5* allele in male and female gamete populations was used to predict the frequencies of genotypic classes among the selfed *duo5* heterozygotes. **(C)** The predicted and observed frequency of *duo5* mutant and wild type plants in *duo5* selfed heterozygotes. The selfed *duo5* heterozygous population showed higher frequency of mutant plants (calculated in Table 3) than predicted.

deviate from expected 1:1 ratio. This confirms that *duo5* is a male specific mutation that blocks transmission of 78% of mutant pollen, but a proportion (22%) of the mutant *duo5* germ nuclei form functional twin sperm cells capable of fertilisation.

Table 3: Genetic transmission analysis of *duo5*

The number of wild type and mutant progeny from reciprocal crosses between heterozygous mutant and wild type plants are shown along with calculated transmission efficiency (TE=number of mutant/number of wild type progeny X 100) through the male (TE^{male}) and female (TE^{female}) gametes. The Chi-squared test suggests that TE values for female do not differ significantly from expected values of 100%, whereas in the case of male transmission, TE values differ significantly from expected 1:0 ratio (χ^2=3.84, p=0.05). TP = Total plants, WTP = Wild type plants.

Genotype	TP	WTP	duo5 plants	TE female	TE male	WT:duo5	Test ratio	X^2 value	Significance (α=0.05) X2=3.84
+/*duo5* X +/+	209	116	93	80	_	1.25 : 0.8	1:1	2.53	ns
+/+ X +/*duo5*	309	253	56	_	22	4.5 : 0.22	1:0	10.148	*

Furthermore, the observed frequency of *duo5* plants in test cross progeny could be utilized to predict the structure of effective gamete population in *duo5* heterozygotes (Figure 3.9A). According to the transmission data, 18% of the pollen population and 44.5% of the available ovules successfully transmit *duo5*. Transmission analysis predicts that the putative *duo5* homozygotes would occur at reduced frequency of 8% (18% of the 44.5% viable *duo5* ovules) (Figure 3.9B). Additionally, *duo5* mutant plants would comprise 54.5% of the heterozygous *duo5* selfed progeny. The frequency of mutant plants in a segregating selfed progeny was determined to be 62%, slightly higher than predicted (Figure 3.9C). The mutant progeny also included two homozygotes identified based on higher percentage of aberrant pollen frequency (discussed in section 3.3.2).

3.3.2 Screening for mutant plants segregating in selfed progeny

A male gametophytic mutation is considered to be fully penetrant if it exhibits a maximum of 50% mutant phenotype in a heterozygous plant and is considered to be male gametophytic lethal if it is specifically not transmitting through the male (Park *et al.*, 1998). In such case the selfed progeny for the mutant segregates 1:1 between wild type and mutant plants, as in *duo1* (Durbarry *et al.*, 2005). In the case of gametophytic mutants that show partially reduced transmission through male, segregation ratio in selfed progeny may not remain 1:1 and could show an increase in the number of mutant

progeny compared to the wild type. The selfed progeny from backcrossed lines (BC2) for *duo5* was screened for pollen phenotype and the proportion of wild type to mutant plants was scored (Table 4).

Table 4: Number of wild type and mutant progeny from selfed heterozygous *duo5* plants

Proportions of wild type and mutant plants from backcrossed lines are counted. The application of Chi-squared test shows that ratios of wild type to *duo5* mutant plants differs significantly from expected 1:1 ratio (χ^2=3.84, p=0.05). * = significantly different, WT = wild type plants.

					Based on 1:1 ratio	
Genotype	**Total plants**	**WT plants**	***duo5* plants**	***WT:duo5***	**X^2 value**	**Significance (α=0.05) X2=3.84**
duo5 het	**169**	**64**	**105**	**1:1.6**	**9.94467**	*

Selfed heterozygous *duo5* plants produced 64 wild type plants to 105 mutant plants. Approximately 62% of the progeny showed mutant phenotype, higher than the expected 50% for a fully penetrant mutation. The higher percentage of the mutant plants indicates the presence of putative homozygotes. Two putative *duo5* homozygotes were identified in heterozygous *duo5* selfed progeny and pollen counts from 5 inflorescences from each homozygote were done to score the percentage mutant phenotype. The results obtained showed double the percentage of aberrant pollen as compared to heterozygous plants. The putative homozygotes were out crossed as females to wild type plants of Nossen ecotype. All *duo5* F1 progeny exhibited the mutant pollen phenotype confirming them to be true homozygotes (n=189). From the Chi-squared test it was found that segregation ratios of wild type to *duo5* mutant plants differ significantly from the expected 1:1 ratio (Table 4). The low frequency of homozygotes observed among selfed heterozygous *duo5* progeny would be expected as a result of reduced transmission through the male parent.

3.3.3 Tetrad analysis

Tetrad analysis can be used as a powerful tool to prove the gametophytic functions of genes required for normal cell division in pollen development in Arabidopsis using the *quartet1 (qrt)* mutants. The *qrt1* mutant is a sporophytic recessive mutation that keeps all of the four microspores produced from single meiosis together throughout pollen development (Preuss *et al.*, 1994). In tetrad analysis, when heterozygous plant for a

gametophytic mutation is introduced into the *qrt (qrt/qrt*) background, not more than two members of the tetrad are expected to show mutant phenotype.

Heterozygous *duo5* plants *(+/+; /+duo*) were crossed as female into *qrt (+/+; qrt/qrt)* plants and the F2 progeny was screened for mutant phenotype in the *quartet* background. In homozygous *qrt1* plants, 100% of the tetrads analysed for tricellular phenotype (n=136) appear wild type, whereas in the case of heterozygous *duo5* plants, approximately 42% (n=188) of tetrads contained two aberrant member, 50% (n=113) possessed a single aberrant member, slightly more than 2% (n=6) showed presence of three aberrant nuclei and 5% (n=12) appeared as wild type with no aberrant members.

Table 5: Tetrad analysis of *duo5* mutant

The heterozygous *duo5* plants are crossed into the *qrt1* mutant, in which the four pollen grains within a tetrad remain associated (Preuss *et al.*, 1994). The phenotypes of pollen grains present within mature tetrads are analysed by epifluorescence microscopy after DAPI staining. The number of bicellular members of each tetrad is scored. WT; wild type, numbers in parenthesis indicate number of tetrads analysed.

Genotype	Ratio of WT to mutant phenotype in each tetrad			
	1:3 WT/*duo5:duo5/duo5*	**2:2** WT/WT:*duo5/duo5*	**3:1** WT/WT:WT/*duo5*	**4:0** WT/WT:WT/WT
WT:*qrt*	0	0	0	100% (n=136)
duo5:qrt	2.66% (n=6)	42% (n=94)	50% (n=113)	5.3% (n=12)

The presence of tetrads with both one and two aberrant pollen grains indicates that *duo5* is an incompletely penetrant gametophytic mutation (Table 5) and that a proportion of mutant germ cells may divide to produce tricellular pollen. The mutant pollen frequency was also calculated from the total pollen population (n=900). About 35% of the total pollen population showed aberrant pollen phenotype, slightly reduced compared with the percentage frequency of heterozygous *duo5* mutant pollen in Nossen background.

3.4 Mapping of the *duo5* mutation

3.4.1 Generation of mapping population

Positional cloning also called map-based cloning approach has been widely used to identify the protein defined by a mutation. The method is based on identifying the mutant locus that is linked to molecular or genetic markers, whose physical location on the chromosome is already known (Jander *et al.*, 2002; Lukowitz *et al.*, 2000). Another

prerequisite is the availability of F2 mapping population that segregates for the locus of interest. The mapping population is generated by crossing the mutant plant in a specific ecotype (Nossen in this work) as female to wild type plants of a different ecotype that has sufficient number of sequence polymorphisms to carry out mapping (Columbia in this work). The map-based cloning approach narrows down the genetic interval containing the mutant locus by successfully excluding all other parts of the genome. To narrow down the mapping region containing *duo5* locus, mapping populations were generated by out crossing heterozygous *duo5* plants as female (Nossen ecotype-No-0) to wild type plants (Columbia ecotype-Col-0). The F1 plants heterozygous for *duo5* mutant were identified by screening DAPI-stained pollen and were allowed to self-fertilise. Leaf DNA from F1 plants was extracted and examined to confirm presence of both Nossen and Columbia genome, using SSLP markers polymorphic between the two ecotypes. Selfed F1 plants produced both wild type and mutant *duo5* plants. In the F2 population both wild type and mutant *duo5* plants were used as the mapping population to identify recombinants (Figure 3.10). Recombinant plants have different ecotype specific genotypes in the two markers present in the mapping interval and recombination can be recorded from both sides of the mutation.

The *duo5* and wild type recombinants could be identified as the *duo5* mutation is in the No-0 background and wild type plants are homozygous for Col-0 alleles (Col-0/ Col-0) at the mutant locus. In the case of wild type recombinant plants, the presence of both the Col-0 and No-0 allele (Col-0/ No-0) would indicate a single crossover event while, two No-0 alleles (No-0/ No-0) would represent double recombination events. However, non-recombinant *duo5* plants would have C and N alleles (Col-0/ No-0) at the *duo5* locus and recombinants would have either Col-0/ Col-0 or No-0/ No-0 alleles. PCR-based molecular markers lying north and south of the mutated locus were utilized for identification of recombinants to narrow down the interval containing the mutation. By knowing the ecotype of the mutant plant, the recombination position of the mutation can identified. This can be done by determining the phenotype of the recombinant plant and comparing its phenotype with the genotypes of the north and south markers. If a *duo5* plant from a segregating F2 mapping population exhibits mutant phenotype and has Col-0/Col-0 and No-0/Col-0 genotypes in the markers flanking the mutation from north to the south respectively, it can be concluded that the mutation is located to the south of the Col-0/Col-0 marker. A wild type plant with the same marker genotype exhibiting

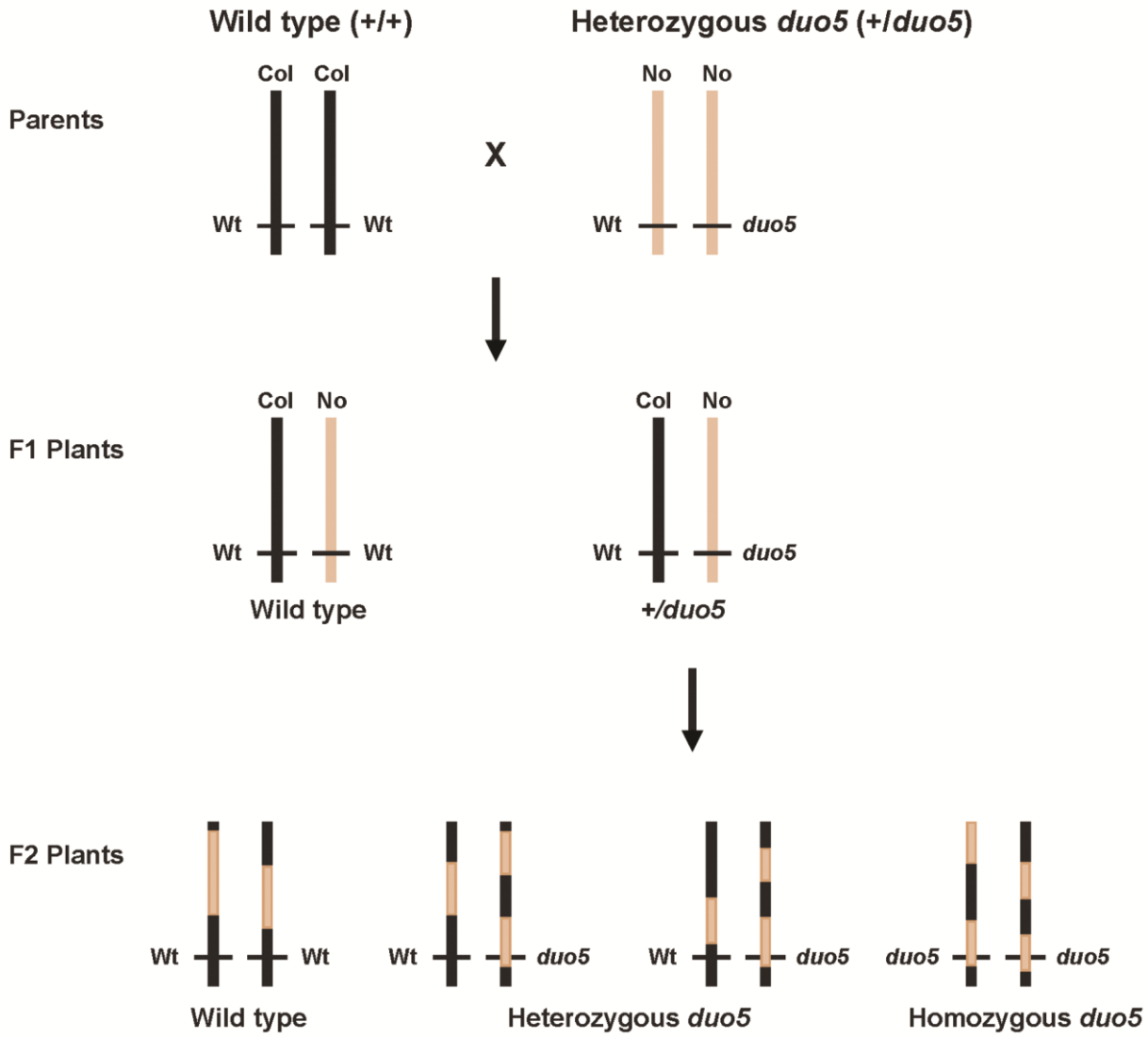

Figure 3.10: Schematic representation of the crosses performed to generate *duo5* mapping population. Heterozygous *duo5* plants in the Nossen (No-0) background were used as female parent and pollinated with pollen from wild type plants in Columbia (Col-0) background. F1 plants were stained with DAPI and screened for mutant phenotype. F1 plants that showed *duo5* phenotype were self-fertilized and the resulting F2 progeny was used as the mapping population. Both wild type and mutant plants in the mapping progeny were used to identify recombinants using SSLP and dCAPS molecular markers.

wild type phenotype would imply that the mutation is to the north of the No-0/Col-0 marker. With the availability of the recombinants and new molecular markers the interval can be further narrowed down by walking towards the mutation site from both north and south.

3.4.2 Molecular markers used to narrow down the *duo5* locus

Molecular markers used in the mapping experiment were already generated in the lab and all of them localised to chromosome IV. A number of simple sequence length polymorphisms (SSLP) (Bell and Ecker, 1994) and dCAPS (derived cleaved amplified polymorphic sequence) (Michaels and Amasino, 1998) were used to narrow down the *duo5* locus. The modification of CAPS (cleaved amplified polymorphic sequence) technique eliminates the need for the SNP to fall within a recognition site for an available restriction site. In this method termed as dCAPS, a restriction enzyme recognition site which includes the SNP is introduced into the PCR product by a primer containing one or more mismatches to the template DNA. The PCR product modified in this manner is then subjected to restriction enzyme digestion and the presence and absence of the SNP is determined by the resulting restriction digest pattern (Figure 3.11). The SSLP method is based on amplification of regions of microsatellite DNA that differ in length between two ecotypes (Bell and Ecker, 1994) (Figure 3.11). Such markers are co-dominant and can be detected on agarose gel as well as also both chromosomes of a plant could be genotyped by using a single PCR fragment amplification method. The TAIR database contains an extensive collection of polymorphisms between the ecotypes Columbia (Col-0) and Landsberg *erecta* (L*er*) but limited information is available about polymorphisms between Nossen (No-0) and Columbia (Col-0) ecotypes. Besides, data about a large number of simple-sequence repeats can be found in TAIR10, which provides a good starting point to develop further SSLP markers. Four established SSLP markers were used, that include F16G20, F27G19 T16L1A as North markers and F6G17 as south marker (Table 6). These markers were tested with wild type (Col-0 and No-0) and F1 DNA samples. The size differences were resolved on 4% agarose gel. Similarly, random fragments of DNA (approximately 1 kb fragments) in the region of interest were sequenced to identify polymorphisms. Stretches of intergenic regions or large introns were selected to maximise the chances to find polymorphisms.

Table 6: Molecular markers used to delimit *duo5* region to 250kb

Markers	BAC clone	Position(bp)	Type	Primer F	Tm ºC	Primer R	Tm ºC	Product size
F16G20	F16G20	12273361	SSLP	TGTCATTTTGTCAACCAATCGCC	66	GTGGCCTAAGTAGATTAGGACG	66	No-0 > Col-0: 144
F27G19	F27G19	13711335	SSLP	GTTCCCACTTCAACACAATTCTTCC	60.7	TGCAGCTACAGATCGCTATTTTACAC	61.7	Col-0: >, No-0: 179
T16L1A	T16L1A	16159348	SSLP	GGGAAGATTTAACACGCCAGAGAGTC	63.5	CAACAGCTCTTACCACGTTTCTACCC	63.6	Col-0: >, No-0: 168
F6G17	F6G17	17611296	SSLP	CCGACTTTGTGGCAACATTA	56.6	CAGAAGGAGCTTGCCTTGTA	57.5	Col-0: >, No-0: 164
DUO5-SNP7-SacI	F23E12	16760201	dCAPS	ATGTTTGAAGTGGTCAGTGGC	63.9	AAACCATGTTATGTAGATCGGAG**C**T	64.6	*SacI* cut *duo5* 195 (No-0)
DUO5-SNP6-NcoI	F23E12	16760061	dCAPS	AGGCTAATGATTGGAAATAGTTC	59.1	AACTATAATAATATTTAAACCC**C**AT	54.3	*NcoI* cut *duo5* 125 (No-0)
DUO5-SNP2-DdeI	F23E12	16759944	dCAPS	CTTCAAGACGAGAACTATTGGC**T**CA	66.4	GCCAATAGTTCTCGGTTCTTGAAG	65.8	*DdeI* cut *duo5* 186(No-0)
DUO5-dCAPS-DdeI	F11I11	16664410	dCAPS	TAGAAGACATGCGTTTCTTTCT**C**TT	63.2	TAAAAGAAAGAAACGCATGTCTTCTA	62.9	*DdeI* cut *Wt* 150 (Col-0)
34990-35000-Col-0_deletion	F11I11	16664039	Indel	GATTGTGGTTTTTATTCTTGTTTG	60.2	TGTCTTTCAGGTATCAAACAAACT	60.5	No-0 > Col-0: 97
34560-70-Nos-0_deletion	T4L20	16509160	Indel	CATAGATAAAGTTCTCGTGGTAA	56.7	GTCACCATGCATTTGTATGTC	60.3	Col-0: >, No-0: 136
DUO5-dCAPS-HinfI	F11I11	16509355	dCAPS	CTAAAGCATCGAATATTTGATA**G**AC	58.9	CCAATAAAAGTGAGACCAAGAT	58.7	*HinfI* cut *duo5* 213 (No-0)
DUO5-dCAPS-DdeI	F11I11	16509279	dCAPS	CATACAAATGCATGGTGACGGT	66.6	TCCAGATTAGGCATTAGCTAGT**C**TG	63.5	*DdeI* cut *duo5* 128 (No-0)
DUO5-dCAPS-HindIII	F11I11	16645623	dCAPS	ACCTGCCGTAATTAAAGTCCAAATA	64.2	ACAAGTCACACTTTCGAATTTCAA**G**	64.2	*HindIII* cut *Wt* 172 (Col-0)
DUO5-dCAPS-DdeI	F11I11	16645623	dCAPS	ACCTGCCGTAATTAAAGTCCAAATA	64.2	ACAAGTCACACTTTCGAATTTC**T**AA	61.8	*DdeI* cut *duo5* 172 (No-0)

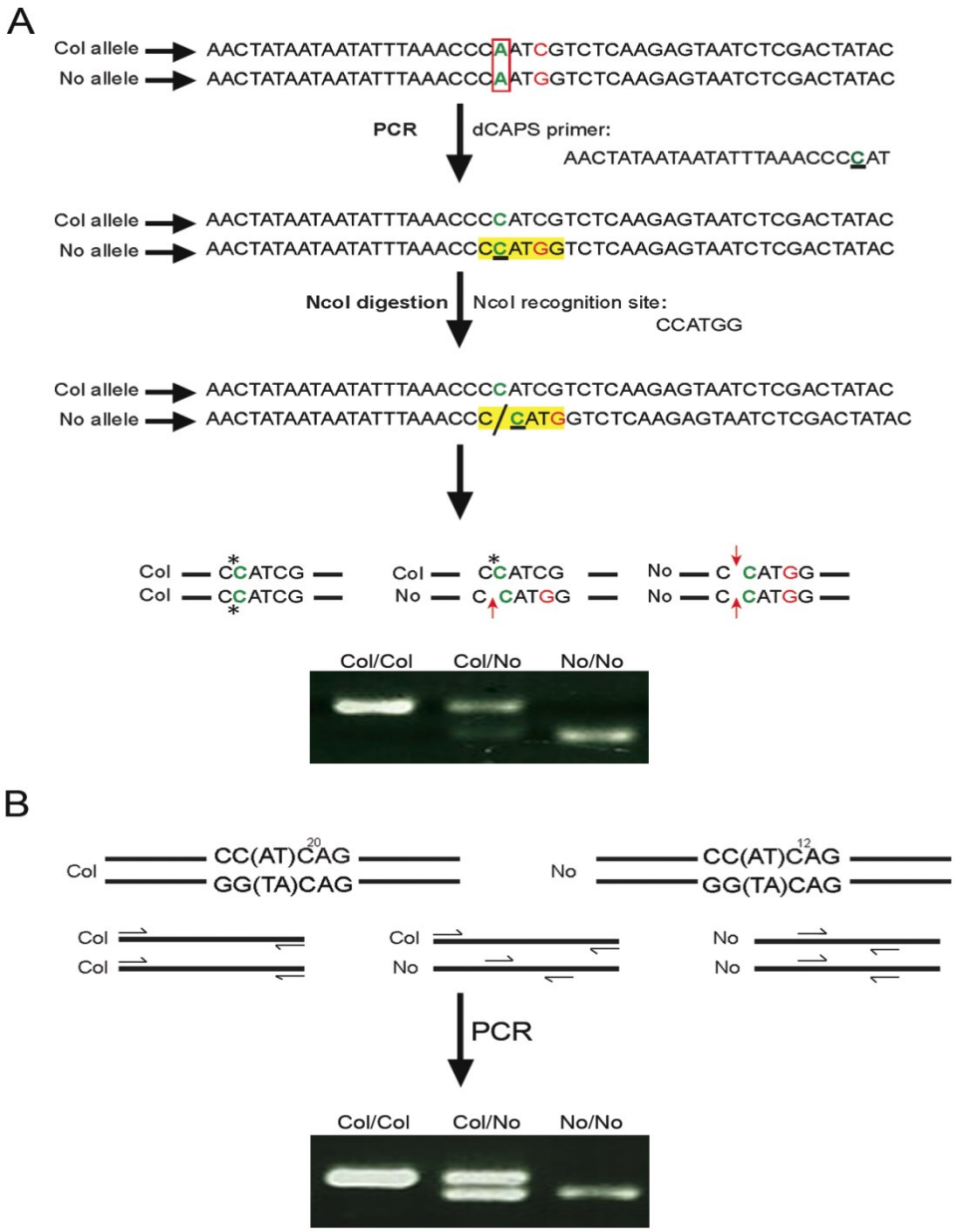

Figure 3.11: Schematic illustration showing genotyping of dCAPS and SSLP markers. (A) A single nucleotide polymorphisms (SNP) exists in Col-0 and No-0 ecotypes at a position indicated in red but does not generate a novel restriction site. To distinguish between the two ecotypes, the region of DNA containing base change is amplified using primers, which contain one mismatch (indicated in green) and incorporates the mutation into the product. The introduction of this mismatch into amplified product generates an NcoI restriction site in PCR product from No-0 allele only and hence can be digested by NcoI enzyme. The region highlighted in yellow represents NcoI restriction site in No-0 allele. The NcoI restriction sequence is written in 5'→3' direction for each homologous chromosome. PCR products are digested with NcoI enzyme and separated on 4% the agarose gel. The gel image shows three different product sizes depicting three genotypes i.e. Col/Col (single longer band), Col/No (two bands: longer Col undigested and shorter No fragment digested), No/No (one shorter band). **(B)** A microsatellite DNA region at the particular locus in Col-0 has more repeats than in No-0 ecotype. Primers are designed to anneal outside the microsatellite regions. PCR products are separated on the 4% (w/v) agarose gel and the three different ecotypes can be detected by different fragments length for the three different size PCR products.

A pair of oligonucleotides was synthesised for each DNA sequence and DNA from wild type Nossen plants was amplified and sequenced. The sequences were then compared with the existing Col-0 sequence on TAIR10 to detect polymorphisms. Simple nucleotide polymorphisms (SNPs), deletions and insertions were identified from the sequencing information. The SNPs and the deletions were used to generate ecotype specific markers (Col-0 or No-0 specific), derived cleaved amplified polymorphic (dCAPS) markers or SSLP markers (Table 6). However, two of the derived cleaved amplified polymorphic (dCAPS) markers, F11/11-Hinf1 and F23E12-Nco1were useful and were used as North and South markers respectively. These markers were also used to delimit the chromosome IV region containing *duo5* mutation to an interval of 250 kb.

3.4.3 Map position of *duo5* locus

Initial linkage was established for *duo5* by using a bulk segregant analysis. The mutation was linked to the lower arm of the chromosome 4, showing 17.5% recombination frequency with marker F16G20. Chromosomal location of *duo5* was defined between the markers nga1139 with 9.52% recombination frequency and the marker nga1107 with recombination frequency of 30.2% (Durbarry, 2004 unpublished).

Initially a small mapping population was grown and DNA was extracted from leaf material of 75 plants using CTAB DNA extraction method. The DNA was screened with SSLP marker F16G20, to confirm linkage previously established. 19 recombinants were identified and recombination of frequency 12.66% was calculated. Another marker F6G17, lying south of F16G20 was used to identify recombinants from south. A total of 9 recombinants were obtained with recombination frequency of 6%.

A new mapping population of approximately 231 F2 plants was grown in 40-compartments trays and leaf material harvested using a high throughput assay. Plant material was harvested for preparation of the DNA from individual plants in a 96-well plate. The DNA was genotyped with a marker and the PCR products were analysed on high-resolution agarose gels (4%) to identify the recombinants near the region of interest. PCR products from 96-well plates were loaded by a multichannel pipette into gel wells and analysed simultaneously in a large gel chamber. Subsequently, recombinants were re-extracted using a CTAB-DNA extraction protocol and genotype investigated with further genetic markers available. In this way, phenotypic screening of

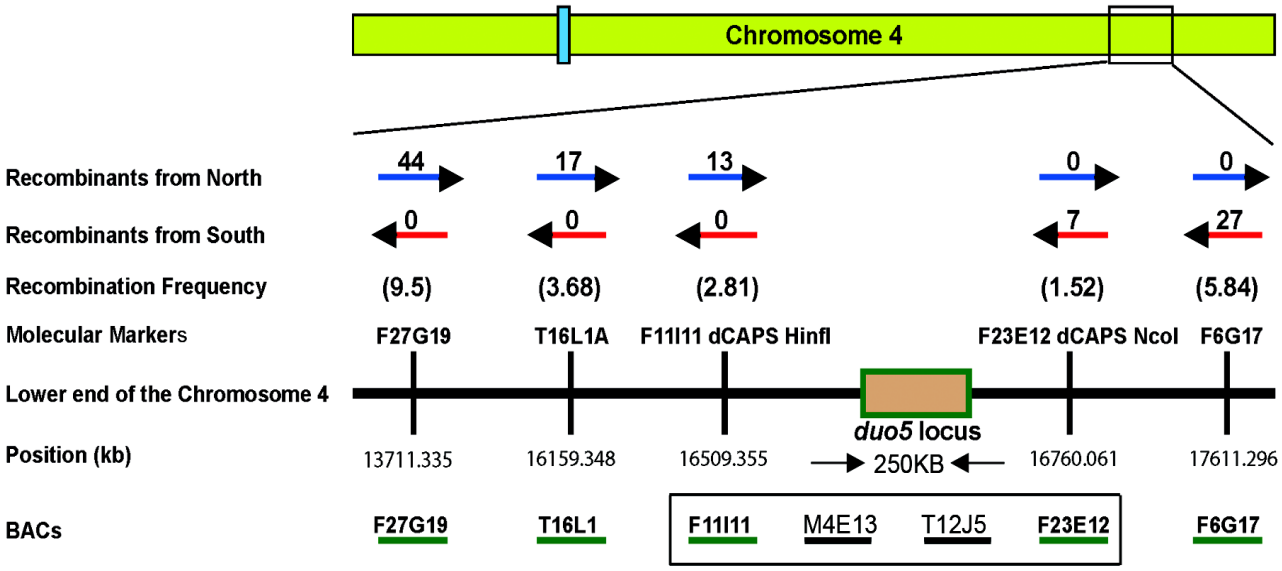

Figure 3.12: Schematic presentation of molecular markers and initial position of *DUO5* gene. Blue and red arrows show number of recombinants for each marker from the North and South, respectively. The numbers in brackets represent the recombination frequency with markers lying north and south of the putative *DUO5* locus. The recombination frequency of 2.81 and 1.52 with North marker F11I11 dCAPS HinfI and South marker F23E12 dCAPS NcoI respectively, has narrowed down the mapping region to approximately 250 kb containing four BACs indicated in a rectangular box.

only the recombinant plants were needed to determine the north and south recombinants.

The F2 mapping population was screened for recombinants with north marker F27G19 and south marker F6G17 and a total of 42 north and 26 south recombinants were selected and a recombination frequency of 9.5% and 5.84% respectively, was obtained. The pollen phenotype of recombinants was determined and both wild type and mutant plants were used for further mapping. The north recombinants were again screened with SSLP marker T16L1A and the number of recombinants was reduced to 17, with a recombination of frequency of 3.68%. Both North and South recombinants were further genotyped with F11I11-Hinf1 from North and F23E12-Nco1 from South and the number of recombinants reduced to 13 from north and 7 from south with the recombination frequency of 2.81% and 1.52% respectively. The genetic interval containing the region of interest was reduced to 250kb between BACs F11I11 and F23E12 (Appendix Table A11, Figure 3.12).

3.4.4 Candidate genes in the Mapping region

Alongside fine mapping another strategy of gene hunting had been adopted and is based on analysis of putative candidate genes located in the 250kb region of predicted *duo5*

Table 7: List of candidate genes located in putative *duo5* mapping region

Candidate genes were selected based on their potential role in cell cycle regulation or cell division processes during male gametophyte development as well as transcripts abundance in mature pollen. The candidate gene functions are listed according to TAIR10 annotation and belong to different protein families with diverse functions.

Type	Gene	BAC	Description
gene/protein	At4G34710	T4L20	ADC2 (ARGININE DECARBOXYLASE 2
gene/protein	At4G34880	F11I11	Amidase family protein
gene/protein	At4G34930	F11I11	1-phosphatidylinositol phosphodiesterase-related
gene/protein	At4G34990	F11I11	AtMYB32 (myb domain protein 32)
gene/protein	At4G35050	M4E13	WD-40 repeat protein (MSI3)
gene/protein	At4G35080	M4E13	High-affinity nickel-transport family protein
gene/protein	At4G35090	M4E13	CAT2 (CATALASE 2)
gene/protein	At4G35120	M4E13	Kelch repeat-containing F-box family protein
gene/protein	At4G35130	M4E13	Pentatricopeptide (PPR) repeat-containing protein
gene/protein	At4G35140	M4E13	WD-40 repeat family protein

locus. This new genetic interval contains four overlapping BACs i.e. F11I11, M4E13, T12J5 and F23E12 (Figure 3.12). According to information on TAIR10, these BACs harbor 73 protein-coding genes with potential roles in cell cycle regulation, cell division, and protein-protein interaction as well as transcriptional regulation. A number of genes residing on these BACs represented valuable candidates for further investigation in an attempt to maximize the chance of identifying the mutant locus. However, as the hypothetical mutation point is located in the region surrounding BACs F11I11 and M4E13, therefore candidate genes located in 25kb region on either side of the putative *duo5* locus were considered suitable candidates. Furthermore, candidate genes had been selected based on their putative function in cell cycle activities and transcriptional regulations as well as sperm cell-enriched expression according to sperm cell transcriptomic data (Borges *et al.*, 2008) (Table 7).

Table 8: List of T-DNA lines in selected *duo5* candidate genes

T-DNA alleles for the genes were ordered from NASC stock centre. Seeds were sown on the soil and plants PCR genotyped to identify hemizygous and homozygous insertion lines. Furthermore, the phenotype of the T-DNA insertion lines was scored by examining DAPI stained pollen with fluorescence microscopy.

Gene	Insertion	location	Coordinates	Gene Product size (bp)	T-DNA Size (bp)
At4g34990	SALK_132874.48.95.x	Exon	W/16661475-16661670	1908	400
At4g35050	GABI_870A03	Intron	W/16684240-16684328	750	900
At4g35140	SAIL_196_H02	5'UTR	W/16726621-16726884	715	800
At4g35270	SALK_009675.40.25.x	Promoter	C/16781120-16781529	1142	500
At4g35270	SALK_009712.14.35.x	Promoter	C/16781197-16781258	1142	500
At4g35370	SALK_005176.54.50.x	5'UTR	C/16814967-16815058	1064	800

The loss-of-function mutants represent valuable resource to investigate gene function and to characterize the phenotypic changes associated with the gene mutation. To determine if the disruption of gene function in candidate genes result in *duo5* phenotype, T-DNA insertions spanning 5'UTR, promoter, intron and exons of the selected candidate genes were chosen for analysis. The T-DNA insertion mutagenesis results in disruption of the DNA sequence due to random integration of the transgene into different locations in the genome (Krysan *et al.*, 1999). This leads to alteration in the normal function of the affected gene, thus creating a loss-of-function mutant. SALK, GABI and SAIL lines in selected genes from the candidate genes list (Table 8) as well as two additional genes that were considered candidates in the previously identified

mapping region of 1452kb, were ordered from the NASC stock centre (Scholl *et al.*, 2000) (Table 8). Seeds were sown on soil and more than 10 plants from each line were PCR screened to identify lines hemizygous or homozygous for the insertion. Mature pollen from these lines was stained with DAPI and analysed with fluorescent microscope to observe possible aberrant germ cell phenotype. According to T-DNA genotyping results, a number of hemizygous and homozygous lines were identified, however, no visible phenotype was detected in mature pollen. The lack of observable phenotypes in these lines could suggest that *duo5* mutation is not a loss-of-function but rather gain-of-function mutation and therefore loss of function T-DNA lines in putative candidate genes do not exhibit observable phenotype. Although the candidate genes selected, showed sperm cell enriched expression, however, additional experiments are required to determine whether the lack of phenotype is due to insertional mutation not affecting expression. This may include performing RT-PCR on the cDNA generated from RNA sample from homozygous *duo5* pollen. If minimal changes in expression of candidate genes are observed this may strengthen the idea that *duo5* represents a gain-of-function mutant and that the loss-of-function T-DNA insertional mutants are unlikely to recreate germ cell division arrest phenotype.

3.5 Discussion

EMS mutagenesis is the most commonly used method in plants to generate a wide range of mutant phenotypes. A unique class of mutants termed as *duo* mutants produce single germ cell at dehisced anther stage. This chapter describes in detail, phenotypic and genetic characteristics of a novel germ cell division mutant termed *duo5*. A series of experiments were performed to determine phenotypic and genetic characters of the *duo5* mutant as well as to delimit the mapping region containing mutant locus responsible for the aberrant germ cell division phenotype.

3.5.1 *duo5* is a novel male germ cell division mutant exhibiting distinct bicellular phenotype

The novel gametophytic mutant, *duo5* belongs to a class of germ cell division mutants that shed bicellular pollen at anthesis. The phenotypic analysis revealed that the mutant pollen grains exhibit different phenotypic classes including round, elongated and

abnormal germ cell nuclei. A male gametophytic mutation is considered fully penetrant if it produces 50% aberrant pollen (Park *et al.*, 1998). Heterozygous *duo1* and *duo2* mutants shed approximately 50% bicellular pollen containing single germ cells and showing complete penetrance of the mutation (Durbarry *et al.*, 2005). In the case of *duo5*, the percentage aberrant pollen varied between 40% to 46% in *duo5* heterozygous and 75% to 82% in homozygous plants, demonstrating the incompletely penetrant gametophytic nature of the mutation. The *duo* mutants (*duo1*, *duo2*, *duo3)* generally possess round germ cell morphology at anthesis (Durbarry *et al.*, 2005), however, *duo5* germ cells displayed abnormally elongated germ cell morphology. The elongated germ nuclei represented a dominant phenotypic class and comprised 62% of the mutant pollen (27% of the total pollen) in a heterozygous line and 48% in *duo5* homozygous lines. Approximately 11% of the mutant germ cells in heterozygous mutant population and 26% of the mutant germs cells in homozygous lines exhibited mitotic figures, suggesting that division is not blocked but delayed. Majority of the germ cells were not able to progress beyond prophase stage indicating that mutant germ cells failed to align on metaphase plate to initiate chromosome separation. In eukaryotes, a core feature of the cell cycle control is the transient and cyclical appearance of the cyclin-dependent kinases that are required for G1/S and G2/M transitions. In *Arabidopsis* male germline, DUO1 is required for the expression of G2/M regulator CYCB1;1 that is expressed in actively dividing cells (Brownfield *et al.*, 2009a), whereas its degradation is mediated by APC, allowing cells to exit mitosis (Pesin and Orr-Weaver, 2008). In *duo5* germ cells proper sequence of mitotic events is impaired suggesting that *duo5* germ cells may undergo checkpoint arrest and therefore exhibit delay in mitotic progression. This delay causes the mutant germ cells to skip PMII and enter another round of DNA replication as observed in *duo1* mutant germ cells (Brownfield *et al.*, 2009a).

Further analysis revealed that *duo5* pollen grains were uniform in morphology and appeared indistinguishable from wild type pollen grains as viewed by bright field microscopy. The mutation appeared to affect germ cell division without causing apparent pollen morphological defects or collapsed pollen. Transmission electron microscopy analysis also revealed that pollen structure, size and cytoplasmic constituents were similar in wild type and mutant pollen. Ultrastructure analysis further showed that *duo5* mutant germ cells were surrounded by intact plasma membranes, validating the fact that mutant *duo5* pollen grains exhibit bicellularity. Interestingly, the

elongated germ cell profiles were also observed in the TEM images. The abnormal elongation phenotype distinguishes *duo5* from other germ cell mutants. The morphogenesis of newly formed germ cell to form an elongated, lenticular or spindle shape is associated with the reorganization of the microtubules arrays located in the cortical region of the cytoplasm. Moreover, previous studies have shown that endoplasmic and sub-cortical microtubules are involved in germ cell shape change (Dubas *et al.*, 2012). In this context, microtubules associated proteins (MAPs) that appear after PMI represent excellent candidates to explore their role in germ cell division and morphogenesis. Miss expression/overexpression of proteins such as Mitogen-activated protein kinases (MAPKs) and MAPs could possibly result in impaired germ cell division causing abnormal elongation of mutant germ cell. Moreover, in *Arabidopsis* a WD40-containing protein called NEDD1 has been investigated for its critical role in microtubule organization during microspores division. In the loss-of-function *nedd1* mutant, the mutant spindle loses length control and expands across the cytoplasm in the dividing microspore resulting in an abnormally elongated spindle (Zeng *et al.*, 2009). Overexpression of WD proteins that show increased expression levels during male germline development could represent potential candidates for further analysis to identify *duo5* mutation.

3.5.2 *duo5* germ cells depart from wild type developmental pathway at germ cell division and continue M phase of the cell cycle

Detailed analysis of progressive bud stages in wild type and mutant *duo5* plants established the precise point in pollen development where *duo5* germ cells deviated from normal developmental pathway. Previous studies have shown that asymmetric division at PMI is critical for the correct cell fate of the male gametophyte (Twell *et al.*, 1998). To determine if the germ cell fate of impaired *duo5* germ cells is maintained, vegetative and germ cell fate markers were analysed in *duo5* heterozygous plants. The analysis indicated that vegetative and germ cell fate markers are correctly expressed in mutant pollen grains suggesting that fate of both vegetative and germ cell is not altered. Cell fate analysis also revealed that the *duo5* mutation specifically affects germ cell division. Furthermore, microspore polarisation and division in mutant and wild type buds followed similar developmental pattern and the earliest defect was only seen at germ cell division. During development, round germ nuclei underwent morphogenesis

and acquired elongated shape that marked entry into M phase of the cell cycle. Wild type germ cells entered M phase of the cell cycle at -5 and -4 bud stages and completed division by -3 bud stage. In contrast, mutant germ cells failed to enter or complete germ cell division. At these bud stages, mutant germ cells exhibited different phenotypic classes including abnormally elongated non-mitotic germ cells, round germ cells, germ cells with abnormal prophasic nuclei as well as mitotic germ cells at different stages of mitosis. In wild type buds, mitotic figures were observed only at -5 and -4 bud stages whereas, in heterozygous and homozygous *duo5* pollen, mitotic stages prevailed until pollen dehiscence. Moreover, frequencies of mitotic figures in wild type (-4, -5) and mutant (*duo5* het = -1 to -5, *duo5* hom = -1 to -4) buds were calculated to determine specific mitotic defects in *duo5* germ cells. According to mean mitotic index, proportion of mitotic figures in heterozygous and homozygous mutant buds was similar to wild type. However, the distribution of mitotic stages differed in wild type and mutant buds. Mitotic figures in wild type buds consisted of 62% of prophases whereas in heterozygous and homozygous mutant buds pollen grains with prophases constituted 90% of the mitotic figures, higher than the wild type. This resulted from the increased frequency of germ cells at prophases and could arise if mutant germ cells stay longer or arrests at prophase stage of mitosis. Furthermore, reduced frequencies of germ cells at later stages of mitosis compared to wild type supports the idea that *duo5* germ cells elongated and entered mitosis but exhibited division defect specifically at prophase stage resulting in delayed mitotic progression and subsequent failed division. *Arabidopsis* male gametophytic mutant *duo2* also displays higher proportions of prometaphase figures as compared to wild type resulting in prometaphase arrest (Durbarry *et al.*, 2005).

3.5.3 *duo5* germ cells appear to be arrested at G2/M phase or endocycle

In addition, to further investigate the cell cycle stage at which *duo5* germ cells were defective, relative DNA content of mutant germ nuclei was determined by measuring DAPI fluorescence relative to germ cell nuclei of *duo2* (Durbarry *et al.*, 2005). It was previously reported that *duo2* germ cell nuclei have C values close to 2C immediately prior to germ cell division, similar to wild type prophasic nuclei and remain constant until anthesis. The mutant germ cells of *duo2* represent good control as aberrant germ cells complete S phase and arrest at prometaphase (Durbarry *et al.*, 2005). Therefore,

DNA content of *duo5* germ cells was calculated relative to *duo2*. Furthermore, relative DNA content measurement revealed that *duo5* germ cells possess average C values of 2.49C similar to mean DNA content of *duo1* germ cells. The increased DNA content indicated that mutant *duo5* germ cells enter another round of DNA replication. DNA content of individual *duo5* germ nuclei varied and distribution of C values ranged from 1.5C to 3.5C, which possibly reflects technical variation in the measurement of fluorescence. However, majority of the germ cells exhibited C values ranging from 2C to 3C. The analysis suggested that 21% of *duo5* germ nuclei exhibited fluorescence values closer to 2C, whereas, majority of mutant germ nuclei contained more than 2C DNA content suggesting that these germ cells skip mitosis and continue S phase similar to the continued replication that occur in wild type sperm cells (Friedman, 1999). Mutant germ cells thus appear to be arrested at two stages of the cell cycle i.e. in G2/M transition and in endocycle According to previous studies germ cells that fail to enter mitosis or display delayed mitotic progression contain DNA content closer to 2C (Brownfield *et al.*, 2009b). It would be interesting to determine whether mature *duo5* germ cells that contain 2C DNA content, exhibit pre-mitotic arrest or delayed mitotic progression phenotype. Moreover, DNA content of developing *duo5* germ cells at early, mid and late interphase could be measured in order to determine whether the mutant germ cells maintain C values similar to wild type germ cells while progressing through S phase of the germ cell cycle or whether DNA replication stage is accelerated in the mutant germ cells prior to germ cell division. Previous studies have shown that presence of non-degradable CYCB1;1 in dividing cells inhibit mitotic exit and subsequent entry into S phase (Weingartner *et al.*, 2004). According to Brownfield *et al*., (2009b), only the population of *duo3* germ cells that degrade CYCB1;1 re-enters S phase. The expression of CYCB1;1 in *duo3* germ cells was monitored by analysing activity of ProCYCB1;1:MDB-GFP construct, in which CYCB1;1 promoter and N-terminal mitotic destruction box (MDB) were fused to GFP. The aberrant *duo3* germ cells that showed persistent GFP expression possessed 2C DNA content at anthesis, whereas undivided *duo3* germ cells in which CYCB1;1 was degraded, had re-entered S phase as they contained more than 2C DNA content. Interestingly, mutant *duo5* germ cells also exhibit variability in DNA content and a population of mutant *duo5* germ cells show persistent GFP expression (ProCYCB1;1:MDB-GFP) in mature pollen at anthesis. Similar analysis could be carried out to measure the DNA content at anthesis of the

mutant *duo5* germ cells harbouring ProCYCB1;1:MDB-GFP. The DNA content could be measured in two distinct *duo5* germ cell populations i.e. population of mutant germ cells containing non-degraded CYCB1;1 and therefore exhibiting persistent GFP expression and group of mutant germ cells that degrade CYCB1;1 and therefore re-enter S-phase. The initial analysis of mature *duo5* pollen exhibiting persistent GFP expression suggests that mutant germ cells failure to exit mitosis could be due to incomplete activation of the Anaphase Promoting Complex (APC), that sequentially degrades its substrate proteins including CYCB1;1 to promote exit from mitosis (Heyman and De Veylder, 2012). Recent studies have shown that plants overexpressing *APC8* in the male germline produces increased numbers of bicellular pollen at anthesis, partially mimicking *duo1* phenotype (Zheng *et al.*, 2011). In this context, it is likely that in *duo5* germ cells, the mitotic division is impaired due to lesions in cell cycle components of APC causing delay of germ cell division thus creating aberrant germ cell phenotype.

3.5.4 *duo5* is a male specific incompletely penetrant gametophytic mutant required for germ cell division

The screening of progeny from selfed heterozygous mutant plants revealed that *duo5* mutant produced higher ratio of mutant plants than wild type plants (Table 4). The increased mutant progeny also contained homozygotes that were verified by progeny testing. The gametophytic nature of the mutant was further analysed in a tetrad background using *qrt1* mutant (Preuss *et al.*, 1994). The existence of tetrads containing one and two aberrant pollen grains indicated that *duo5* is an incompletely penetrant gametophytic mutation. Moreover, the genetic transmission of the *duo5* mutant was assayed by counting the frequency of mutant plants in the F1 generation resulting from a cross between wild type (No-0) pistils and pollen from heterozygous *duo5* plants. The transmission analysis revealed that *duo5* is normally transmitted through female parent but show reduced transmission through the male parent indicating that *duo5* specifically affect male gametophyte development. According to the analysis, approximately 78% of *duo5* germ cells are unable to transmit through the male parent, whereas, a proportion of 22% of the mutant germ cells form functional twin sperm cells capable of fertilisation. In the case of other *duo* mutants including *duo1*, *duo2* and *duo3,* male transmission is strongly reduced through the male parent (Brownfield *et al.*, 2009a; Durbarry *et al.*, 2005). In order to identify the lesion causing germ cell division defect, map-based

cloning approach was adopted. A number of molecular markers were employed to identify recombinants from north and south. This mapping strategy delimited the *duo5* locus to a 250 kb region on lower arm of chromosome four. Furthermore, candidate genes within the interval were identified based on the increased transcripts levels in the transcriptomic data at mature pollen stage. Mature pollen from loss-of-function T-DNA lines in the selected candidate genes did not show observable phenotype, suggesting that T-DNA insertional mutants did not affect expression. This also indicates that *duo5* mutation could be gain-of-function mutant; however, further expression analysis of candidate genes is required to determine whether lack of phenotype is due to insertional mutation not affecting expression.

3.5.5 Candidate genes in *duo5* locus

List of candidate genes contain protein encoding genes with novel functions. Two of these candidate genes include WD-40 repeat proteins (At4g35050, At4g35140). The WD40 repeats are short and approximately 40 amino acid motifs that represent prominent features within proteins that mediate diverse protein-protein interactions. Studies suggest that repeated WD40 domains play central roles in biological processes such as cell division and cytokinesis, apoptosis, light signalling and vision, cell motility, flowering, floral development, meristem organization, protein trafficking, cytoskeleton dynamics, chemotaxis, nuclear export to RNA processing, chromatin modification, and transcriptional mechanism (Stirnimann *et al.*, 2010).

In *Arabidopsis* several WD40-domain containing proteins act as key regulators of plant-specific developmental events. A WD40 repeat protein related to the animal NEDD1/GCP-WD protein also termed as NEDD1 has been investigated for its role in cell division in microspores. The analysis of T-DNA insertion allele of the single NEDD1 gene showed negative effect on the microtubule organization by altering organization of phragmoplast microtubules. The dividing microspores exhibited aberrant MT organization and spindles were no longer restricted to the cell periphery and became abnormally elongated (Zeng *et al.*, 2009).

Another candidate gene is a member of R2R3 MYB gene (At4g34990) coding for transcription factors in *Arabidopsis thalaiana* and change in levels of this protein may affect pollen development by affecting the composition of the pollen wall.

Kelch repeat containing F-box family protein is another gene (At4g35120) which plays critical role in the controlled degradation of cellular regulatory proteins via the ubiquitin pathway.

Chapter 4 Characterization of a pair of novel C2H2 zinc finger encoding proteins DAZ3 and DAZ3L

4.1 Introduction

The development of male gametophyte is governed by the interplay of regulatory mechanisms that are necessary to ensure production of twin sperm cells. To understand the molecular events that play key role during male gametophyte development, a series of transcriptome data sets have been generated in the genetic model *Arabidopsis*. Key studies have been conducted using the Affymetrix ATH1 GeneChip platform to characterize the transcriptomes of mature pollen grains and earlier developmental stages. The studies have generated large amounts of data and has revealed genome-wide expression profiles from microspores to mature pollen (Honys and Twell, 2004; Pina *et al.*, 2005), the sperm cell transcriptome (Borges *et al.*, 2008) and transcript changes associated with pollen germination and tube growth (Qin *et al.*, 2009; Wang *et al.*, 2008). The wealth of information these datasets offer will play an enormous role in deciphering various regulatory networks governing the male germline development.

Both forward and reverse genetic studies targeted at male gametophyte development have been utilized to isolate and characterize several germline genes that affect germline development. DUO1 is one such important germline regulator, identified in a forward genetics screen. DUO1 represents the first characterized male germline transcription factor (Rotman *et al.*, 2005). It has already been established that *DUO1* coordinates cell cycle progression with germ cell fate to ensure formation of two functional sperm cells. It is achieved by regulating germline specific genes i.e. *MGH3* (Okada *et al.*, 2005), *GEX2* (Engel *et al.*, 2005) and *GCS1 (HAP2)* (Mori *et al.*, 2006). *DUO1* is also required for germline expression of the G2/M regulator *Cyclin B1:1* (Brownfield *et al.*, 2009a). Further studies targeting the function of DUO1 has revealed that ectopic expression of *DUO1* in an estradiol-inducible manner in seedlings activates its target genes in sporophytic tissues. This ability of *DUO1* to activate its targets in ectopic tissues has been exploited by carrying out a time-course microarray experiment using an estradiol-inducible m*DUO1* cDNA altered at the microRNA binding site. Seedlings were grown in the presence and absence of inducer for three independent time points of 6, 12 and 24

hours. RNA was isolated from three biological replicates for the uninduced and induced seedlings at each time point and subjected to microarray analysis using Affymetrix *Arabidopsis* ATH1 genome arrays. The output of this study revealed 63 putative targets that showed a 3-fold increase in signal between uninduced and induced samples at the 24 hour time point after induction of *DUO1*. Out of these, 14 target genes have been validated as DUO1-targets by demonstrating their promoter activity in the male germline and their promoter transactivation in transient luciferase assays. The genes in DUO1 regulatory network have been termed as DUO1-activated target (DAT) genes (Borg *et al.*, 2011). These putative *DUO1*-targets represent various gene families including transcription factors. Three of the targets discovered in the experiment belong to C2H2 transcription factors family of zinc finger proteins and hence referred to as DUO1-activated zinc finger proteins i.e. DAZ1, DAZ2, and DAZ3. Further *in silico* analysis has identified a homologue of DAZ3 in *Arabidopsis,* termed as DAZ3L. The first part of this chapter describes the independent validation of DAZ3 and DAZ3L genes as DUO1 targets using transient luciferase assays and also by monitoring expression of these two novel zinc finger proteins in the *duo1* background by generating stable H2B-GFP marker lines driven by their native promoters. The second part of this chapter discusses structural and functional domains of the two novel genes and identifying putative regulatory regions in the promoter of both genes. The final part of this chapter highlights the importance of putative MYB sites in these target promoters, which play critical role in the transactivation of these targets by DUO1.

4.2 Regulation of genes encoding novel zinc finger proteins, DAZ3 and DAZ3L, by DUO1

4.2.1 Expression profiles of DAZ3 and DAZ3L from microarray data

The ability of DUO1 to activate its target genes in sporophytic tissues was further exploited by carrying out a time-course microarray experiment using an estradiol-inducible mDUO1 cDNA. Seedlings were grown in the presence and absence of inducer for three independent time points of 6, 12 and 24 hours. RNA was isolated from induced and uninduced seedlings at each time point and subjected to microarray analysis. The DUO1-activated target genes were selected for further analysis on the basis of their 3-fold induction between the mean expression values of induced and uninduced replicates

Figure 4.1: Expression analysis of DAZ3 and DAZ3L from microarray data and their activation by DUO1 in transient assays and in the male germline. (A) Graphical representation of the fold induction of three putative DUO1-activated genes during a time course microarray experiment. These three genes belong to two different groups based on their response to ectopic DUO1 expression (Borg *et al.,* 2011). DAT genes, DAA1 and PCR11 showed a 3-fold increase after 12 hours of induction, whereas DAZ3 responded after 24hour induction. **(B)** Line graph depicting expression of DAZ3 and DAZ3L during pollen development as predicted by AGRONOMICS microarray data, unpublished work conducted in Twell lab (Le Trionnaire and Twell unpublished). Both DAZ3 and DAZ3L show marginal hybridization signal at unicellular and bicellular pollen stage, and show a marked increase at tricellular and mature pollen stages. Signal values shown signify data from AGRONOMIC microarray analysis, which corresponds to single hybridization event. UNM, unicellular microspore, BCP, bicellular pollen, TCP, immature tricellular pollen, MPG, mature pollen grain. **(C)** DAZ3 and DAZ3L promoters show DUO1 dependency for activation in a transient expression assays in tobacco leaves. Bar chart represents relative luciferase activity (FLuc/RLuc) of both target promoters in the absence (-) and presence (+) of mDUO1 as an effector. Data was gathered from at least eight independent infiltrations and the standard error of the mean calculated, as indicated by error bars. The experiment was repeated twice on two different days and the graph here represents data from one of the experiments. Assays were performed two days after infiltration of tobacco leaves. **(D-E)** Images representing expression of ProDAZ3:H2B-GFP and ProDAZ3L:H2B-GFP marker lines in the *duo1* background. Pollen from these lines was stained with DAPI and analyzed with fluorescence microscopy. Counts for GFP expressing pollen were carried out on mature pollen shed from T1 lines with *duo1* phenotype. DAPI fluorescent images are shown in the top panel with corresponding GFP images below. The expression of GFP reporter is visible in the sperm cells in the wild type pollen population (indicated by arrows), while no GFP could be detected in the *duo1* germ cells (indicated by arrowhead). Scale bar represents 10μm **(F-G)** Bar charts representing mean percentage frequency of pollen in T1 Lines expressing GFP in the wild type sperm cells and mutant *duo1* germ cells harboring ProDAZ3:H2B-GFP and ProDAZ3L:H2B-GFP constructs. Means were calculated from at least three lines. Both DAZ3 and DAZ3L show significantly reduced activity in *duo1* germ cells as compared with wild type sperm cells (Chi-squared analysis: $p<0.001$).

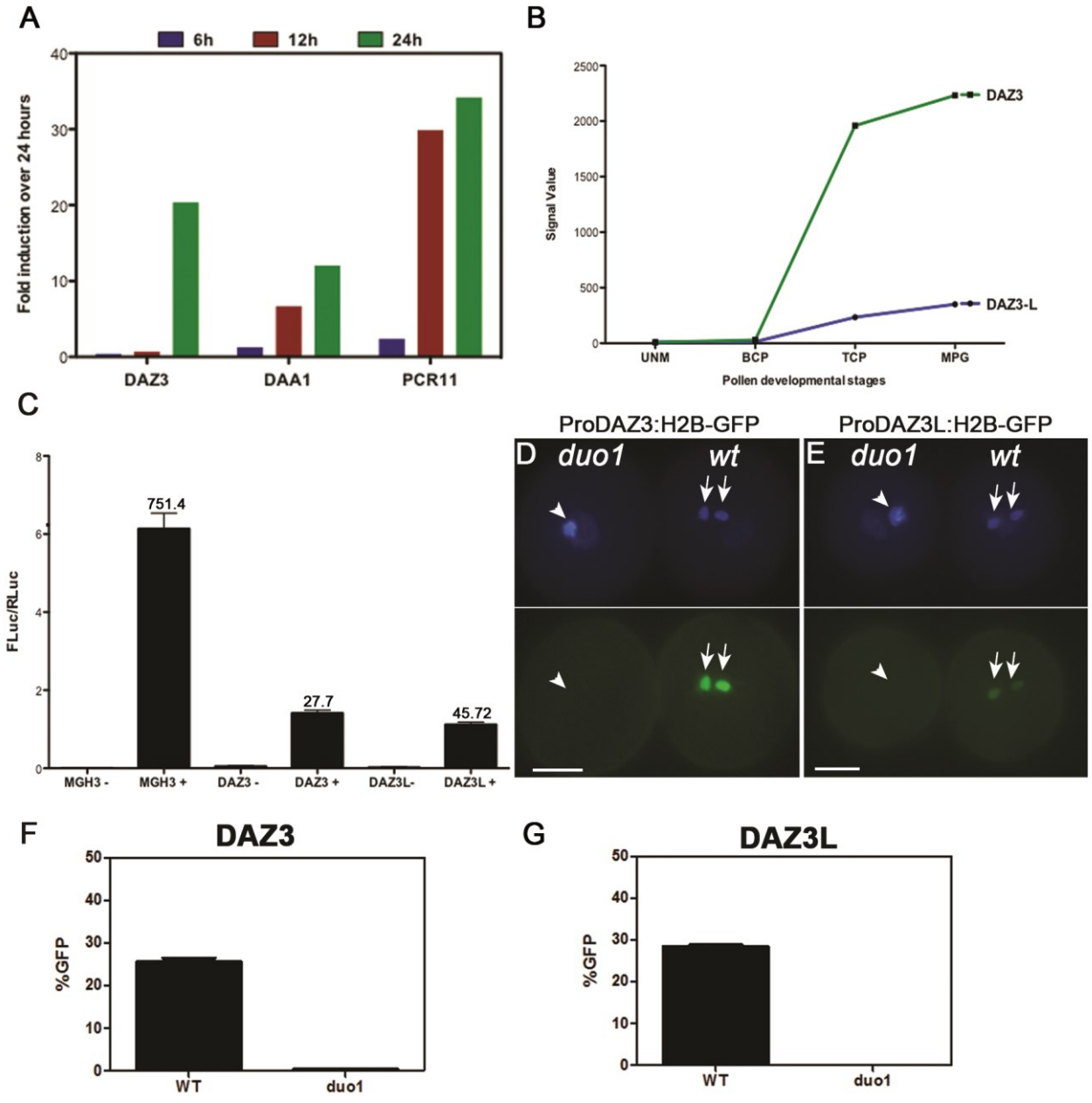
A
6h
12h
24h
Fold induction over 24 hours
40
30
20
10
0
DAZ3
DAA1
PCR11
B
2500
2000
1500
1000
500
0
Signal Value
DAZ3
DAZ3-L
UNM
BCP
TCP
MPG
Pollen developmental stages
C
FLuc/RLuc
8
6
4
2
0
751.4
27.7
45.72
MGH3 -
MGH3 +
DAZ3 -
DAZ3 +
DAZ3L-
DAZ3L +
ProDAZ3:H2B-GFP
ProDAZ3L:H2B-GFP
D
duo1
wt
E
duo1
wt
F
DAZ3
%GFP
50
40
30
20
10
0
WT
duo1
G
DAZ3L
%GFP
50
40
30
20
10
0
WT
duo1

at different time points. Interestingly among the set of 14 genes being validated as DUO1 targets, the promoter activity of three target genes, DAA1, PCR11 and DAZ3 appear to be sperm cell-specific and have enriched transcripts in sperm cells (Borg *et al.*, 2011; Borges *et al.*, 2008). The first two genes, DAA1 and PCR11 responded to DUO1 activation after 12 hours of induction, whereas DAZ3 showed a 3-fold increase only after 24 hours of induction (Figure 4.1A). DAZ3L was not present on the Affymetrix *Arabidopsis thaliana* ATH1 array that contains probes sets representing approximately 23000 genes that covers about 80% of *Arabidopsis* genes. In another study, a new Affymetrix *Arabidodpsis* microarray called AGRONOMICS1 was used, that contains probes for more than 30,000 *Arabidopsis* genes, representing more than 90% of *Arabidopsis* annotated genes (Rehrauer *et al.*, 2010). The data from AGRONOMICS1 microarray analysis which corresponds to one hybridization event shows that the transcript levels of both DAZ3 and DAZ3L are detectable at microspore and bicellular stage but show increase at tricellular and mature pollen stage (Le Trionnaire and Twell unpublished). The trend in DAZ3 transcript profiles between different pollen developmental stages both in ATH1 and AGRONOMICS1 datasets was comparable. According to AGRONOMICS1 microarray data both DAZ3 and DAZ3L show absent signals at unicellular microspore (UNM) and bicellular pollen stage (BCP), however, a sharp increase in transcript abundance is observed at tricellular pollen stage (TCP), which peaks at mature pollen stage (MPG) (Figure 4.1B). There is a 66-fold increase in transcript abundance at tricellular pollen stage and 75-fold at mature pollen stage for DAZ3, whereas transcript abundance of 17-fold at tricellular pollen stage and 26-fold at mature pollen stage is observed for DAZ3L. Interestingly the signal value for DAZ3 was 8-fold higher at tricellular pollen stage and 6–fold at mature pollen stage compared with DAZ3L. This analysis validates that DAZ3 is one of the highly expressed late genes in the *Arabidopsis* sperm cells also identified in the transcriptome of sperm cells (Borges *et al.*, 2008). The higher expression values in the tricellular pollen stage for DAZ3 and DAZ3L distinguish them from other DAT genes where in majority of the targets expression appears after the formation of germ cell. The increase in transcript levels after division of the germ cell suggests that both these novel zinc finger proteins could be an integral part of the DUO1 regulatory pathway active at later stages of pollen development.

4.2.2 DUO1 transactivates the DAZ3 and DAZ3L promoters

To further validate that both DAZ3 and DAZ3L expression is DUO1-dependent, a transient luciferase assay was employed to determine transactivation of target promoters in tobacco leaves (Borg *et al.*, 2011). Assaying the expression of luciferase provides a rapid and inexpensive method for monitoring promoter activity. The primary objective of the assay was to quantify promoter strength by fusing the promoter sequence to a heterologous reporter gene that encodes a quantifiable enzyme using highly sensitive assays. The dual luciferase assay has been widely used to determine rapidly but accurately the activity of a given gene promoter. Bioluminescent reporters' i.e Fire fly luciferase and Renilla luciferase are ideal because of their exceptional sensitivity, instantaneous measurement as well as 10-fold to 1000-fold higher assay sensitivity than fluorescent reporters such as GFP. These assays have been proved useful in quantifying promoter activity of various plant genes promoters (Bate and Twell, 1998; Borg *et al.*, 2011; Dare *et al.*, 2008; Espley *et al.*, 2009). The luciferase gene from the firefly *Photinus pyralis* is a commonly used reporter gene that encodes the luciferase enzyme. This firefly luciferase is capable of oxidizing its substrate, D-Luciferin, in the presence of adenosine triphosphate (ATP), oxygen and magnesium ions, emitting light that can be quantified (DeLuca and McElroy, 1978). Renilla luicferase is another useful luciferase based reporter gene from a soft coral, *Renilla reniformis that* is used as an internal control to normalize the values of experimental reporter gene for variations that could be caused by transfection efficiency and sample handling. Renilla luciferase enzyme catalyzes a luminescent reaction utilizing oxygen and coelenterate luciferin (coelenterazine), emitting carbondioxide and light (Matthews *et al.*, 1977). Due to the dissimilar enzyme structures and substrate requirements, the two bioluminescent reporters have been combined together in an integrated single assay, often referred to as dual luciferase assay (Sherf *et al.*, 1996).

It has already been shown that *Agrobacterium*-mediated transient transformation of tobacco leaves could be used for fluorescent protein expression studies (Sparkes *et al.*, 2006). To perform the dual luciferase assay, existing *Agrobacterium* strains harbouring an effector plasmid in which DUO1 is driven by CAMV-35S promoter (35S-mDUO1), a control vector in which Renilla luciferase is driven by CAMV-35S promoter (35S-RenLUC) and a reporter vector where promoter DAZ3 drives the expression of firefly

luciferase (ProDAZ3-LUC) were used (Borg *et al.*, 2011). The luciferase reporter construct for DAZ3L (Pro-DAZ3L-LUC) was generated using Multisite Gateway recombination vectors (Invitrogen) (Karimi *et al.*, 2002). As ProMGH3 has already been established to be strongly transactivated in the transient assay by DUO1, it was used as a positive control to monitor transactivation potential of DUO1 in this analysis. The *Agrobacterium* strains containing the DAZ3 and DAZ3L reporter vectors were used to infiltrate *Nicotiana tabacum* (tobacco) leaves with and without an *Agrobacterium* strain harbouring the 35S-mDUO1 effector plasmid. Each infiltration also contained the 35S-RenLUC control plasmid to monitor variation in transformation efficiency. The assay for dual luciferase activity was performed after two days. The resulting activity of the firefly luciferase was normalized to that of Renilla luciferase. FLuc/RLuc ratio was used to quantify promoter activity and represented measure of luciferase expression relative to the expression of the 35S-RenLUC in both with and without effector infiltrations. Minimal background levels of promoter activity were observed in the absence of the 35S-mDUO1 effector strain for both DAZ3 and DAZ3L, which suggests that both promoters are not activated in the absence of DUO1 and that low FLuc/RLuc ratio was due to presence of other transcription factors causing basal levels of transactivation (Figure 4.1C). However, by adding the 35S-mDUO1 effector to the infiltration mixture a significant increase in the relative luciferase activity for the three reporter genes was observed. When ProMGH3-LUC was co-infiltrated with 35S-mDUO1, a 751.4-fold increase in relative luciferase activity was observed compared to infiltration of the reporter alone (Figure 4.1C). Similarly, ProDAZ3-LUC and ProDAZ3L-LUC showed 27.7-fold and 45.72-fold increase respectively in relative LUC activity compared to the background. The transactivation levels of the two genes varied since the two proteins differ in their promoter architecture and hence their associated response to DUO1. The increased levels of luciferase activity suggest that DUO1 is necessary for the transactivation of both DAZ3 and DAZ3L promoters in tobacco leaves. The presence of MBSs in promoters of the two genes and their increased luciferase activity in the presence of DUO1 suggests that their activation is more likely direct. This hypothesis that DAZ3 and DAZ3L are direct DUO1 targets is further tested by quantifying luciferase activity of the 5` deletions in the two promoters as well measuring luciferase activity of promoter variants with mutagenized MBSs in context of full-length promoter. The results are discussed in section 4.4.

4.2.3 Expression analysis of DAZ3 and DAZ3Lin wild type and *duo1* pollen

In order to determine whether DAZ3 and DAZ3L require DUO1 for their expression *in planta*, stable transgenic H2B-GFP marker lines driven by the promoters of both DAZ3 and DAZ3L promoters were generated in the *duo1* background and their expression monitored in *duo1* germ cells. The T1 generation was analysed by monitoring H2B-GFP expression in mature pollen from several independent T1 lines in the *duo1* background. Heterozygous *duo1* plants at anthesis shed 50% wild type pollen with twin sperm cells and 50% mutant pollen with a single germ cell (Durbarry *et al.*, 2005). The GFP expression of both reporter constructs was detected in the wild type pollen whereas no or very weak GFP signal could be detected in *duo1* mutant germ cells (Figure 4.1D-E). The percentage of GFP expression scored in the germ nuclei of *duo1* pollen was 0.3% and 0% in the DAZ3 and DAZ3L marker lines respectively. This reduction in the proportion of germ cells with GFP fluorescence was statistically significant compared with wild type pollen (Chi-squared test: $p<0.001$). These data suggest that DAZ3 and DAZ3L are male germline specific genes and extend the evidence that DUO1 is required for the expression of multiple germline specific genes belonging to different functional classes (Borg *et al.*, 2011; Brownfield *et al.*, 2009a).

4.3 Features and domains of DAZ3 and DAZ3L

DUO1 is an important transcriptional factor regulating a network of diverse DAT genes with different functions (Borg *et al.*, 2011). It belongs to R2-R3 MYB transcription factor family and contains a MYB DNA binding domain that binds the specific MYB sites in the target promoters (Rotman *et al.*, 2005). Three highly overrepresented MYB DNA binding motifs (*motif 1*, mwwAACCGTCwa; *motif 2*, awAAACCGCta; and *motif 3*, adwAACCGTywh) in the DAT promoters have already been identified. The analysis of DAZ3 and DAZ3L promoters utilizing the motif analysis suite Regulatory Sequence Analysis Tools identified overrepresented DUO1-binding DNA motifs or MYB binding sites. Each motif has a typical MYB core sequence containing nucleotide AAC and is most frequently present in the proximity of TATA box (Figure 4.2A). Interestingly, the group of DAT genes that responded earliest to ectopically expressed DUO1 possess on average more MYB binding sites (MBSs) in their promoters compared to late

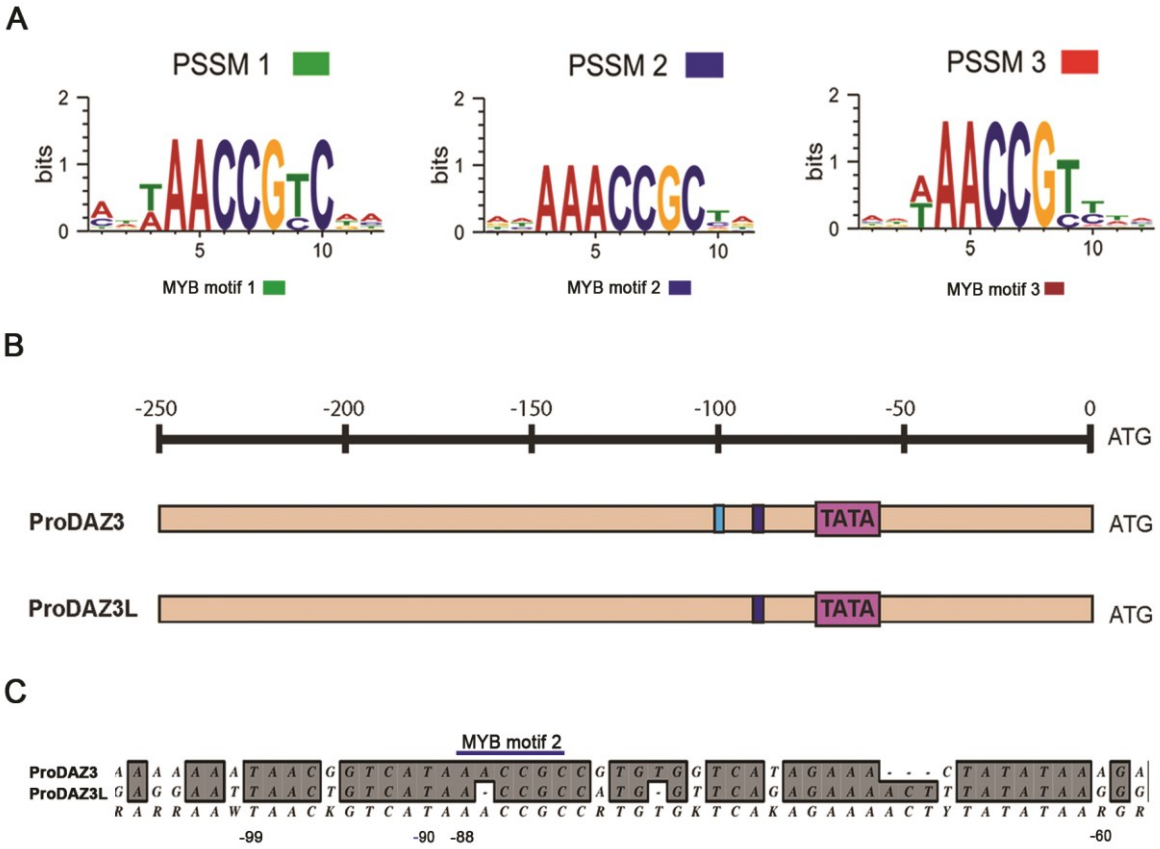

Figure 4.2: Putative MYB binding sites are present in regulatory regions of DAZ3 and DAZ3L surrounding putative TATA box. (A) Sequence analysis of the promoters of candidate DAT genes identified three overrepresented MYB binding motifs. The consensus sequence of the motifs is represented as a PSSM logo. Each PSSM has a high information content showing high sequence conservation within the PSSM. Adapted from (Borg *et al.,* 2011). **(B)** Schematic diagram of the promoter region of DAZ3 and DAZ3L -250bp upstream of ATG, illustrating regulatory regions with putative MYB binding sites shown as dark and light blue rectangular boxes in the proximity of a putative TATA box. The MYB sites are contained within -130bp upstream of ATG. **(C)** ClustalW alignments of promoters of both DAZ3 and DAZ3L showing the putative TATA box and the MYB binding motif 2 present in both promoters.

responding genes. For example *MGH3* promoter contain five MBSs and out of these, four are present in the proximal promoter region surrounding the TATA box (Borg *et al.*, 2011).

Both DAZ3 and DAZ3L belong to the group of late responding genes and contain the putative MBSs within -150bp region upstream of ATG (Borg *et al.*, 2011). DAZ3 promoter contains two MBSs, with an additional MYB binding motif adjacent to MYB motif 2. The second MYB site apart from MYB motif 2 was identified from a databank for motifs found in plant *cis*-acting regulatory DNA element, called PLACE. Furthermore, the occurrence of MBSs in close proximity is a trait also found in other DUO1 target gene promoters. The two putative MYB sites centred at -88 and -99 promoter regions respectively. In the case of DAZ3L, only one MYB site could be identified in the proximal promoter region and is centred at -88 (Figure 4.2B). The ClustalW alignment of proximal region of both promoter regions shows the identical MYB motif 2 in DAZ3 and DAZ3L upstream of putative TATA box (Figure 4.2C).

The two genes, DAZ3 and DAZ3L belong to the C2H2 zinc finger family, which constitute the most abundant family of putative transcriptional regulators in *Arabidopsis*. Both DAZ3 and DAZ3L belong to the C1-1iCa subgroup and are characterized by having single zinc finger domain (Englbrecht *et al.*, 2004). The coding sequence of both genes has a single exon. The number of amino acid residues in DAZ3 and DAZ3L protein sequence is 275 and 271 respectively (Figure 4.3B). ClustalW alignment of protein sequences of both genes indicates 46% protein identity and 14% similarity. Both proteins have a single zinc finger domain. A basic stretch of amino acids is present at the N-terminal portion of each protein and may serve as putative Nuclear Localisation Signal (NLS). The C terminal region has an acidic stretch of amino acids as well as a leucine-rich region. This leucine-rich stretch is known as an Ethylene-responsive element binding factor-associated amphiphilic repression (ERF-associated amphiphilic repression or EAR) motif. The DAZ3 and DAZ3L protein harbours two putative ERF-associated repression (EAR) motifs (Figure 4.3A) (Kagale *et al.*, 2010). The single zinc finger domain in both proteins contains two cysteine and two histidine residues that tetrahedrally coordinate a zinc atom. In the zinc finger domain, the spacing between the two zinc coordinating histidine residues is three and hence placed in the group C1. This group is considered evolutionarily younger compared to

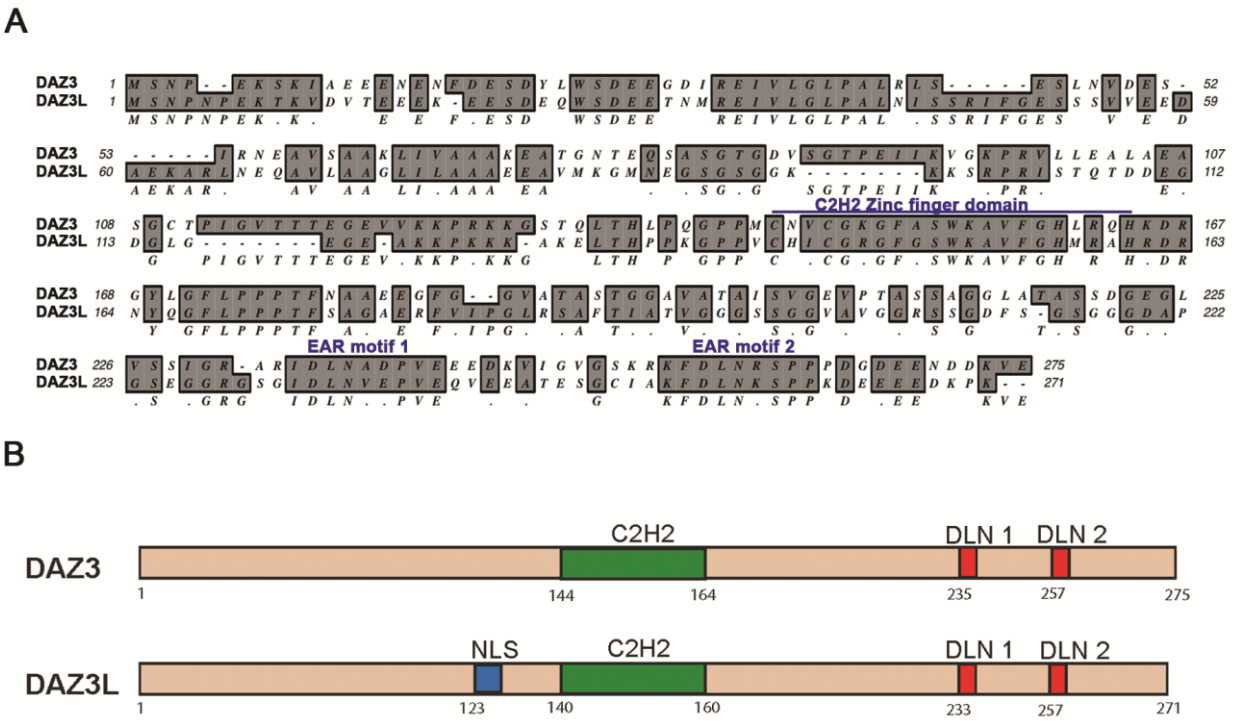

Figure 4.3: ClustalW alignment of DAZ3 and DAZ3L amino acid sequences. (A) Sequences were aligned with ClustalW using default parameters. Grey shading indicates identical residues. Gaps required for optimal alignment are indicated by dashes. The putative zinc finger domains and EAR motifs are indicated by a line above the sequences. **(B)** Schematic representation of the coding region of the two zinc finger proteins. The position of the zinc finger domains and putative EAR motifs has been illustrated with colored boxes and the start position of amino acid signified below each structural component. **(C)** The K2-2 type helix signature present in the zinc finger helix of DAZ3 and DAZ3L. Amino acids are shown in helix position -1 to 10 where Q at position 2 is replaced with K and hence called K2-2 helix signature.

other groups of C2H2 zinc finger proteins (Englbrecht *et al.*, 2004). The zinc finger domain of DAZ3 and DAZ3L does not contain the signature QALGGH sequence but instead Q is replaced with K at helix position 2 and hence the signature K2-2 where K2 refers to lysine at position 2. Also the signature K2-2 zinc finger motif has W in position 1 and R in position 9 (Figure 4.3C) (Englbrecht *et al.*, 2004). The C terminal region of the two proteins harbours two EAR motifs of DLNxxP type (Kagale *et al.*, 2010). The two motifs have been labelled as DLN1 and DLN2 (Figure 4.3A-B) and have been identified in other zinc finger proteins with repression functions (Hiratsu *et al.*, 2002; Ohta *et al.*, 2001). These EAR motifs containing proteins have been implicated in inhibiting transcription by modifying chromatin structure of regulatory regions by histone deacetylation or by interacting with components of basal transcriptional machinery (Pazin and Kadonaga, 1997). The mode of action of these EAR proteins is to recruit co-repressors such as SAP18 (SIN3-associated polypeptide of 18 kDa) or TPL (TOPLESS), which interact with HDA19 (Histone deacetylase 19) to bring about repression (Kagale and Rozwadowski, 2011). The presence of putative transcriptional repression motifs makes DAZ3 and DAZ3L ideal candidates to investigate transcriptional repression pathways in plant germline.

4.4 DUO1 is able to activate DAZ3 and DAZ3L through binding MYB sites in their promoters

It has been already established that promoters of both DAZ3 and DAZ3L respond to DUO1 in transient assay and that this response correlates with the fact that DUO1 binds positive promoter elements or putative MBSs present in the promoters of both zinc finger genes. The next logical step was to investigate the functionality of these identified putative biding sites, which was investigated by quantifying the reporter luciferase activity of promoter variants of both DAZ3 and DAZ3L in transient assays. Two strategies were employed to determine DAZ3 and DAZ3L promoter response to DUO1. For each gene two types of promoter variants were generated, a series of 5' deletions and promoter fragments in which the MBSs were mutated using site-directed mutagenesis. These promoter variants were fused to the luciferase reporter and the quantified expression of luciferase reporter driven by different promoter variants of each gene was compared to the native full-length promoter. The assay was performed in

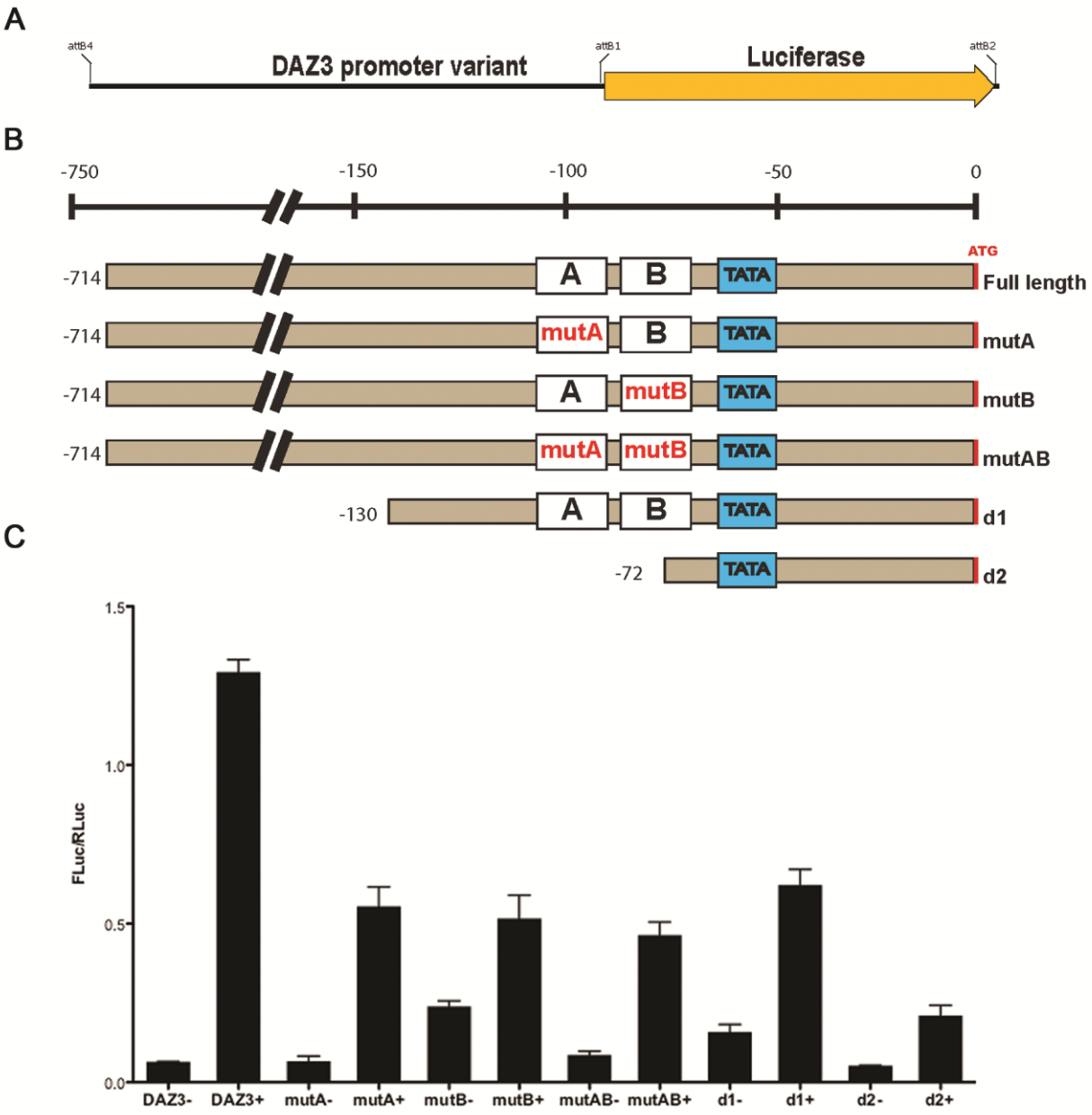

Figure 4.4: The presences of MYB binding sites in the DAZ3 promoter are important for its transactivation by mDUO1. **(A)** Schematic illustration of the functional constructs depicting DAZ3 promoter variant driving luciferase. A number of such constructs were generated and utilized in the dual luciferase assay. **(B)** Diagrams illustrating the different DAZ3 promoter variants generated. These include DAZ3 promoter fragments with either mutated MYB site A, B or both together, in the context of the full-length promoter as well as promoter deletions both with (-130) and without (-72) the two MYB sites. **(C)** Results of the experiment are shown as bar charts illustrating the significance of the MYB sites. The relative luciferase activity of each promoter variant is determined alone (-) and upon co infiltration with 35S-mDUO1(+). The relative luciferase activity (FLuc/RLuc) of the DAZ3 variant promoters is presented with error bars signifying the mean of at least four independent infiltrations. The experiment was performed twice and data presented here belongs to one representative experiment.

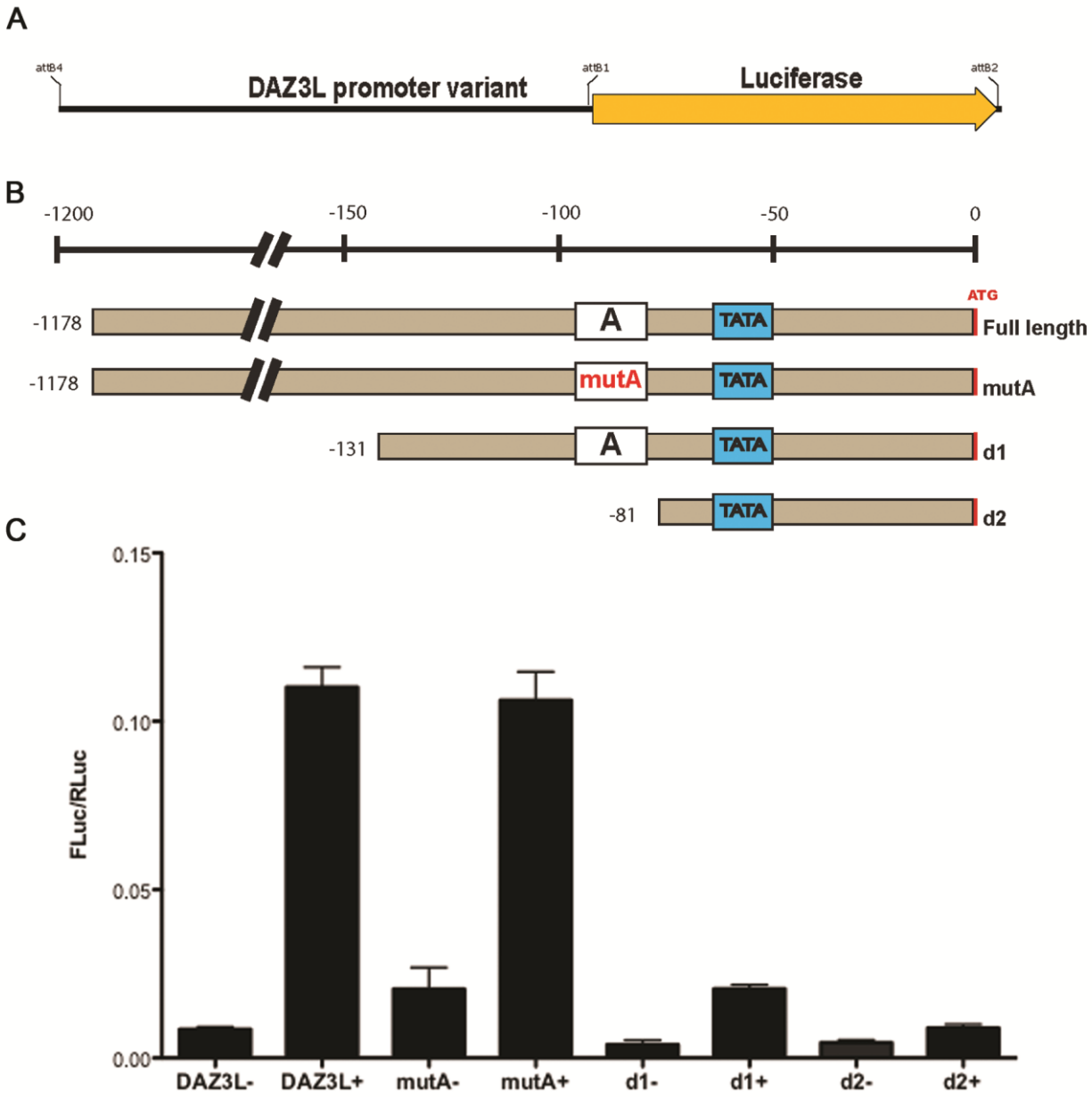

Figure 4.5: The significance of single MYB binding site in DAZ3L promoter in its transactivation by mDUO1. (A) Schematic diagram representing functional construct of DAZ3L promoter variant driving luciferase. A number of such constructs were generated and utilized in the dual luciferase assay. **(B)** DAZ3L promoter variants are shown here schematically to illustrate the position of the single MYB site and to represent mutagenesis and deletion approaches used to generate DAZ3L promoter fragment with mutated MYB site A in the context of full-length promoter and promoter deletions upstream of ATG both with (-131) and without (-81) the MYB site. **(C)** The relative luciferase activity (FLuc/RLuc) of the DAZ3L promoter variants alone (-) and upon co-infiltration with 35S-mDUO1 (+), is presented in bar charts illustrating the significance of the MYB sites. Error bars signify the mean of independent infiltrations. The experiment was performed twice and data presented here belongs to one of the experiments performed on a different day.

tobacco leaves where DUO1 is repressed by microRNA 159 (Palatnik *et al.*, 2007) and hence DUO1 cDNA altered at microRNA binding site was used for transactivation of the target promoters (Brownfield *et al.*, 2009a).

Both DAZ3 and DAZ3L promoters have putative MYB sites within -150bp region upstream of the ATG and surrounds the putative TATA box. In this context, the first aim of the experiment was to narrow down the responsive region of both promoters required for DUO1-dependent transactivation. The promoter region of DAZ3 and DAZ3L was removed upto -131bp (-130bp for DAZ3 and -131bp for DAZ3L) upstream of the MBSs and was referred to as deletion 1 (d1). Similarly promoter regions of DAZ3 and DAZ3L were further deleted upto -72bp for DAZ3 and -81bps for DAZ3L. The deletions also resulted in the removal of MBSs and were referred to as deletion 2 (d2). Previously it was established that DAZ3 promoter deletion 1 exhibited the same levels of expression as its native promoter (Esparaza and Twell unpublished). To validate these previous results, the assay was repeated for DAZ3 using already established constructs. In order to analyse DAZ3L promoter, a new set of 5' promoter deletion constructs were generated using Gateway recombination procedures. In the case of DAZ3, the results showed that removal of -130bp (d1) upstream of MYB sites reduces the luciferase activity by 52% as compared to the full-length promoter. The removal of the DAZ3 promoter region including the MYB sites upstream of the TATA box (d2) abolishes the luciferase activity by 84% (Figure 4.4C). The assay was repeated and showed the same trend. In the case of DAZ3L, analysis of promoter deletion 1 (-131bp), the relative luciferase activity was reduced to ~81%, whereas in the case of deletion 2, there was further reduction to basal levels. This result implied that the upstream region of both DAZ3 and DAZ3L might be important for the DUO1-dependent activation of these genes (Figure 4.4C and Figure 4.5C).

In order to determine the importance of putative MBSs (A and B in DAZ3 and A in DAZ3L) in the context of full-length promoters, MYB sites were mutagenised (mutA, mutB in DAZ3, mutA in DAZ3L). Constructs for mutagenised MYB site A and B in the context of the full-length DAZ3 promoter were already established and hence a double MYB mutagenised construct for DAZ3 and single MYB mutagenised construct for DAZ3L were generated. Analysis of mutagenised MYB sites, mutA or mutB in DAZ3 showed 57% and 60 % reduction in relative luciferase activity, respectively compared to

full-length promoter, suggesting that the both MYB act synergistically and are required for the DUO1-dependent activation. Whereas mutagenizing both MYB A (mutA) and MYB B (mutB) does not abolish the relative luciferase activity but reduces it to 64% of the full-length promoter suggesting that absence of MBSs does not hinder DUO1 ability to activate DAZ3 promoter. Furthermore, upstream regulatory region may harbour additional binding sites either for DUO1 binding or for other DUO1-dependent intermediate factors that may contribute in DAZ3 promoter activation. To determine if reduction of 64% is significantly different from 57% and 60%, post hoc analysis was carried out with Tukey-Kramer test following ANOVA analysis and it was found that the reduction in the luciferase activity was not significant among three DAZ3 promoter variants analysed. These results demonstrate that mutagenesis of the MYB sites significantly reduces the DAZ3 promoter activity ($p<0.05$) and hence these sites are of fundamental importance for DUO1-dependent transactivation of DAZ3 promoter. The analysis for DAZ3L promoter was also carried out in the same fashion and the luciferase activity for a construct with single mutagenised MYB site (mutA) was quantified. Unlike DAZ3, there was no significant reduction in the mutagenized promoter luciferase activity compared to full-length DAZ3L promoter, suggesting that other *cis*-regulatory elements maybe involved in the DUO1-dependent activation of the promoter. Another explanation could be that DUO1 alone is not sufficient for activating the promoter and indirect mechanism is utilized to control activity of the gene.

4.5 Significance of upstream promoter region and MYB binding sites in germline expression of DAZ3

The result that DUO1 is able to transactivate DAZ3 promoter variant 5' upstream region deleted just prior to the MYB sites gave rise to an interesting question of whether there is any effect on the expression pattern of the deleted DAZ3 promoter in pollen. To analyse the expression of DAZ3 promoter deletions (d1 and d2) in pollen, promoter variant H2B-GFP fusion constructs were generated and introduced into plants to generate stable T1 lines (Figure 4.6A). Mature pollen was analysed from T1 lines transformed with ProDAZ3:H2B-GFP, ProDAZ3d1:H2B-GFP and ProDAZ3d2:H2B-GFP using DAPI staining and examination by fluorescence microscopy (Figure 4.6B-G). The percentage of T1 plants harbouring ProDAZ3:H2B-GFP construct and

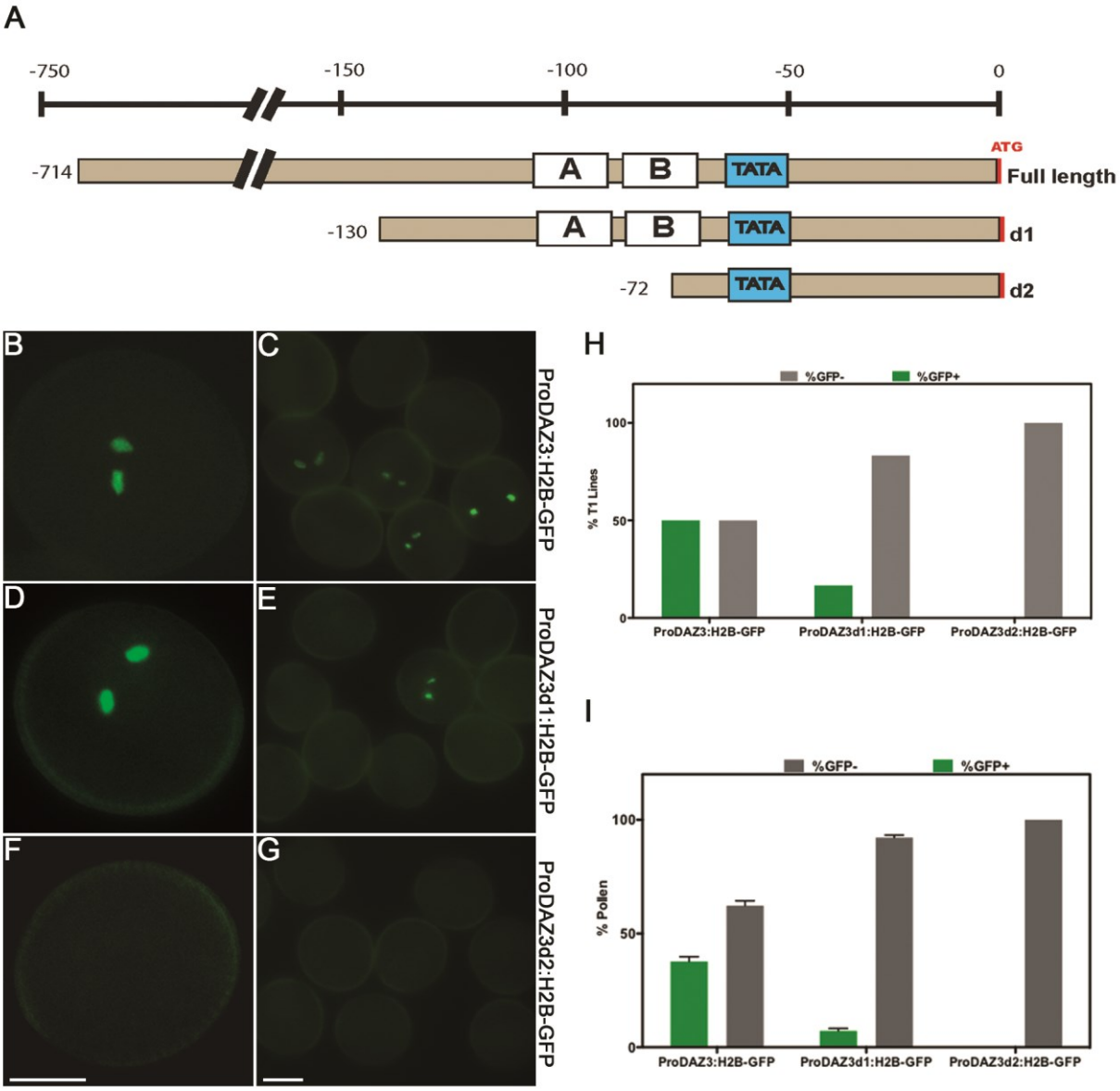

Figure 4.6: Significance of the upstream region and MYB binding sites in germline expression of DAZ3 promoter. (A) Schematic diagram illustrating strategies to determine importance of upstream region and the two MYB sites for the DAZ3 promoter activity. DAZ3 promoter constructs, with promoter deletion1 (d1) and deletion2 (d2) were generated and mature pollen from T1 lines harbouring these constructs was stained with DAPI analyzed under GFP fluorescence. GFP counts were carried out on pollen population from T1 lines. Images shown illustrate expression of **(B-C)** full-length DAZ3 promoter driving H2B-GFP, **(D-E)** DAZ3 promoter deletion1 driving H2B-GFP and **(F-G)** DAZ3 promoter deletion2 driving H2B-GFP. Images on the left show single pollen from a population, whereas images on the right represent a group of pollen harbouring one of the three constructs. Scale bar represents 10µm **(H)** Bar charts represent the percentage T1 lines harbouring the DAZ3 promoter variant constructs and expressing GFP signal in sperm cells. **(I)** The mean percentage frequency of GFP positive pollen, identified in the DAZ3 promoter variant T1 lines is presented in the bar graph. GFP positive pollen counts were carried out from several independent T1 lines. Error bars represent the standard error of the mean.

exhibiting GFP expression was 50% (n=6/12) (Figure 4.6B-C), while percentage of T1 plants with GFP expression for ProDAZ3d1:H2B-GFP was 16.6% (n=4/24) (Figure 4.6D-E). No GFP could be detected in ProDAZ3d2:H2B-GFP lines (n=24) (Figure 4.6F-G). The percentage of tricellular pollen expressing uniform bright GFP in 6 independent lines ranged between 30.8% and 45.65% (Figure 4.6H). Interestingly only 3 lines could be identified from T1 population harbouring ProDAZ3d1:H2B-GFP construct. The reason being a small proportion of pollen population in these lines expressed GFP. The percentage of GFP counted in the three lines was 9.9%, 6% and 5.66% (Figure 4.6I). Interestingly, the pollen expressing GFP showed uniform bright signal. No GFP signal could be detected in the vegetative cell nucleus. This interesting result gives an insight into the complex transcriptional mechanisms playing their role in gene transcription and clearly suggests that a framework of different transcriptional proteins maybe needed to help DUO1 switch on the transcription of DAZ3. Moreover, the presence of upstream region of the DAZ3 promoter seems essential for reliable expression of DAZ3 as well as to stabilize the transcription machinery to switch on the gene.

4.6 Discussion

This chapter describes a subset of sperm cell-specific genes, DAZ3 and DAZ3L, which encode EAR (ERF-associated amphiphilic repression)-motif containing C2H2 type zinc finger proteins. Both genes become active, late after germ cell division, specifically at tricellular stage of pollen development. Detailed analysis has been carried out to elucidate the DUO1-dependent activation of DAZ3 and DAZ3L genes and to validate them as DUO1 targets. The functionality of the putative MYB binding sites has also been investigated in a transient luciferase assay to determine their significance in DUO1-dependent transactivation of the two target promoters.

4.6.1 DAZ3 and DAZ3L are activated late during male germline development

The first evidence that the activation of DAZ3 requires DUO1 comes from the landmark time-course microarray experiment where DAZ3 was identified as late gene that exhibited 3-fold increase after 24 hours in response to ectopic DUO1 expression. In

contrast to other DUO1 target genes which show increase in transcripts levels earlier when the germ cell is formed, transcripts for DAZ3 and two other DUO1 target genes, PCR11 and DAA1 were detected after germ cell has divided. These three genes exhibited sperm cell enriched expression with DAZ3 being the most highly expressed gene according to the sperm cell transcriptomic data (Borg *et al.*, 2011; Borges *et al.*, 2008). On the other hand, DAZ3L was absent from Affymetrix ATH1 microarray and hence could not be identified as DUO1 target. Interestingly, DAZ3L was discovered in bioinformatics search as a putative DAZ3 homologue and hence most likely a DUO1 target. In another study, DAZ3L probe sets were found on a new Affymetrix microarray chip called AGRONOMICS1 (Le Trionnaire and Twell unpublished) and exhibited the same trend in transcript profiles between different pollen developmental stages as observed in DAZ3. According to the AGRONOMICS1 microarray data, both DAZ3 and DAZ3L show increase in transcripts level specifically at tricellular and mature pollen stage. Interestingly, signal value for DAZ3 was 6-8 folds higher at both tricellular stage and mature pollen stages compared with DAZ3L. The similar trend in transcripts abundance specifically at tricellular stage suggests sperm cell-specific activation as well as functional redundancy between the two proteins.

The fact that DAZ3 shows high-fold induction after 24 hours suggests that DUO1 may activate late responding genes after the necessary upstream factors have been activated. Additionally, the earliest responding genes possess on average more MBSs in their promoters as compared to late responding genes (Borg *et al.*, 2011). Thus the rapid response of early responding genes may relate to the increased number of MBSs in their promoters, facilitating direct activation by DUO1, whereas, late responding genes require interaction of DUO1 with other factors that are activated later during development. In summary, two mechanisms could be accounted for late activation of DAZ3 and DAZ3L promoters. In first instance, DAZ3 and DAZ3L promoters may undergo chromatin remodelling from a closed or repressive state in germ cells to an open or permissive state in sperm cells. In this context, DUO1 acting alone or in association with other germline factors (potentially DUO3 and DAZ) may recruit chromatin remodelling complexes to create a chromatin environment that is permissive for DUO1 binding. The other possible mechanism could be that the promoters are bound by a germ cell-specific repressor which is progressively inactivated or degraded in the differentiating germline to the extent that critical threshold level is reached in

sperm cells allowing DUO1 to activate DAZ3 and DAZ3L promoters.

4.6.2 DUO1 is essential for the transactivation of DAZ3 and DAZ3L

The similarity in expression pattern, sperm cell specificity and late activation make these two genes interesting candidates to further analyse their role at later stages of pollen development. Moreover, the transcriptomic data provided a solid ground to test the hypothesis that similar to DAZ3, the expression of its homologue, DAZ3L is most likely DUO1-dependent. The two zinc finger proteins were validated as DUO1 targets by monitoring their promoter activity in a transient luciferase assay. Interestingly, the regulatory regions of both genes responded positively upon co-transformation with DUO1. Both DAZ3 and DAZ3L promoters showed 27.7-fold and 45.72-fold increase in relative luciferase activity respectively, compared to infiltration of the reporter alone. The result strongly suggested that DUO1 is essential for transactivation of DAZ3 and DAZ3L in tobacco leaves. These results were further supported by a separate analysis where the nuclear-localised expression of the two promoters was monitored in *duo1* germ cells. The significant reduction of DAZ3 and DAZ3L promoter activity in *duo1* germ cells further validated the luciferase assay results indicating that DUO1 is required for activation and germline expression of the two zinc finger proteins.

It has been shown that a subset of DUO1 target gene promoters including GEX2 and GCS1 display low levels of expression in DUO3 germ cells proposing the idea that coordinated activity of DUO1 and DUO3 may be required for activation of common target genes (Brownfield *et al.*, 2009b). Similarly, low expression levels of DAZ3 driven GFP reporter in *duo3* mutant background suggest that the promoter is partially active in *duo3* germ cells (discusses in Chapter 5). Furthermore, the possible role of DUO3 in activation of DAZ3 and DAZ3L could further be explored by employing transient luciferase assay in tobacco leaves. Likewise, DAZ1 and DAZ2 represent a subset of DUO1-activated zinc finger transcriptional repressors that are functionally redundant and specifically express in the germline (Borg *et al.*, 2014). The promoter activity of ProDAZ3:H2B-GFP marker line in *daz* (*daz1daz2*-homhet) germ cells is completely abolished implying the possible involvement of DAZ in late activation of DAZ3 (discussed in Chapter 5). Also the analysis of DAZ3L promoter activity in *duo3* and *daz* mutant background as well as possible activation in luciferase assay would

further increase our understanding of the mechanisms that modulate late activation of DAZ3L promoter during germline development. Based on the reduced DAZ3 marker expression in these three G2/M regulators it can be proposed that the master regulator, DUO1 may interact with DUO3 and/or DAZ in a transcriptional complex. This interaction could involve DUO3-dependent chromatin remodelling at DAZ3 and DAZ3L promoters resulting in DUO1 access to the binding sites. Alternatively, DUO1-dependent DAZ which is a potential transcriptional repressor, may interact with co-repressor TOPLESS in an EAR dependent manner (Kagale and Rozwadowski, 2011). This potential co-repressor complex may recruit chromatin remodelling factors resulting in transcriptional repression of another repressor thereby optimizing DUO1 access to the target promoters.

4.6.3 MYB binding sites represent core features of DAZ3 and DAZ3L promoters and are required for DUO1 dependent activation

The ability of DUO1 to activate its target genes is dependent on its ability to bind positive regulatory sequences in the target promoters. DUO1 is an R2-R3 MYB transcription factor and therefore, require specific MYB sites in target promoters for binding and subsequent transcription. According to Borg *et al*. (2011), the search for putative MYB sites in the target promoters resulted in identification of three highly over represented MYB binding DNA motifs in DUO1 target gene promoters. These motifs contain a typical MYB core sequence consisting of nucleotides AAC and are frequently present in the close proximity of TATA box in candidate DUO1 target promoters. Studies have shown that several other transcription factors also bind the typical MYB core AAC/GTT. These include maize R2R3‑MYB C1 protein (Roth *et al.*, 1991), maize P gene (Grotewold *et al.*, 1994), MYB Ph3 protein from *Petunia hybrida* (Solano *et al.*, 1995), GAMYB in cereal aleurone cells (Gubler *et al.*, 1999) as well as *Arabidopsis* MYB98 (Punwani *et al.*, 2007). DAZ3 and DAZ3L upstream regulatory regions also possess one of the MYB consensus sequences identified as MYB motif 2. Interestingly, the ClustalW alignment of the proximal region of DAZ3 and DAZ3L promoters showed that the MYB motif 2 lies within -150bp region upstream of ATG consistent with the findings reported by Borg *et al.* (2011). DAZ3 promoter region contains an additional MYB motif that was identified in a separate bioinformatics search, and was retrieved from database PLACE, a databank for motifs found in plant *cis*-acting regulatory DNA

elements. The presence of MBSs in target promoters correlates well with the transactivation of both DAZ3 and DAZ3L in a DUO1-dependent manner and supports the idea that DUO1 activate these target genes through binding the MYB sites within their promoters.

This idea was further put to test and DAZ3, DAZ3L promoter variants were analysed to investigate the functionality of these putative MBSs as well as the role of upstream region in transactivation of DAZ3 and DAZ3L. It was hypothesised that the deletion of upstream region should not affect promoter activity if the intact MYB sites are critical for DUO1-dependent promoter activation. However, in DAZ3, a 5' promoter deletion (d1) upstream of the two MBSs showed 52% luciferase activity, which is significantly reduced ($P < 0.05$) compared to full-length promoter. Furthermore, analysis of promoter fragments with mutagenized MYB A or B exhibited significant reduction of 57% and 60% respectively, which implied the loss of a major promoter element. Furthermore, it also suggested that the two MBSs may act synergistically. In this context it was expected that the mutagenesis of both MBSs together may further reduce promoter activity. However, 64% reduction in luciferase activity was observed, similar to the percentage reduction in the case of mMBS A or mMBS B, suggesting that both MBSs are activated to the same extent indicating that both types of binding sites are functionally equivalent. Taken together, these results provided robust evidence that the two MBSs are critical for DUO1-dependent transactivation of the DAZ3 promoter. In addition, alongside the MBSs, an intact upstream regulatory region is also essential for DUO1 to fully activate its targets. The results further suggests that the upstream regulatory region may contain an enhancer or additional binding sites required for optimal DUO1 binding and thus contributing to full DAZ3 activation. Alternatively, in the absence of MBSs, DUO1 may indirectly control transcription of DAZ3 through intermediate factors that are also under DUO1 regulation.

The absence of DAZ3L marker activity in *duo1* germ cells as well as DAZ3L promoter transactivation in the presence of DUO1 validates the fact that DAZ3L is indeed a DUO1 target. However, relative luciferase activity of DAZ3L promoter deletion1 reduced by 81%, whereas, mutagenesis of single MBS showed promoter activity similar to full-length DAZ3L promoter. This result reflects the fact that the upstream *cis* regulatory region may contain novel binding sites essential for DUO1-dependent

promoter activation. Alternatively, DAZ3L promoter is activated via indirect route involving enhancers that facilitate formation of stable and active transcriptional state within which promote activity is permitted and therefore, removal of the upstream region disrupts stability of the transcriptional complex, thereby reducing the rate of transcription. This idea could be further exploited by generating transgenic lines harbouring sequential deletions of the DAZ3L promoter fused with nuclear localised H2B-GFP. The quantitative analysis of the reporter may help identify enhancers and other elements modulating DAZ3L promoter activity.

In summary, the analysis clearly suggests that DUO1 activates the expression DAZ3 and DAZ3L by employing both direct and indirect transcriptional mechanisms. In the case of DAZ3, presence of both MBSs is required for DUO1 to directly bind MBSs and activate DAZ3 promoter, whereas, putative MBS in DAZ3L promoter does not seem functional. Moreover, intact upstream regulatory region of both promoters is necessary for the full activation of DAZ3 and DAZ3L promoters.

4.6.4 Significance of MYB binding sites for expression of DAZ3 in the male germline

The analysis of DAZ3 promoter deletions (d1 and d2) fused to H2B-GFP was carried out *in planta* to determine the significance of the two binding sites for expression of DAZ3 in the male germline. A full-length DAZ3 promoter marker line (ProDAZ3:H2B-GFP) was also examined alongside promoter deletion constructs. Stable transgenic lines were identified and mature pollen from T1 lines was stained with DAPI and analysed with epifluorescence microscopy. The percentage of pollen exhibiting GFP expression in full-length DAZ3 promoter marker lines was approximately 45%. Interestingly, the number of T1 lines harbouring ProDAZ3d1:H2B-GFP as well as the percentage of GFP expressing pollen in these lines was significantly reduced compared with full-length construct. The percentage of pollen population that showed uniform bright GFP signal ranged between 5.66% and 9.9%. This reduced population penetrance could possibly result from inability of the transcriptional complex to successfully assemble at the target promoter. Moreover, a framework of different transcriptional proteins maybe required to help DUO1 switch on transcription of the target promoter. Another explanation for the reduced penetrance could be that a ‘switch’ mechanism is involved which turns on gene

transcription only when transcription complex is successfully formed rather than a mechanism producing continuous spectrum of expression levels. This gene regulatory mechanism has already been reported in other eukaryotes (Walters *et al.*, 1995). The inability of majority of pollen harbouring ProDAZ3d1:H2B-GFP construct to exhibit GFP expression suggests that the transcriptional complex fails to assemble successfully, thereby switching off transcription. The presence of upstream region of the DAZ3 promoter is therefore required to successfully assemble and stabilize the transcription machinery thereby ensuring reliable expression of DAZ3. The presence of MBSs as well as upstream regulatory region is therefore required for full activation of DAZ3 promoter. Furthermore, to determine whether the two MBSs are necessary for DAZ3 expression *in planta,* promoter variants could be constructed harbouring the mMBS A and B driving expression of H2B-GFP fusion. The resulting constructs could be introduced into wild type plants and the GFP signal in pollen population from single locus T1 lines could be quantified to determine the significance of these MBSs for expression of DAZ3 in the male germline.

Chapter 5 Expression analysis of DAZ3 and DAZ3L

5.1 Introduction

The division of the germ cell switches on a group of genes specific to the late phase of pollen development. An estimated 12000 genes are expressed at microspore and bicellular stage of pollen development but this number decreases to 7000 genes in mature pollen (Honys and Twell, 2004). According to the sperm cell transcriptomic data (Borges *et al.*, 2008), nearly 11% of the sperm cell-expressed genes appear to be sperm cell-specific. Identification and characterization of many germline expressed genes in other species provided a platform to identify and characterize their homologues in *Arabidopsis*. These include a homologue of lily gene GCS1 (also called HAP2) and three genes homologous to maize sperm cell express genes (GEX1, GEX2, and GEX3) (Alandete-Saez *et al.*, 2008; Engel *et al.*, 2005; Mori *et al.*, 2006; Von Besser *et al.*, 2006). Similarly analysis of the histone family in *Arabidopsis* revealed a germline specific Histone H3 Related 10 variant (HTR10) also known as Male Gamete Histone 3 (MGH3) (Okada *et al.*, 2005). Studies of the promoter activities of these germline specific genes have been useful in not only understanding their role in male germline regulation but they have also provided useful tool to carry out cell fate analysis of various mutants defective in germ cell division. The germ cell fate of various mutants including *duo1, duo3, cdka;1 , fbl17, caf1* and *rbr,* has been analysed by monitoring the promoter activity of these markers (Borg *et al.*, 2011; Brownfield *et al.*, 2009a; Brownfield *et al.*, 2009b; Chen *et al.*, 2009; Chen *et al.*, 2008; Gusti *et al.*, 2009).

These recent transcriptomic studies and the identification of male germline regulators e.g. DUO1 have profound importance in analysing regulatory mechanisms governing the formation of twin sperm cells. In addition it has also been shown that, DUO3, which encodes a conserved plant protein, is also required for normal expression of sperm cell genes and sperm differentiation. DUO1 is needed for activation of different sets of genes with different timings. DUO3 also promotes the expression of a subset of genes that depend on DUO1 activity and plays related yet distinct role in germline development (Brownfield *et al.*, 2009a; Brownfield *et al.*, 2009b).

The promoter activity of DUO1 first appears in the germ cell after asymmetric division

and continues to accumulate in later developmental stages. The expression profiles of DUO1 target genes i.e. *MGH3* (Okada *et al.*, 2005), *GEX2* (Engel *et al.*, 2005) are also germline specific and are expressed throughout the male germline development until the formation of mature pollen (Borg *et al.*, 2011; Brownfield *et al.*, 2009a). Previously it was reported that promoter activity of GCS1/HAP2 is only detected in sperm cells (Von Besser *et al.*, 2006) but later it was shown that its expression is first detected in germ cells soon after the asymmetric division and peaks in the sperm cells (Brownfield *et al.*, 2009a). According to *in planta* analysis, promoter activity of most of the newly discovered DUO1 target genes appear in the newly formed germ cell after the first asymmetric division of the microspore (Borg *et al.*, 2011), followed by an increase in expression in the later stages of development. However, a small number of genes show sperm cell-specific activity which appears after germ cell division. These include PCR11, DAA1 and DAZ3. The expression of these late genes specifically in the sperm cell suggests that these maybe a part of DUO1 regulatory pathways active late in pollen development (Borg *et al.*, 2011). The master regulator, DUO1, thus controls two subsets of genes with different timings. An early subset of genes that appear in the germ cell after first microspore division and a late group of genes that appears after germ cell division. DAZ3 and DAZ3L belong to the late subset of genes and their promoter activity is detected after the two sperm cells are formed. According to microarray data both DAZ3 and its homologue DAZ3L show reduced signal values at microspore and bicellular stage and higher expression values at mature pollen stage (Borges *et al.,* 2008; Le Trionnaire and Twell unpublished).

This chapter describes the expression profiles of both DAZ3 and DAZ3L with special emphasis on DAZ3 being one of the most highly expressed sperm cell-specific genes. The first part of the chapter describes the expression of both genes in progressive pollen developmental stages and in sporophytic tissues. The second part of the chapter describes the germline-specific expression of the two genes by monitoring their promoter activity throughout pollen development and also by analysing their protein expression profiles using H2B-GFP and mCherry fluorescent protein as reporters respectively. Analysis of protein fusion constructs of both zinc finger proteins also reveal differences between the two in their localisation patterns. The third part of the chapter gives an insight into the value of DAZ3 as a sperm cell-specific marker in the characterization of various germ cell division mutants for germ cell fate. It also

describes the successful knockdown of DAZ3 in homozygous ProDAZ3:DAZ3-mCherry background using RNAi and artificial micro RNA (amiRNA) tools providing evidence that small RNA pathways are active in the plant male germline.

5.2 Expression analysis of DAZ3 and DAZ3L in pollen and sporophytic tissues by RT-PCR

It has already been established that both DAZ3 and DAZ3L are sperm cell-specific genes and is also evident by the microarray data from both ATH1 (Borges *et al.*, 2008; Honys and Twell, 2004) and AGRONOMICS1 array (Figure 5.1B) (Le Trionnaire and Twell unpublished). To further investigate the expression pattern of these genes in pollen as well as other sporophytic tissues, two approaches were used. To get an insight into the expression pattern of these genes, microarray data available in public databases was utilized and was further validated by RT-PCR analysis of cDNA generated from different sporophytic tissues and pollen developmental stages.

Arabidopsis Gene Family Profiler (aGFP) database (Dupl'akova *et al.*, 2007) contains a large collection of normalized Affymetrix ATH1 microarray datasets including NASCArray and AtGenExpress transcriptomic datasets for various tissues at different developmental stages. AtGenExpress contains a set of experiments, involving Columbia-0 plants grown under comparable conditions to provide a gene expression atlas at several developmental stages from various sporophytic tissues (Schmid *et al.*, 2005)**.** Similarly NASCArrays is a compilation of all other datasets deposited at Nottingham *Arabidopsis* Stock Centre (NASC) (Craigon *et al.*, 2004) and contains experiments carried out in various ecotypes grown under various conditions. All gametophytic and sporophytic transcriptomic data from aGFP database was gathered from nearly 350 gene chips and normalized using dChip software. The MAS5 algorithm was used to determine the present and absent calls for hybridization events. Only the expression of DAZ3 in both sporophytic and pollen developmental stages could be analysed form the online transcriptomic datasets, as DAZ3L probe sets are absent from the ATH1 microarray. Analysis of DAZ3 expression in sporophytic tissues with AtGenExpress dataset from aGFP database showed absent expression in different sporophytic tissues including seedlings, shoot, leaf and root. Furthermore, analysis of transcriptomic profile using NASC dataset at aGFP showed reduced expression at

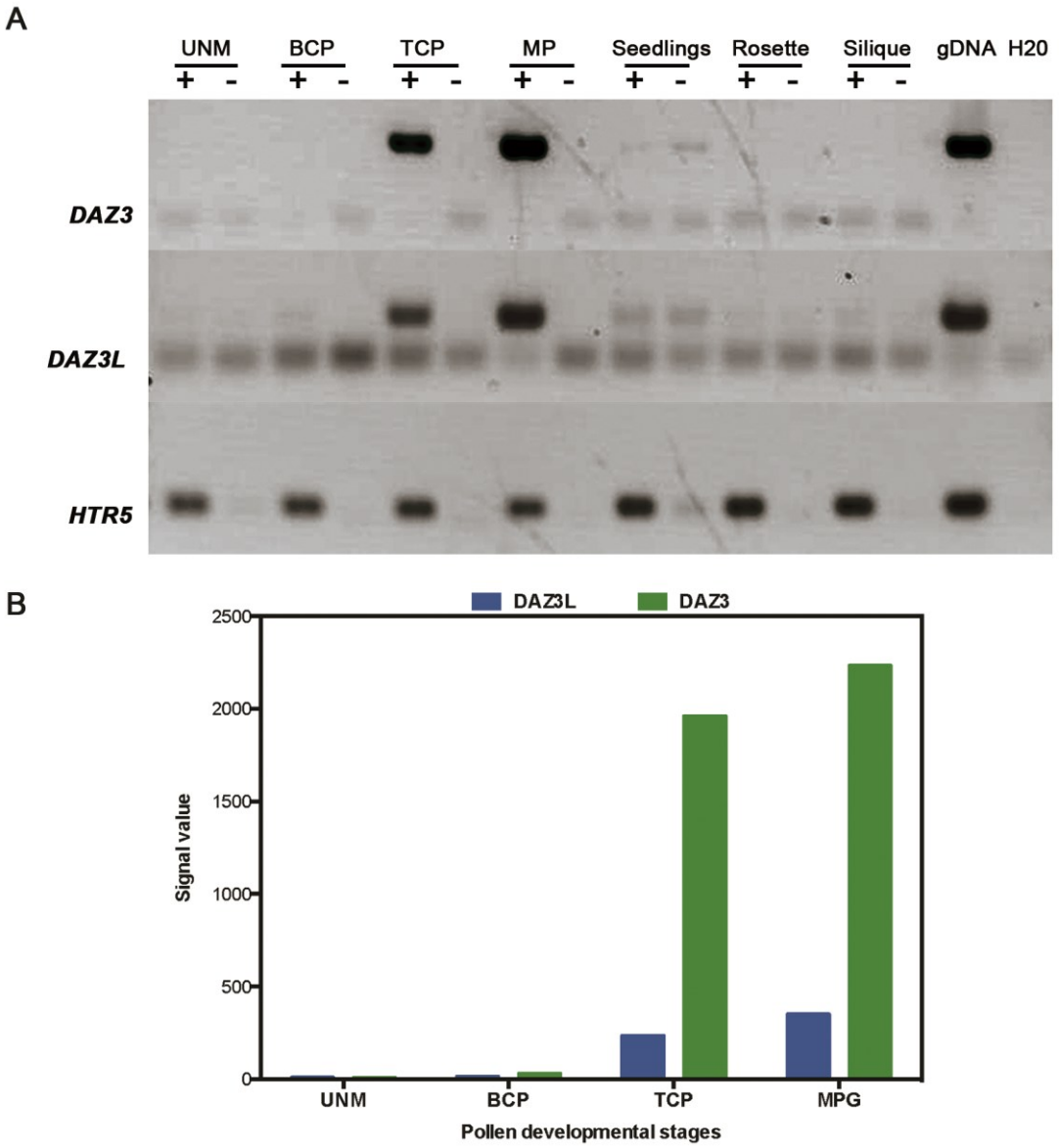

Figure 5.1: Analysis of DAZ3 and DAZ3L expression from microarray data and in plant tissues using RT-PCR. (A) Results from RT-PCR analysis of DAZ3 and DAZ3L in sporophytic tissues and pollen developmental stages illustrating restricted expression to tricellular pollen. PCR reactions were performed on the cDNA synthesised from total RNA samples of different sporophytic and pollen developmental stages as well as genomic DNA. A mock –RT control was also synthesized containing all the RT-PCR reagents except the reverse transcriptase and used as control for potential contamination from gDNA. Both +RT and –RT cDNA samples were used for amplifications. The primers used amplified PCR products specific for DAZ3 (top panel), DAZ3L (middle panel) and Histone HTR5 (at4g40040) that was used as positive control. The transcripts of DAZ3 and DAZ3L are detected at tricellular and mature pollen stage. No expression could be detected in other tissues. **(B)** A bar graph representing transcriptome data derived from AGRONOMICS microarray experiment depicting normalized signal values for the two zinc finger proteins (Le Trionnaire and Twell unpublished). The data shows reduced transcripts of DAZ3 and DAZ3L at unicellular and bicellular stages. The transcripts for both genes increase significantly at tricellular stage and mature pollen stage. UNM;unicellular microspore, BCP;bicellular pollen, TCP;tricellular pollen, MPG; mature pollen grain, gDNA; genomic DNA.

microspore and bicellular stage but the expression value increased many fold at tricellular and mature pollen stage. The expression of DAZ3 and DAZ3L in other sporophytic tissues and pollen developmental stages was verified further by reverse transcription polymerase chain reaction (RT-PCR) analysis. Total RNA was extracted from several vegetative tissues including seedlings, root, shoot apex, silique and from different pollen developmental stages. A reverse transcription polymerase chain reaction (RT-PCR) was performed on cDNA generated from total RNA samples and PCR amplification was performed using 1 in 5 dilutions of cDNA. A pair of PCR primers was designed for both intron-less genes and genomic DNA was also amplified to check primer efficiency and for the correct size of amplicon. For each sample, an RT control reaction was performed with no reverse transcriptase enzyme to detect any genomic contamination in the total RNA samples. Histone H3.2 gene *HTR5* (At4g40040) is constitutively expressed in all tissues and was used as a positive control for the assay.

The transcripts for *DAZ3* and *DAZ3L* were not detected in sporophytic tissues i.e. seedlings, siliques and rosette stage whereas transcripts for both genes were detected at tricellular pollen and mature pollen stages (Figure 5.1A). These results show that the expression of both *DAZ3* and *DAZ3L* is highly restricted to the pollen and remains at low levels in the sporophytic tissues. In pollen developmental stages expression of both genes is not detected at unicellular microspore stage (UNM) and bicellular pollen stage (BCP). The transcripts rapidly accumulate at tricellular pollen stage and higher transcript levels are observed at mature pollen stage. The expression profile observed using RT-PCR for DAZ3 are in agreement with the microarray data from the aGFP database confirming that DAZ3 is highly expressed at mature pollen stage. Moreover high protein identity between DAZ3 and DAZ3L and their similar expression patterns in sporophytic and pollen tissues implies that both genes may play similar role in later stages of pollen development.

5.3 Analysis of DAZ3 and DAZ3L promoter activity during pollen development

The expression analysis of DUO1 target genes have been shown to exhibit similar expression profiles and are expressed throughout pollen development. The activity of the target promoters is first detected after pollen mitosis I (Borg *et al.*, 2011; Brownfield

et al., 2009a). To verify that DAZ3 and DAZ3L show more or less same behaviour and to investigate the spatio-temporal activity of both DAZ3 and DAZ3L promoters, a set of constructs were generated with each of the native target promoters driving the expression of a histone and GFP fusion (H2B-GFP) fusion that localises fluorescence to the nucleus. These constructs were introduced into plants through floral dipping. Plants generated were initially analysed by examining developing pollen from different bud stages stained with DAPI and observations made under fluorescent microscope by using DAPI and GFP filters. Later several independent single loci homozygous T2 lines were analysed by releasing pollen from different bud stages dissected directly in 0.3M mannitol and subsequently examined by fluorescent microscopy using differential interference contrast and GFP filter sets. The developing pollen from bud stages was analysed in mannitol to avoid any background fluorescence observed in some pollen when stained with DAPI solution. The phenomenon was also previously reported as not the true expression of transgene but autofluorescence and was observed in the earlier stages of pollen development in plants heterozygous for the transgene as well as in wild type plants (Engel *et al.*, 2005).

Detailed analysis of the 714bp DAZ3 promoter during pollen development revealed late activity of the gene. As predicted by the microarray data no GFP could be detected in earlier bud stages until formation of tricellular pollen (Figure 5.2A-E). According to Lalanne and Twell (2002), -1 and -2 buds represent immature tricellular pollen while -3 bud stage represents a mixture tricellular and bicellular pollen. Interestingly a small proportion of tricellular pollen (3% to 6%) was observed that expressed faint GFP signal at -3 bud stage. A remarkable increase in the number of tricellular pollen with GFP signal was observed in -2 bud stage where 91% of the tricellular pollen showed strong GFP signal. The subsequent -1 and mature pollen stages showed further increase in the number of tricellular pollen expressing GFP from 99% in -1 bud stage to 100% in the mature pollen (Figure 5.2K). Similarly a 1.2kb DAZ3L promoter showed the same expression pattern with GFP signal first detected in tricellular pollen at -3 bud stage that increased remarkably in later bud stages. The data discussed here represents individual lines analysed for GFP expression (Figure 5.2F-J). Several other independent homozygous T2 lines for both DAZ3 and DAZ3L showed very similar patterns of expression.

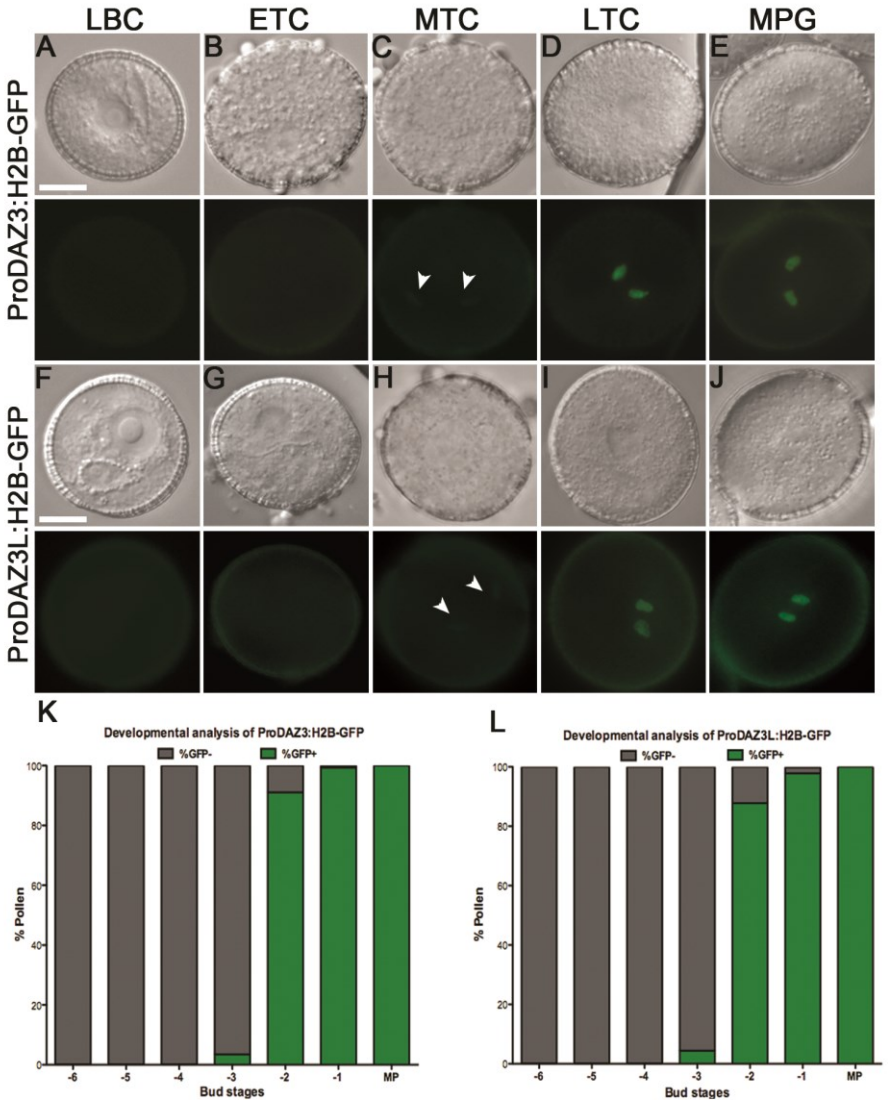

Figure 5.2: Analysis of DAZ3 and DAZ3L promoter activity during pollen development. (A-E) Expression of ProDAZ3:H2B-GFP in pollen developmental stages. Top panel (A-E) shows five progressive stages: **(A)** late bicellular (LBC), **(B)** early tricellular (ETC), **(C)** mid tricellular (MTC), **(D)** late tricellular (LTC) and **(E)** mature pollen grain (MPG). Buds from plants containing reporter constructs were separated and sequentially arranged based on their position on the floral axis. The first fully open flower represented +1 bud stage, whereas the first and second unopened flowers were termed as -1 and -2 bud stage respectively (Lalanne and Twell, 2002). Pollen from successive bud stages was dissected out in 0.3M mannitol and analysed using fluorescent microscope at DIC and GFP filter sets. GFP expression was first detected in mid tricellular pollen stage (indicate by arrowheads) (MTC), with increased expression in late tricellular pollen (LTC). The GFP expression peaked at mature pollen stage (MPG). **(F-J)** The same trend of GFP expression was observed for ProDAZ3L:H2B-GFP construct during pollen development, with appearance of GFP signal at **(H)** mid tricellular pollen stage as indicated by arrowheads (MTC) a increase in the GFP signal at **(I)** late tricellular and peaking at **(J)** mature pollen stage**.** Scale bars represent 10µm. **(K-L)** Bar graphs representing percentage counts of pollen population expressing GFP signal in DAZ3 and DAZ3L marker lines during pollen development. The higher percentages of pollen expressing GFP at tricellular stage suggest that DAZ3 and DAZ3L are sperm cell specific genes. LBC;Late bicellular, ETC;early tricellular, MTC;mid tricellular pollen, MPG;mature pollen grain.

Following the division of the germ cell, the two newly formed sperm cells appear round (anaphase and telophase) and represent early tricellular pollen stage (ETC) mostly observed at -3 and -4 bud stages. The two incipient sperm cells then undergo a series of morphological changes and appear elongated, here referred to as mid tricellular stage (MTC) observed at -2 and -1 bud stages. The two sperm cells then elongate further and mature at anther dehiscence a state referred to as mature pollen grain stage (MPG). One remarkable similarity in expression pattern of both promoters is the first appearance of GFP in tricellular pollen that could be classified as mid tricellular based on their advanced developmental stage compared to early tricellular pollen. This mid tricellular stage could be identified in -3 stage buds based on the morphology of sperm cells and representing a small proportion that showed elongating sperm cells. However the subsequent -2 bud stage is composed of maximum number of mid tricellular pollen and more than 90% of the tricellular pollen expresses GFP signal. As the sperm cells progressed in maturity, the number of GFP expressing tricellular pollen peaked to 100% at -1 bud stage and at anther dehiscence (Figure 5.2K-L). The specific increase in promoter activity of both DAZ3 and DAZ3L in sperm cells makes them one of the novel categories of late germline genes with possible roles after germ cell division and in sperm cells in pollen tubes and/or fertilisation.

The promoter activities of both DAZ3 and DAZ3L were specifically detected in the sperm cells and no GFP signal was observed in the earlier microspore or the vegetative cell validating their tight germline specificity confined to developing sperm cells.

5.4 Protein localisation of DAZ3 and DAZ3L in developing pollen and in germinating pollen tubes

5.4.1 Analysis of DAZ3 and DAZ3L proteins fused to the mCherry reporter in developing pollen

According to sperm cell transcriptomic data DAZ3 represents one of the most abundant transcripts in the sperm cells (Borges *et al.*, 2008) and together with DAZ3L represents one of the few known sperm cell-specific genes. As discussed earlier both DAZ3 and DAZ3L show higher activity specifically in the tricellular pollen. This was validated by RT-PCR analysis and expression profiling of sperm cell-specific promoter activity

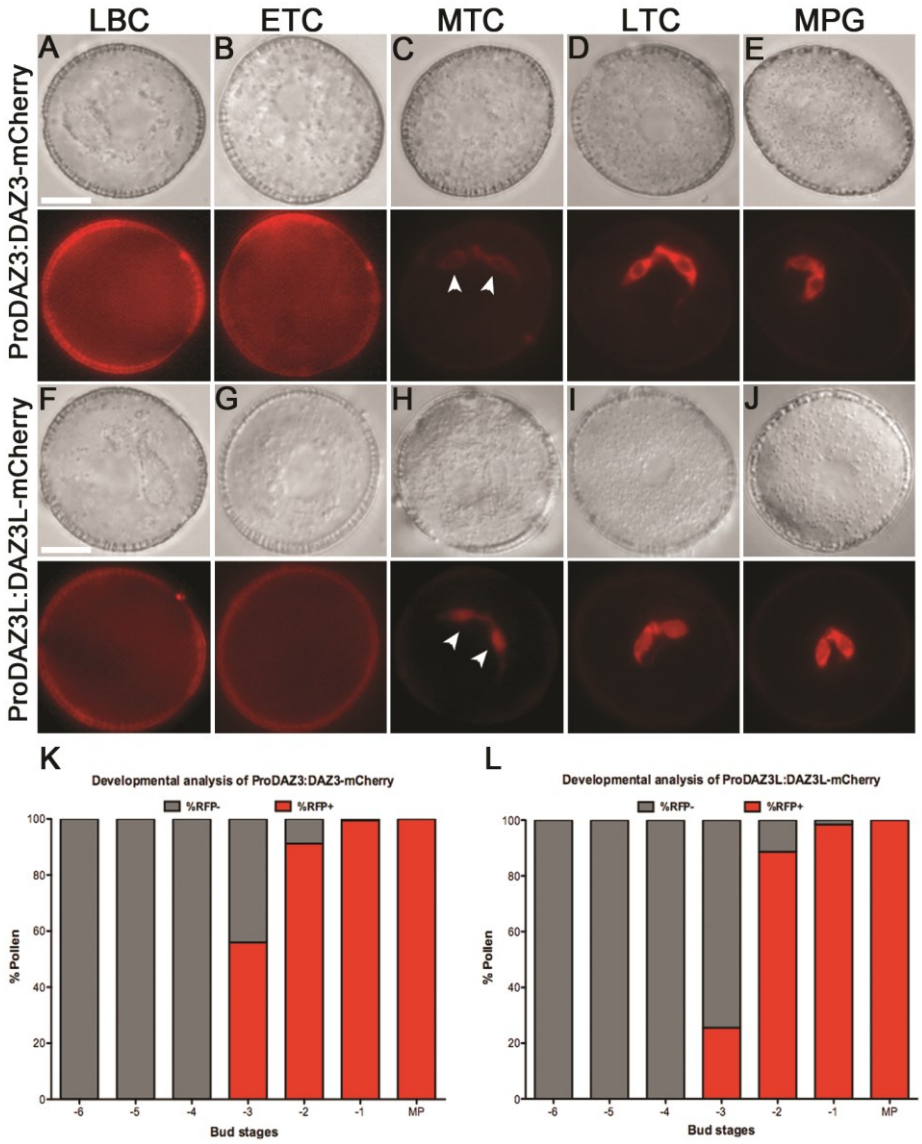

Figure 5.3: Analysis of DAZ3 and DAZ3L protein fusion constructs during pollen development. (A-E) Expression of ProDAZ3:DAZ3-RFP in pollen developmental stages. Top panel **(A-E)** shows five progressive stages: **(A)** late bicellular (LBC), **(B)** early tricellular (ETC), **(C)** mid tricellular (MTC), **(D)** late tricellular (LTC) and **(E)** mature pollen grain (MPG). Buds from plants expressing the reporter constructs were separated and analysed based on their position on the floral axis (Lalanne and Twell, 2002). Pollen from bud stages was dissected out in 0.3M mannitol and examined with fluorescent microscope using DIC and RFP filter sets. Counts for pollen with RFP signal were carried out in different bud stages. RFP expression was detected in the mid tricellular pollen stage (MTC) (indicated by arrowheads), which increased in late tricellular pollen (LTC) and peaked at mature pollen stage (MPG). **(F- J)** The same trend of RFP expression was observed for ProDAZ3L:DAZ3L-RFP construct during pollen development. The expression of RFP signal was first detected at **(H)** mid tricellular pollen stage (MTC) (indicated by arrowheads) with subsequent increase at **(I)** late tricellular and **(J)** mature pollen grain stage. Scale bars represent 10µm**. (K-L)** Bar graphs representing percentage counts of pollen expressing RFP signal in DAZ3 and DAZ3L marker lines during pollen development. The higher percentages of RFP+ pollen at tricellular pollen stage suggest that DAZ3 and DAZ3L are sperm cell specific genes. The data presented here is consistent with percentage counts for promoter activity of DAZ3 and DAZ3L. LBC;Late bicellular, ETC;early tricellular, MTC;mid tricellular pollen, MPG;mature pollen grain.

for both genes. To further investigate the specific localisation of DAZ3 and DAZ3L proteins during transcript accumulation, a pair of protein fusion constructs was generated by multisite gateway recombination. Each construct comprised of DAZ3 or DAZ3L promoters driving expression of their respective coding regions as red fluorescent protein (mCherry) fusions i.e. ProDAZ3:DAZ3-mCherry and ProDAZ3L:DAZ3L-mCherry. Wild type plants were transformed with each construct and stable transgenic lines were generated. T1 and subsequent T2 lines were analysed for expression and localisation of DAZ3 and DAZ3L protein fusion constructs. Pollen from different bud stages was dissected out in 0.3M mannitol and subsequently examined by fluorescence microscopy. The expression of both DAZ3 and DAZ3L protein fusion constructs mirrored the activity of their promoter alone and showed expression specifically in the developing sperm cells in tricellular pollen. The mCherry reporter expression was first detected in the immature tricellular pollen, which can be referred to as mid-tricellular pollen based on the developing sperm cell morphology (Figure 5.3C, H). In the following bud stages the number of tricellular pollen expressing the RFP signal increased remarkably and at anthesis all the tricellular pollen displayed 100% positive RFP signal (Figure 5.3D-E, I-L). Interestingly the mCherry fluorescence was observed in both sperm cells throughout the cytoplasm, extending into the longer tail-like cytoplasmic extensions associated with sperm cell 1 (SC1) which is closest to the vegetative nucleus. Fluorescence could also be seen in the shorter cytoplasmic extension of sperm cell 2 (SC2), which is farther from the vegetative nucleus (Figure 5.4) (McCue *et al.*, 2011). The expression was also observed in the region connecting the two sperms. This analysis confirmed that DAZ3 and DAZ3L expression is not detected in other pollen developmental stages including the vegetative cell and that the activity of both genes is restricted to the sperm cells.

An interesting phenomenon encountered was the difficulty of using DAPI to analyse nuclear DNA and reporter expression for both DAZ3 and DAZ3L. DAZ3 being the most abundant sperm cell-specific gene was expected to exhibit higher fluorescent intensity of mCherry in the sperm cells. The blue fluorescent DAPI is used to stain the nuclear double stranded DNA and appears to associate with AT clusters in the minor groove. DAPI solution used in the analysis contains 0.8 µg/ml DAPI in GUS buffer (100 mM sodium-phosphate, pH 7; 5 mM EDTA, 0.1% Triton X-100) that contains Triton X-100 detergent. The use of detergent in DAPI solution is important for rapid

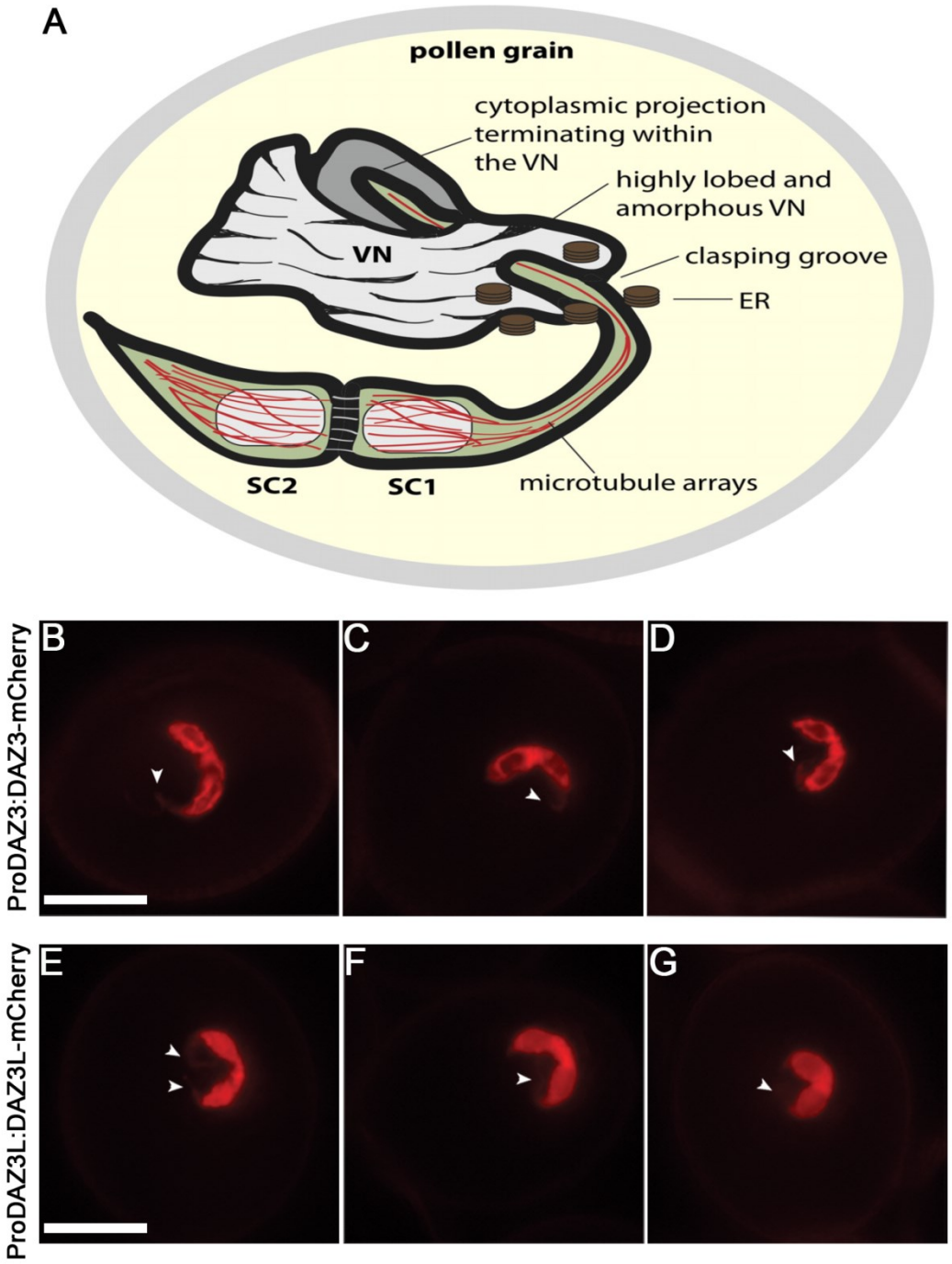

Figure 5.4: Fluorescent micrographs of pollen illustrating tail-like cytoplasmic extensions associated with sperm cells. (A) A schematic diagram of the sperm cell cytoplasmic extension connected with the vegetative nucleus. The illustration depicts the highly lobed structure of the vegetative nucleus containing indentations referred to as 'clasping grooves'. The cytoplasmic extensions/projections of sperm cells associate with the vegetative nucleus at these sites (adapted from Mc Cue *et al.*, 2011)**. (B-G)** Mature pollen from DAZ3 and DAZ3L mCherry reporter lines was mounted in 0.3 M mannitol and examined by fluorescence microscopy using RFP filter. The red fluorescence is observed in pollen harbouring **(B-D)** DAZ3 and (**E-G)** DAZ3L reporter constructs. Images presented here illustrate the expression of red fluorescent protein in the sperm cells as well as tail-like cytoplasmic extensions in both marker lines. The arrowheads indicate the tail-like extensions of the two sperm cells. Scale bars represent 10µm.

uptake of the dye by the sperm cell and subsequently by the nucleus, ultimately staining the DNA. The use of DAPI solution thus creates pores in the plasma membrane of the sperm cells, which allows the highly abundant DAZ3 protein to escape from the sperm cells and thus creating a halo around the sperm cells. No such fluorescence was observed when mature pollen carrying ProDAZ3:DAZ3-mCherry was mounted in mannitol which maintains pollen membrane integrity and viability. This observation suggests that sperm cells have abundant DAZ3 protein evident from the high levels of reporter expression in the whole sperm cells, consistent with the transcriptomic predictions for the gene.

5.4.2 Analysis of DAZ3 and DAZ3L fluorescent protein localisation in sperm cells

Another important question to address was to determine if these remarkably similar proteins share the same location in the sperm cells. To determine the subcellular localisation of the DAZ3 and DAZ3L proteins, mature pollen from plants expressing ProDAZ3:DAZ3-mCherry and ProDAZ3L:DAZ3L-mCherry was scored for mRFP expression utilizing fluorescent and confocal laser scanning microscopy. DAZ3 and DAZ3L belong to the C2H2 transcription factor family and hence it is logical to expect their activity to be localised to the nucleus. Mature pollen from several independent homozygous T2 lines was mounted in mannitol and mCherry reporter expression was scored using fluorescent microscopy and later by confocal laser scanning microscopy. Interestingly, in DAZ3, mCherry fluorescence is exclusively localised to the cytoplasm. Nearly 98% of pollen showed mCherry reporter expression specifically in the cytoplasm and only 2% of the pollen showed both nuclear and cytoplasmic expression (Figure 5.5A-G). The nuclei in the sperm cells appeared dark compartments suggesting that DAZ3 mCherry is excluded from the nucleus. The absence of putative Nuclear Localisation Signal in DAZ3 protein is consistent with the absence of DAZ3 protein from the nucleus. In the case of DAZ3L, majority of the pollen population showed cytoplasmically enriched expression with a detectable signal in the nucleus. A significant proportion of the DAZ3L pollen (25%) showed both nuclear and cytoplasmic localisation. A uniform fluorescence was observed in the DAZ3L pollen population staining the nucleus and cytoplasm in the sperm cells. This pattern can clearly be distinguished from that of DAZ3 sperm cells (Figure 5.5H-N). This result suggests that

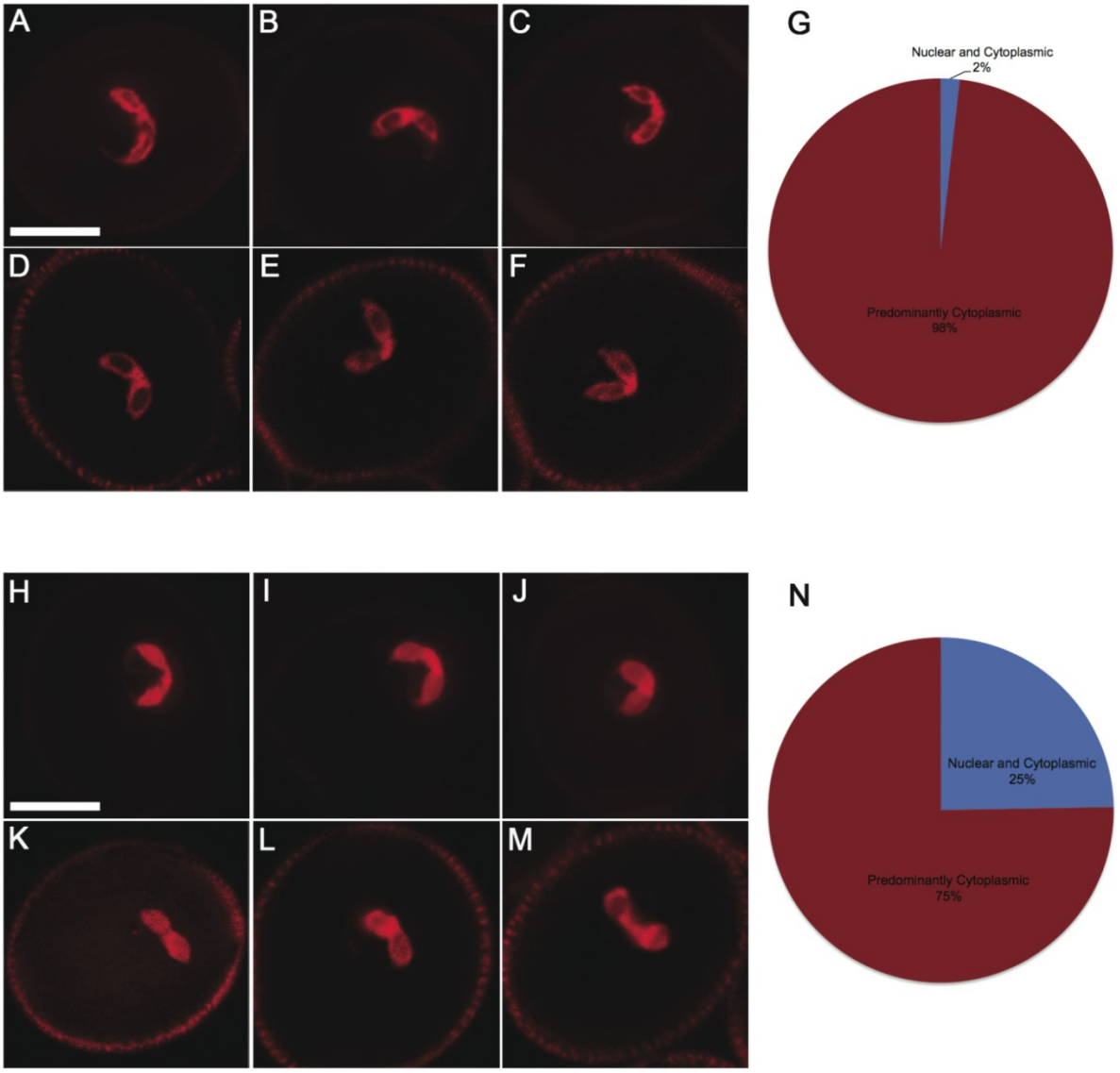

Figure 5.5: Analysis of DAZ3 and DAZ3L fluorescent protein localization in sperm cells. Mature pollen from plants expressing DAZ3 and DAZ3L mCherry reporter constructs under the regulation of their native promoters was mounted in mannitol and visualized with the fluorescent microscope. **(A-C)** Top panel shows representative images of pollen expressing ProDAZ3:DAZ3-mCherry construct as analysed with fluorescent and **(D-F)** confocal laser scanning microscope. In sperm cells expressing DAZ3 driven mCherry reporter, fluorescence is exclusively localized to the cytoplasm. The sperm nuclei can be seen as dark, hollow compartments devoid of RFP signal. **(G)** Approximately 98% of pollen analysed showed predominantly cytoplasmic expression. **(H-M)** The lower panel shows images of mature pollen expressing ProDAZ3L:DAZ3L-mCherry construct. **(H-J)** Mature pollen analysed with fluorescent microscope and **(K-M)** confocal laser scanning microscope, showed that majority of pollen has cytoplasmically enriched expression with detectable signal in the nucleus. **(N)** A significant proportion of DAZ3L pollen (25%) showed both nuclear and cytoplasmic localization. Scale bars represent 10μm.

putative NLS in DAZ3L protein may be partly functional in assisting the protein transport in to the nucleus. It also suggests that these two similar proteins may be a part of the same regulatory pathway but with different functions and hence have different locations in the sperm cells.

5.4.3 Analysis of DAZ3 and DAZ3L fluorescent fusion proteins localisation in germinated pollen tubes

The analysis of mature pollen shows that both DAZ3 and DAZ3L proteins show predominantly cytoplasmic localisation. The expression of the two proteins was further analysed in the germinated pollen tubes to determine whether both DAZ3 and DAZ3L protein remain localised in their respective locations as observed in the mature pollen or whether there is a shift in the localisation after the sperm cells have undergone further development during their transport to the ovule for double fertilisation event. A newly developed *in vitro* pollen germination protocol (Rodriguez-Enriquez *et al.*, 2013) was used. According to the protocol, pollen was placed in contact with a cellulose membrane overlying an agarose-based pollen germination media. The slides were placed in a vertical position in a humid sealed box and incubated in the dark at 24°C for 10 to 12 hours. The cellophane membrane with germinated pollen was carefully removed with forceps from the agarose pad and placed on drop of the liquid germination media of same composition as the solid germination media without agarose on a new slide. A cover slip was placed on the cellophane membrane and then sealed with nail varnish. The germinating pollen tubes expressing ProDAZ3:DAZ3-mCherry and ProDAZ3L:DAZ3L-mCherry construct were observed with fluorescent microscopy using partial bright field optics and mRFP filter set.

The pollen tubes (n=50) carrying sperm cells expressing DAZ3 fluorescent protein showed no change in the localisation of the DAZ3 protein and remained exclusively cytoplasmic as observed in mature dehisced pollen (Figure 5.6A-F). The expression of DAZ3L fluorescent protein in the germinating pollen tubes (n=50) also remained partly nuclear and cytoplasmic as observed in mature pollen (Figure 5.6G-K). The result shows that both proteins remain localised in their respective locations in the sperm cells inside the growing pollen tubes. Based on their expression in pollen tubes it could be speculated that both proteins may persist in the sperm cells even after being delivered to

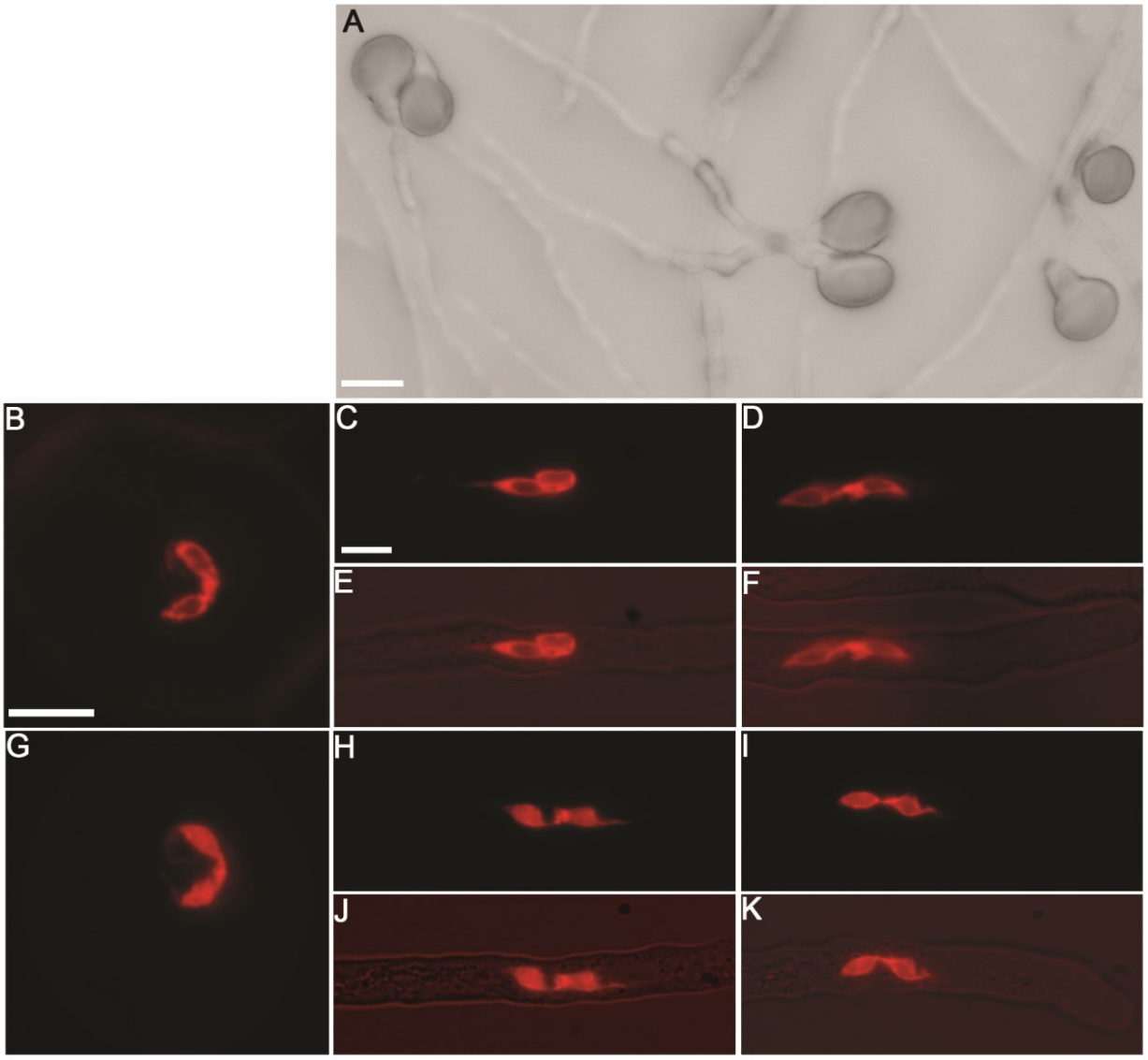

Figure 5.6: Expression of DAZ3 and DAZ3L fluorescent proteins in germinated pollen tubes. Pollen from lines harbouring DAZ3 and DAZ3L m Cherry constructs was germinated on agarose-based pollen germination media. Germinated pollen tubes were observed with partial bright field optics and RFP filters. **(A)** Bright field image of germinated pollen tubes after 10 hours incubation. **(B)** Dehisced pollen image showing ProDAZ3:DAZ3-mCherry expression localized to cytoplasm. **(C-F)** Microscopic observations of two sperm cells in pollen tubes with RFP filter **(C-D)** and partial bright field optics **(E-F)** showed localization of RFP signal to the sperm cell cytoplasm as observed in **(B)** mature pollen. Similarly, observation of DAZ3L fluorescent protein construct in **(G)** mature pollen and germinated pollen **(H-K)** showed similar expression trends. The RFP expression remained partly nuclear and cytoplasmic, with varied expression in the sperm nucleus. Scale bars represent 10µm.

the embryo sac for double. It also suggests that the two proteins remain non-degraded in the pollen tubes and hence may have a role in events taking place before or after fertilisation.

5.5 DAZ3 promoter is active normally in germ cells defective in division

It has already been established that *DAZ3* promoter activation requires direct binding of *DUO1* to the MYB sites in the *DAZ3* promoter. While *DUO1* accumulates in germ cells before division, *DAZ3* is not expressed until after second mitotic division unlike other direct *DUO1* target promoters (e.g. *MGH3, DAZ1, DAZ2*) and hence is specifically expressed in sperm cells. This analysis raises some questions about the delayed activation of DAZ3 and its putative role in sperm cells differentiation. One of the important questions to address is whether the passage of germ cell through division is required for DAZ3 promoter activation or alternatively progressive germline differentiation determines the late onset of DAZ3 promoter.

To investigate the possible role of germ cell division in DAZ3 activation a number of germ cell division mutants were analysed. Two of the mutants analysed are required for cell cycle regulation and include *fbl17* and *cdka;1* (Iwakawa *et al.*, 2006; Kim *et al.*, 2008) which affect the activity of the A-type cyclin-dependent kinase (CDKA;1) and have very similar phenotypes. Similarly DUO1 and DUO3 (Brownfield *et al.*, 2009a; Brownfield *et al.*, 2009b) are important transcriptional regulators and both *duo1* and *duo3* division mutants affects germ cell division and differentiation. DAZ1 and DAZ2 (Borg *et al.*, 2011) are DUO1 regulated transcriptional factors that are also important components of germ cell division and differentiation machinery. Other important germ cell division mutants investigated include *duo2* (Durbarry *et al.*, 2005)*, duo4* and over expression lines of *ccs52* (Cell Cycle Switch protein 52) (Khatab and Twell unpublished).

The experiment was approached with two strategies. In the case of *daz1-1 +/- daz2-1-/-* and *daz1-1 -/- daz2-1+/-,* double hom-het mutant lines were transformed with ProDAZ3:H2B-GFP construct and T1 lines were examined by fluorescence microscopy to analyse the expression of *DAZ3* marker line in *daz1-1 +/- daz2-1-/-* and

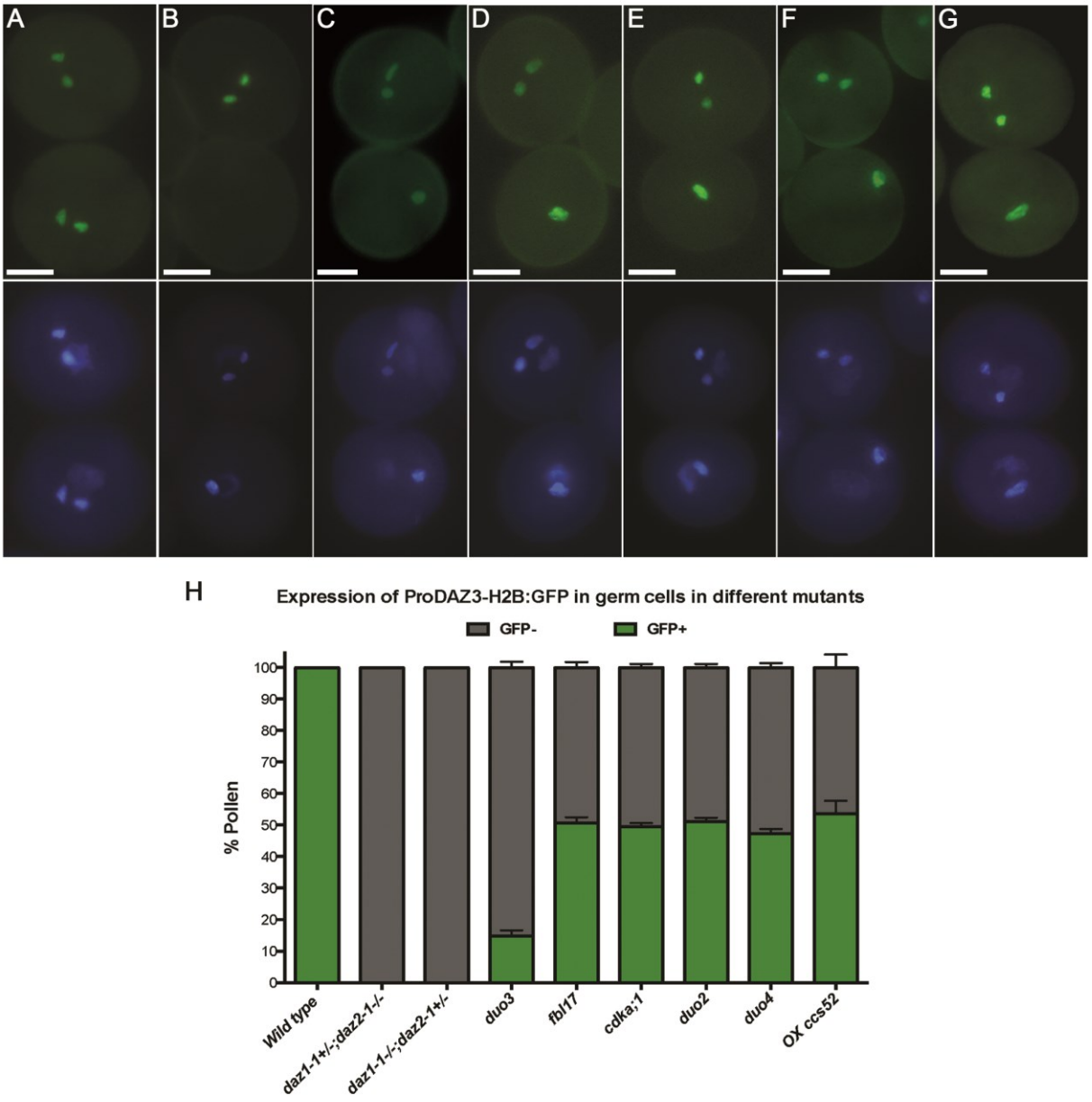

Figure 5.7: Expression analysis of ProDAZ3:H2B-GFP marker in germ cell division mutants. The expression of DAZ3 marker lines was analysed in different single germ cell mutants to investigate the role of division in DAZ3 activation. The marker line was crossed to a number of germ cell division mutants and GFP expression was scored in the germ cells. In the case of *daz1-1 +/- daz2-1-/-* and *daz1-1 -/- daz2-1+* mutants, T1 lines transformed with ProDAZ3:H2B-GFP construct were analysed for GFP expression. Mature pollen from at least three F1 and T1 plants was stained with DAPI and analysed with fluorescent microscope. **(A)** Image illustrating expression of DAZ3 marker line in specifically in sperm cells in wild type plants. (**B-G)** Images illustrating expression of DAZ3 driven H2B-GFP construct in mutant germ cells. The top panel shows both mutant and wild type pollen images with GFP fluorescence and bottom panel represent corresponding DAPI images. **(B)** No GFP signal could be detected in *daz* double mutant, whereas **(C)** a small proportion of *duo3* mutant germ cells showed low GFP levels. Normal GFP expression was observed in mutant germs cells of **(D)** *fbl17*, **(E)** *cdka;1*, **(F)** d*uo2* and **(G)** *duo4* and *OXccs52*. Scale bars represent 10μm. **(H)** Bar chart illustrates mean percentage GFP expression in mutant germ cells. Error bars represent the standard error of the mean of at least four lines examined.

daz1-1 -/- daz2-1+/- mutant germ cells. No GFP expression could be detected in mutant germ cells in both double hom het *daz* mutants (Figure 5.7A-B). The expression could only be seen in wild type pollen where 50% of wild type pollen expressed GFP signal.. In another approach crosses were made between single locus homozygous ProDAZ3:H2B-GFP lines and germ cell division mutants including *fbl17*, *cdka;1, duo3, duo2, duo4* and *OXccs52* and reporter expression was analysed in the mutant germ cells in each mutant. F1 progeny were analysed for GFP signal in mutant germ cells and the expression scored. The GFP signal was detected in wild type sperm cells and mutant germ cells in both *fbl17* and *cdka;1* mutants. Similarly mutant single germ cells in *duo2, duo4* and OX*ccs52* showed normal DAZ3 expression. In the case of *duo3*, less than one third of the mutant germ cells variably expressed GFP signal (Figure 5.7C-G).

The absence of DAZ3 from *daz1-1 +/- daz2-1-/-* and *daz1-1 -/- daz2-1+/-* double hom-het mutant lines can be attributed to the fact the mutant germ cells are not fully differentiated and lack important differentiation factors and as a result are unable to express DAZ3 which is active presumably in the functionally mature germ cells. It also suggests the importance of DAZ1 and DAZ2 in activation of DAZ3 and it could be speculated that presence of both DAZ1 and DAZ2 is necessary for the normal activation of DAZ3. The *duo3* mutant germ cells also exhibited reduced DAZ3 expression implying the possible involvement of DUO3 in modulating DAZ3 activity in the germline. The normal expression of DAZ3 in cell cycle mutants *fbl17* and *cdka;1* suggest its cell cycle independent activation in the germline. Similarly other novel germ cell division mutants, *duo2, duo4* and *OXccs52* also normally express DAZ3 expression (Figure 5.7H). These observations demonstrate that late activation of DAZ3 promoter is not dependent on passage through division but germ cells must go through a progressive germline differentiation to mature and to normally express DAZ3 and other germline and fertilisation factors including MGH3, GEX2 and GCS1. In this regard DAZ3 is a part of germ/sperm cell maturation pathway and is active only in cells that have begun to differentiate.

5.6 RNAi and artificial microRNA (ami) Knockdown of DAZ3

The identification of DAZ3 as a late gene and exhibiting one of the most abundant

transcripts in the mature pollen raise questions about its possible functions in the sperm cell differentiation and other important roles before and after delivery of sperm cells to the embryo sac. The highly specific male gametophytic expression can be attributed to fundamental functions of DAZ3 during sperm cell formation. To understand mode of action of this gene, the best strategy was to analyse DAZ3 knockout T-DNA lines. Due to unavailability of the DAZ3 knockout T-DNA insertions another strategy was devised to uncover its functional role during pollen development. A knockdown approach was adopted exploiting small RNA pathways or RNA interference (RNAi) as well as targeted artificial microRNA (amiRNA) as tools. A number of studies have shown that many of the transcripts involved in different small RNA pathways could be detected in pollen that are required for miRNA and siRNA biogenesis (Grant-Downton *et al.*, 2009). The artificial microRNA has already been successfully employed in *Arabidopsis* pollen to characterize pollen genes (Coimbra *et al.*, 2009). Similarly small interfering RNAs (siRNAs) have also been shown to be present in sperm cells (Slotkin *et al.*, 2009).

A series of constructs were generated that targeted DAZ3 transcripts in the tricellular pollen. The functional knockdown of DAZ3 was achieved by following two strategies. In one instant 21-mer artificial microRNAs directed against DAZ3 transcripts were designed exploiting online web tool Web MicroRNA Designer. Two different artificial microRNAs, termed amiR1 and amiR2 were selected for targeting DAZ3 transcripts. The two microRNAs chosen had two different recognition sites in the DAZ3 mRNA to maximize chances of successful knockdown. The two ami's were cloned into entry clone pDONR221 and subsequently inserted in a gateway vector, pBDAZ3GW7/pB2GW7 using one part cloning. The destination vector already had DAZ3 promoter cloned into the vector.

Similarly existing gateway sense-antisense vectors i.e. pB7GWIWG2 (II, 0) (Karimi *et al.*, 2002) was modified and the amplified DAZ3 promoter with SacI and SpeI restriction sites was introduced into the vector using conventional cloning methods. Two target regions in DAZ3 coding sequence were selected and referred to as hairpin target fragment 1 or hp1 (188 bp long) and hairpin target fragment 2 or hp2 (187 bp long). These sequences were PCR amplified using gene specific primers tagged with recombination adapter sequences and cloned into donor vector (pDONR221) to generate

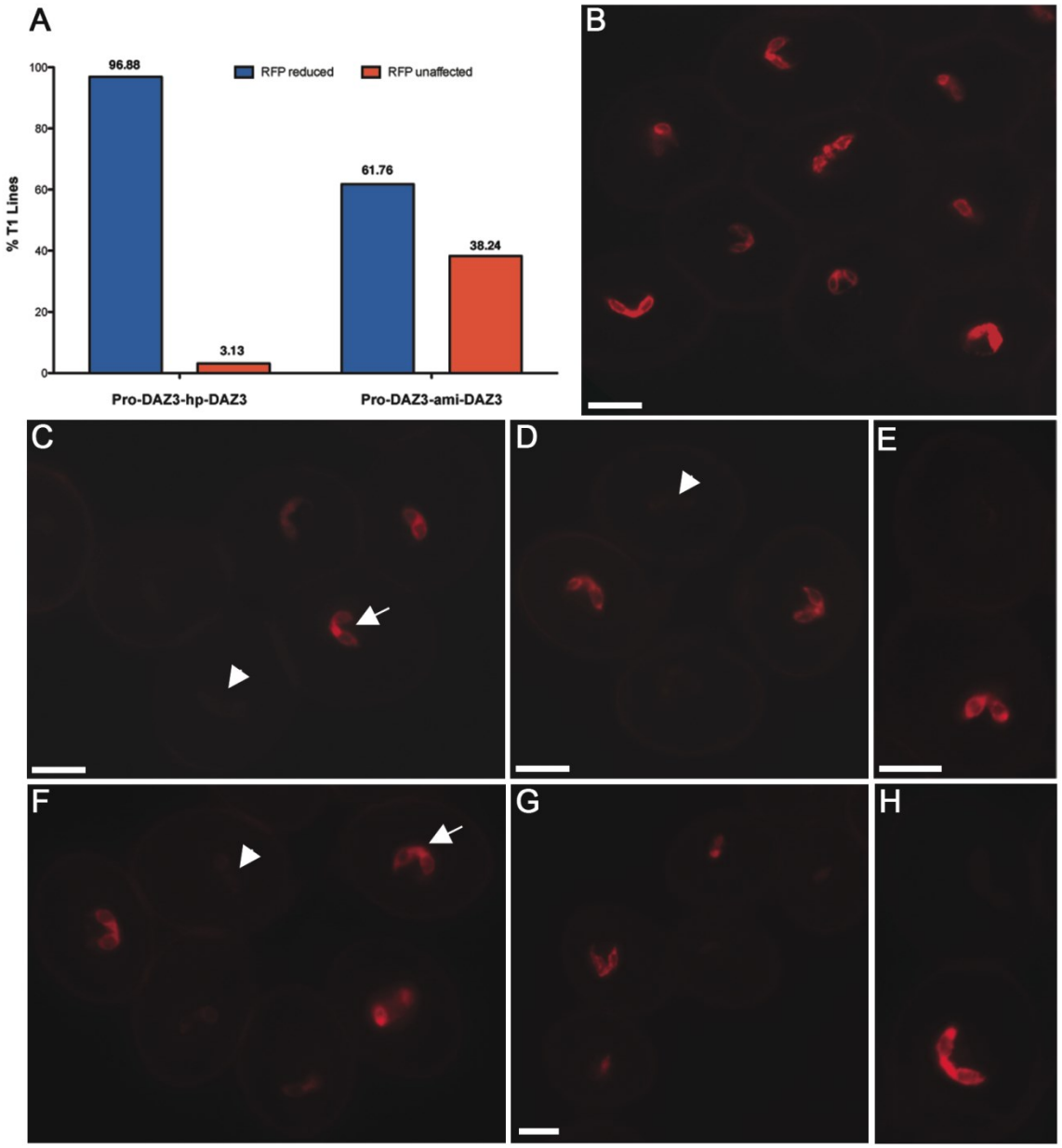

Figure 5.8: Knockdown of ProDAZ3:DAZ3-mCherry expression in sperm cells using hairpin and artificial microRNA constructs. A series of hairpin and artificial microRNA constructs were generated to knockdown DAZ3 transcripts in pollen. Homozygous ProDAZ3:DAZ3-mCherry lines were transformed with construct carrying DAZ3 targeted hairpin and ami constructs driven by DAZ3 promoter. **(A)** Bar chart representing percentage T1 knockdown lines harbouring hp and ami constructs. **(B)** Image illustrating a homozygous marker line exhibiting uniform bright RFP expression, whereas **(C-H)** reduction in expression can clearly be seen in knockdown lines. Approximately 97% of homozygous marker lines transformed with hairpin constructs showed successful knockdown. **(C-E)** Representative images showing reduced RFP levels in pollen from T1 lines carrying hairpin construct targeted against DAZ3. In the case of ami knockdown, 62% of the marker lines **(F-H)** displayed reduction in RFP levels. Arrowheads indicate sperm cells with reduced RFP levels, while; arrows indicate sperm cells showing normal expression of DAZ3 protein construct. The morphology of pollen containing the knockdown transgene appear normal similar to wild type pollen. Scale bars represent 10μm.

entry clones. Verified entry clones were used in an LR reaction with modified destination vector, pBDAZ3GW7, to generate final expression vectors. Both amiRNA and hairpin constructs targeting DAZ3 transcripts were transformed into single locus homozygous ProDAZ3:DAZ3-mCherry lines (Col-0). Knockdown constructs carried resistance marker to BASTA herbicide whereas homozygous marker lines carried resistance marker to antibiotic Kanamycin. T1 seed from transformed plants were sown on soil hydrated with 30mg/ml BASTA to select individuals harbouring knockdown constructs. Mature pollen from about 16 lines from each construct was mounted in mannitol and examined by fluorescence microscopy. The mature pollen from knockdown lines were expected to show reduced RFP expression reflecting the down regulation of DAZ3 transcripts. As expected the analysis of RFP expression in the lines carrying the knockdown constructs showed visible reduction in the mCherry reporter levels compared to the pollen not carrying the knockdown transgene. Homozygous DAZ3-mCherry lines were also used as control to determine the extent of DAZ3 reporter knockdown in T1 lines (Figure 5.8B). The number of T1 lines with reduced RFP levels was recorded for both ProDAZ3-hp and ProDAZ3-ami lines and their knockdown efficiency determined. A comparison between the amiRNA and hairpin knockdown revealed that more T1 lines harbouring hairpin constructs had reduced RFP levels compared to lines carrying amiRNA constructs (Figure 5.8A). Approximately 97% of the ProDAZ3-hp lines showed successful knockdown of the homozygous DAZ3-mCherry expression (Figure 5.8C-E), whereas approximately 62% of the ProDAZ3-ami lines exhibited reduced mCherry levels (Figure 5.8F-H). Another interesting observation was the relatively efficient knockdown of DAZ3 transcripts in ProDAZ3-hp lines where DAZ3-mCherry levels in the sperm cells appeared reduced compared to its reduction in the sperm cells analysed in ProDAZ3-ami lines. Knockdown of DAZ3 did not yield a visible mutant phenotype, as all screened pollen had wild type appearance; however in some hp and ami T1 lines a proportion of collapsed pollen was also observed. The general plant morphology of the plants carrying knockdown constructs appeared normal showing no effects on general sporophyte development. Although late timing and high levels of DAZ3 activation in pollen may suggest its putative role in events after pollen is shed, however the formation of siliques appeared normal indicating that pollen carrying the knockdown transgene was capable of fertilisation.

Although DAZ3 transcripts were successfully targeted for degradation exploiting small RNA as tools, further analysis of the DAZ3 knockdown lines is required to determine its functional role. This could be done by male transmission crosses and segregation analysis of single locus T2 generation to assess transmission through both parents. In the case of segregation distortion, seed set and fertilisation defects could be examined in both heterozygous and homozygous knockdown lines to characterize the developmental role of DAZ3.

5.7 Discussion

This chapter has described the sperm cell-specific expression profiles of DAZ3 and DAZ3L by using fluorescently labelled promoter and protein fusion constructs with special emphasis on the expression profile of DAZ3 which according to microarray data (Borges *et al.*, 2008) represents one of the highly expressed genes in the *Arabidopsis* germline. Analysis of datasets derived from gametophytic and sporophytic tissues clearly indicated that DAZ3 expression is germline specific. According to microarray expression dataset AtGenExpress from aGFP database, DAZ3 expression could not be detected in the sporophytic tissues including seedlings, shoot, leaf and root. Moreover, NASCArray dataset also showed highly reduced DAZ3 expression at microspore stage and bicellular stage, that peaked manifolds at tricellular and mature pollen stage (Dupl'akova *et al.*, 2007). The expression profiles of DAZ3 and DAZ3L were further verified by performing a reverse transcription polymerase chain reaction (RT-PCR) on cDNA generated from total RNA samples. These RNA samples were extracted from various sporophytic tissues and pollen developmental stages. The results clearly suggested that expression of DAZ3 and DAZ3L is highly restricted to tricellular and mature pollen. These results were further put to test and fluorescently labelled promoter and protein fusion constructs were analysed *in planta.* The analysis clearly indicated that DAZ3 and DAZ3L expression is absent from any other sporophytic tissues but show increased expression specifically in developing sperm cells.

After it was established that activity of both proteins is restricted to the sperm cells, it was necessary to determine their location in the sperm cells. For this purpose both fluorescent and laser scanning microscopy was used to analyse reporter expression in the nucleus and cytoplasm of the sperm cells. As discussed in section 4.3, a basic stretch

of amino acids is present at the N-terminal portion of each protein that may serve as putative Nuclear Localisation Signal (NLS) (Lange *et al.*, 2007). However, microscopic analysis suggested that DAZ3 protein is absent from the nucleus and is exclusively cytoplasmic, whereas, DAZ3L show both nuclear and cytoplasmic localization suggesting that putative NLS in DAZ3L C-terminal region is functional. The reporter expression was also determined in the germinated pollen tubes to monitor any shift in localization after the sperm cells have undergone further development during their transport to the embryo sac. The results suggested that both proteins remain localized in their respective compartments in the sperm cells.

One of the important issues discussed in the thesis is the delayed activation of DAZ3 and its putative role in sperm cell differentiation. An important question to address was whether late activation of DAZ3 is dependent on passage through germ cell division or is it progressive differentiation of developing germline that determines the late onset of DAZ3 expression. A number of germline division mutants were crossed with single locus homozygous ProDAZ3:H2B-GFP marker lines and the GFP expression was specifically scored in the aberrant germ cells. The results showed that germ cell division mutants normally express DAZ3 marker line eliminating the idea that passage through division is required for its activation. However, germ cells must undergo progressive germline differentiation to mature and therefore express DAZ3 and other germline and fertilization factors including MGH3, GEX2 and GCS1. As discussed earlier, DAZ3 represents one of the most abundant transcripts in the sperm cells indicating that DAZ3 is required for sperm cell differentiation and maturation. In order to test functional role of DAZ3 in the germline a knockdown approach was adopted. DAZ3 transcripts were targeted using amiRNA and hairpin constructs and knockdown was performed in ProDAZ3:DAZ3-mCherry background. The reporter mCherry provided a good control to determine the extent of knockdown by visibly scoring pollen with reduced RFP levels. According to microscopic analysis of T1 pollen carrying knockdown amiRNA and hairpin constructs, a number of T1 lines with reduced RFP levels were scored for both ami and hp constructs. ProDAZ3-hp lines showed 97% successful knockdown as compared to 62% knockdown exhibited by ProDAZ3-ami lines. The successful knockdown did not yield a visible phenotype suggesting that the function of DAZ3 is substituted by its *Arabidopsis* homologue, DAZ3L. To test the functional role of DAZ3 and DAZ3L, efficient knockdown of both proteins could be performed to determine

their role in sperm cell functions. Furthermore, male transmission crosses and segregation analysis of single locus T2 lines will assess transmission through male and female parents further characterizing their function.

Chapter 6 General discussion

6.1 Summary

The formation of twin sperm cells in *Arabidopsis* requires interplay of division and specification programmes activated at specific points during germline development. A recent discovery of regulatory pathway of genes controlled by the master regulator DUO1 provides a unique opportunity to decipher various mechanisms underlying male gametophyte development. The utilization of forward and reverse genetics approaches have proved useful in identifying mutants affecting male and female gametophyte development. The use of EMS-mutagenesis screens has yielded a number of germ cell division mutants as well as mutants defective at later stages of pollen development. The cloning and further analysis of these mutants have increased our understanding of developmental and differentiation programmes that govern male germline development. In particular, the morphological screen using DAPI staining (Park *et al.*, 1998) yielded a novel class of mutants termed the *duo pollen* mutants. DUO1, that coordinates germ cell division with specification, is an important germline regulator and the first transcription factor identified in the screen (Brownfield *et al.*, 2009a).

The work presented in thesis aims to understand the mechanisms controlling the germ cell division and differentiation. The work described in the thesis has investigated phenotypic and genetic aspects of a novel *duo5* mutant, an EMS-induced mutation that affects germ cell division. The phenotypic analysis focuses on the analysis of the germ cell phenotype as well as determination of the point in development where mutant deviates from the wild type developmental pattern. Two approaches were used i.e. microscopic examination of DAPI-stained pollen from successive bud stages in the wild type and mutant plants and DNA content measurement of the mutant germ cells relative to that of prometaphase arrest mutant, *duo*2 that exhibits approximately 2C DNA content at anthesis. Both approaches confirmed that *duo5* pollen deviated from normal development at germ cell stage and more specifically at prophase stage. Pollen viability assays used included staining with fluorescein diacetate (FDA), *in vitro* pollen germination assay and analysis of the seed set in siliques form heterozygous and homozygous *duo5* plants. The analysis revealed that pollen viability of heterozygous

mutant pollen was similar to wild type pollen. However, homozygous mutant pollen displayed significant reduction in percentage of pollen viability and was evident from the reduced seed set in siliques from homozygous *duo5* plants as compared with wild type (Figure A2). Furthermore, genetic analysis revealed that *duo5* is an incompletely penetrant gametophytic mutation, displaying reduced transmission though the male parent. Established and newly developed PCR based markers including SSLP and dCAPS markers delimited the mutant *duo5* locus to 250 kb region on the lower arm of chromosome IV. Although not discussed in the thesis, additional approached were also employed to identify *duo5* mutation. These included analysis of heterozygous *duo5* pollen in tetraploid background to determine the dominant or recessive nature of the mutation and unsuccessful transformation attempts of a number of JAtY clones into the *duo5* mutant plants to identify clones that complement the *duo5* division defect if the mutation is loss-of-function, to further resolve the position of the mutation. Phenotypic analysis of loss-of-function T-DNA lines in candidate genes was also performed to identify mutation causing germ cell division defect. The preliminary results from tetraploid analysis as well as lack of observable phenotype in candidate *duo5* T-DNA lines revealed that *duo5* locus could represent a semi-dominant gain-of-function mutation. In this respect, whole genome sequencing (WGS) as well as gain-of-function approach named as the FOX (Full-length cDNA Over-eXpressor gene) hunting system would further contribute in identifying the elusive *duo5* mutation (Ichikawa *et al.*, 2006; Sakurai *et al.*, 2011).

The thesis also discusses the expression pattern as well as DUO1-dependent transactivation of the two zinc finger proteins. The first piece of evidence suggesting that both genes are putative DUO1 targets that are activated both directly and indirectly; originate from the expression analysis of DAZ3 and DAZ3L marker lines in *duo1* germ cells. The lack of expression in mutant *duo1* germ cells supports the idea that the two zinc finger proteins are integral part of DUO1 regulatory network active late after germ cell has divided. Both genes have similar sperm cells enriched gene expression profiles as evident form the AGRONOMICS and ATH1 microarray data. The upstream regulatory regions of the two promoters harbour putative MYB binding sites. DAZ3 promoter contains two whereas, DAZ3L promoter has single MBS. Interestingly, both promoters share identical binding site referred to as MYB motif 2 (awAAACCGCta) (Borg *et al.*, 2011). The significance of the MYB binding sites is further investigated by

analysing magnitude of luciferase expression of 5'deletion and mutagenized promoters of the two late genes using transient luciferase assays. The analysis established that upstream regulatory regions as well as MYB binding sites are involved in the activation of the two genes. More precisely, the experimental evidence strongly suggests that MBSs in the DAZ3 promoter contribute in the DUO1-dependent transactivation of the promoter *in vivo*. The single MBS in DAZ3L promoter appear to have no functional role in promoter activation; however, loss of upstream regulatory region causes significant reduction in luciferase activity. In addition, both proteins share 60% similarity in their protein structure. According to the classification of zinc finger proteins in *Arabidopsis* genome based on *in silico* analysis of the whole proteome, DAZ3 and DAZ3L belong to the C1-1iCa subgroup of the C2H2-type zinc finger family harbouring a single zinc finger domain (Englbrecht *et al.*, 2004). The N-terminal portion of DAZ3L contains a basic stretch of amino acids that is predicted to act as a nuclear localisation signal and is absent from DAZ3 protein. In the C-terminal region, are present a pair of repression motifs called EAR motifs that are implicated in inhibiting transcription by modifying chromatin structure of regulatory regions (Hiratsu *et al.*, 2003; Ohta *et al.*, 2001). The similarity in protein structure is also reflected in the promoter and protein expression profiles that are strictly sperm cell-specific. The analysis of DAZ3 marker line (ProDAZ3:H2B-GFP) in germ cell division mutants revealed that DAZ3 promoter activation is cell cycle independent further suggesting that mutant germ cells must undergo a progressive germline differentiation programme to mature and therefore normally express DAZ3 marker line. This identifies DAZ3 as an important germ/sperm cell maturation factor that is only expressed in differentiated germ or sperm cells. The absence of transcripts in sporophytic tissues and the germline specific expression shows that DAZ3 and DAZ3L act redundantly to participate in germline differentiation events that occur after the germ cell has divided. Interestingly, DAZ3 protein construct exclusively localises to the cytoplasm whereas, in DAZ3L, 25% of pollen exhibit both nuclear and cytoplasmic localisation of the mCherry reporter. The predominantly cytoplasmic expression of the two proteins remains unaltered while the sperm cells are inside the growing pollen tubes. This observation also suggests that the two proteins may remain non-degraded even after the sperm cells have entered the embryo sac and hence may have a role in the events taking place before or after fertilisation. In addition, these proteins may represent candidate transcription factors that may have a role in

activating and regulating de novo transcription during pollen tube growth (Loraine *et al.*, 2013). The most abundant transcripts profile as well as highly specific male gametophytic expression of DAZ3 at mature pollen stage makes it an ideal candidate to explore its function. Hence to determine its functional role knockdown approach was adopted utilizing targeted artificial microRNA and RNA interference (RNAi) as tools. Although DAZ3 knockdown lines produced pollen population with visibly reduced mCherry levels exhibiting successful knockdown of the gene, further analysis is required to determine the effect of the knockdown on pollen development. Furthermore, double knockdown of DAZ3 and DAZ3L would elucidate the role of this redundant gene pair encompassing various aspects of sperm cell formation including sperm cell differentiation and function in fertilisation thereby affecting male transmission, fertilisation and seed set. This analysis would provide insights into novel role of the two DUO1-dependent zinc finger proteins that are activated late in development.

6.2 Delayed mitotic progression of *duo5* germ cells may impact germ/sperm cell maturation

One of the major objectives set out in this thesis was the characterization and identification of *duo5* mutation that specifically impairs germ cell division. The frequency of mutant *duo5* germ cells in heterozygous plants comprises 43% of total pollen population at anthesis, whereas in homozygous condition approximately 74% of mature pollen consists of single germ cells. The mutant phenotype can be categorized in different classes based on the shape of germ cell nucleus as well as shape of the germ cell. A number of male gametophytic mutants such as *cdka;1*, *fbl17*, *duo1, duo2* and *duo3* cause arrest or delay in germ cell division thus producing pollen containing round germ cells (Aw *et al.*, 2010; Brownfield *et al.*, 2009b; Durbarry *et al.*, 2005; Iwakawa *et al.*, 2006; Kim *et al.*, 2008; Nowack *et al.*, 2006; Rotman *et al.*, 2005). A distinguishing character of *duo5* mutant is abnormally elongated germ cell phenotype that represents a novel phenotypic class exhibited by a proportion of mutant germ cells. Mutant germ cells also display other phenotypic classes including round, mitotic and irregular germ cells. It has been established that *duo5* germ cells arrest at G2 and M phase of the cell cycle. In majority of the *duo5* germ cells further progression to form sperm cells is delayed and therefore, proportion of mutant *duo5* germ cells remain in different mitotic

stages when pollen is shed suggesting that germ cell division is not blocked but delayed. In a similar study Aw *et al.,* (2010) reported that a predominant proportion of germinated *cdka;1* pollen tubes contain two sperm cells, thus concluding that *cdka;1* delayed but did not prevent germ cell division.

Successful fertilisation and zygote formation depends on the development of the fully mature gametes that are able to undergo plasma membrane fusion, cytoplasm mixing or plasmogamy and fusion between gamete nuclei or karyogamy. One strategy to determine if the aberrant male gametes are mature and able to perform fertilisation is to investigate expression of cell fate markers in mutant germ/sperm cells. The effect of *duo5* mutation on the expression of sperm cell differentiation genes was also tested by analysing expression of germ and vegetative cell fate markers, indicating that cell fate is not altered. Apart from normal expression of the majority of the cell fate markers tested, the absence of sperm cell-specific maturation marker, ProDAZ3:H2B-GFP, suggested possible impact on *duo5* male gamete maturation. Similar analysis of *cdka;1* also suggested that aberrant germ cells exhibit normal cell fate. However, variable expression levels of ProHTR10-RFP (Okada *et al.*, 2005) was observed in *cdka;1* pollen carrying one or two sperm cells compared with wild type pollen thus leading to altered chromatin composition (Aw *et al.*, 2010). Similarly, progression delay in *duo5* germ cells could also have impact on differentiation programmes at mature pollen stage. The absence of DAZ3 supports the hypothesis that delayed M phase in *duo5* germ cells correlates with delayed differentiation of *duo5* male gametes. The incomplete differentiation of these germ cells is carried over in the divided germ cells, resulting in immature sperm cells incapable of fertilisation. Previously it was reported that single germ/sperm cell in *cdka;1* and *fbl17* preferentially fertilises egg cells (Kim *et al.*, 2008; Nowack *et al.*, 2006), however, recent reassessment of the *cdka;1* mutant demonstrated an equal capacity to fertilise the egg cell or the central cell. Similarly, CAF-1 pathway-deficient mutant germ cells as well as single sperm cells produced by expression of diphtheria toxin A subunit of *Arabidopsis GCS1* promoter are functional and are able to fertilise the egg or central cell indiscriminately (Chen *et al.*, 2008; Frank and Johnson, 2009). Initial analysis of mutant *duo5* siliques suggested that a proportion of *duo5* germ cells are able to initiate fertilization but fail to produce healthy seeds (discussed in section 3.2.3). However, further analysis is required to determine if *duo5* germ cells undergo division during pollen tube germination thereby delivering two sperm cells to

the two female gametes. Also investigating expression of *GCS1* in *duo5* germ cells will further provide information about fertility of *duo5* male gametes (Mori *et al.*, 2006). Moreover, to establish the ability of *duo5* germ cells to perform fertilisation, crosses of *duo5* pollen onto *ms1-1* or wild type pistils could be performed and analysing siliques 3 days after pollination (DAP) by clearing and examining the number of ovules. This will help in identifying fertilisation defects in the developing embryo and/or endosperm. Furthermore, the expression of DAZ3 marker in divided *duo5* germ cells later in pollen tube would provide an estimate of *duo5* sperm cells that have undergone maturation and therefore are able to fuse with female gametes (egg cell and central cell). In the absence of DAZ3, The delay in division and differentiation of these DAZ3 devoid/lacking *duo5* mutant germ cells can potentially cause post fertilisation defects with possible ovule and seed abortion.

6.3 DUO1-dependent DAZ3 and DAZ3L promoter activation requires presence of MYB binding sites and upstream regulatory region

It has already been established that DUO1-activated target gene transcripts begin to accumulate rapidly following a peak in DUO1 expression consolidating the idea that these target genes are downstream of DUO1. Furthermore, a bioinformatics search identified MYB binding sites in the proximal promoter regions of target genes. The MYB binding sites identified represented DNA motifs enriched in A and C residues (Borg *et al.*, 2011). Studies have shown that other R2R3 MYB transcription factors identified also bind DNA sequences enriched in A and C residues. In the case of AtMYB61, such motifs have been identified using cyclic amplification and selection of targets (CASTing) approach (Prouse and Campbell, 2013).

A major objective of the thesis was to determine how DUO1 activates the two late target genes. Promoter regions of DAZ3 and DAZ3L contain MYB binding motif 2 (AACCGC) residing in the proximal promoter region. Furthermore, promoter analysis suggests that presence of MBSs in DAZ3 promoter is critical for DUO1-dependent activation, whereas single binding site in DAZ3L promoter is not functional. Interestingly, the analysis suggested that the upstream regulatory region plays important role in DUO1-dependent activation of DAZ3 and DAZ3L. Therefore, it can be

concluded that DUO1 directly binds MBSs to transactivate DAZ3 promoter. The putative direct relationship between DUO1 and DAZ3 can be further verified by employing *in vitro* and *in vivo* MYB-DNA interaction studies. This can be demonstrated by performing an *in vitro* Electrophoretic mobility shift assay (EMSA) or gel shift assay to detect physical interaction between DUO1 MYB domain and MYB binding sties in DAZ3 promoter. In the case of DAZ3L, the experimental evidence that mutagenized MBS has no effect on the DAZ3L promoter activity, weighs more in favour of the fact that DAZ3L activation is indirect although initial transient assay as well absence of DAZ3L promoter activity in mutant *duo1* germ cells suggest that DUO1 MYB domain may directly bind MYB sites in DAZ3L promoter. It has already been established *in vitro* that interaction between DUO1 MYB domain and the proximal target DNA site in *MGH3* promoter is direct, indicating that these motifs are critical for *MGH3* promoter activation (Borg *et al.*, 2011). In another study another R2R3 MYB transcription factor called MYB98 has been shown to directly bind specific DNA sequences in the target gene promoter thereby regulating its expression in synergids. Interestingly, the promoter region of the target gene *DD11* contained six binding sites but only one site remained functional (Punwani *et al.*, 2007). Several other MYB transcription factors have been shown to interact with other cofactors in a combinatorial fashion. These include WEREWOLF and GLABRA1 (Schiefelbein, 2003) and C1 (Grotewold, 2005). DAZ3L promoter may also harbour other binding sites located at an optimal distance containing adjacent sequences required for optimal DUO1 binding. It is also possible that DUO1 activates expression of another MYB protein that binds novel binding sites in DAZ3L promoter. Furthermore, the number and arrangement of these motifs is also critical for DUO1-dependent activation. It would be interesting to analyse DAZ3L promoter deletion 1 fragment with multiple *MGH3* MYB sites positioned in the proximal region to determine whether this modified promoter architecture would show increased activation in response to DUO1. Further analysis is required to ascertain the nature of DUO1-dependent DAZ3L activation.

6.4 DAZ3 and DAZ3L promoters are activated late after germ cell has divided

One interesting observation is the timing of the DAZ3 and DAZ3L promoter activation

late after division exhibiting a novel phenomenon of separation of transcription factor activity and target promoter activation in the male germline. The late activation of the DAZ3 promoter is also evident from the time-course overexpression microarray experiment, where DAZ3 transcripts were induced after 24 hours of DUO1 induction (Borg *et al.*, 2011). Promoter analysis of DAZ3 and DAZ3L showed increased promoter activity specifically confined to the developing sperm cells. Similarly, expression of both proteins mirrored the activity of their promoters exhibiting transcript accumulation specifically in sperm cells (discussed in sections 5.3 and 5.4.1). How DUO1 extends its regulatory authority in inducing expression of the two genes late after the division of germ cell remains elusive. In this context, two mechanisms could be accounted for their late activation. In first instance a direct repression mechanism could be involved in which a putative germ cell-specific repressor binds DAZ3 and DAZ3L promoters thereby masking binding sites rendering them inaccessible to DUO1. This repressor may undergo progressive inactivation or degradation until a critical threshold level is reached in the sperm cells allowing DUO1 to activate transcription of the two promoters. Till date single experimental evidence has emerged which showed that a repressor protein called GERMLINE-RESTRICTIVE SILENCING FACTOR (GRSF) specifically bind to a 10 bp silencer region GGCTGAATTT in the promoter of *LGC1* in lily thereby conferring strict gene repression in every cell except the sperm cells in pollen (Haerizadeh *et al.*, 2006). In another example, non-phosphorylated RBR binds to heterodimeric transcription factor E2F/DP thereby masking its transcriptional activation domain. This RBR-E2F repressor complex actively represses transcription of genes involved in DNA replication thus blocking G1 to S phase transition (Attwooll *et al.*, 2004).

In the second instance, an epigenetic repression mechanism could possibly involve alteration of chromatin structure from a repressive state in germ cells to an open permissive state in sperm cells. Studies of epigenetic modifications in *Arabidopsis* have shown that expressed and repressed genes carry different epigenetic marks. A large number of genes were found to contain H3K4me3 marks and have been shown to be associated with transcribed genes (Zhang *et al.*, 2009), whereas, trimethylation of Lys-9 on histone-3 (H3K27me3) represent a dominant repressive mark associated with repressed genes. Recent analysis has revealed that in *Arabidopsis* seedlings, the majority of pollen specific genes carry histone-3 marked by mono- or trimethylation of Lys-27

(H3K27me1/H3K27me3) marks in their promoters where H3K27me3 was identified as a predominant repressive mark resulting in transcriptional repression of male gametophytic genes in sporophyte. Interestingly, independent studies have found DAZ3 gene to be associated with the histone modification H3K27me3 indicating that novel mechanisms are at play that repress highly expressed pollen genes in *Arabidopsis* sporophyte (Hoffmann and Palmgren, 2013; Lafos *et al.*, 2011; Roudier *et al.*, 2011). In a recent study, low-cell-number chromatin immunoprecipitation assay (ChIP) was developed to investigate the chromatin of mouse primordial germ cells. The results demonstrated the existence of H3K4me3/H3K27me3 bivalent domains highly enriched at developmental regulatory genes at multiple stages of primordial germ cell development (Sachs *et al.*, 2013). Similarly, chromatin state in *Arabidopsis* germline can be characterized by utilizing ChIP protocol as well as ChIP sequencing (ChIP-seq) and ChIP-quantitative PCR (ChIP-qPCR) to demonstrate presence of such repressive marks in the developing *Arabidopsis* germline.

Furthermore, other mechanisms of chromatin repression also exist in eukaryotes. Many histone-modifying enzymes are able to remodel the chromatin state to favour or inhibit transcription initiation. Studies suggest that such mechanisms can actively repress transcription activity by interfering with non-DNA-binding proteins such as the co-repressors which in turn recruit chromatin remodelling factors for example histone deacetylases (HDACs). These HDACs may further remove acetyl groups from lysine residues of histone amino terminal tails resulting in tightening of chromatin and gene silencing (Krogan and Long, 2009). Interestingly, a new study has emerged that demonstrates the importance of a pair of DUO1-dependent C2H2 zinc finger proteins called DAZ1 and DAZ2 that are required to promote germ cell division and gamete differentiation in *Arabidopsis*. Most importantly, the study shows that the carboxy terminal of the two proteins harbour a repression motif called EAR motif. The EAR motif of DAZ1 has been shown to interact with a co-repressor called TOPLESS in an EAR-dependent manner. This interaction could result in transcriptional repression of factors that could limit expression of germline genes (Borg *et al.*, 2014). In this context, DAZ1/DAZ2 and TPL co-repressor complex may mediate derepression of DAZ3 and DAZ3L promoters thereby activating their expression in the sperm cells. However, further analysis of DAZ3, DAZ3L promoter repression will provide valuable insights into late activation as well as the novel roles of the two proteins in the male germline.

6.5 Future work

The work presented in the thesis focuses on the characterization and isolation of a novel germ cell division mutant, *duo5* as well as investigation of the role of a redundant pair of DUO1-dependent zinc finger proteins, DAZ3 and DAZ3L in the male gametophyte development. Several approaches have been utilized to decipher roles of these germline factors in controlling germ cell division and differentiation.

Map-based cloning was used to isolate *duo5* mutant, an EMS-induced mutation, in order to study its protein structure and to understand its role in the formation of sperm cells. Such methods have been frequently used to identify mutations induced by a commonly used mutagen, EMS and have been useful in identifying various other mutants including *duo1* and *duo3* (Brownfield *et al.*, 2009b; Durbarry *et al.*, 2005), however, the whole procedure is tedious and time-consuming. The identification of the affected gene takes approximately 1 year largely due to the fact that the process incorporates five cycles of the plant growth assuming 2 moths/cycle (Jander *et al.*, 2002). An alternative to the map-based cloning would be to utilize whole-genome re-sequencing strategy in order to uncover the mutation, potentially a SNP that is responsible for the phenotype. Whole-genome sequencing (WGS) approach has already been successfully used in both plants and animals to identify point mutations. (Ashelford *et al.*, 2011; Uchida *et al.*, 2011; Zuryn *et al.*, 2010). Similar approach could also be utilised to identify *duo5* mutation that has already been restricted to a 250kb region. Seeds stocks of homozygous *duo5* lines are in No-0 background and have been backcrossed four times. These lines could be sown on MS media and two weeks old seedlings collected in eppendorf tubes. DNA extracted from the pooled mutant seedlings as well as wild type segregant could be sequenced using Applied Biosystems SOLiD, sequencing by ligation technology or deep sequencing techniques. The analysis of sequenced data will further provide information about the genes containing C to T and G to A changes resulting in premature stop codons. Further expression of analysis of the candidate genes can be performed by RT-PCR analysis of the cDNA generated from homozygous *duo5* mature pollen RNA. Similarly, sequence data of the wild type segregant can be utilized to generate molecular markers that can be used to further pursue mapping.

In addition, to determine the functional role of the DUO1-activated, DAZ3 and DAZ3L,

double knockdown lines could be generated and analysed for their effect on the developing pollen. In this context, previously established T2 lines harbouring pKDAZ3:DAZ3-mCHERRY, knocked down with pBDAZ3:ami-DAZ3 and pBDAZ3:hp-DAZ3 constructs could be grown and plants screened for reduced RFP levels (50% for heterozygotes and 90 to 100% for homozygotes) and heterozygous and homozygous plants identified. In the meantime, DAZ3L ami and hairpin constructs could be cloned in a marked (LAT52-GFP) two-part vector. In this regard two different promoters, early promoter MGH3 and late promoter DAZ3 could be utilized to drive the expression of DAZ3L ami and hairpin constructs. Both wild type homozygous ProDAZ3L:DAZ3L-mCherry marker lines and homozygous DAZ3 ami and hairpin lines could be dipped with the four constructs (pHDAZ3:ami1-DAZ3-L, pHDAZ3:ami2-DAZ3-L, pHMGH3:ami1-DAZ3-L and pHMGH3:ami2-DAZ3-L) and T1 generation grown to identify single locus lines based on GFP expression (LAT52-GFP). The strategy should be to select best knockdown lines (with early or late promoter) in the single knockdown DAZ3L and double knock down DAZ3/DAZ3L mutant backgrounds. Also the single knockdown DAZ3L and Double knockdown DAZ3/DAZ3L T1 lines exhibiting reduced RFP levels in 50% of the pollen or GFP signal in 50% pollen population in a marked vector background could be considered as single locus lines. The DAZ3L ami knockdown T1 lines are also an important source for male transmission analysis and could be utilized to generate F1 crosses. These T1 lines as well as control wild type lines could also be analysed to determine seed gaps, seed abortion or silique length. T2 seed thus generated from the single and double knockdown lines could be further used to calculate segregation ratio of the transgene to determine segregation ratio distortions. Flowers from heterozygous and homozygous individuals from segregating DAZ3DAZ3L knockdown lines could be collected and RT performed to quantify the levels of reporter mCherry as well as endogenous DAZ3/DAZ3L transcript levels which will further provide molecular evidence for the knockdown of the two genes.

Appendices

Table A1: Sequences of oligonucleotide primers used

Primer	Sequence 5'→3' (attB sequences shown in bold)
At4g35060-70-Left Primer	CGACCTATTGGTGCTTGGAGAAC
At4g35060-70-Right Primer	CTCCAAAACGCTTTAGTTGACCAC
At4g35010-20-Left Primer	CCATCGATGATCAAAGAGGTTCC
At4g35010-20-Right Primer	CAAGTCTTTCCAACAGCACCGTC
At4g35160-65-Left Primer	TTCTGAACCGGACTGAACCCAAC
At4g35160-65-Right Primer	CACGAGATTAGCGACACTCACGG
At4g35230-40-Left Primer	AAAGGCAAAGAGTGAAGTGATCCG
At4g35230-40-Right Primer	AAAAGCGCCTTTCAGGATGATG
At4g34990-35000-Left Primer	TAAGGAGGTTGTAAAGGGCATC
At4g34990-35000-Right Primer	CCTGAAACTTGACCTAACCTGG
At4g35090-35100-Left Primer	CACCTATGGCTATGAGTGCTTG
At4g35090-35100-Right Primer	CGTGTATCGTATCTGGTAACGG
DUO5-SNP7-SacI-Forward	ATGTTTGAAGTGGTCAGTGGC
DUO5-SNP7-SacI-Reverse	AAACCATGTTATGTAGATCGGAG**C**T
DUO5-SNP6-NcoI-Forward	AGGCTAATGATTGGAAATAGTTC
DUO5-SNP6-NcoI-Reverse	AACTATAATAATATTTAAACCC**C**AT
DUO5-SNP2-DdeI-Forward	CTTCAAGACGAGAACTATTGGC**T**CA
DUO5-SNP2-DdeI-Reverse	GCCAATAGTTCTCGGTTCTTGAAG
At4g34670-34680-Left Primer	ACTCTCTCCCATTTTCTTGACG
At4g34670-34680-Right Primer	ATCAAGTCTAATCCACTCGCCTC
at4g34560-34570-Left Primer	GTTGGGGTAAAACTGAGTCCATC
At4g34560-34570-Right Primer	GTCTACATCCAAGAATCCTAAGGG
At4g34950-34960-Left Primer	GAAGATGTAAAGAGAGCGATAGCC
At4g34950-34960-Right Primer	ATAAGGAGGCGGCTAAGGATAAC
DUO5-dCAPS-DdeI-Forward-34990-35000	TAGAAGACATGCGTTTCTTTCT**C**TT
DUO5-dCAPS-DdeI-Reverse-34990-35000	TAAAAGAAAGAAACGCATGTCTTCTA
DUO5-dCAPS-AflII-Forward-34990-35000	TAGAAGACATGCGTTTCTTTCTT**AA**
DUO5-dCAPS-AflII-Reverse-34990-35000	TAAAAGAAAGAAACGCATGTCTTCTA
34990-35000-Col-0_deletion-Forward	GATTGTGGTTTTTATTCTTGTTTG
34990-35000-Col-0_deletion-Reverse	TGTCTTTCAGGTATCAAACAAACT
34560-70-Nos-0_deletion-Forward	CATAGATAAAGTTCTCGTGGTAA
34560-70-Nos-0_deletion-Reverse	GTCACCATGCATTTGTATGTC
DUO5-dCAPS-HinfI-Forward-34560-70	CTAAAGCATCGAATATTTGATA**G**AC
DUO5-dCAPS-HinfI-Reverse-34560-70	CCAATAAAAGTGAGACCAAGAT
DUO5-dCAPS-DdeI-Forward-34560-70	CATACAAATGCATGGTGACGGT
DUO5-dCAPS-DdeI-Reverse-34560-70	TCCAGATTAGGCATTAGCTAGT**C**TG
DUO5-dCAPS-HindIII-Forward-34950-60	ACCTGCCGTAATTAAAGTCCAAATA
DUO5-dCAPS-HindIII-Reverse-34950-60	ACAAGTCACACTTTCGAATTTCAA**G**
DUO5-dCAPS-DdeI-Forward-34950-60	ACCTGCCGTAATTAAAGTCCAAATA
DUO5-dCAPS-DdeI-Reverse-34950-60	ACAAGTCACACTTTCGAATTTC**T**AA
At4g34990-TDNA-LP	GCGACACTTACAAATGGCGAAC

Primer	Sequence 5'→3' (attB sequences shown in bold)
At4g34990-TDNA-RP	TGGATGCCCTTTACAACCTCC
At4g35050-TDNA-LP	TCCTCCTCTCTCTTTTTGGGCG
At4g35050-TDNA-RP	GGCTTTTGTGGCATACACCTCG
N505867-At4g35140-TDNA-LP	GGTTAGTGGGTCAGACTGTGGGA
N505867-At4g35140-TDNA-RP	TCTCTGGACTACTACTGCTTCGG
N809234-At4g35140-TDNA-LP	GCCAAACAATCTTCTCTCTCCCG
N809234-At4g35140-TDNA-RP	CCATCAGCAGCACAGGTTACTATC
At4g35270-TDNA-LP	GGTCCACTTTGTTCTTGGGGAAA
At4g35270-TDNA-RP	CCATCAAACAAGAGTTCATCCAT
At4g35220-TDNA-LP	CGTCTATGACAAGTATTACGATG
At4g35220-TDNA-RP	ACAGAGTAGAGTCCTGCCTTCAC
At4g35370-TDNA-LP	ACAGAATCACGAGAGAGAGATGC
At4g35370-TDNA-RP	TGGATAATAAAGGTGTCCCTGC
Left primer-ProDAZ3L-attB4-F	TGTATAGAAAAGTTGTGTGTGTGGTGGCTCTCTCTTTC
Right primer-ProDAZ3L-attB1-R	TTTTGTACAAACTTGACTATTTTCGCACTTTAGTCTAGG
At4g35610-attB1-F	**ACAAAAAAGCAGGCT**CTATGAGTAATCCGAACCCAGAGA
At4g35610-attB2-nsR	**ACAAGAAAGCTGGGT**CCTTGGGTTTGTCCTCTTCC
DAZ3L-RT-Left Primer	ATCTGCTTTTACTATTGCCACTGTC
DAZ3L-RT-Right Primer	ACAGGTTCCACATTCAAATCAATAC
pDAZ3-ΔD-R	CACACGGCGGTTTATGAGAGCTCTTTTTTTATGTGTGTC
pDAZ3-ΔD-F	GACACACATAAAAAAAGAGCTCTCATAAACCGCCGTGTG
pDAZ3-ΔR3-R	GTTTCTATGACCACACGGAGCTCTATGACCGTTATTTTTT
pDAZ3-ΔR3-F	AAAAAATAACGGTCATAGAGCTCCGTGTGGTCATAGAAAC
pDAZ3-ΔD-ΔR3_F	GAGCTCTCATAGAGCTCCGTGTGGTC
pDAZ3-ΔD-ΔR3_R	GAGCTCTATGAGAGCTCTTTTTTTATG
pDAZ3-L-ΔMYB1-F	GAGCTCCATGGTTCAGAGAAAACTTTATATAAG
pDAZ3-L-ΔMYB1-R	CTCTGAACCATGGAGCTCATGACAGTTAATTC
pDAZ3-Lke-Δ1-attB4-F	**TGTATAGAAAAGTTG**CAAATCTTCAAACGAAAAGGC
pDAZ3-Lke-Δ2-attB4-F	**TGTATAGAAAAGTTG**TGGTTCAGAGAAAACTTTATATAAGG

Table A2: Frequency of pollen phenotypic classes in wild type plants

EGC = elongated germ cell, RGC = round germ cell, P = prophase, MAT = meta-, ana- and telophase, AGC = abnormal germ cell.

	Mutant Pollen Classes										WT Pollen		
Line	**EGC**	**%EGC**	**RGC**	**%RGC**	**P**	**%P**	**MAT**	**MAT%**	**AGC**	**%AGC**	**TCP**	**%TCP**	**%Aberrant**
1	0	0.00	0	0.00	0	0.00	0	0.00	0	0.00	213	100	0.00
2	0	0.00	0	0.00	0	0.00	0	0.00	0	0.00	183	100	0.00
3	0	0.00	0	0.00	0	0.00	0	0.00	0	0.00	203	100	0.00
4	0	0.00	0	0.00	0	0.00	0	0.00	0	0.00	196	100	0.00
Total	0	0.00	0	0.00	0	0.00	0	0.00	0	0.00	795	100	0.00

Table A3: Frequency of pollen phenotypic classes in heterozygous *duo5* plants

EGC = elongated germ cell, RGC = round germ cell, P = prophase, MAT = meta-, ana-, and telophase, AGC = abnormal germ cell.

	Mutant Pollen Classes										**WT Pollen**		
Line	**EGC**	**%EGC**	**RGC**	**%RGC**	**P**	**%P**	**MAT**	**MAT%**	**AGC**	**%AGC**	**TCP**	**%TCP**	**%Aberrant**
1	110	27.16	37	9.14	14	3	6	1.48	11	2.72	227	56.0	43.95
2	63	27.75	20	8.81	6	2.64	4	1.76	4	1.76	130	57.3	42.73
3	76	26.30	8	2.77	11	3.81	8	2.77	13	4.50	173	59.9	40.14
4	69	26.54	36	13.85	4	1.54	3	1.15	8	3.08	140	53.8	46.15
Total	318	26.93	101	8.55	35	2.96	21	1.78	36	3.05	670	57	43.27

Table A4: Frequency of pollen phenotypic classes in homozygous *duo5* plants

EGC = elongated germ cell, RGC = round germ cell, P = prophase, MAT = meta-, ana-, and telophase, AGC = abnormal germ cell.

	Mutant Pollen Classes										WT Pollen		
Line	**EGC**	**%EGC**	**RGC**	**%RGC**	**P**	**%P**	**MAT**	**MAT%**	**AGC**	**%AGC**	**TCP**	**%TCP**	**%Aberrant**
1	59	37.34	25	15.82	11	6.96	11	6.96	24	15.3	28	17.83	82.39
2	45	28.66	7	4.46	17	10.83	23	14.65	16	10.2	49	31.2	68.80
3	64	36.57	12	6.86	18	10.29	13	7.43	17	9.7	51	29.14	70.84
4	52	41.94	3	2.42	13	10.48	14	11.29	11	8.87	31	25	75.00
Total	220	35.83	47	7.65	59	9.61	61	9.93	68	11.07	159	25.90	74.10

Table A5: The frequency of tricellular pollen at different bud stages in wild type, heterozygous and homozygous *duo5* plants, before, during and after germ cell division

SD = standard deviation, SEM = standard error of mean, N = number of lines

	%Tricellular pollen in wild type buds				%Tricellular pollen in heterozygous *duo5* buds				%Tricellular pollen in homozygous *duo5* buds			
	Mean	**SD**	**N**	**SEM**	**Mean**	**SD**	**N**	**SEM**	**Mean**	**SD**	**N**	**SEM**
-7	0	0	2	0	0.00	0.00	2	0	0.00	0.00	0	0
-6	0	0	3	0	2.72	3.84	3.00	2.22	0.00	0.00	0.00	0
-5	8.71	10.04	4	5.02	16.96	17.26	4.00	8.63	0.00	0.00	3.00	0
-4	49.15	21.54	4	10.77	25.63	21.01	5	9.4	0.00	0.00	5.00	0
-3	100	0	5	0	31.85	16.06	6.00	6.56	0.00	0.00	5.00	0
-2	100	0	4	0	45.80	6.36	6.00	2.6	4.04	4.64	5.00	2.07
-1	100	0	5	0	53.4	8.04	6	3.28	10.4	9.61	5	4.3

Table A6: The composition of pollen population in individual buds in wild type plants

RG = round germ cell, EG = elongated germ cell, MF = mitotic figures, ETC = early tricellular pollen, LTC = late tricellular pollen.

Pollen classes/Buds	**-8**	**-7**	**-6**	**-5**	**-4**	**-3**	**-2**	**-1**
RG	100	95.83	84.87	41.6	13.27	0.00	0.00	0.00
EG	0.00	4.17	14.72	22.38	16.74	0.00	0.00	0.00
MF	0.00	0.00	0.41	27.31	20.83	0.00	0.00	0.00
ETC	0.00	0.00	0.00	7.79	32.03	14.9	12.17	3.75
LTC	0.00	0.00	0.00	0.92	17.12	85.1	87.83	96.25

Table A7: The composition of pollen population in individual buds in heterozygous *duo5* plants

RG = round germ cell, EG = elongated germ cell, MF = mitotic figures, Bi-ACG = bicellular abnormally condensed germ cell nuclei, Bi-AEG = bicellular abnormally elongated germ cell nuclei, ETC = early tricellular pollen, LTC = late tricellular pollen.

Pollen classes/Buds	**-8**	**-7**	**-6**	**-5**	**-4**	**-3**	**-2**	**-1**
RG	100.00	80.80	70.60	36.79	28.91	12.58	2.03	0.00
EG	0.00	19.20	26.68	25.71	8.00	0.00	0.00	0.00
MF	0.0	0.0	0.0	15.9	22.7	27.7	28.4	22.5
Bi-ACG	0.00	0.00	0.00	4.15	2.69	2.73	5.09	7.53
Bi-AEG	0.0	0.0	0.0	0.5	12.0	25.2	18.7	16.6
ETC	0.00	0.00	0.91	9.19	15.40	10.90	9.58	2.84
LTC	0.00	0.00	1.81	7.77	10.23	20.94	36.22	50.55

Table A8: The composition of pollen population in individual buds in homozygous *duo5* plants

RG = round germ cell, EG = elongated germ cell, MF = mitotic figures, Bi-ACG = bicellular abnormally condensed germ cell nuclei, Bi-AEG = bicellular abnormally elongated germ cell nuclei, ETC = early tricellular pollen, LTC = late tricellular pollen.

Pollen classes/Buds	-7	-6	-5	-4	-3	-2	-1
RG	100	100	95.76	60.82	1.69	0.00	0.00
EG	0.00	0.00	4.24	21.52	0.00	0.00	0.00
MF	0.00	0.00	0.00	8.98	21.49	29.45	34.50
Bi-ACG	0.00	0.00	0.00	3.41	7.89	4.93	1.31
Bi-AEG	0.00	0.00	0.00	5.27	68.94	61.58	53.78
ETC	0.00	0.00	0.00	0.00	0.00	0.17	0.09
LTC	0.00	0.00	0.00	0.00	0.00	3.87	10.31

Table A9: The frequency of mitotic figures at different bud stages in wild type, heterozygous and homozygous *duo5* plants during development

P, M, A, T = prophase, metaphase, anaphase and telophase. SD = standard deviation, SEM = standard error of mean, N = number of lines.

	%Mitotic figures in wild type buds				%Mitotic figures in heterozygous *duo5* buds				%Mitotic figures in homozygous *duo5* buds			
	Mean	**SD**	**N**	**SEM**	**Mean**	**SD**	**N**	**SEM**	**Mean**	**SD**	**N**	**SEM**
P	62.13	7.78	2	5.5	90.02	4.38	5	1.96	91.01	6.67	4	3.34
M	13.51	3.01	2	2.13	4.84	2.36	5	1.06	3.15	1.98	4	0.99
A	7.96	1.13	2	0.8	1.15	0.72	5	0.32	0.84	0.77	4	0.38
T	16.4	5.9	2	4.17	3.99	2.02	5	0.91	4.99	5.25	4	2.62

Table A10: Mitotic index of wild type, heterozygous and homozygous *duo5* pollen calculated from bud stages in mitosis

MI = mitotic index, SD = standard deviation, SEM = standard error of mean, N = number of lines

Genotype	MI	SD	SEM	N
Wild type	24.06	3.23	2.29	8
Heterozygous *duo5*	23.43	4.47	2.00	27
Homozygous *duo5*	23.6	9.64	4.82	19

Table A11: Mapping data derived from wild type and mutant *duo5* F2 mapping population

Recombinants indicated in green are identified from North and the ones highlighted in blue reside towards the south of the predicted locus. RCF = recombination frequency.

Sample NO.	Parent	Phenotype	Genotype	F27G19	RCF	T16L1A	RCF	F11/11-dCAPS-HinfI	RCF	Predicted Genotype	F23E12-dCAPs-Nco1	RCF	F6G17	RCF
1	**T1B4**	WT	C	C						C			C	
2	T1B4	WT	C	C						C			C	
7	T1B4	WT	C	C						C			C	
13	T1B4	WT	C	C						C			C	
19	T1B4	WT	C	C						C	C		C/N	1
21	T1B4	WT	C	C/N	1	C/N	1	C/N	1	C			C	
26	T1B4	WT	C	C/N	1	C/N	1	C/N	1	C			C	
27	T1B4	WT	C	C/N	1	C/N	1	C/N	1	C			C	
29	T1B4	WT	C	C						C			C	
30	T1B4	WT	C	C						C			C	
33	T1B4	WT	C	C						C			C	
41	T1B4	WT	C	N	2	C/N	1	C/N	1	C			C	
42	T1B4	WT	C	C						C			C	
47	T1B4	WT	C	C						C			C	
53	T1B4	WT	C	C						C			C	
57	T1B4	WT	C	C						C			C	
58	T1B4	WT	C	C						C			C	
63	T1B4	WT	C	C						C			C	
65	T1B4	WT	C	C						C			C	
66	T1B4	WT	C	C/N	1	C				C			C	
67	T1B4	WT	C	C						C	C		C/N	1
69	T1B4	WT	C	C						C			C	
71	T1B4	WT	C	C						C			C	
73	T1B4	WT	C	C						C			C/N	1
74	T1B4	WT	C	C						C			C	
75	T1B4	WT	C	C						C			C	
76	T1B4	WT	C	C						C			C	
77	T1B4	WT	C	C						C			C	
80	T1B4	WT	C	C/N	1	C/N	1	C		C			C	
82	T1B3	WT	C	C						C			C	
84	T1B3	WT	C	C						C			C	
88	T1B3	WT	C	C						C			C	
92	T1B3	WT	C	C						C			C	
94	T1B3	WT	C	C						C			C	
95	T1B3	WT	C	C/N	1	C				C			C	
96	T1B3	WT	C	C						C			C	
99	T1B3	WT	C	C						C			C	
101	T1B3	WT	C	C						C			C	
103	T1B3	WT	C	C						C			C	
105	T1B3	WT	C	C						C			C	
111	T1B3	WT	C	C						C			C	
118	T1B3	WT	C	C						C			C	
119	T1B3	WT	C	C						C			C	
120	T1B3	WT	C	C						C	C		C/N	1
121	T1B3	WT	C	C						C			C	
123	T1B3	WT	C	C						C	C		C/N	1

125	T1B3	WT	C	C						C			C	
127	T1B3	WT	C	C/N	1	C				C			C	
128	T1B3	WT	C	C						C			C	
129	T1B3	WT	C	C						C			C	
131	T1B3	WT	C	C						C			C	
133	T1B3	WT	C	C						C			C	
134	T1B3	WT	C	C						C			C	
135	T1B3	WT	C	N	2	C/N	1	C/N	1	C	C/N	1	C/N	1
138	T1B3	WT	C	C						C			C	
150	T1B3	WT	C	C						C			C	
151	T1B3	WT	C	C						C	C		C/N	1
152	T1B3	WT	C	C/N	1	C				C			C	
154	T1B3	WT	C	C						C			C	
156	T1B3	WT	C	C						C			C	
160	T1B3	WT	C	C/N	1	?				C			C	
161	T1B3	WT	C	C/N	1	C				C			C	
162	T1B3	WT	C	C						C			C	
163	T1B3	WT	C	C						C			C	
167	T1B3	WT	C	C/N	1	C				C			C	
170	T1B3	WT	C	C/N	1	C				C			C	
175	T1B3	WT	C	C						C			C	
180	T1B3	WT	C	C						C			C	
182	T1B3	WT	C	C						C			C	
184	T1B3	WT	C	C						C			C	
187	T1B3	WT	C	C						C			C	
188	T1B3	WT	C	C						C			C	
189	T1B3	WT	C	C/N	1	C/N	1	C/N	1	C			C	
190	T1B3	WT	C	C						C			C	
191	T1B3	WT	C	C						C	C		C/N	1
192	T1B3	WT	C	C						C			C	
198	T1B3	WT	C	C						C			C	
204	T1B3	WT	C	C						C			C	
205	T1B3	WT	C	C						C	C/N	1	N	2
209	T1B3	WT	C	C						C			C	
212	T1B3	WT	C	C						C			C	
214	T1B3	WT	C	C						C			C	
216	T1B3	WT	C	C						C			C	
220	T1B3	WT	C	C						C	C		C/N	1
227	T1B3	WT	C	C						C			C	
231	T1B3	WT	C	C						C			C	
3	T1B4	duo	C/N	C/N						C/N			C/N	
4	T1B4	duo	C/N	C/N						C/N			C/N	
5	T1B4	duo	C/N	C/N						C/N			C/N	
6	T1B4	duo hom	N	N						N			N	
8	T1B4	duo	C/N	C/N						C/N			C/N	
9	T1B4	duo	C/N	C/N						C/N			C/N	
10	T1B4	duo	C/N	C/N						C/N			C/N	
11	T1B4	duo hom	N	N						N			N	
12	T1B4	duo	C/N	N	1	C/N				C/N			C/N	
14	T1B4	duo	C/N	C/N						C/N			C/N	
15	T1B4	duo	C/N	N	1	C/N				C/N			C/N	
17	T1B4	duo hom	N	N						N	N		C/N	1
18	T1B4	duo	C/N	C/N						C/N			C/N	

20	T1B4	duo	C/N	C/N					C/N			C/N		
22	T1B4	duo	C/N	C/N					C/N			C/N		
23	T1B4	duo	N	N					N			N		
24	T1B4	duo	C/N	C/N					C/N			C/N		
25	T1B4	duo	C/N	C/N					C/N			C/N		
28	T1B4	duo	C/N	C/N					C/N			C/N		
31	T1B4	duo	C/N	C/N					C/N			C/N		
32	T1B4	duo	C/N	C/N					C/N	N	1	N	1	
34	T1B4	duo	C/N	C/N					C/N			C/N		
35	T1B4	duo hom	N	N					N			N		
36	T1B4	duo hom	N	C	2	N			N			N		
37	T1B4	duo	C/N	C/N					C/N			C/N		
38	T1B4	duo	C/N	C/N					C/N			C/N		
39	T1B4	duo	C/N	C/N					C/N			C/N		
40	T1B4	duo	C/N	C/N					C/N			C/N		
43	T1B4	duo	C/N	C/N					C/N			C/N		
44	T1B4	duo	C/N	C	1	C/N			C/N			C/N		
45	T1B4	duo	C/N	C/N					C/N			C/N		
46	T1B4	duo	N	N					N			N		
48	T1B4	duo	C/N	C	1	C	1	C/N	C/N			C/N		
49	T1B4	duo	C/N	C/N					C/N			C/N		
50	T1B4	duo	C/N	C/N					C/N			C/N		
51	T1B4	duo	C/N	C/N					C/N			C/N		
52	T1B4	duo	C/N	C/N					C/N			C/N		
54	T1B4	duo hom	N	N				N	N	N		C/N	1	
55	T1B4	duo	C/N	C/N					C/N			C/N		
56	T1B4	duo	C/N	N	1				C/N			C/N		
59	T1B4	duo	C/N	C/N					C/N	C/N		C	1	
60	T1B4	duo	C/N	C/N					C/N			C/N		
61	T1B4	duo	C/N	C/N					C/N	N	1	N	1	
62	T1B4	duo	C/N	N					C/N			N		
64	T1B4	duo	C/N	C/N					C/N			C/N		
68	T1B4	duo	C/N	C/N					C/N			C/N		
70	T1B4	duo	C/N	C	1	C	1	C/N	C/N			C/N		
72	T1B4	duo	C/N	C	1	C/N			C/N			C/N		
78	T1B4	duo hom	N	N					N			N		
79	T1B4	duo	C/N	C/N					C/N			?		
81	**T1B3**	duo	C/N	C	1	C/N			C/N			C/N		
83	T1B3	duo	C/N	C/N					C/N			C/N		
85	T1B3	duo	C/N	C/N					C/N			C/N		
86	T1B3	duo	C/N	C/N					C/N			C/N		
87	T1B3	duo	C/N	C/N					C/N	N	1	N	1	
89	T1B3	duo	C/N	C/N					C/N	C	1	C	1	
90	T1B3	duo	C/N	C/N					C/N	C/N		N	1	
91	T1B3	duo	C/N	C/N					C/N			C/N		
93	T1B3	duo	C/N	N	1	N	1	N	1	C/N		C/N		
97	T1B3	duo	C/N	C/N					C/N			C/N		
98	T1B3	duo	C/N	C/N					C/N			C/N		
100	T1B3	duo	C/N	C/N					C/N			C/N		
102	T1B3	duo	C/N	N	1	C/N			C/N			C/N		
104	T1B3	duo	C/N	C/N					C/N	C/N		C		
106	T1B3	duo	C/N	C/N					C/N			C/N		
107	T1B3	duo	C/N	C/N					C/N			C/N		

108	T1B3	duo	C/N	N	1	N	1	N	1	C/N		C/N	
109	T1B3	duo hom	N	N						N		N	
110	T1B3	duo	C/N	C/N						C/N		C/N	
112	T1B3	duo	C/N	N		N				C/N		N	
113	T1B3	duo	C/N	C/N						C/N	C/N	C	1
114	T1B3	duo hom	N	N						N		N	
115	T1B3	duo	C/N	C/N						C/N		C/N	
117	T1B3	duo	C/N	C/N						C/N		C/N	
122	T1B3	duo	C/N	N	1	N	1	N	1	C/N		C/N	
124	T1B3	duo	C/N	C/N						C/N		C/N	
126	T1B3	duo	C/N	C/N						C/N		C/N	
130	T1B3	duo	C/N	C/N						C/N	C/N	N	1
132	T1B3	duo hom	N	N						N		N	
136	T1B3	duo	C/N	C/N						C/N	C/N	N	1
137	T1B3	duo	C/N	C/N						C/N		C/N	
139	T1B3	duo	C/N	N	1	N	1	N	1	C/N		C/N	
140	T1B3	duo	C/N	C/N						C/N	C/N	N	1
141	T1B3	duo	C/N	C/N						C/N		C/N	
142	T1B3	duo hom	N	N						N		N	
143	T1B3	duo	C/N	C/N						C/N		C/N	
144	T1B3	duo	C/N	C/N						C/N		C/N	
145	T1B3	duo	C/N	C/N						C/N		C/N	
146	T1B3	duo	C/N	C/N						C/N		C/N	
147	T1B3	duo	C/N	C/N						C/N		C/N	
148	T1B3	duo	C/N	C/N						C/N		C/N	
149	T1B3	duo	C/N	C/N						C/N		C/N	
153	T1B3	duo	C/N	N	1	N	1	C/N		C/N		C/N	
155	T1B3	duo	C/N	C	1	C	1	C	1	C/N		C/N	
157	T1B3	duo	C/N	C/N						C/N		C/N	
158	T1B3	duo	C/N	N	1	C/N				C/N		C/N	
159	T1B3	duo	C/N	C/N						C/N		C/N	
164	T1B3	duo	C/N	C/N						C/N		C/N	
165	T1B3	duo	C/N	C/N						C/N		C/N	
166	T1B3	duo	N OR C/N	C/N						C/N		C/N	
168	T1B3	duo	C/N	C	1	C/N				C/N		C/N	
169	T1B3	duo	C/N	C/N						C/N		C/N	
171	T1B3	duo	C/N	C/N						C/N	C/N	C	1
172	T1B3	duo	C/N	C/N						C/N		C/N	
173	T1B3	duo	C/N	C/N						C/N		C/N	
174	T1B3	duo	C/N	C/N						C/N		C/N	
176	T1B3	duo	C/N	C/N						C/N		C/N	
177	T1B3	duo	C/N	C/N						C/N		C/N	
178	T1B3	duo	C/N	C/N						C/N		C/N	
179	T1B3	duo hom	N	N						N		N	
181	T1B3	duo	C/N	C/N						C/N		C/N	
183	T1B3	duo hom	N	**N**						N		N	
185	T1B3	duo	C/N	C/N						C/N		C/N	
186	T1B3	duo	C/N	N	1	C/N				C/N		C/N	
193	T1B3	duo	C/N	C/N						C/N		C/N	
194	T1B3	duo	C/N	C/N						C/N		C/N	
195	T1B3	duo	C/N	C/N						C/N		C/N	
196	T1B3	duo	C/N	C/N						C/N		C/N	
197	T1B3	duo	C/N	C/N						C/N		C/N	

199	T1B3	duo	C/N	C/N						C/N			C/N	
200	T1B3	duo hom	N	N						N			N	
201	T1B3	duo hom	N	N						N			N	
202	T1B3	duo	C/N	C/N						C/N			C/N	
203	T1B3	duo	C/N	C/N						C/N			C/N	
206	T1B3	duo hom	N	N						N			N	
207	T1B3	duo	C/N	C/N						C/N			C/N	
208	T1B3	duo	C/N	C/N						C/N			C/N	
210	T1B3	duo	C/N	C/N						C/N			C/N	
211	T1B3	duo	C/N	C/N						C/N			C/N	
213	T1B3	duo	C/N	N	1	C/N				C/N			C/N	
215	T1B3	duo	C/N	C/N						C/N	N	1	N	1
217	T1B3	duo	C/N	C	1	C/N				C/N			C/N	
218	T1B3	duo	C/N	C/N						C/N			C/N	
219	T1B3	duo	C/N	N	1	N	1	N	1	C/N			C/N	
221	T1B3	duo	C/N	C/N						C/N			C/N	
222	T1B3	duo	C/N	N	1	C/N				C/N			C/N	
223	T1B3	duo	C/N	N	1	C/N				C/N			C/N	
224	T1B3	duo hom	N	N						N			N	
225	T1B3	duo	C/N	C/N						C/N	C/N		N	1
226	T1B3	duo	C/N	C/N						C/N			C/N	
228	T1B3	duo hom	N	N						N			N	
229	T1B3	duo	C/N	C	1	C	1	C	1	C/N	C/N		N	1
230	T1B3	duo hom	N	N						N			N	
232	T1B3	duo hom	N	N						N			N	
233	T1B3	duo	C/N	C/N						C/N			C/N	
234	T1B3	duo	C/N	C/N						C/N			C/N	
235	T1B3	duo	C/N	N	1	C/N				C/N			C/N	
236	T1B3	duo	C/N	C/N						C/N			C/N	
238	T1B3	duo	C/N	C/N						C/N			C/N	
239	T1B3	duo	C/N	C/N						C/N			C/N	
240	T1B3	duo	C/N	C/N						C/N			C/N	

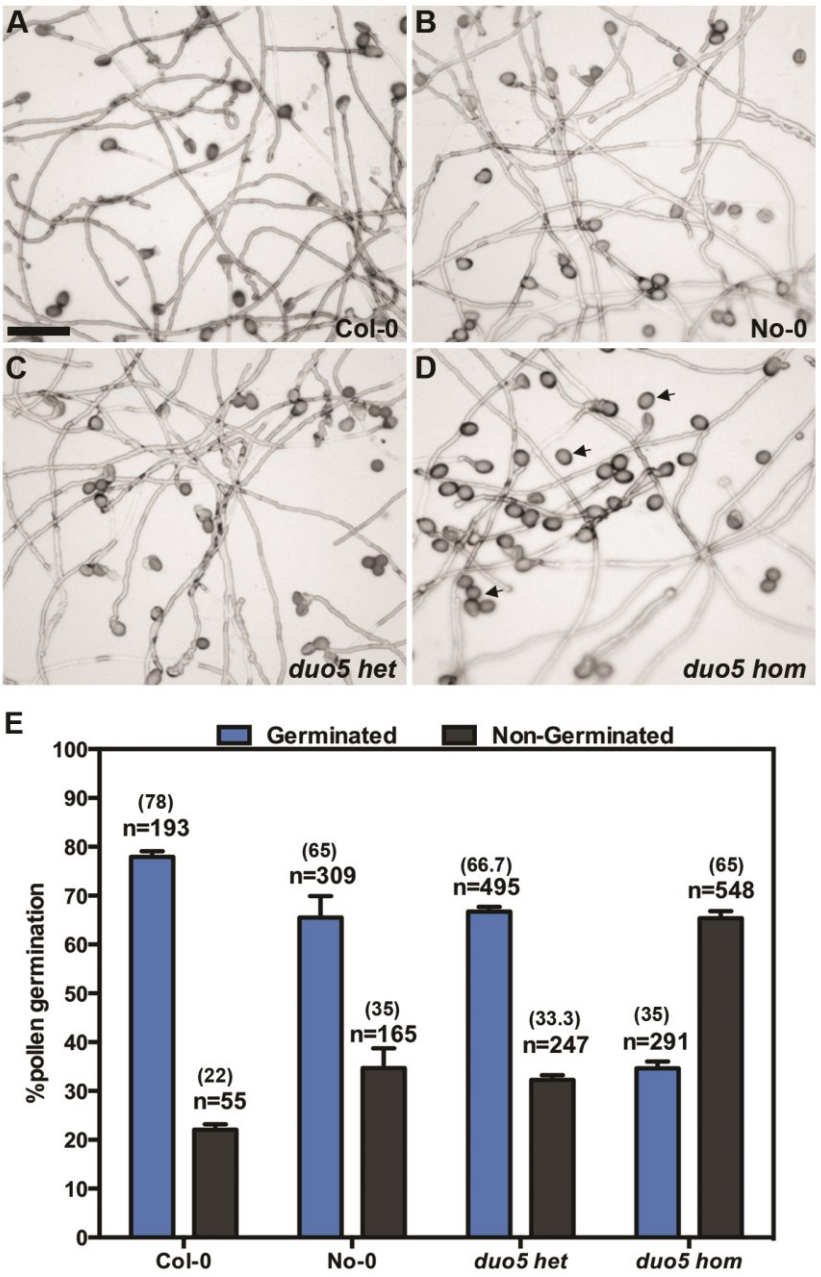

Figure A1: Pollen germination efficiency of wild type and *duo5* mutant heterozygotes and homozygotes *in vitro*. (A-D) Pollen from wild type (No-0 and Col-0) and mutant *duo5* plants was germinated on agarose-based pollen germination media. Pollen tubes are shown following 10-12 hours culture at 24°C on a cellophane membrane overlying a 0.5% agarose medium containing 1 mM CaCl2, 0.01% Boric Acid, 18% Sucrose, 1 mM Ca(NO3)2, 1 mM MgSO4 and 10 % Sucrose in distilled water, pH adjusted to 7. **(E)** Bar chart representing mean percentage pollen germination rates of wild type and *duo5* mutant pollen. Error bars represents the standard error of the mean calculated from at least three different samples. Approximately 78% and 65% of the pollen from wild type Col-0 and No-0 respectively show pollen tube growth after 10 to 12 hours of incubation at 24°C. The mean percentage germination rate of *duo5* pollen was 66.7% similar to wild type No-0 ecotype. However, Chi-squared analysis revealed that germination rate of homozygous *duo5* pollen reduced significantly ($X^2 = 41.096$, $p < 0.05$) from heterozygous *duo5* and wild type pollen grains. Arrows indicate the non-germinated pollen grains. Scale bars represent100µm.

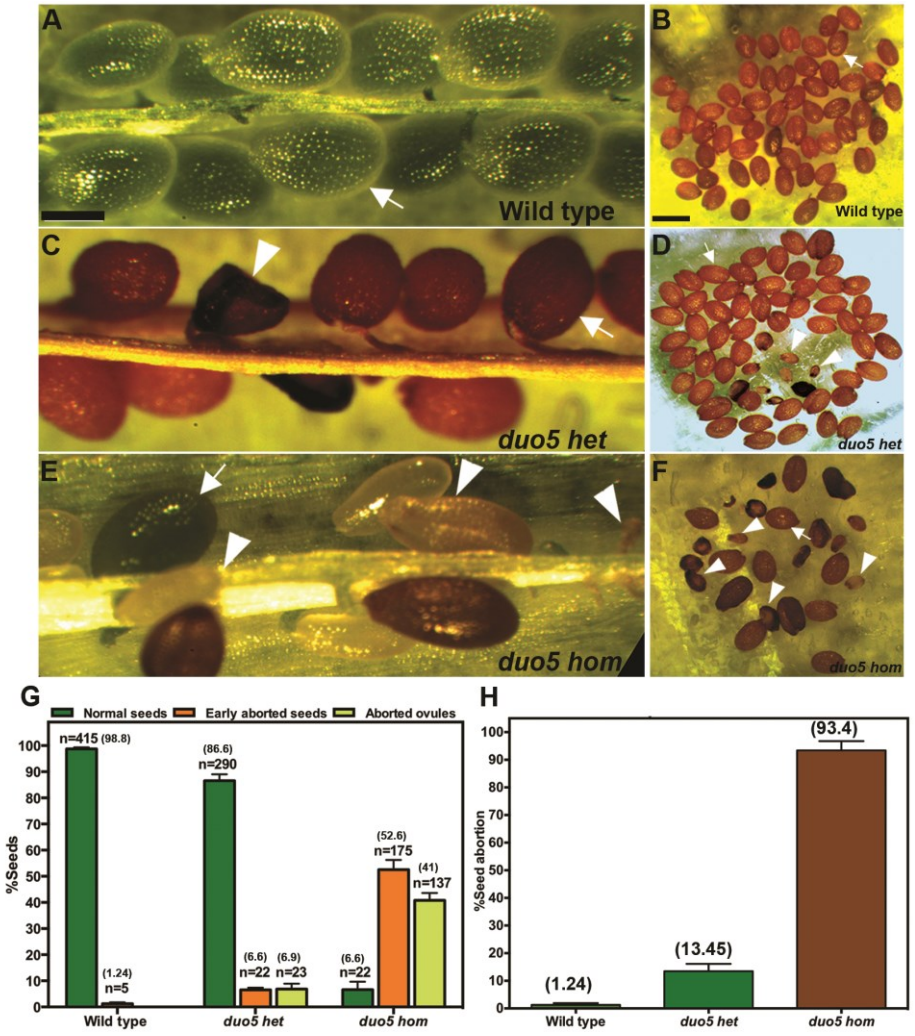

Figure A2: Seed set of mature siliques from wild type and *duo5* mutant plants. (A) Mature siliques from self-fertilized wild type plants contain full and green seeds that mature into **(B)** viable seeds. Arrows indicate wild type developing green seeds and mature dehisced seeds. The wild type siliques on average contain 59 green seeds (n=415). **(C)** In comparison, mature siliques from *duo5* heterozygous selfed plants also contain approximately 87% normal seeds (n=290) as well as aborted seeds (6.6%) and undeveloped ovules (6.9%). Aborted seeds are indicated by arrowheads, whereas, normal developing seeds are indicted by arrow. A Chi-squared analysis indicates that seed failure in siliques from heterozygous mutant plants is significantly lower than expected 50% for a fully penetrant gametophytic mutation. **(D)** Mature normal seeds in siliques from heterozygous mutant plants are similar to wild type plants and each silique on average contains approximately 48 viable seeds. **(E)** Representative silique from a self-pollinated *duo5* homozygous plant showing reduced seed set. Mutant seeds appear as white to pale green translucent seeds as wells as **(F)** shriveled brown early aborted seeds (52.6%) indicated by arrowhead. Undeveloped ovules (41%) also appear as white stubs (indicate by arrowhead). **(G)** Bar graph illustrating mean percentage seed set in selfed siliques from wild type, heterozygous and homozygous *duo5* plants. Error bars represent the standard error of the mean. **(H)** Bar charts representing percentage seed failure in the genotypes analyzed. According to Kruskal-Wallis ANOVA and Dunn's *post ad hoc* test, homozygous *duo5* mature siliques have significantly reduced seed set compared to wild type and heterozygous plants ($p < 0.001$). Error bars represent standard error of the mean. Scale bars for Fig A, C, E = 200µm and scale bars for B, D, F = 500µm.

References

Alandete-Saez M, Ron M, McCormick S. 2008. GEX3, Expressed in the Male Gametophyte and in the Egg Cell of Arabidopsis thaliana, Is Essential for Micropylar Pollen Tube Guidance and Plays a Role during Early Embryogenesis. *Molecular Plant* **1**, 586-598.

Alexander MP. 1969. Differential Staining of Aborted and Nonaborted Pollen. *Biotechnic & Histochemistry* **44**, 117-122.

Allen RS, Li J, Stahle MI, Dubroué A, Gubler F, Millar AA. 2007. Genetic analysis reveals functional redundancy and the major target genes of the Arabidopsis miR159 family. *Proceedings of the National Academy of Sciences* **104**, 16371-16376.

Amasino R. 2010. Seasonal and developmental timing of flowering. *The Plant Journal* **61**, 1001-1013.

Araki S, Ito M, Soyano T, Nishihama R, Machida Y. 2004. Mitotic Cyclins Stimulate the Activity of c-Myb-like Factors for Transactivation of G2/M Phase-specific Genes in Tobacco. *Journal of Biological Chemistry* **279**, 32979-32988.

Ashelford K, Eriksson ME, Allen CM, D'Amore R, Johansson M, Gould P, Kay S, Millar AJ, Hall N, Hall A. 2011. Full genome re-sequencing reveals a novel circadian clock mutation in Arabidopsis. *Genome Biol* **12**, R28.

Attwooll C, Lazzerini Denchi E, Helin K. 2004. The E2F family: specific functions and overlapping interests. *Embo Journal* **23**, 4709-4716.

Aw SJ, Hamamura Y, Chen Z, Schnittger A, Berger F. 2010. Sperm entry is sufficient to trigger division of the central cell but the paternal genome is required for endosperm development in Arabidopsis. *Development* **137**, 2683-2690.

Aya K, Ueguchi-Tanaka M, Kondo M, Hamada K, Yano K, Nishimura M, Matsuoka M. 2009. Gibberellin Modulates Anther Development in Rice via the Transcriptional Regulation of GAMYB. *The Plant Cell Online* **21**, 1453-1472.

Bachmair A, Novatchkova M, Potuschak T, Eisenhaber F. 2001. Ubiquitylation in plants: a post-genomic look at a post-translational modification. *Trends Plant Sci* **6**, 463-470.

Banaś M, Tirlapur U, Charzyńska M, Cresti M. 1996. Some events of mitosis and cytokinesis in the generative cell of Ornithogalum virens L. *Planta* **199**, 202-208.

Barrett SCH. 2002. The evolution of plant sexual diversity. *Nature Reviews Genetics* **3**, 274-284.

Bate N, Twell D. 1998. Functional architecture of a late pollen promoter: pollen-specific transcription is developmentally regulated by multiple stage-specific and co-dependent activator elements. *Plant Molecular Biology* **37**, 859-869.

Bäurle I, Dean C. 2006. The Timing of Developmental Transitions in Plants. *Cell* **125**, 655-664.

Becker JD, Boavida LC, Carneiro J, Haury M, Feijo JA. 2003. Transcriptional profiling of Arabidopsis tissues reveals the unique characteristics of the pollen transcriptome. *Plant Physiology* **133**, 713-725.

Bell CJ, Ecker JR. 1994. Assignment of 30 microsatellite loci to the linkage map of Arabidopsis. *Genomics* **19**, 137-144.

Benjamini Y, Braun H. 2002. John W. Tukey's contributions to multiple comparisons. *Annals of Statistics* **30**, 1576-1594.

Berger F. 2008. Double-fertilization, from myths to reality. *Sexual Plant Reproduction* **21**, 3-5.

Berger F, Grini PE, Schnittger A. 2006. Endosperm: an integrator of seed growth and development. *Current Opinion in Plant Biology* **9**, 664-670.

Berger F, Twell D. 2011. Germline Specification and Function in Plants. *Annual Review of Plant Biology* **62**, 461-484.

Bhatt AM, Canales C, Dickinson HG. 2001. Plant meiosis: the means to 1N. *Trends Plant Sci* **6**, 114-121.

Boavida LC, Becker JD, Feijo JA. 2005. The making of gametes in higher plants. *International Journal of Developmental Biology* **49**, 595-614.

Bonhomme S, Horlow C, Vezon D, de Laissardière S, Guyon A, Férault M, Marchand M, Bechtold N, Pelletier G. 1998. T-DNA mediated disruption of essential gametophytic genes in Arabidopsis is unexpectedly rare and cannot be inferred from segregation distortion alone. *Molecular & general genetics : MGG* **260**, 444-452.

Boniotti MB, Gutierrez C. 2001. A cell-cycle-regulated kinase activity phosphorylates plant retinoblastoma protein and contains, in Arabidopsis, a CDKA/cyclin D complex. *The Plant Journal* **28**, 341-350.

Borg M, Brownfield L, Khatab H, Sidorova A, Lingaya M, Twell D. 2011. The R2R3 MYB Transcription Factor DUO1 Activates a Male Germline-Specific Regulon Essential for Sperm Cell Differentiation in Arabidopsis. *The Plant Cell Online* **23**, 534-549.

Borg M, Brownfield L, Twell D. 2009. Male gametophyte development: a molecular perspective. *Journal of Experimental Botany* **60**, 1465-1478.

Borg M, Rutley N, Kagale S, Hamamura Y, Gherghinoiu M, Kumar S, Sari U, Esparza-Franco MA, Sakamoto W, Rozwadowski K, Higashiyama T, Twell D. 2014. An EAR-Dependent Regulatory Module Promotes Male Germ Cell Division and Sperm Fertility in Arabidopsis. *The Plant Cell Online*.

Borges F, Gomes G, Gardner R, Moreno N, McCormick S, Feijó JA, Becker JD. 2008. Comparative Transcriptomics of Arabidopsis Sperm Cells. *Plant Physiology* **148**, 1168-1181.

Borghi L, Gutzat R, Fütterer J, Laizet Yh, Hennig L, Gruissem W. 2010. Arabidopsis RETINOBLASTOMA-RELATED Is Required for Stem Cell Maintenance,

Cell Differentiation, and Lateral Organ Production. *The Plant Cell Online* **22**, 1792-1811.

Boruc J, Van den Daele H, Hollunder J, Rombauts S, Mylle E, Hilson P, Inzé D, De Veylder L, Russinova E. 2010. Functional Modules in the Arabidopsis Core Cell Cycle Binary Protein–Protein Interaction Network. *The Plant Cell Online* **22**, 1264-1280.

Boudolf V, Lammens T, Boruc J, Van Leene J, Van Den Daele H, Maes S, Van Isterdael G, Russinova E, Kondorosi E, Witters E, De Jaeger G, Inzé D, De Veylder L. 2009. CDKB1;1 Forms a Functional Complex with CYCA2;3 to Suppress Endocycle Onset. *Plant Physiology* **150**, 1482-1493.

Brewbaker JL. 1967. The Distribution and Phylogenetic Significance of Binucleate and Trinucleate Pollen Grains in the Angiosperms. *American Journal of Botany* **54**, 1069-1083.

Brown RC, Lemmon BE. 1991. Pollen development in orchids: 3. A novel generative pole microtubule system predicts unequal pollen mitosis. *Journal of Cell Science* **99**, 273-281.

Brown RC, Lemmon BE. 1994. Pollen mitosis in the slipper orchid Cypripedium fasciculatum. *Sexual Plant Reproduction* **7**, 87-94.

Brownfield L, Hafidh S, Borg M, Sidorova A, Mori T, Twell D. 2009a. A plant germline-specific integrator of sperm specification and cell cycle progression. *PLoS Genet* **5**, e1000430.

Brownfield L, Hafidh S, Durbarry A, Khatab H, Sidorova A, Doerner P, Twell D. 2009b. Arabidopsis DUO POLLEN3 Is a Key Regulator of Male Germline Development and Embryogenesis. *Plant Cell* **21**, 1940-1956.

Burgess J. 1970. Cell shape and mitotic spindle formation in the generative cell of Endymion non-scriptus. *Planta* **95**, 72-85.

Cai G, Cresti M. 2006. The Microtubular Cytoskeleton in Pollen Tubes: Structure and Role in Organelle Trafficking. In: Malhó R, ed. *The Pollen Tube*, Vol. 3: Springer Berlin Heidelberg, 157-175.

Capron A, Serralbo O, Fülöp K, Frugier F, Parmentier Y, Dong A, Lecureuil A, Guerche P, Kondorosi E, Scheres B, Genschik P. 2003. The Arabidopsis Anaphase-Promoting Complex or Cyclosome: Molecular and Genetic Characterization of the APC2 Subunit. *The Plant Cell Online* **15**, 2370-2382.

Cebolla A, Vinardell JM, Kiss E, Olah B, Roudier F, Kondorosi A, Kondorosi E. 1999. The mitotic inhibitor ccs52 is required for endoreduplication and ploidy-dependent cell enlargement in plants. *Embo Journal* **18**, 4476-4484.

Charzyńska M, Ciampolini F, Cresti M. 1988. Generative cell division and sperm cell formation in barley. *Sexual Plant Reproduction* **1**, 240-247.

Charzynska M, Cresti M. 1993. Early events in division of the generative cell ofOrnithogalum virens. *Protoplasma* **172**, 77-83.

Charzynska M, Lewandowska E. 1990. Generative Cell Division and Sperm Cell Association in the Pollen Grain of Sambucus nigra. *Annals of Botany* **65**, 685-689.

Charzynska M, Murgia M, Milanesi C, Cresti M. 1989. Origin of sperm cell association in the "male germ unit" ofBrassica pollen. *Protoplasma* **149**, 1-4.

Chen SH, Liao JP, Kuang AX, Tian HQ. 2006. Isolation of two populations of sperm cells from the pollen tube of Torenia fournieri. *Plant Cell Rep* **25**, 1138-1142.

Chen YC, McCormick S. 1996. sidecar pollen, an Arabidopsis thaliana male gametophytic mutant with aberrant cell divisions during pollen development. *Development* **122**, 3243-3253.

Chen Z, Hafidh S, Poh SH, Twell D, Berger F. 2009. Proliferation and cell fate establishment during Arabidopsis male gametogenesis depends on the Retinoblastoma protein. *Proc Natl Acad Sci U S A* **106**, 7257-7262.

Chen Z, Hui JTL, Ingouff M, Sundaresan V, Berger F. 2008. Chromatin assembly factor 1 regulates the cell cycle but not cell fate during male gametogenesis in Arabidopsis thaliana. *Development* **135**, 65-73.

Cheng Y, Cao L, Wang S, Li Y, Shi X, Liu H, Li L, Zhang Z, Fowke LC, Wang H, Zhou Y. 2013. Downregulation of multiple CDK inhibitor ICK/KRP genes upregulates the E2F pathway and increases cell proliferation, and organ and seed sizes in Arabidopsis. *The Plant Journal* **75**, 642-655.

Choo Y, Klug A. 1997. Physical basis of a protein-DNA recognition code. *Curr Opin Struct Biol* **7**, 117-125.

Churchman ML, Brown ML, Kato N, Kirik V, Hulskamp M, Inze D, De Veylder L, Walker JD, Zheng Z, Oppenheimer DG, Gwin T, Churchman J, Larkin JC. 2006. SIAMESE, a plant-specific cell cycle regulator, controls endoreplication onset in Arabidopsis thaliana. *Plant Cell* **18**, 3145-3157.

Clough SJ, Bent AF. 1998. Floral dip: a simplified method forAgrobacterium-mediated transformation ofArabidopsis thaliana. *The Plant Journal* **16**, 735-743.

Coimbra S, Costa M, Jones B, Mendes MA, Pereira LG. 2009. Pollen grain development is compromised in Arabidopsis agp6 agp11 null mutants. *Journal of Experimental Botany* **60**, 3133-3142.

Coleman AW, Goff LJ. 1985. Applications of fluorochromes to pollen biology. I. Mithramycin and 4',6-diamidino-2-phenylindole (DAPI) as vital stains and for quantitation of nuclear DNA. *Stain Technol* **60**, 145-154.

Cools T, De Veylder L. 2009. DNA stress checkpoint control and plant development. *Current Opinion in Plant Biology* **12**, 23-28.

Craigon DJ, James N, Okyere J, Higgins J, Jotham J, May S. 2004. NASCArrays: a repository for microarray data generated by NASC's transcriptomics service. *Nucleic Acids Research* **32**, D575-D577.

Dare AP, Schaffer RJ, Lin-Wang K, Allan AC, Hellens RP. 2008. Identification of a

cis-regulatory element by transient analysis of co-ordinately regulated genes. *Plant Methods* **4**.

De Clercq AD, Inzé D. 2006. Cyclin-Dependent Kinase Inhibitors in Yeast, Animals, and Plants: A Functional Comparison. *Critical Reviews in Biochemistry and Molecular Biology* **41**, 293-313.

De Veylder L, Beeckman T, Beemster GTS, Krols L, Terras F, Landrieu I, Van Der Schueren E, Maes S, Naudts M, Inzé D. 2001. Functional Analysis of Cyclin-Dependent Kinase Inhibitors of Arabidopsis. *The Plant Cell Online* **13**, 1653-1668.

De Veylder L, Beeckman T, Inze D. 2007. The ins and outs of the plant cell cycle. *Nat Rev Mol Cell Biol* **8**, 655-665.

De Veylder L, Segers G, Glab N, Casteels P, Van Montagu M, Inze D. 1997. The Arabidopsis Cks1At protein binds the cyclin-dependent kinases Cdc2aAt and Cdc2bAt. *FEBS Lett* **412**, 446-452.

Del casino C, Tiezzi A, Wagner VT, Cresti M. 1992. The Organization of the Cytoskeleton in the Generative Cell and Sperm of Hyacinthus-Orientalis. *Protoplasma* **168**, 41-50.

DeLuca MA, McElroy WD. 1978. Purification and properties of firefly luciferase. *Methods Enzymol.* **57**, 3-15.

Desvoyes B, Ramirez-Parra E, Xie Q, Chua N-H, Gutierrez C. 2006. Cell Type-Specific Role of the Retinoblastoma/E2F Pathway during Arabidopsis Leaf Development. *Plant Physiology* **140**, 67-80.

Dewitte W, Murray JAH. 2003. The plant cell cycle. *Annual Review of Plant Biology* **54**, 235-264.

Dewitte W, Riou-Khamlichi C, Scofield S, Healy JMS, Jacqmard A, Kilby NJ, Murray JAH. 2003. Altered Cell Cycle Distribution, Hyperplasia, and Inhibited Differentiation in Arabidopsis Caused by the D-Type Cyclin CYCD3. *The Plant Cell Online* **15**, 79-92.

Dinneny JR, Weigel D, Yanofsky MF. 2006. NUBBIN and JAGGED define stamen and carpel shape in Arabidopsis. *Development* **133**, 1645-1655.

Doerner P, Jorgensen J-E, You R, Steppuhn J, Lamb C. 1996. Control of root growth and development by cyclin expression. *Nature* **380**, 520-523.

Drews GN, Goldberg RB. 1989. Genetic-Control of Flower Development. *Trends in Genetics* **5**, 256-261.

Drews GN, Yadegari R. 2002. Development and function of the angiosperm female gametophyte. *Annu Rev Genet* **36**, 99-124.

Dubas E, Wedzony M, Custers J, Kieft H, van Lammeren AA. 2012. Gametophytic development of Brassica napus pollen in vitro enables examination of cytoskeleton and nuclear movements. *Protoplasma* **249**, 369-377.

Dubos C, Stracke R, Grotewold E, Weisshaar B, Martin C, Lepiniec L. 2010. MYB transcription factors in Arabidopsis. *Trends Plant Sci* **15**, 573-581.

Dumas C, Berger F, Faure J-E, Matthys-Rochon E. 1998. Gametes, Fertilization and Early Embryogenesis in Flowering Plants. In: Callow JA, ed. *Advances in Botanical Research*, Vol. Volume 28: Academic Press, 231-261.

Dupl'akova N, Renak D, Hovanec P, Honysova B, Twell D, Honys D. 2007. Arabidopsis Gene Family Profiler (aGFP)--user-oriented transcriptomic database with easy-to-use graphic interface. *Bmc Plant Biology* **7**, 39.

Durbarry A, Vizir I, Twell D. 2005. Male germ line development in Arabidopsis. duo pollen mutants reveal gametophytic regulators of generative cell cycle progression. *Plant Physiology* **137**, 297-307.

Dyer BW, Ferrer FA, Klinedinst DK, Rodriguez R. 2000. A noncommercial dual luciferase enzyme assay system for reporter gene analysis. *Anal Biochem* **282**, 158-161.

Eady C, Lindsey K, Twell D. 1995. The Significance of Microspore Division and Division Symmetry for Vegetative Cell-Specific Transcription and Generative Cell Differentiation. *The Plant Cell Online* **7**, 65-74.

Ebel C, Mariconti L, Gruissem W. 2004. Plant retinoblastoma homologues control nuclear proliferation in the female gametophyte. *Nature* **429**, 776-780.

Edwards K, Johnstone C, Thompson C. 1991. A Simple and Rapid Method for the Preparation of Plant Genomic DNA for Pcr Analysis. *Nucleic Acids Research* **19**, 1349-1349.

Eloy NB, de Freitas Lima M, Van Damme D, Vanhaeren H, Gonzalez N, De Milde L, Hemerly AS, Beemster GTS, Inzé D, Ferreira PCG. 2011. The APC/C subunit 10 plays an essential role in cell proliferation during leaf development. *The Plant Journal* **68**, 351-363.

Engel ML, Chaboud A, Dumas C, McCormick S. 2003. Sperm cells of Zea mays have a complex complement of mRNAs. *Plant Journal* **34**, 697-707.

Engel ML, Davis RH, McCormick S. 2005. Green sperm. Identification of male gamete promoters in Arabidopsis. *Plant Physiology* **138**, 2124-2133.

Englbrecht CC, Schoof H, Bohm S. 2004. Conservation, diversification and expansion of C2H2 zinc finger proteins in the Arabidopsis thaliana genome. *Bmc Genomics* **5**.

Espley RV, Brendolise C, Chagne D, Kutty-Amma S, Green S, Volz R, Putterill J, Schouten HJ, Gardiner SE, Hellens RP, Allan AC. 2009. Multiple repeats of a promoter segment causes transcription factor autoregulation in red apples. *Plant Cell* **21**, 168-183.

Evans T, Rosenthal ET, Youngblom J, Distel D, Hunt T. 1983. Cyclin: a protein specified by maternal mRNA in sea urchin eggs that is destroyed at each cleavage division. *Cell* **33**, 389-396.

Feldmann KA. 1991. T-DNA Insertion Mutagenesis in Arabidopsis - Mutational

Spectrum. *Plant Journal* **1**, 71-82.

Feldmann KA, Coury DA, Christianson ML. 1997. Exceptional segregation of a selectable marker (KanR) in Arabidopsis identifies genes important for gametophytic growth and development. *Genetics* **147**, 1411-1422.

Foucher F, Kondorosi E. 2000. Cell cycle regulation in the course of nodule organogenesis in Medicago. *Plant Molecular Biology* **43**, 773-786.

Francis KE, Lam SY, Copenhaver GP. 2006. Separation of Arabidopsis pollen tetrads is regulated by QUARTET1, a pectin methylesterase gene. *Plant Physiology* **142**, 1004-1013.

Frank AC, Johnson MA. 2009. Expressing the diphtheria toxin A subunit from the HAP2(GCS1) promoter blocks sperm maturation and produces single sperm-like cells capable of fertilization. *Plant Physiology* **151**, 1390-1400.

Friedman WE. 1999. Expression of the cell cycle in sperm of Arabidopsis: implications for understanding patterns of gametogenesis and fertilization in plants and other eukaryotes. *Development* **126**, 1065-1075.

Goldberg RB, Beals TP, Sanders PM. 1993. Anther Development - Basic Principles and Practical Applications. *Plant Cell* **5**, 1217-1229.

Grant-Downton R, Hafidh S, Twell D, Dickinson HG. 2009. Small RNA Pathways Are Present and Functional in the Angiosperm Male Gametophyte. *Molecular Plant* **2**, 500-512.

Grini PE, Schnittger A, Schwarz H, Zimmermann I, Schwab B, Jurgens G, Hulskamp M. 1999. Isolation of ethyl methanesulfonate-induced gametophytic mutants in Arabidopsis thaliana by a segregation distortion assay using the multimarker chromosome 1. *Genetics* **151**, 849-863.

Grotewold E. 2005. Plant metabolic diversity: a regulatory perspective. *Trends Plant Sci* **10**, 57-62.

Grotewold E, Drummond BJ, Bowen B, Peterson T. 1994. The Myb-Homologous P-Gene Controls Phlobaphene Pigmentation in Maize Floral Organs by Directly Activating a Flavonoid Biosynthetic Gene Subset. *Cell* **76**, 543-553.

Gubler F, Kalla R, Roberts JK, Jacobsen JV. 1995. Gibberellin-Regulated Expression of a Myb Gene in Barley Aleurone Cells - Evidence for Myb Transactivation of a High-Pl Alpha-Amylase Gene Promoter. *Plant Cell* **7**, 1879-1891.

Gubler F, Raventos D, Keys M, Watts R, Mundy J, Jacobsen JV. 1999. Target genes and regulatory domains of the GAMYB transcriptional activator in cereal aleurone. *Plant Journal* **17**, 1-9.

Gusti A, Baumberger N, Nowack M, Pusch S, Eisler H, Potuschak T, De Veylder L, Schnittger A, Genschik P. 2009. The Arabidopsis thaliana F-Box Protein FBL17 Is Essential for Progression through the Second Mitosis during Pollen Development. *Plos One* **4**.

Haerizadeh F, Singh MB, Bhalla PL. 2006. Transcriptional Repression Distinguishes Somatic from Germ Cell Lineages in a Plant. *Science* **313**, 496-499.

Haga N, Kobayashi K, Suzuki T, Maeo K, Kubo M, Ohtani M, Mitsuda N, Demura T, Nakamura K, Jürgens G, Ito M. 2011. Mutations in MYB3R1 and MYB3R4 Cause Pleiotropic Developmental Defects and Preferential Down-Regulation of Multiple G2/M-Specific Genes in Arabidopsis. *Plant Physiology* **157**, 706-717.

Hanahan D. 1983. Studies on transformation of Escherichia coli with plasmids. *Journal of Molecular Biology* **166**, 557-580.

Hause B, Hause G, Pechan P, Vanlammeren AAM. 1993. Cytoskeletal Changes and Induction of Embryogenesis in Microspore and Pollen Cultures of Brassica-Napus L. *Cell Biology International* **17**, 153-168.

Hayashi K, Surani MA. 2009. Resetting the Epigenome beyond Pluripotency in the Germline. *Cell Stem Cell* **4**, 493-498.

Heese M, Gansel X, Sticher L, Wick P, Grebe M, Granier F, Jurgens G. 2001. Functional characterization of the KNOLLE-interacting t-SNARE AtSNAP33 and its role in plant cytokinesis. *J Cell Biol* **155**, 239-249.

Hennig L, Menges M, Murray JAH, Gruissem W. 2003. Arabidopsis transcript profiling on Affymetrix GeneChip arrays. *Plant Molecular Biology* **53**, 457-465.

Heyman J, De Veylder L. 2012. The anaphase-promoting complex/cyclosome in control of plant development. *Mol Plant* **5**, 1182-1194.

Hiratsu K, Matsui K, Koyama T, Ohme-Takagi M. 2003. Dominant repression of target genes by chimeric repressors that include the EAR motif, a repression domain, in Arabidopsis. *Plant Journal* **34**, 733-739.

Hiratsu K, Ohta M, Matsui K, Ohme-Takagi M. 2002. The SUPERMAN protein is an active repressor whose carboxy-terminal repression domain is required for the development of normal flowers. *FEBS Lett* **514**, 351-354.

Hoffmann RD, Palmgren MG. 2013. Epigenetic repression of male gametophyte-specific genes in the Arabidopsis sporophyte. *Mol Plant* **6**, 1176-1186.

Honys D, Oh SA, Renak D, Donders M, Solcova B, Johnson JA, Boudova R, Twell D. 2006. Identification of microspore-active promoters that allow targeted manipulation of gene expression at early stages of microgametogenesis in Arabidopsis. *Bmc Plant Biology* **6**.

Honys D, Twell D. 2003. Comparative analysis of the Arabidopsis pollen transcriptome. *Plant Physiology* **132**, 640-652.

Honys D, Twell D. 2004. Transcriptome analysis of haploid male gametophyte development in Arabidopsis. *Genome Biol* **5**, R85.

Howden R, Park SK, Moore JM, Orme J, Grossniklaus U, Twell D. 1998. Selection of T-DNA-tagged male and female gametophytic mutants by segregation distortion in Arabidopsis. *Genetics* **149**, 621-631.

Ichikawa T, Nakazawa M, Kawashima M, Iizumi H, Kuroda H, Kondou Y, Tsuhara Y, Suzuki K, Ishikawa A, Seki M, Fujita M, Motohashi R, Nagata N, Takagi T, Shinozaki K, Matsui M. 2006. The FOX hunting system: an alternative gain-of-function gene hunting technique. *Plant Journal* **48**, 974-985.

Imai KK, Ohashi Y, Tsuge T, Yoshizumi T, Matsui M, Oka A, Aoyama T. 2006. The A-type cyclin CYCA2;3 is a key regulator of ploidy levels in Arabidopsis endoreduplication. *Plant Cell* **18**, 382-396.

Inze D, De Veylder L. 2006. Cell cycle regulation in plant development. *Annu Rev Genet* **40**, 77-105.

Irish VF. 2010. The flowering of Arabidopsis flower development. *Plant Journal* **61**, 1014-1028.

Ito M, Araki S, Matsunaga S, Itoh T, Nishihama R, Machida Y, Doonan JH, Watanabe A. 2001. G2/M-Phase–Specific Transcription during the Plant Cell Cycle Is Mediated by c-Myb–Like Transcription Factors. *The Plant Cell Online* **13**, 1891-1905.

Iwakawa H, Shinmyo A, Sekine M. 2006. Arabidopsis CDKA;1, a cdc2 homologue, controls proliferation of generative cells in male gametogenesis. *Plant Journal* **45**, 819-831.

Jander G, Norris SR, Rounsley SD, Bush DF, Levin IM, Last RL. 2002. Arabidopsis map-based cloning in the post-genome era. *Plant Physiology* **129**, 440-450.

Jenik PD, Irish VF. 2000. Regulation of cell proliferation patterns by homeotic genes during Arabidopsis floral development. *Development* **127**, 1267-1276.

Johnson-Brousseau SA, McCormick S. 2004. A compendium of methods useful for characterizing Arabidopsis pollen mutants and gametophytically-expressed genes. *Plant Journal* **39**, 761-775.

Johnson MA, von Besser K, Zhou Q, Smith E, Aux G, Patton D, Levin JZ, Preuss D. 2004. Arabidopsis hapless mutations define essential gametophytic functions. *Genetics* **168**, 971-982.

Johnson SA, McCormick S. 2001. Pollen germinates precociously in the anthers of raring-to-go, an Arabidopsis gametophytic mutant. *Plant Physiology* **126**, 685-695.

Jones KH, Senft JA. 1985. An Improved Method to Determine Cell Viability by Simultaneous Staining with Fluorescein Diacetate Propidium Iodide. *Journal of Histochemistry & Cytochemistry* **33**, 77-79.

Joubès J, Chevalier C. 2000. Endoreduplication in higher plants. *Plant Molecular Biology* **43**, 735-745.

Joubès J, Chevalier C, Dudits D, Heberle-Bors E, Inzé D, Umeda M, Renaudin J-P. 2000. CDK-related protein kinases in plants. *Plant Molecular Biology* **43**, 607-620.

Kagale S, Links MG, Rozwadowski K. 2010. Genome-Wide Analysis of Ethylene-Responsive Element Binding Factor-Associated Amphiphilic Repression Motif-Containing Transcriptional Regulators in Arabidopsis. *Plant Physiology* **152**, 1109-

1134.

Kagale S, Rozwadowski K. 2011. EAR motif-mediated transcriptional repression in plants An underlying mechanism for epigenetic regulation of gene expression. *Epigenetics* **6**, 141-146.

Kaneko M, Inukai Y, Ueguchi-Tanaka M, Itoh H, Izawa T, Kobayashi Y, Hattori T, Miyao A, Hirochika H, Ashikari M, Matsuoka M. 2004. Loss-of-function mutations of the rice GAMYB gene impair alpha-amylase expression in aleurone and flower development. *Plant Cell* **16**, 33-44.

Kang YH, Kirik V, Hulskamp M, Nam KH, Hagely K, Lee MM, Schiefelbeind J. 2009. The MYB23 Gene Provides a Positive Feedback Loop for Cell Fate Specification in the Arabidopsis Root Epidermis. *Plant Cell* **21**, 1080-1094.

Karimi M, Inze D, Depicker A. 2002. GATEWAY vectors for Agrobacterium-mediated plant transformation. *Trends Plant Sci* **7**, 193-195.

Kim HJ, Oh SA, Brownfield L, Hong SH, Ryu H, Hwang I, Twell D, Nam HG. 2008. Control of plant germline proliferation by SCF(FBL17) degradation of cell cycle inhibitors. *Nature* **455**, 1134-1137.

Kipreos ET, Pagano M. 2000. The F-box protein family. *Genome Biol* **1**, Reviews3002.

Klempnauer KH, Gonda TJ, Bishop JM. 1982. Nucleotide sequence of the retroviral leukemia gene v-myb and its cellular progenitor c-myb: the architecture of a transduced oncogene. *Cell* **31**, 453-463.

Kliwer I, Dresselhaus T. 2010. Establishment of the male germline and sperm cell movement during pollen germination and tube growth in maize. *Plant Signal Behav* **5**, 885-889.

Klug A, Schwabe JW. 1995. Protein motifs 5. Zinc fingers. *FASEB J* **9**, 597-604.

Komaki S, Sugimoto K. 2012. Control of the Plant Cell Cycle by Developmental and Environmental Cues. *Plant and Cell Physiology* **53**, 953-964.

Kost B, Mathur J, Chua NH. 1999. Cytoskeleton in plant development. *Current Opinion in Plant Biology* **2**, 462-470.

Krizek BA, Lewis MW, Fletcher JC. 2006. RABBIT EARS is a second-whorl repressor of AGAMOUS that maintains spatial boundaries in Arabidopsis flowers. *Plant Journal* **45**, 369-383.

Krogan NT, Long JA. 2009. Why so repressed? Turning off transcription during plant growth and development. *Current Opinion in Plant Biology* **12**, 628-636.

Krysan PJ, Young JC, Sussman MR. 1999. T-DNA as an insertional mutagen in Arabidopsis. *Plant Cell* **11**, 2283-2290.

Kubo K-i, Sakamoto A, Kobayashi A, Rybka Z, Kanno Y, Nakagawa H, Nishino T, Takatsuji H. 1998. Cys2/His2 zinc-finger protein family of petunia: Evolution and

general mechanism of target-sequence recognition. *Nucleic Acids Research* **26**, 608-615.

Kwee H-S, Sundaresan V. 2003. The NOMEGA gene required for female gametophyte development encodes the putative APC6/CDC16 component of the Anaphase Promoting Complex in Arabidopsis. *The Plant Journal* **36**, 853-866.

Lafos M, Kroll P, Hohenstatt ML, Thorpe FL, Clarenz O, Schubert D. 2011. Dynamic regulation of H3K27 trimethylation during Arabidopsis differentiation. *PLoS Genet* **7**, e1002040.

Lalanne E, Michaelidis C, Moore JM, Gagliano W, Johnson A, Patel R, Howden R, Vielle-Calzada JP, Grossniklaus U, Twell D. 2004. Analysis of transposon insertion mutants highlights the diversity of mechanisms underlying male progamic development in arabidopsis. *Genetics* **167**, 1975-1986.

Lalanne E, Twell D. 2002. Genetic control of male germ unit organization in Arabidopsis. *Plant Physiology* **129**, 865-875.

Landy A. 1989. Dynamic, Structural, and Regulatory Aspects of Lambda-Site-Specific Recombination. *Annual Review of Biochemistry* **58**, 913-949.

Lange A, Mills RE, Lange CJ, Stewart M, Devine SE, Corbett AH. 2007. Classical nuclear localization signals: definition, function, and interaction with importin alpha. *J Biol Chem* **282**, 5101-5105.

Lee J, Das A, Yamaguchi M, Hashimoto J, Tsutsumi N, Uchimiya H, Umeda M. 2003. Cell cycle function of a rice B2-type cyclin interacting with a B-type cyclin-dependent kinase. *The Plant Journal* **34**, 417-425.

Lee JY, Lee DH. 2003. Use of serial analysis of gene expression technology to reveal changes in gene expression in Arabidopsis pollen undergoing cold stress. *Plant Physiology* **132**, 517-529.

Lee Y-RJ, Li Y, Liu B. 2007. Two Arabidopsis Phragmoplast-Associated Kinesins Play a Critical Role in Cytokinesis during Male Gametogenesis. *The Plant Cell Online* **19**, 2595-2605.

Lima d, Eloy N, Pegoraro C, Sagit R, Rojas C, Bretz T, Vargas L, Elofsson A, de Oliveira A, Hemerly A, Ferreira P. 2010. Genomic evolution and complexity of the Anaphase-promoting Complex (APC) in land plants. *Bmc Plant Biology* **10**, 1-18.

Liu B, Ho CM, Lee YR. 2011. Microtubule Reorganization during Mitosis and Cytokinesis: Lessons Learned from Developing Microgametophytes in Arabidopsis Thaliana. *Front Plant Sci* **2**, 27.

Liu B, Palevitz BA. 1991. Kinetochore Fiber Formation in Dividing Generative Cells of Tradescantia - Kinetochore Reorientation Associated with the Transition between Lateral Microtubule Interactions and End-on Kinetochore Fibers. *Journal of Cell Science* **98**, 475-482.

Liu J, Zhang Y, Qin G, Tsuge T, Sakaguchi N, Luo G, Sun K, Shi D, Aki S, Zheng N, Aoyama T, Oka A, Yang W, Umeda M, Xie Q, Gu H, Qu LJ. 2008a. Targeted degradation of the cyclin-dependent kinase inhibitor ICK4/KRP6 by RING-type E3

ligases is essential for mitotic cell cycle progression during Arabidopsis gametogenesis. *Plant Cell* **20**, 1538-1554.

Liu L, Du H, Tang XF, Wu YM, Huang YB, Tang YX. 2008b. The roles of MYB transcription factors on plant defense responses and its molecular mechanism. *Yi Chuan* **30**, 1265-1271.

Liu Z, Bao W, Liang W, Yin J, Zhang D. 2010. Identification of gamyb-4 and analysis of the regulatory role of GAMYB in rice anther development. *J Integr Plant Biol* **52**, 670-678.

Loraine AE, McCormick S, Estrada A, Patel K, Qin P. 2013. RNA-seq of Arabidopsis pollen uncovers novel transcription and alternative splicing. *Plant Physiology* **162**, 1092-1109.

Lui H, Wang H, DeLong C, Fowke LC, Crosby WL, Fobert PR. 2000. The Arabidopsis Cdc2a-interacting protein ICK2 is structurally related to ICK1 and is a potent inhibitor of cyclin-dependent kinase activity in vitro. *The Plant Journal* **21**, 379-385.

Lukowitz W, Gillmor CS, Scheible WR. 2000. Positional cloning in Arabidopsis. Why it feels good to have a genome initiative working for you. *Plant Physiology* **123**, 795-805.

Maheshwari P. 1950. An introduction to the embryology of angiosperms.

Mandaokar A, Browse J. 2009. MYB108 Acts Together with MYB24 to Regulate Jasmonate-Mediated Stamen Maturation in Arabidopsis. *Plant Physiology* **149**, 851-862.

Mandaokar A, Thines B, Shin B, Lange BM, Choi G, Koo YJ, Yoo YJ, Choi YD, Choi G, Browse J. 2006. Transcriptional regulators of stamen development in Arabidopsis identified by transcriptional profiling. *Plant Journal* **46**, 984-1008.

Mascarenhas JP. 1975. The biochemistry of angiosperm pollen development. *The Botanical Review* **41**, 259-314.

Mascarenhas JP. 1990. Gene Activity during Pollen Development. *Annual Review of Plant Physiology and Plant Molecular Biology* **41**, 317-338.

Matthews JC, Hori K, Cormier MJ. 1977. Purification and Properties of Renilla-Reniformis Luciferase. *Biochemistry* **16**, 85-91.

McCormick S. 2004. Control of male gametophyte development. *Plant Cell* **16**, S142-S153.

McCue AD, Cresti M, Feijo JA, Slotkin RK. 2011. Cytoplasmic connection of sperm cells to the pollen vegetative cell nucleus: potential roles of the male germ unit revisited. *Journal of Experimental Botany* **62**, 1621-1631.

Menges M, De Jager SM, Gruissem W, Murray JAH. 2005. Global analysis of the core cell cycle regulators of Arabidopsis identifies novel genes, reveals multiple and highly specific profiles of expression and provides a coherent model for plant cell cycle

control. *The Plant Journal* **41**, 546-566.

Michaels SD, Amasino RM. 1998. A robust method for detecting single-nucleotide changes as polymorphic markers by PCR. *Plant Journal* **14**, 381-385.

Millar AA, Gubler F. 2005. The Arabidopsis GAMYB-like genes, MYB33 and MYB65, are MicroRNA-regulated genes that redundantly facilitate anther development. *Plant Cell* **17**, 705-721.

Mironov V, De Veylder L, Van Montagu M, Inzé D. 1999. Cyclin-Dependent Kinases and Cell Division in Plants—The Nexus. *The Plant Cell Online* **11**, 509-521.

Moore JM, Calzada JPV, Gagliano W, Grossniklaus U. 1997. Genetic characterization of hadad, a mutant disrupting female gametogenesis in Arabidopsis thaliana. *Cold Spring Harbor Symposia on Quantitative Biology* **62**, 35-47.

Mori T, Kuroiwa H, Higashiyama T, Kuroiwa T. 2006. GENERATIVE CELL SPECIFIC 1 is essential for angiosperm fertilization. *Nature Cell Biology* **8**, 64-71.

Nakai T, Kato K, Shinmyo A, Sekine M. 2006. Arabidopsis KRPs have distinct inhibitory activity toward cyclin D2-associated kinases, including plant-specific B-type cyclin-dependent kinase. *FEBS Lett* **580**, 336-340.

Noda K, Glover BJ, Linstead P, Martin C. 1994. Flower Color Intensity Depends on Specialized Cell-Shape Controlled by a Myb-Related Transcription Factor. *Nature* **369**, 661-664.

Nowack MK, Grini PE, Jakoby MJ, Lafos M, Koncz C, Schnittger A. 2006. A positive signal from the fertilization of the egg cell sets off endosperm proliferation in angiosperm embryogenesis. *Nature Genetics* **38**, 63-67.

Oh S-A, Bourdon V, Das 'Pal M, Dickinson H, Twell D. 2008. Arabidopsis Kinesins HINKEL and TETRASPORE Act Redundantly to Control Cell Plate Expansion during Cytokinesis in the Male Gametophyte. *Molecular Plant* **1**, 794-799.

Oh SA, Allen T, Twell D. 2010a. A ticket for the live show: Microtubules in male gametophyte development. *Plant Signal Behav* **5**, 614-617.

Oh SA, Das Pal M, Park SK, Johnson JA, Twell D. 2010b. The tobacco MAP215/Dis1-family protein TMBP200 is required for the functional organization of microtubule arrays during male germline establishment. *Journal of Experimental Botany* **61**, 969-981.

Oh SA, Johnson A, Smertenko A, Rahman D, Park SK, Hussey PJ, Twell D. 2005. A divergent cellular role for the FUSED kinase family in the plant-specific cytokinetic phragmoplast. *Current Biology* **15**, 2107-2111.

Oh SA, Park KS, Twell D, Park SK. 2010c. The SIDECAR POLLEN gene encodes a microspore-specific LOB/AS2 domain protein required for the correct timing and orientation of asymmetric cell division. *Plant Journal* **64**, 839-850.

Ohta M, Matsui K, Hiratsu K, Shinshi H, Ohme-Takagi M. 2001. Repression domains of class II ERF transcriptional repressors share an essential motif for active

repression. *Plant Cell* **13**, 1959-1968.

Okada T, Endo M, Singh MB, Bhalla PL. 2005. Analysis of the histone H3 gene family in Arabidopsis and identification of the male-gamete-specific variant AtMGH3. *Plant Journal* **44**, 557-568.

Oppenheimer DG, Herman PL, Sivakumaran S, Esch J, Marks MD. 1991. A Myb Gene Required for Leaf Trichome Differentiation in Arabidopsis Is Expressed in Stipules. *Cell* **67**, 483-493.

Owen HA, Makaroff CA. 1995. Ultrastructure of Microsporogenesis and Microgametogenesis in Arabidopsis-Thaliana (L) Heynh Ecotype Wassilewskija (Brassicaceae). *Protoplasma* **185**, 7-21.

Pacini E. 1996. Types and meaning of pollen carbohydrate reserves. *Sexual Plant Reproduction* **9**, 362-366.

Page DR, Grossniklaus L. 2002. The art and design of genetic screens: Arabidopsis thaliana. *Nature Reviews Genetics* **3**, 124-136.

Palatnik JF, Wollmann H, Schommer C, Schwab R, Boisbouvier J, Rodriguez R, Warthmann N, Allen E, Dezulian T, Huson D, Carrington JC, Weigel D. 2007. Sequence and expression differences underlie functional specialization of Arabidopsis MicroRNAs miR159 and miR319. *Developmental Cell* **13**, 115-125.

Palevitz BA. 1990. Kinetochore Behavior during Generative Cell-Division in Tradescantia-Virginiana. *Protoplasma* **157**, 120-127.

Palevitz BA. 1993. Organization of the Mitotic Apparatus during Generative Cell-Division in Nicotiana-Tabacum. *Protoplasma* **174**, 25-35.

Palevitz BA, Cresti M. 1989. Cytoskeletal Changes during Generative Cell-Division and Sperm Formation in Tradescantia-Virginiana. *Protoplasma* **150**, 54-71.

Palevitz BA, Tiezzi A. 1992. Organization, Composition, and Function of the Generative Cell and Sperm Cytoskeleton. *International Review of Cytology-a Survey of Cell Biology* **140**, 149-185.

Parcy F. 2005. Flowering: a time for integration. *International Journal of Developmental Biology* **49**, 585-593.

Park S, Rahman D, Oh S, Twell D. 2004. Gemini pollen 2, a male and female gametophytic cytokinesis defective mutation. *Sexual Plant Reproduction* **17**, 63-70.

Park SK, Howden R, Twell D. 1998. The Arabidopsis thaliana gametophytic mutation gemini pollen1 disrupts microspore polarity, division asymmetry and pollen cell fate. *Development* **125**, 3789-3799.

Park SK, Twell D. 2001. Novel patterns of ectopic cell plate growth and lipid body distribution in the Arabidopsis gemini pollen1 mutant. *Plant Physiology* **126**, 899-909.

Pastuglia M, Azimzadeh J, Goussot M, Camilleri C, Belcram K, Evrard JL, Schmit AC, Guerche P, Bouchez D. 2006. Gamma-tubulin is essential for microtubule

organization and development in Arabidopsis. *Plant Cell* **18**, 1412-1425.

Payne T, Johnson SD, Koltunow AM. 2004. KNUCKLES (KNU) encodes a C2H2 zinc-finger protein that regulates development of basal pattern elements of the Arabidopsis gynoecium. *Development* **131**, 3737-3749.

Paz-Ares J, Ghosal D, Wienand U, Peterson PA, Saedler H. 1987. The Regulatory C1 Locus of Zea-Mays Encodes a Protein with Homology to Myb Protooncogene Products and with Structural Similarities to Transcriptional Activators. *Embo Journal* **6**, 3553-3558.

Pazin MJ, Kadonaga JT. 1997. What's up and down with histone deacetylation and transcription? *Cell* **89**, 325-328.

Pedersen S, Simonsen V, Loeschcke V. 1987. Overlap of gametophytic and sporophytic gene expression in barley. *Theoretical and Applied Genetics* **75**, 200-206.

Pereira AP, Francisco VS, Becker. JD. 2012. Decision-Making in the Plant Cell Cycle. *canalBQ*, 48-62.

Pesin JA, Orr-Weaver TL. 2008. Regulation of APC/C activators in mitosis and meiosis. *Annu Rev Cell Dev Biol* **24**, 475-499.

Pina C, Pinto F, Feijo JA, Becker JD. 2005. Gene family analysis of the Arabidopsis pollen transcriptome reveals biological implications for cell growth, division control, and gene expression regulation. *Plant Physiology* **138**, 744-756.

Planchais S, Samland AK, Murray JAH. 2004. Differential stability of Arabidopsis D-type cyclins: CYCD3;1 is a highly unstable protein degraded by a proteasome-dependent mechanism. *The Plant Journal* **38**, 616-625.

Preuss D, Rhee SY, Davis RW. 1994. Tetrad Analysis Possible in Arabidopsis with Mutation of the Quartet (Qrt) Genes. *Science* **264**, 1458-1460.

Procissi A, de Laissardiere S, Ferault M, Vezon D, Pelletier G, Bonhomme S. 2001. Five gametophytic mutations affecting pollen development and pollen tube growth in Arabidopsis thaliana. *Genetics* **158**, 1773-1783.

Prouse MB, Campbell MM. 2013. Interactions between the R2R3-MYB transcription factor, AtMYB61, and target DNA binding sites. *Plos One* **8**, e65132.

Punwani JA, Rabiger DS, Drews GN. 2007. MYB98 positively regulates a battery of synergid-expressed genes encoding filiform apparatus localized proteins. *Plant Cell* **19**, 2557-2568.

Punwani JA, Rabiger DS, Lloyd A, Drews GN. 2008. The MYB98 subcircuit of the synergid gene regulatory network includes genes directly and indirectly regulated by MYB98. *Plant Journal* **55**, 406-414.

Qin Y, Leydon AR, Manziello A, Pandey R, Mount D, Denic S, Vasic B, Johnson MA, Palanivelu R. 2009. Penetration of the stigma and style elicits a novel transcriptome in pollen tubes, pointing to genes critical for growth in a pistil. *PLoS Genet* **5**, e1000621.

Redman JC, Haas BJ, Tanimoto G, Town CD. 2004. Development and evaluation of an Arabidopsis whole genome Affymetrix probe array. *Plant Journal* **38**, 545-561.

Rehrauer H, Aquino C, Gruissem W, Henz SR, Hilson P, Laubinger S, Naouar N, Patrignani A, Rombauts S, Shu H, Van de Peer Y, Vuylsteke M, Weigel D, Zeller G, Hennig L. 2010. AGRONOMICS1: A New Resource for Arabidopsis Transcriptome Profiling. *Plant Physiology* **152**, 487-499.

Rhee SY, Osborne E, Poindexter PD, Somerville CR. 2003. Microspore Separation in the quartet 3 Mutants of Arabidopsis Is Impaired by a Defect in a Developmentally Regulated Polygalacturonase Required for Pollen Mother Cell Wall Degradation. *Plant Physiology* **133**, 1170-1180.

Riechmann JL, Heard J, Martin G, Reuber L, -Z. C, Jiang, Keddie J, Adam L, Pineda O, Ratcliffe OJ, Samaha RR, Creelman R, Pilgrim M, Broun P, Zhang JZ, Ghandehari D, Sherman BK, -L. Yu G. 2000. Arabidopsis Transcription Factors: Genome-Wide Comparative Analysis Among Eukaryotes. *Science* **290**, 2105-2110.

Rodriguez-Enriquez MJ, Mehdi S, Dickinson HG, Grant-Downton RT. 2013. A novel method for efficient in vitro germination and tube growth of Arabidopsis thaliana pollen. *New Phytologist* **197**, 668-679.

Roeder AHK, Chickarmane V, Cunha A, Obara B, Manjunath BS, Meyerowitz EM. 2010. Variability in the Control of Cell Division Underlies Sepal Epidermal Patterning in *Arabidopsis thaliana*. *PLoS Biol* **8**, e1000367.

Roth BA, Goff SA, Klein TM, Fromm ME. 1991. C1- and R-dependent expression of the maize Bz1 gene requires sequences with homology to mammalian myb and myc binding sites. *The Plant Cell Online* **3**, 317-325.

Rotman N, Durbarry A, Wardle A, Yang WC, Chaboud A, Faure J-E, Berger F, Twell D. 2005. A Novel Class of MYB Factors Controls Sperm-Cell Formation in Plants. *Current Biology* **15**, 244-248.

Roudier F, Ahmed I, Berard C, Sarazin A, Mary-Huard T, Cortijo S, Bouyer D, Caillieux E, Duvernois-Berthet E, Al-Shikhley L, Giraut L, Despres B, Drevensek S, Barneche F, Derozier S, Brunaud V, Aubourg S, Schnittger A, Bowler C, Martin-Magniette ML, Robin S, Caboche M, Colot V. 2011. Integrative epigenomic mapping defines four main chromatin states in Arabidopsis. *Embo Journal* **30**, 1928-1938.

Rozen S, Skaletsky H. 2000. Primer3 on the WWW for general users and for biologist programmers. *Methods Mol Biol* **132**, 365-386.

Rudall PJ, Bateman RM. 2007. Developmental bases for key innovations in the seed-plant microgametophyte. *Trends Plant Sci* **12**, 317-326.

Russell SD. 1991. Isolation and Characterization of Sperm Cells in Flowering Plants. *Annual Review of Plant Physiology and Plant Molecular Biology* **42**, 189-204.

Sachs M, Onodera C, Blaschke K, Ebata KT, Song JS, Ramalho-Santos M. 2013. Bivalent chromatin marks developmental regulatory genes in the mouse embryonic germline in vivo. *Cell Rep* **3**, 1777-1784.

Saikumar P, Murali R, Reddy EP. 1990. Role of Tryptophan Repeats and Flanking Amino-Acids in Myb-DNA Interactions. *Proceedings of the National Academy of Sciences of the United States of America* **87**, 8452-8456.

Sakai H, Medrano LJ, Meyerowitz EM. 1995. Role of SUPERMAN in maintaining Arabidopsis floral whorl boundaries. *Nature* **378**, 199-203.

Sakamoto H, Maruyama K, Sakuma Y, Meshi T, Iwabuchi M, Shinozaki K, Yamaguchi-Shinozaki K. 2004. Arabidopsis Cys2/His2-type zinc-finger proteins function as transcription repressors under drought, cold, and high-salinity stress conditions. *Plant Physiology* **136**, 2734-2746.

Sakurai T, Kondou Y, Akiyama K, Kurotani A, Higuchi M, Ichikawa T, Kuroda H, Kusano M, Mori M, Saitou T, Sakakibara H, Sugano S, Suzuki M, Takahashi H, Takahashi S, Takatsuji H, Yokotani N, Yoshizumi T, Saito K, Shinozaki K, Oda K, Hirochika H, Matsui M. 2011. RiceFOX: a database of Arabidopsis mutant lines overexpressing rice full-length cDNA that contains a wide range of trait information to facilitate analysis of gene function. *Plant and Cell Physiology* **52**, 265-273.

Sambrook J, Russell David W. 1989. *Molecular cloning: a laboratory manual. Vol. 3*: Cold spring harbor laboratory press.

Sanger JM, Jackson WT. 1971. Fine structure study of pollen development in Haemanthus katherinae Baker. II. Microtubules and elongation of the generative cells. *J Cell Sci* **8**, 303-315.

Schiefelbein J. 2003. Cell-fate specification in the epidermis: a common patterning mechanism in the root and shoot. *Current Opinion in Plant Biology* **6**, 74-78.

Schmid M, Davison TS, Henz SR, Pape UJ, Demar M, Vingron M, Scholkopf B, Weigel D, Lohmann JU. 2005. A gene expression map of Arabidopsis thaliana development. *Nature Genetics* **37**, 501-506.

Scholl RL, May ST, Ware DH. 2000. Seed and Molecular Resources for Arabidopsis. *Plant Physiology* **124**, 1477-1480.

Schwacke R, Grallath S, Breitkreuz KE, Stransky E, Stransky H, Frommer WB, Rentsch D. 1999. LeProT1, a transporter for proline, glycine betaine, and gamma-amino butyric acid in tomato pollen. *Plant Cell* **11**, 377-391.

Scott RJ, Spielman M, Dickinson HG. 2004. Stamen structure and function. *Plant Cell* **16**, S46-S60.

Segarra G, Van der Ent S, Trillas I, Pieterse CMJ. 2009. MYB72, a node of convergence in induced systemic resistance triggered by a fungal and a bacterial beneficial microbe. *Plant Biology* **11**, 90-96.

Sherf B, Navarro S, Hannah R. 1996. Dual-luciferase reporter assay: an advanced co-reporter technology integrating firefly and Renilla luciferase assays. *Promega Notes* **57**.

Singh MB, Bhalla PL. 2007. Control of male germ-cell development in flowering plants. *Bioessays* **29**, 1124-1132.

Singh MB, Xu HL, Bhalla PL, Zhang ZJ, Swoboda I, Russell SD. 2002. Developmental expression of polyubiquitin genes and distribution of ubiquitinated proteins in generative and sperm cells. *Sexual Plant Reproduction* **14**, 325-329.

Slotkin RK, Vaughn M, Borges F, Tanurdzic M, Becker JD, Feijo JA, Martienssen RA. 2009. Epigenetic Reprogramming and Small RNA Silencing of Transposable Elements in Pollen. *Cell* **136**, 461-472.

Smyth DR, Bowman JL, Meyerowitz EM. 1990. Early Flower Development in Arabidopsis. *Plant Cell* **2**, 755-767.

Solano R, Nieto C, Avila J, Canas L, Diaz I, Paz-Ares J. 1995. Dual DNA binding specificity of a petal epidermis-specific MYB transcription factor (MYB.Ph3) from Petunia hybrida. *Embo Journal* **14**, 1773-1784.

Sorrell DA, Marchbank A, McMahon K, Dickinson JR, Rogers HJ, Francis D. 2002. A WEE1 homologue from Arabidopsis thaliana. *Planta* **215**, 518-522.

Sparkes IA, Runions J, Kearns A, Hawes C. 2006. Rapid, transient expression of fluorescent fusion proteins in tobacco plants and generation of stably transformed plants. *Nature Protocols* **1**, 2019-2025.

Stals H, Inze D. 2001. When plant cells decide to divide. *Trends Plant Sci* **6**, 359-364.

Stirnimann CU, Petsalaki E, Russell RB, Muller CW. 2010. WD40 proteins propel cellular networks. *Trends in Biochemical Sciences* **35**, 565-574.

Stracke R, Werber M, Weisshaar B. 2001. The R2R3-MYB gene family in Arabidopsis thaliana. *Current Opinion in Plant Biology* **4**, 447-456.

Strome S, Lehmann R. 2007. Germ versus soma decisions: Lessons from flies and worms. *Science* **316**, 392-393.

Sun YJ, Dilkes BP, Zhang CS, Dante RA, Carneiro NP, Lowe KS, Jung R, Gordon-Kamm WJ, Larkins BA. 1999. Characterization of maize (Zea mays L.) Wee1 and its activity in developing endosperm. *Proceedings of the National Academy of Sciences of the United States of America* **96**, 4180-4185.

Sundaresan V, Springer P, Volpe T, Haward S, Jones JDG, Dean C, Ma H, Martienssen R. 1995. Patterns of Gene-Action in Plant Development Revealed by Enhancer Trap and Gene Trap Transposable Elements. *Genes & Development* **9**, 1797-1810.

Takahashi I, Kojima S, Sakaguchi N, Umeda-Hara C, Umeda M. 2010. Two Arabidopsis cyclin A3s possess G1 cyclin-like features. *Plant Cell Rep* **29**, 307-315.

Takahashi N, Lammens T, Boudolf V, Maes S, Yoshizumi T, De Jaeger G, Witters E, Inze D, De Veylder L. 2008. The DNA replication checkpoint aids survival of plants deficient in the novel replisome factor ETG1. *Embo Journal* **27**, 1840-1851.

Takatsuji H. 1999. Zinc-finger proteins: the classical zinc finger emerges in contemporary plant science. *Plant Molecular Biology* **39**, 1073-1078.

Takatsuji H, Mori M, Benfey PN, Ren L, Chua NH. 1992. Characterization of a Zinc Finger DNA-Binding Protein Expressed Specifically in Petunia Petals and Seedlings. *Embo Journal* **11**, 241-249.

Tanaka I. 1988. Isolation of Generative Cells and Their Protoplasts from Pollen of Lilium-Longiflorum. *Protoplasma* **142**, 68-73.

Tanaka I. 1997. Differentiation of generative and vegetative cells in angiosperm pollen. *Sexual Plant Reproduction* **10**, 1-7.

Tanaka I, Ito M. 1980. Induction of Typical Cell-Division in Isolated Microspores of Lilium-Longiflorum and Tulipa-Gesneriana. *Plant Science Letters* **17**, 279-285.

Tanaka I, Ito M. 1981. Control of Division Patterns in Explanted Microspores of Tulipa-Gesneriana. *Protoplasma* **108**, 329-340.

Tarayre S, Vinardell JM, Cebolla A, Kondorosi A, Kondorosi E. 2004. Two Classes of the Cdh1-Type Activators of the Anaphase-Promoting Complex in Plants: Novel Functional Domains and Distinct Regulation. *The Plant Cell Online* **16**, 422-434.

Taylor P, Kenrick J, Li Y, Kaul V, Gunning BES, Knox RB. 1989. The male germ unit of Rhododendron: quantitative cytology, three-dimensional reconstruction, isolation and detection using fluorescent probes. *Sexual Plant Reproduction* **2**, 254-264.

Terasaka O, Niitsu T. 1989. Peculiar spindle configuration in the pollen tube revealed by the anti-tubulin immunofluorescence method. *The botanical magazine = Shokubutsu-gaku-zasshi* **102**, 143-147.

Terasaka O, Niitsu T. 1990. Unequal Cell-Division and Chromatin Differentiation in Pollen Grain Cells .2. Microtubule Dynamics Associated with the Unequal Cell-Division. *Botanical Magazine-Tokyo* **103**, 133-142.

Terasaka O, Niitsu T. 1995. The mitotic apparatus during unequal microspore division observed by a confocal laser scanning microscope. *Protoplasma* **189**, 187-193.

Torres Acosta JA, Fowke LC, Wang H. 2011. Analyses of phylogeny, evolution, conserved sequences and genome-wide expression of the ICK/KRP family of plant CDK inhibitors. *Annals of Botany* **107**, 1141-1157.

Tsuji H, Aya K, Ueguchi-Tanaka M, Shimada Y, Nakazono M, Watanabe R, Nishizawa NK, Gomi K, Shimada A, Kitano H, Ashikari M, Matsuoka M. 2006. GAMYB controls different sets of genes and is differentially regulated by microRNA in aleurone cells and anthers. *The Plant Journal* **47**, 427-444.

Twell D. 1992. Use of a nuclear-targeted β-glucuronidase fusion protein to demonstrate vegetative cell-specific gene expression in developing pollen. *The Plant Journal* **2**, 887-892.

Twell D, Oh S-A, Honys D. 2006. Pollen Development, a Genetic and Transcriptomic View. In: Malhó R, ed. *The Pollen Tube*, Vol. 3: Springer Berlin Heidelberg, 15-45.

Twell D, Park SK, Hawkins TJ, Schubert D, Schmidt R, Smertenko A, Hussey PJ. 2002. MOR1/GEM1 has an essential role in the plant-specific cytokinetic phragmoplast.

Nature Cell Biology **4**, 711-714.

Twell D, Park SK, Lalanne E. 1998. Asymmetric division and cell-fate determination in developing pollen. *Trends Plant Sci* **3**, 305-310.

Uchida N, Sakamoto T, Kurata T, Tasaka M. 2011. Identification of EMS-induced causal mutations in a non-reference Arabidopsis thaliana accession by whole genome sequencing. *Plant and Cell Physiology* **52**, 716-722.

Uchiumi T, Komatsu S, Koshiba T, Okamoto T. 2006. Isolation of gametes and central cells from Oryza sativa L. *Sexual Plant Reproduction* **19**, 37-45.

Umeda M, Shimotohno A, Yamaguchi M. 2005. Control of Cell Division and Transcription by Cyclin-dependent Kinase-activating Kinases in Plants. *Plant and Cell Physiology* **46**, 1437-1442.

Urao T, Yamaguchi-Shinozaki K, Urao S, Shinozaki K. 1993. An Arabidopsis myb homolog is induced by dehydration stress and its gene product binds to the conserved MYB recognition sequence. *The Plant Cell Online* **5**, 1529-1539.

Van Lammeren AA, Keijzer CJ, Willemse MT, Kieft H. 1985. Structure and function of the microtubular cytoskeleton during pollen development in Gasteria verrucosa (Mill.) H. Duval. *Planta* **165**, 1-11.

Van Leene J, Boruc J, De Jaeger G, Russinova E, De Veylder L. 2011. A kaleidoscopic view of the Arabidopsis core cell cycle interactome. *Trends Plant Sci* **16**, 141-150.

Van Leene J, Hollunder J, Eeckhout D, Persiau G, Van de Slijke E, Stals H, Van Isterdael G, Verkest A, Neirynck S, Buffel Y, De Bodt S, Maere S, Laukens K, Pharazyn A, Ferreira PCG, Eloy N, Renne C, Meyer C, Faure JD, Steinbrenner J, Beynon J, Larkin JC, Van de Peer Y, Hilson P, Kuiper M, De Veylder L, Van Onckelen H, Inze D, Witters E, De Jaeger G. 2010. Targeted interactomics reveals a complex core cell cycle machinery in Arabidopsis thaliana. *Molecular Systems Biology* **6**.

Vandepoele K, Raes J, De Veylder L, Rouzé P, Rombauts S, Inzé D. 2002. Genome-Wide Analysis of Core Cell Cycle Genes in Arabidopsis. *The Plant Cell Online* **14**, 903-916.

Vandepoele K, Vlieghe K, Florquin K, Hennig L, Beemster GTS, Gruissem W, Van de Peer Y, Inzé D, De Veylder L. 2005. Genome-Wide Identification of Potential Plant E2F Target Genes. *Plant Physiology* **139**, 316-328.

Vinardell JM, Fedorova E, Cebolla A, Kevei Z, Horvath G, Kelemen Z, Tarayre S, Roudier F, Mergaert P, Kondorosi A, Kondorosi E. 2003. Endoreduplication Mediated by the Anaphase-Promoting Complex Activator CCS52A Is Required for Symbiotic Cell Differentiation in Medicago truncatula Nodules. *The Plant Cell Online* **15**, 2093-2105.

Vodermaier HC. 2004. APC/C and SCF: controlling each other and the cell cycle. *Current Biology* **14**, R787-796.

Von Besser K, Frank AC, Johnson MA, Preuss D. 2006. Arabidopsis HAP2 (GCS1) is a sperm-specific gene required for pollen tube guidance and fertilization. *Development* **133**, 4761-4769.

Walbot V, Evans MMS. 2003. Unique features of the plant life cycle and their consequences. *Nature Reviews Genetics* **4**, 369-379.

Walters MC, Fiering S, Eidemiller J, Magis W, Groudine M, Martin DI. 1995. Enhancers increase the probability but not the level of gene expression. *Proceedings of the National Academy of Sciences* **92**, 7125-7129.

Wang G, Kong H, Sun Y, Zhang X, Zhang W, Altman N, dePamphilis CW, Ma H. 2004. Genome-Wide Analysis of the Cyclin Family in Arabidopsis and Comparative Phylogenetic Analysis of Plant Cyclin-Like Proteins. *Plant Physiology* **135**, 1084-1099.

Wang H, Fowke LC, Crosby WL. 1997. A plant cyclin-dependent kinase inhibitor gene. *Nature* **386**, 451-452.

Wang H, Zhou Y, Fowke LC. 2006. The emerging importance of cyclin-dependent kinase inhibitors in the regulation of the plant cell cycle and related processesThis review is one of a selection of papers published in the Special Issue on Plant Cell Biology. *Canadian Journal of Botany* **84**, 640-650.

Wang Y, Zhang WZ, Song LF, Zou JJ, Su Z, Wu WH. 2008. Transcriptome Analyses Show Changes in Gene Expression to Accompany Pollen Germination and Tube Growth in Arabidopsis. *Plant Physiology* **148**, 1201-1211.

Watanabe N, Arai H, Nishihara Y, Taniguchi M, Watanabe N, Hunter T, Osada H. 2004. M-phase kinases induce phospho-dependent ubiquitination of somatic Wee1 by SCFβ-TrCP. *Proceedings of the National Academy of Sciences of the United States of America* **101**, 4419-4424.

Weimer AK, Nowack MK, Bouyer D, Zhao XA, Harashima H, Naseer S, De Winter F, Dissmeyer N, Geldner N, Schnittger A. 2012. RETINOBLASTOMA RELATED1 Regulates Asymmetric Cell Divisions in Arabidopsis. *The Plant Cell Online* **24**, 4083-4095.

Weingartner M, Criqui M-C, Mészáros T, Binarova P, Schmit A-C, Helfer A, Derevier A, Erhardt M, Bögre L, Genschik P. 2004. Expression of a Nondegradable Cyclin B1 Affects Plant Development and Leads to Endomitosis by Inhibiting the Formation of a Phragmoplast. *The Plant Cell Online* **16**, 643-657.

Weterings K, Russell SD. 2004. Experimental Analysis of the Fertilization Process. *The Plant Cell Online* **16**, S107-S118.

Whittington AT, Vugrek O, Wei KJ, Hasenbein NG, Sugimoto K, Rashbrooke MC, Wasteneys GO. 2001. MOR1 is essential for organizing cortical microtubules in plants. *Nature* **411**, 610-613.

Xu G, Ma H, Nei M, Kong H. 2009. Evolution of F-box genes in plants: Different modes of sequence divergence and their relationships with functional diversification. *Proceedings of the National Academy of Sciences* **106**, 835-840.

Xu H, Swoboda I, Bhalla PL, Singh MB. 1999a. Male gametic cell-specific expression of H2A and H3 histone genes. *Plant Molecular Biology* **39**, 607-614.

Xu H, Weterings K, Vriezen W, Feron R, Xue Y, Derksen J, Mariani C. 2002. Isolation and characterization of male-germ-cell transcripts in Nicotiana tabacum. *Sexual Plant Reproduction* **14**, 339-346.

Xu HL, Swoboda I, Bhalla PL, Singh MB. 1999b. Male gametic cell-specific gene expression in flowering plants. *Proceedings of the National Academy of Sciences of the United States of America* **96**, 2554-2558.

Xu S-x, Zhu C, Hu S-y. 1990. Changes in the Organization of Microtubules During Generative Cell Division and Sperm Formation in Lilium. . *Acta Botanica Sinica* **32**, 821-826.

Yamamoto Y, Nishimura M, Hara-Nishimura I, Noguchi T. 2003. Behavior of vacuoles during microspore and pollen development in Arabidopsis thaliana. *Plant and Cell Physiology* **44**, 1192-1201.

Yang YO, Klessig DF. 1996. Isolation and characterization of a tobacco mosaic virus-inducible myb oncogene homolog from tobacco. *Proceedings of the National Academy of Sciences of the United States of America* **93**, 14972-14977.

Yanhui C, Xiaoyuan Y, Kun H, Meihua L, Jigang L, Zhaofeng G, Zhiqiang L, Yunfei Z, Xiaoxiao W, Xiaoming Q, Yunping S, Li Z, Xiaohui D, Jingchu L, Xing-Wang D, Zhangliang C, Hongya G, Li-Jia Q. 2006. The MYB transcription factor superfamily of Arabidopsis: expression analysis and phylogenetic comparison with the rice MYB family. *Plant Molecular Biology* **60**, 107-124.

Yu HS, Russell SD. 1993. Three-dimensional ultrastructure of generative cell mitosis in the pollen tube of Nicotiana tabacum. *Eur J Cell Biol* **61**, 338-348.

Zeng CJT, Lee Y-RJ, Liu B. 2009. The WD40 Repeat Protein NEDD1 Functions in Microtubule Organization during Cell Division in Arabidopsis thaliana. *The Plant Cell Online* **21**, 1129-1140.

Zhang X, Bernatavichute YV, Cokus S, Pellegrini M, Jacobsen SE. 2009. Genome-wide analysis of mono-, di- and trimethylation of histone H3 lysine 4 in Arabidopsis thaliana. *Genome Biol* **10**, R62.

Zhang Z, Xu H, Singh MB, Russell SD. 1998. Isolation and collection of two populations of viable sperm cells from the pollen of Plumbago zeylanica. *Zygote* **6**, 295-298.

Zhao XA, Harashima H, Dissmeyer N, Pusch S, Weimer AK, Bramsiepe J, Bouyer D, Rademacher S, Nowack MK, Novak B, Sprunck S, Schnittger A. 2012. A General G1/S-Phase Cell-Cycle Control Module in the Flowering Plant *Arabidopsis thaliana*. *PLoS Genet* **8**, e1002847.

Zheng B, Chen X, McCormick S. 2011. The Anaphase-Promoting Complex Is a Dual Integrator That Regulates Both MicroRNA-Mediated Transcriptional Regulation of Cyclin B1 and Degradation of Cyclin B1 during Arabidopsis Male Gametophyte Development. *The Plant Cell Online* **23**, 1033-1046.

Zhou C, Yang HY. 1991. Microtubule changes during the development of generative cells in Hippeastrum vittatum pollen. *Sexual Plant Reproduction* **4**, 293-297.

Zhou YM, Wang H, Gilmer S, Whitwill S, Fowke LC. 2003. Effects of co-expressing the plant CDK inhibitor ICK1 and D-type cyclin genes on plant growth, cell size and ploidy in Arabidopsis thaliana. *Planta* **216**, 604-613.

Zhu Q-H, Ramm K, Shivakkumar R, Dennis ES, Upadhyaya NM. 2004. The ANTHER INDEHISCENCE1 Gene Encoding a Single MYB Domain Protein Is Involved in Anther Development in Rice. *Plant Physiology* **135**, 1514-1525.

Zimmermann P, Hirsch-Hoffmann M, Hennig L, Gruissem W. 2004. GENEVESTIGATOR. Arabidopsis microarray database and analysis toolbox. *Plant Physiology* **136**, 2621-2632.

Zonia L, Tupý J, Staiger CJ. 1999. Unique actin and microtubule arrays co-ordinate the differentiation of microspores to mature pollen in Nicotiana tabacum. *Journal of Experimental Botany* **50**, 581-594.

Zuo JR, Niu QW, Chua NH. 2000. An estrogen receptor-based transactivator XVE mediates highly inducible gene expression in transgenic plants. *Plant Journal* **24**, 265-273.

Zuryn S, Le Gras S, Jamet K, Jarriault S. 2010. A strategy for direct mapping and identification of mutations by whole-genome sequencing. *Genetics* **186**, 427-430.